BMR JOURNAL of Australian Geology & Geophysics

VOLUME 1, NUMBER 3,

SEPTEMBER 1976

Department of National Resources, Australia

Minister: The Rt Hon. J. D. Anthony, M.P.

Secretary: J. Scully

Bureau of Mineral Resources, Geology and Geophysics

Director: L. C. Noakes

Editor, BMR Journal: J. F. Truswell

The BMR Journal of Australian Geology and Geophysics is a quarterly journal of research and related activities. Contributions are from officers of the BMR, from BMR officers working in collaboration with others, or requested work sponsored by the BMR. In addition to articles the Journal may include shorter notes and discussion of papers published in it. Discussion of papers is invited from anyone.

Annual subscription to the Journal is at the rate of $10 (Australian). Individual numbers, if available, cost $3. Subscriptions, etc., made payable to the Receiver of Public Moneys in Australian dollars, should be sent to the Director, Bureau of Mineral Resources, Geology & Geophysics, P. O. Box 378, Canberra, A.C.T. 2601, Australia. The Journal can also be obtained from the offices of the Department of National Resources in Sydney and Melbourne.

Other matters concerning the Journal should be sent to the Director, marked for the attention of the Editor, BMR Journal.

B M R JOURNAL

of Australian Geology and Geophysics

Volume 1, Number 3

September 1976

AUSTRALIAN GOVERNMENT PUBLISHING SERVICE
CANBERRA 1976

Front cover:

Looking southwest across the Styx and Hoogly estuaries, Broad Sound, Queensland. White areas are saline supratidal flats, which are flanked by mangrove swamps (dark areas) on their seaward side. Light-coloured intertidal sands, with some megaripples, can be seen.

BMR has recently completed a comprehensive study of the sedimentological and geochemical processes operative in this tropical estuarine system, the main results of which will appear in Bulletin form in the near future. A paper in this number of the Journal discusses numerical techniques applied to aspects of the geochemistry of the estuary.

Photograph: J. E. Zawartko

ISSN 0312-9608

Printed by Kerton Bros (S.A.) Pty Ltd, Edwardstown, S.A.

Environmental geology for urban development—Tuggeranong, Australian Capital Territory

G. Jacobson, P. H. Vanden Broek, and J. R. Kellett

Geological and soils mapping and an assessment of groundwater conditions has been carried out to assist development planning in the new town of Tuggeranong, in the Australian Capital Territory. The rocks of the area are mainly volcanic rhyodacites and the depth of weathering is generally less than 15 m. Residual soils are mainly podzolic clays; transported soils range from partly cemented gravelly, sandy silts (slope-wash) to complex layered clays (alluvium).

Foundation conditions are generally expected to be satisfactory in most areas for single-storey structures, and large buildings are expected to be founded within 5-10 m of the surface in the town centre area. Excavation conditions will be variable because of the irregular weathering profiles characteristic for the volcanic rocks.

Groundwater occurs in fractured rock, colluvial, and alluvial aquifers, and could be used for irrigation in places. Groundwater seepage problems are associated with the pediplain basins, and some remedial drainage works are necessary.

Sand deposits in the bed of the Murrumbidgee River constitute a major resource but supplies of rock aggregate will have to come from outside the area. The location of sanitary landfill sites will require detailed study to evaluate the risk of surface water and groundwater pollution.

Introduction

The proposed urban development area of Tuggeranong (Fig. 1) lies immediately south of the Woden/Weston Creek area and is planned to eventually house up to 180 000 people. Construction commenced in 1974 and will continue for about 10 years.

The Tuggeranong area consists of undulating slopes in the broad valley of the Murrumbidgee River (Fig. 2) which is bounded on the west by the Murrumbidgee fault scarp (Fig. 3) and on the east by a range of hills, the most prominent of which are Rob Roy (1099 m) and Tuggeranong Hill (805 m). The Murrumbidgee River is incised into the lower part of its valley, which is liable to flooding, and constitutes a major obstacle to access between the east and west sides of the valley.

Tuggeranong will be the first application by the National Capital Development Commission of the 'territorial unit concept' in urban planning (Westerman, 1973). Territorial units are flexible land divisions with their boundaries governed by topographic and land use barriers; they have, where possible, a linear activity spine containing schools, shops and other centres. Consequently the Tuggeranong urban outline plan (Fig. 4) shows a structure based on a linear transport corridor and town spine, with a linear belt of parkland adjacent to the Murrumbidgee River. Many of the roads will follow the natural topographic contours. The steeper slopes will not be developed and the ridges will be left as natural reserves.

A geological survey was requested by the National Capital Development Commission in 1972 to assist preliminary urban planning and was carried out by A. T. Laws, J. Saltet, P. H. Vanden Broek, and J. R. Kellett. It included surface mapping of the geology and soils, an assessment of groundwater conditions, and an augering and drilling programme. The information was presented to the NCDC town planners as a series of thematic maps at a scale of 1:25 000. From these maps an assessment of geological constraints to urban planning could be made.

A series of more detailed engineering geological and geophysical investigations was carried out for foundation conditions in the town centre area (Vanden Broek, 1973, 1974; Pettifer, 1974); for groundwater drainage problem areas at Lanyon and Isabella Plains; for the proposed water feature (Purcell & Goldsmith, 1975); and for the location of sewer lines, bridges and other engineering works. The more

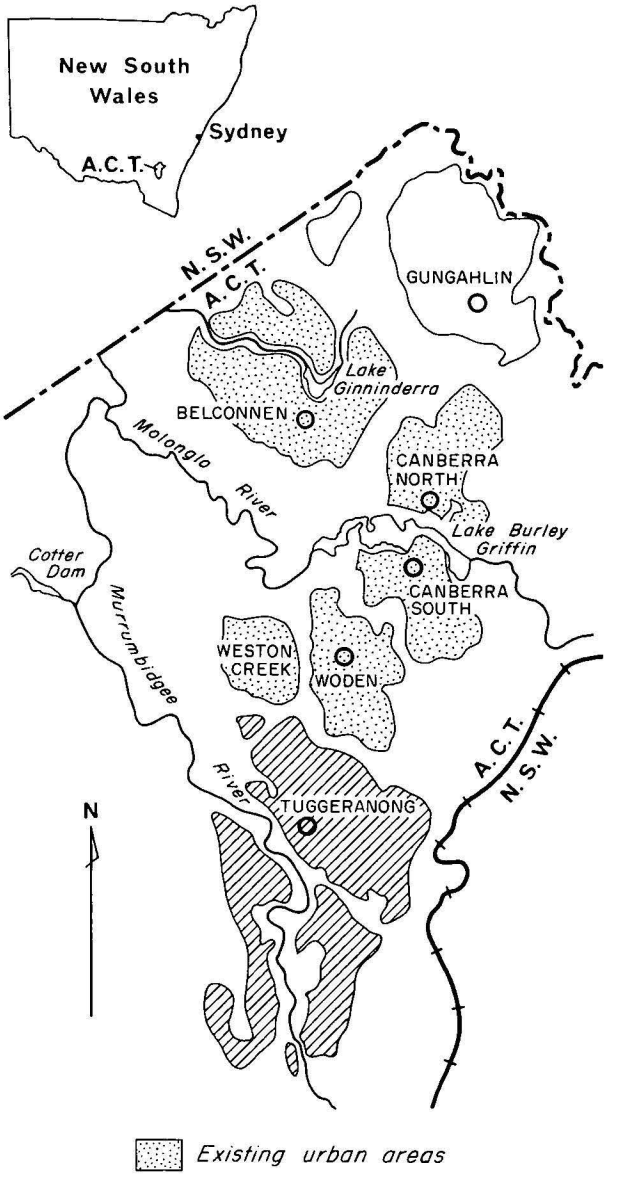

Figure 1. Locality map

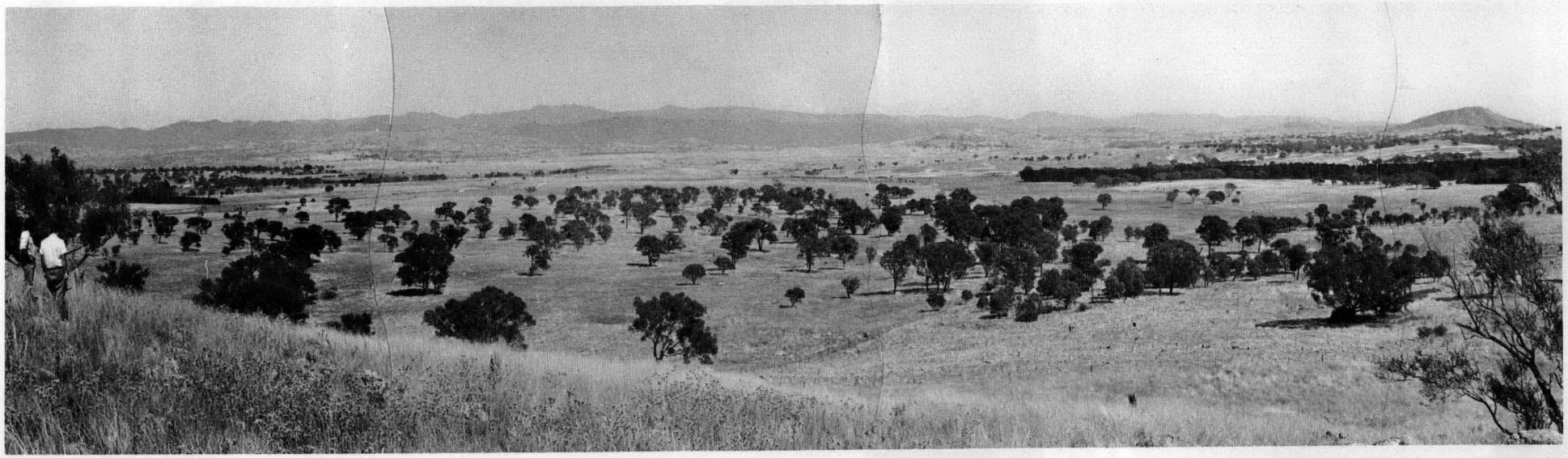

Figure 2. **Panorama of the Tuggeranong urban development area, looking northwest**

Figure 3. **The Murrumbidgee fault scarp at Freshford**

detailed investigations included seismic refraction surveys, drilling, and aquifer testing where appropriate.

Acknowledgement

The illustrations were drawn by J. Stirzacker, R. R. Melsom, and W. Shafron of the BMR geological drawing office.

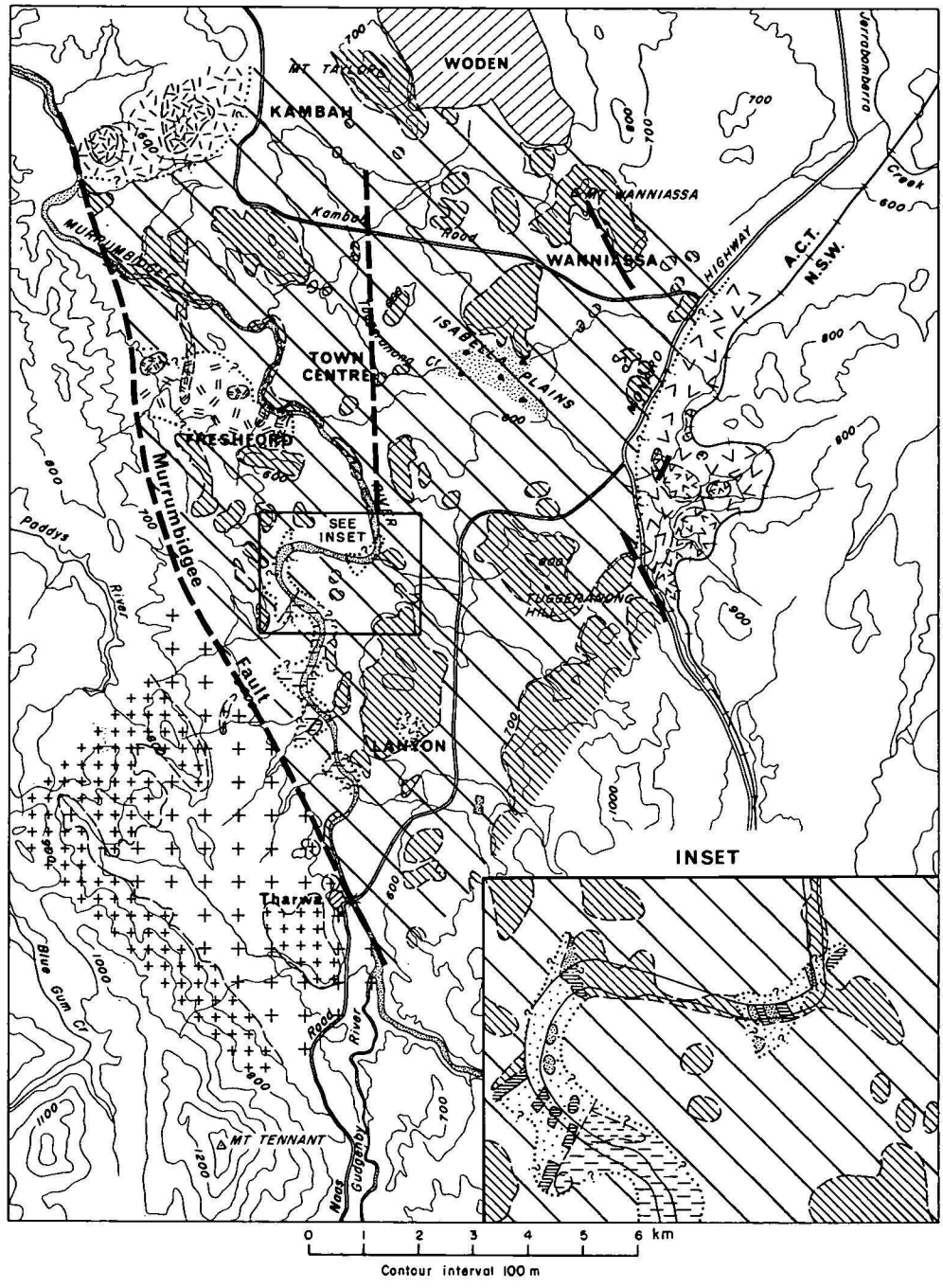

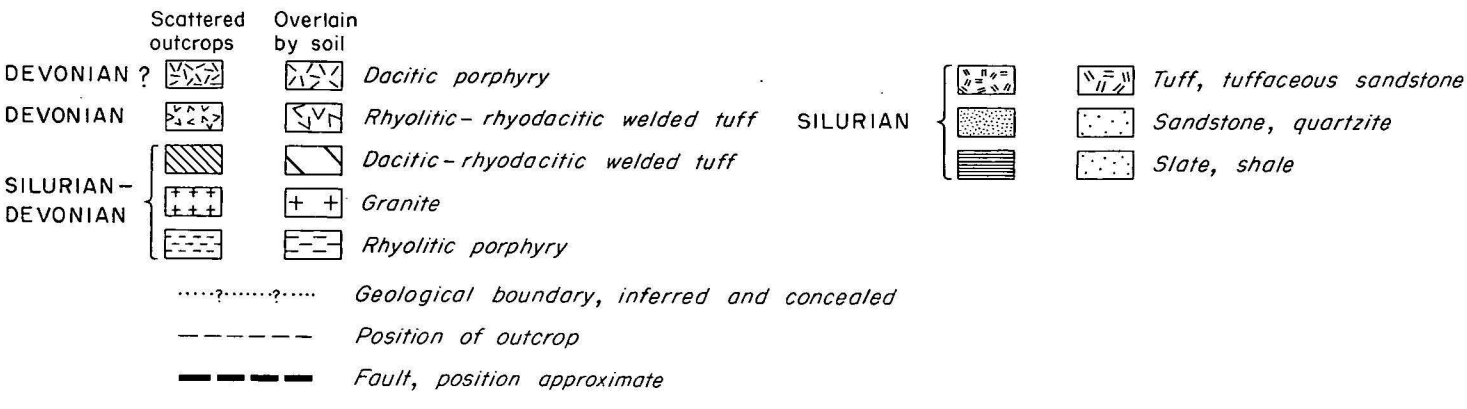

Figure 4. General geology

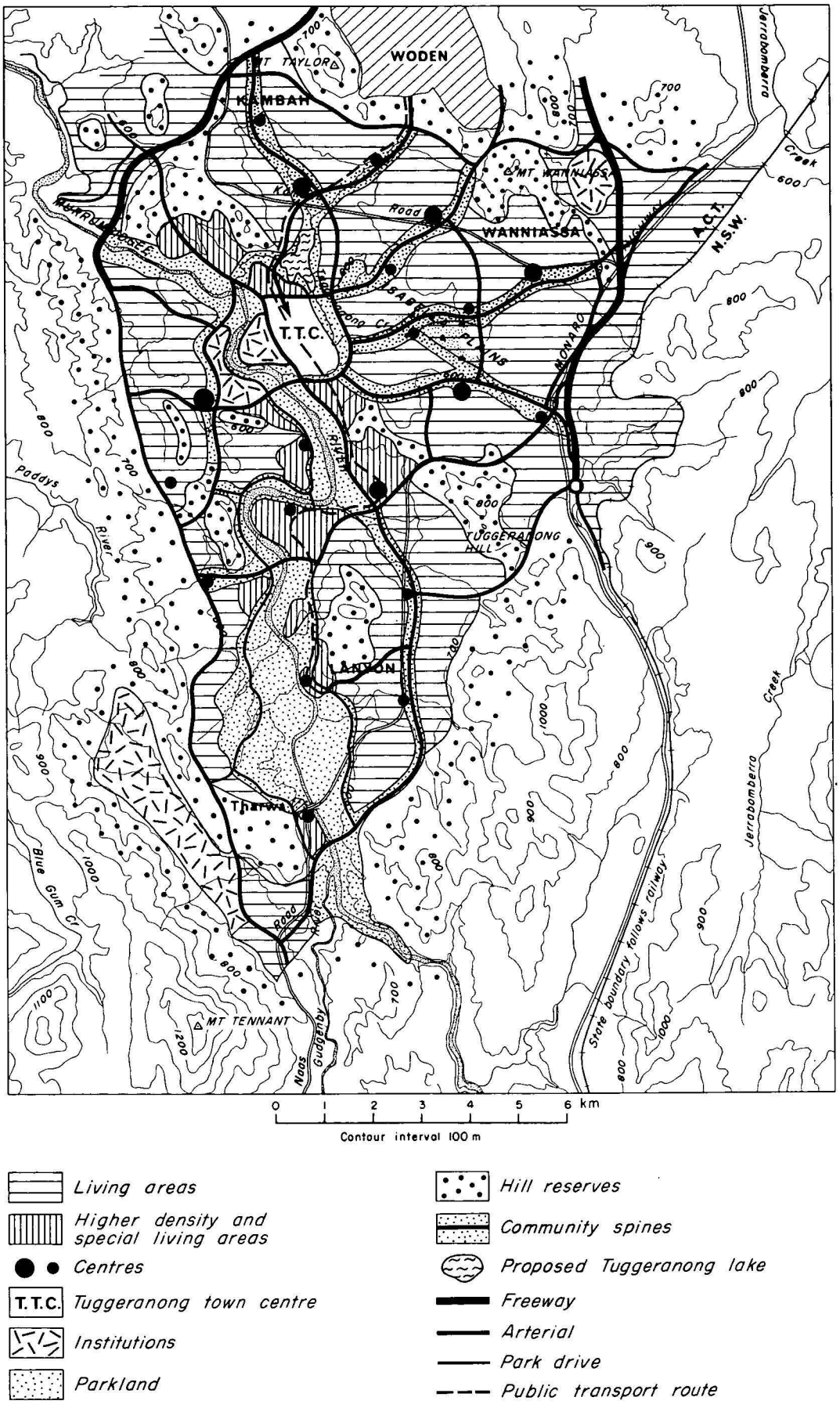

Figure 5. Urban outline plan

Map unit	*Probable age*	*Lithology*	*Structure*	*Structural relationships*	*Topography*	*Weathering*	*Fracturing, bedding, Foliation*	*Excavation characteristics*
Dacitic porphyry	Siluro-Devonian	Quartz and light green plagioclase phenocrysts, (20 mm) and some biotite phenocrysts, in grey-green groundmass.	Intrusive, no foliation observed. Massive. No folding observed.	Intrusive into dacitic and rhyodacitic welded tuff	Crops out only upper slopes, possibly underlying some lower ground in NW	Generally slightly weathered in outcrops	Massive, no obvious fracture pattern	Massive, hard, sound rock, difficult to excavate, little to moderate overbreak.
Rhyolite and rhyodacitic welded tuff	Siluro-Devonian	Quartz and plagioclase phenocrysts (5 mm), pink orthoclase phenocrysts (10 mm) in light to dark pink groundmass, few biotite phenocrysts. Rock is very light to dark pink.	Well-bedded gently dipping (20-40°) to E, general strike N-S	Conformably overlying dacitic and rhyodacitic and welded tuff	Outcropping on upper slopes and underlying the lower ground, covered with alluvium and soil E of Monaro Highway	Slightly to moderately weathered in outcrops	Well-bedded, parting along bedding planes	Hard, but well-bedded rock, moderate overbreak
Dacitic and rhyodacitic welded tuff	Siluro-Devonian	Phenocrysts of quartz, plagioclase and pink orthoclase (10 mm), in dark grey to purple or blue grey groundmass. Rock is generally dark	Massive nature of rock makes full structural analysis impossible: where observed mostly moderate to sub-horizontal dips, general strike approximately N-S.	Unconformably overlying steeply folded Silurian rocks	Crops out on upper slopes of hills and underlies most of the lower ground beneath soil and alluvium, in most of central part of area	Dacitic tuff, generally slightly weathered. Rhyodacitic tuff slightly to moderately weathered in outcrops. Weathering may extend to 15 m or more; weathering pattern regular	Few indications of bedding, main fracture system N-S, vertical	Hard, massive. Little overbreak, except in fractured zones
Granite	Siluro-Devonian	Porphyritic texture and pronounced foliation near Murrumbidgee Fault. Westwards becomes equigranular and less foliated	Generally foliated close to Murrumbidgee Fault.	Faulted against dacitic and rhyodacitic welded tuff along Murrumbidgee Fault	Cropping out mainly at higher elevation, but underlying soil and alluvium in depressions in SW and W of Murrumbidgee River	Moderately weathered in outcrops. Weathered profile deeper and more irregular than in the volcanic rocks. Fresh to moderately weathered boulders ('tors') surrounded by highly weathered rock	Foliation generally 340°, vertical. Main fracture parallel to foliation	Because of its irregular weathering pattern, major excavations should be thoroughly investigated before construction
Rhyolitic porphyry	Siluro-Devonian	Phenocrysts of quartz. Plagioclase, and characteristic conspicuous pink orthoclase (—20 mm) in dark groundmass.	Massive. No apparent structure	Intrusive in Silurian sandstone and shale	Scattered outcrops along Murrumbidgee River upstream from Point Hut Crossing	Outcrops are moderately weathered	Few fractures, no foliation observed	Massive, hard, difficult to excavate, little overbreak
Freshford Beds	Silurian	Interbedded slate, sandstone, ashstone, and rhyodacite with brecciated structure. Average thickness of beds 10 m	Sedimentary and volcanic components bedded. Strike ranges from N-S to E-W. Dips moderate, average 30°	Unconformably underlies dacitic and rhyodacitic welded tuff. Forms Silurian basement.	On lower ground and creek beds in NW	In general— Slate: moderately weathered Sandstone: slightly to highly weathered. Ashstone: Fresh Rhyodacite: slightly weathered	Main fractures parallel to bedding	Varying lithology, each excavation needs individual assessment
Sandstone, quartzite, shale, and slate	Silurian	Interbedded sandstone, quartzite, slate, and shale. Some calcareous shale.	Well-bedded, strike N-S; dips: steep, average 80°	Relation to Freshford Beds unknown.	Along Murrumbidgee River at and upstream from Point Hut Crossing. Isolated steeply dipping lenses exposed in river beneath dacitic and rhyodacitic welded tuff.	In general— Slate, sandstone and shale: moderately weathered Quartzite: Fresh	Parting along bedding planes	Varying lithology, excavation easy to very hard

Table 1. General geology—explanatory notes to accompany Figure 5

General Geology

The general geology of Tuggeranong is shown in Figure 5 and explanatory notes which outline the stratigraphy and structure are given in Table 1. Previous geological mapping by BMR geologists (Gardner, 1968; Jackson, 1970; Rossiter, 1971; Mendum, 1975) has been incorporated into the map.

Stratigraphy and structure

The rocks of the Tuggeranong area east of the Murrumbidgee Fault comprise a lower sequence of tightly folded and faulted Silurian sedimentary and volcanic rocks (Fig. 6) which are unconformably overlain by massive, gently folded Siluro-Devonian volcanic rocks (Figs. 7, 8). The latter plunge about 10° southwest and comprise volcanic flows and interbedded tuffaceous sediments of dominantly rhyolitic and rhyodacitic composition, intruded by sills and dykes ranging in composition from rhyolite to dolerite. Granite crops out to the west of the Murrumbidgee Fault, which defines the western margin of the Canberra graben.

Figure 6. Steeply dipping and faulted tuffaceous sediments, left bank of Murrumbidgee River, Point Hut Crossing

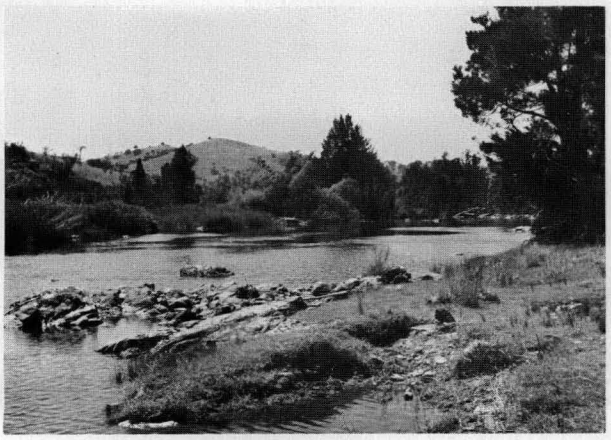

Figure 7. Outcrops of rhyodacite, right bank of Murrumbidgee River near Pine Island

Weathering

Weathering of the various rock types was investigated by drilling in order to provide a guide to foundation and excavation conditions for engineering works. The weathering classification used is shown in Table 2.

All the units mapped consist of rocks which are hard and strong where fresh, as in river-bed outcrops (Fig. 7). Elsewhere they are weathered to varying degrees and depths. Dacite, rhyodacite, and rhyolitic welded tuff underlie 70 percent of the mapped area. The rhyolite weathers to greater depths (up to 40 m) and more uniformly than the dacite and rhyodacite, which generally weather irregularly to about 15 m.

Figure 8. Rhyodacitic agglomerate, right bank of Murrumbidgee River, Pine Island

Fresh:	No discolouration or loss in strength.
Fresh stained:	Limonitic staining along fractures, rock otherwise fresh and shows no loss of strength.
Slight weathered:	Rock is slightly discoloured, but not noticeably lower in strength than the fresh rock.
Moderately weathered:	Rock is discoloured and noticeably weakened; N-size drill core generally cannot be broken by hand across the rock fabric.
Highly weathered:	Rock is discoloured and weakened; N-size drill core can generally be broken by hand across the rock fabric.
Extremely weathered:	Rock is decomposed to a soil, but the original rock fabric is mostly preserved.

Table 2. Rock weathering classification

Seismicity

An assessment of seismic risk has been made in general terms, as detailed records of earthquakes have only been available since 1960, and extrapolation from records covering such a short period of time is difficult.

Felt intensities of earthquakes that have been recorded in the Canberra region are listed in Table 3. A return period of 50 years is estimated for an earthquake with a felt intensivty of V on the Modified *Mercalli scale* (A. J. McEwin, BMR, pers. comm.). Felt intensities are likely to be greater in areas of silty and sandy alluvium and colluvium.

Minor seismicity has been attributed to the release of stress along the Murrumbidgee Fault (Cleary, 1967).

Geomorphology and soils

The landscape at Tuggeranong has been developed by a number of successive landsurfaces. Pediplanation has been the dominant erosion process during the development of a number of these landsurfaces (Van Dijk, 1959). The most recent event, related to the Kosciusko uplift, rejuvenated the Murrumbidgee River forming a valley-in-valley structure. Downward incision by the river has left a series of pediplain

Earthquake	Date	Hypocentre Lat.	Hypocentre Long.	Magnitude	Maximum felt intensity at epicentre	Intensity felt in ACT and environs
Kurrajong	15 Aug 1919	33.5°S	150.7°E	4.6ML	V	I-II
Murrumbateman	6 Mar 1924	34.9°S	149.0°E	5.0MB	IV	I-II
Dalton-Gunning	10 Mar 1949	34.74°S	149.20°E	5.5ML	VIII	III-IV
Rock Flat	1 Sep 1958	36.40°S	149.24°E	4.0ML	V	I-II
Berridale	18 May 1959	36.22°S	148.66°E	5.0ML	VI	III
Robertson-Bowral	21 May 1961	34.55°S	150.50°E	5.6ML	VII	III
Mt. Hotham	3 May 1966	37.04°S	147.13°E	5.7ML	V	II
Dalton	3 Nov 1971	37.76°S	149.16°E	4.2ML	V	III
Picton	9 Mar 1973	34.14°S	150.29°E	5.5ML	VI	IV

Table 3. Felt intensities of earthquakes in the Canberra region

Thickness (metres)	Morphological position	Soil types	Profiles	Origin	Terrain
	Upper slopes	Skeletal soil between areas of solid or scattered rock outcrop.	ML/SM/GM	Residual/colluvial	Hilly or mountainous
0-1	Monadnocks	Skeletal soil between areas of scattered rock outcrops or scattered boulders commonly underlain by completely weathered volcanic rock.	ML/SC	Residual	Rolling or undulating; gently sloping to flat
	Rejuvenated river valley	Skeletal soil between areas of scattered rock outcrop or scattered boulders.	ML/GM	Residual/colluvial	Hilly to undulating; steeply to gently sloping
	Upper pediment	Minimal podzolics. Slope wash.	OL/ML/CL/SC OL/ML/SM	Residual Colluvial	Undulating; moderately sloping
	Lower pediment	1. Red and yellow podzolics	OL/ML/CL/CH/SC	Residual	Gently undulating; gently sloping
		2. Layered soils, often truncated	Variable e.g. OL/ML/CL/CH/ CL/CH/ML/SC	Colluvial/alluvial	
		3. Slopewash	ML/SM	Colluvial	
1-2	Interfluves	Red and yellow earths	ML/CL/GP	Aeolian, alluvial or residual	Gently undulating; gently sloping
		Minimal podzolics	OL/ML/CL/SC	Residual	
	Small perched basins	Minimal soil developed on alluvium or layered soils.	Variable	Colluvial/alluvial	Hilly, moderately sloping
	Upper pediplain	Layered soils, colluvium		Colluvial/residual	Gently undulating
	Old ground surfaces	Maximal podzolics	OL/ML/CH/SC	Residual	Planar; gently sloping
2-3	Stream deposits	Interbedded gravel, sand, sift, and clay	Variable	Alluvial	Planar; gently sloping
	Lower pediplain	Interbedded sand, silt, gravel, and clay including laminated clay	GP to CH	Alluvial, including flood-plain deposits	Planar; flat
	Stream deposits	Interbedded gravel, sand, silt, and clay	GP-CH	Alluvial	
3-5		Interbedded sandy, silty, and clayey organic loams, heavy organic clays	OL-OH	Alluvial	Planar; gently sloping
>5	Pediplain basin	Interbedded gravel, sand, silt, and clay including heavy organic clay	GW-OH	Alluvial	Planar; depressions
Variable	river deposits	Well-sorted sand and gravel	GP and SP	Alluvial	Planar; flat

Table 4. Geomorphology and soils—explanatory notes to accompany Figure 9

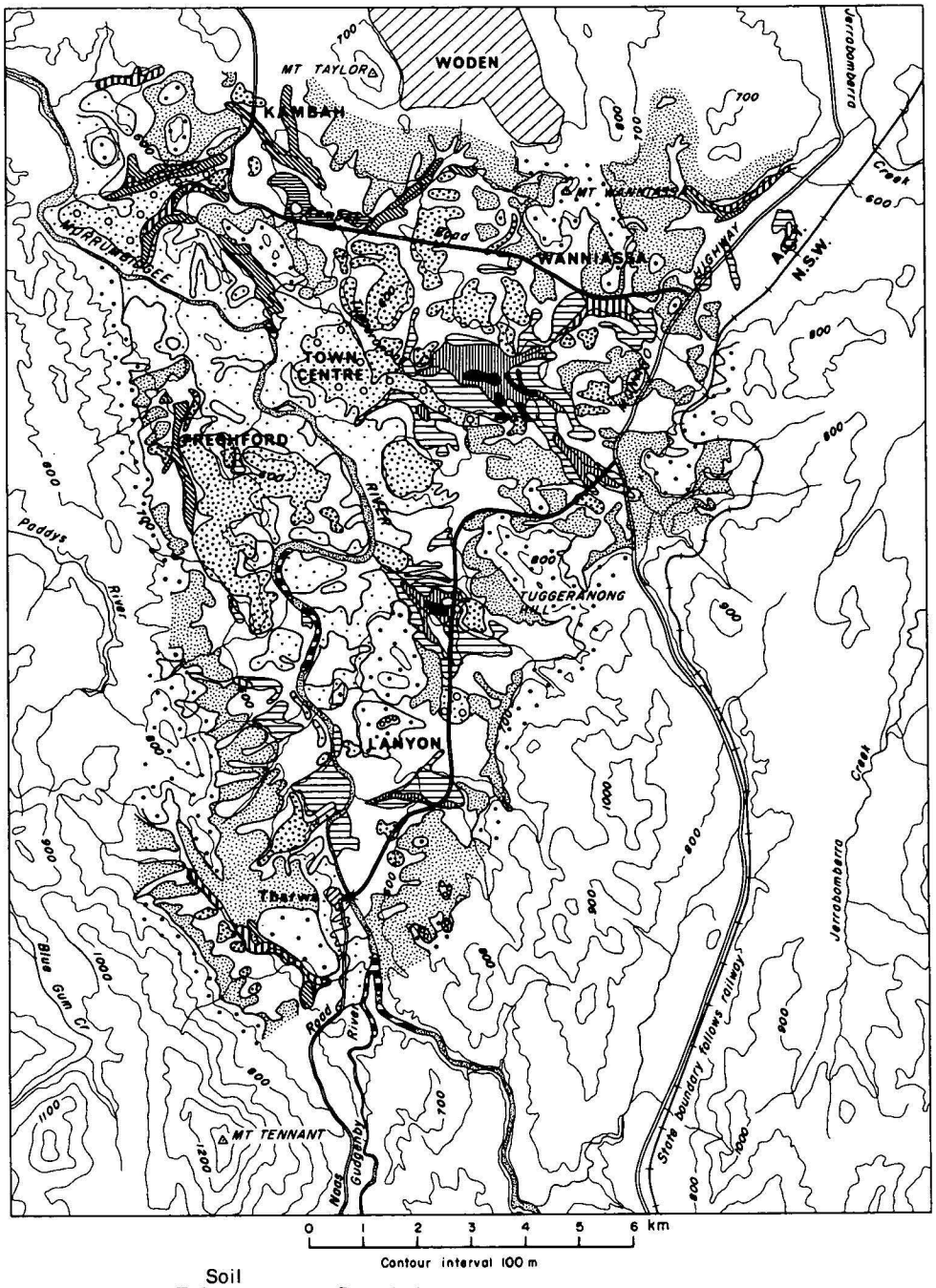

Soil Thickness	Description
0–1 metres	*Upper slopes : skeletal soil* *Monadnocks : skeletal soil* *Rejuvenated river valley : skeletal soil* *Upper pediments : minimal podzolics*
1–2 metres	*Lower pediments : podzolics* *Interfluves : red and yellow earths, podzolics* *Small perched basins : prairie soil on alluvium*
2–3 metres	*Upper pediplain : layered colluvium* *Older groundsurfaces : podzolics and residual clay* *Stream deposits : alluvium*
3–5 metres	*Lower pediplains : alluvium (poorly sorted)* *Stream deposits alluvium (well sorted)*
>5 metres	*Pediplain basin : alluvium*
variable	*River deposits : alluvium*

Figure 9. Soil thickness and geomorphology

basins perched in the valley at a height of 30 to 50 m above river level.

Geomorphological events have determined the distribution of the various soil types (Fig. 9). Table 4 gives the position of the various soil types as related to the development of the landscape, and shows typical thickness, soil profiles, mode of origin and terrain associated with the soil types.

Soil erosion

A study of soil erosion in Tuggeranong was completed by the Department of Forestry, Australian National University (1970) and many occurrences of moderate to severe erosion were recorded (Fig. 10). Severe erosion occurs in areas blanketed by unconsolidated colluvial material, which in some cases, contains dispersive clays.

Figure 10. Soil erosion, Tuggeranong Creek

River erosion

River erosion due to the effects of sand-winning operations has been described by the Commonwealth Department of Works (1971), which recommended strict control of the operations. Sand extraction has since been banned within Tuggeranong. The proposed construction of flood-control weirs could cause erosion problems downstream of the weirs.

Landslips

Occasional landslips occur on the steeper grassy hill slopes; generally in saturated colluvium. In some places large boulders are potentially unstable, particularly on the northern slopes of Castle Hill.

Hydrogeology

The hydrology and drainage features of Tuggeranong are shown in Figure 11. The Murrumbidgee River has a permanent flow; its tributaries mostly have a seasonal flow.

Flooding

An assessment of flooding of the Murrumbidgee River has been made by the Commonwealth Department of Works (1971), which recommended construction of a series of low flood-control weirs. The area which would be affected by a 100-years average return frequency flood is shown in Figure 11. Most of this area has been designated as parkland.

Groundwater

There are three types of groundwater aquifers in Tuggeranong. These comprise fractured-rock aquifers; lenticular aquifers in colluvial sand and gravel; and more continuous alluvial sand and gravel aquifers (Figs. 12, 13).

Groundwater was formerly extracted from several bores in the valley for domestic and stock use. Yields of the bores were generally low (Table 5), but representative of fractured-rock aquifers.

Monitoring of groundwater levels in the fractured rock aquifers indicates a seasonal fluctuation with recharge occurring in the winter months.

Water quality is variable with total dissolved solids content ranging from 195 to 1150 parts per million. The chemical composition of some groundwater and surface water samples is illustrated by Figure 14, which shows that bicarbonate is the dominant anion in most of the groundwater, with calcium

Bore	*Aquifer*	*Depth (m)*	*Yield (m^3/hour)*	*Salinity (ppm)*	*Use*
57	Shale	17	4.5	1040	Abandoned
396	—	—	4.6	920	Stock
56	—	26	0.5	235	Stock, domestic
372	—	76	—	285	Tunnel observation
43	Porphyry	37	2.3	220	Stock, domestic
162	Porphyry	18	3.9	275	Stock, domestic
45	Porphyry	43	6.1	1060	Stock
373	—	55	6.1	—	Tunnel observation
42	—	26	6.6	1100	Stock
335	—	—	5.4	485	Observation
44	—	48	2.0	940	Stock
323	Rhyodacite	43	2.0	—	Observation
330	Rhyodacite	31	0.7	—	Observation
324	Rhyodacite	31	0.7	—	Observation
325	Rhyodacite	31	1.1	—	Observation
49	—	29	4.1	1080	Stock
322	Rhyolite	49	4.1	—	Observation
331	Rhyodacite	26	1.1	—	Observation
328	Rhyodacite	31	1.1	—	Observation
334	Alluvium	—	0.5	195	Abandoned
50	Alluvium	20	0.6	405	Stock
329	Rhyodacite	31	0.5	—	Observation
326	Rhyodacite	31	0.5	—	Observation
327	Rhyodacite	31	0.2	—	Observation
336	Rhyodacite	31	5.4	470	Observation
337	—	31	5.4	—	Observation
334	—	31	1.8	1150	Abandoned
338	—	31	2.7	210	Observation
310	Dacite	41	0.1	—	Observation
313	Rhyodacite	47	0.4	—	Observation
314	Shale	16	0.3	—	Observation
312	Shale	40	8.2	—	Observation
311	Porphyry	40	4.3	—	Observation

Table 5. Groundwater boreholes

or sodium the dominant cation. The sodium absorption ratio is generally low and groundwater could be used for irrigation where sufficient quantities are available. It is a potential resource of 'second class' water to supplement the town water supply.

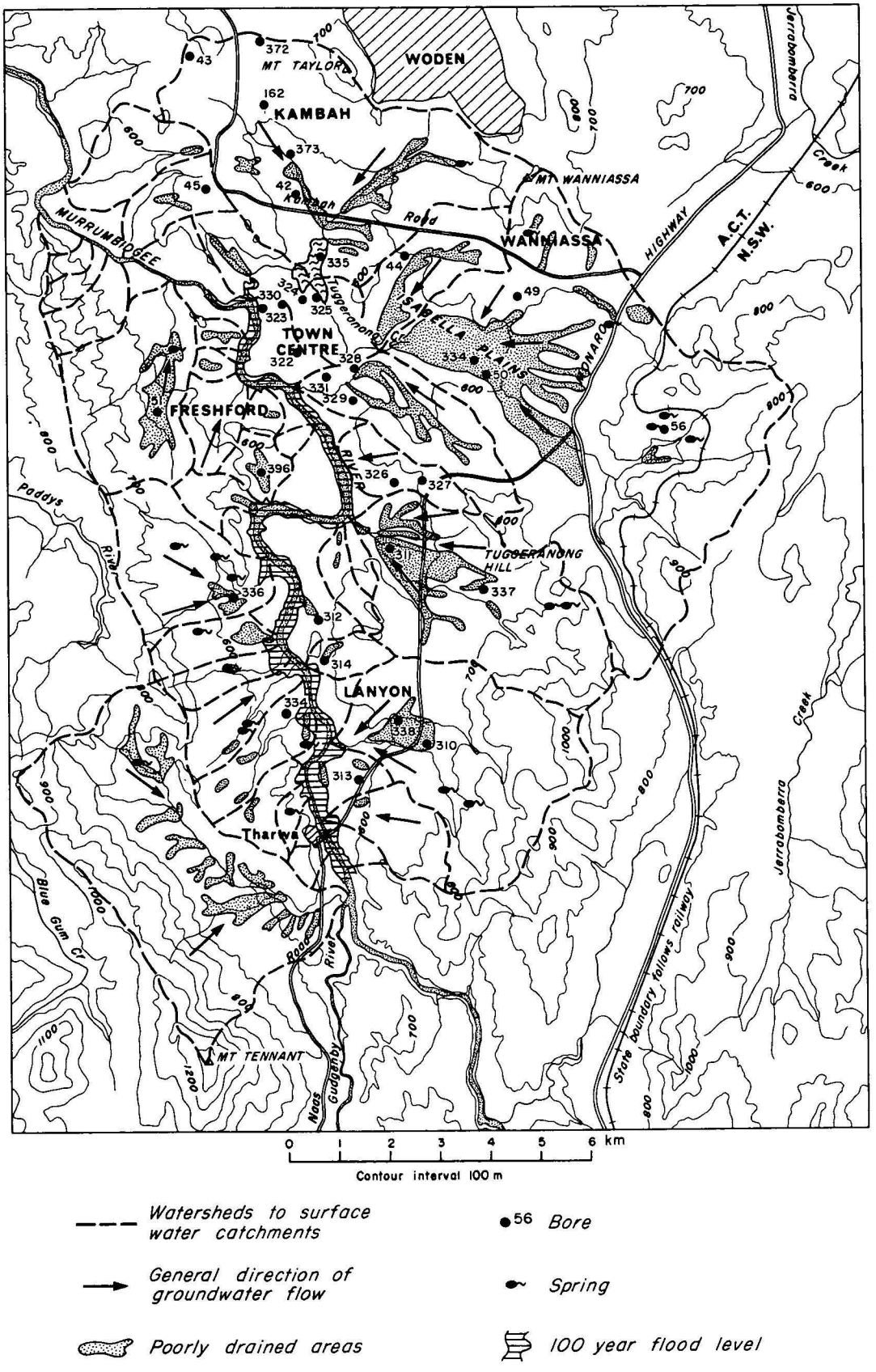

Figure 11. Hydrology and drainage

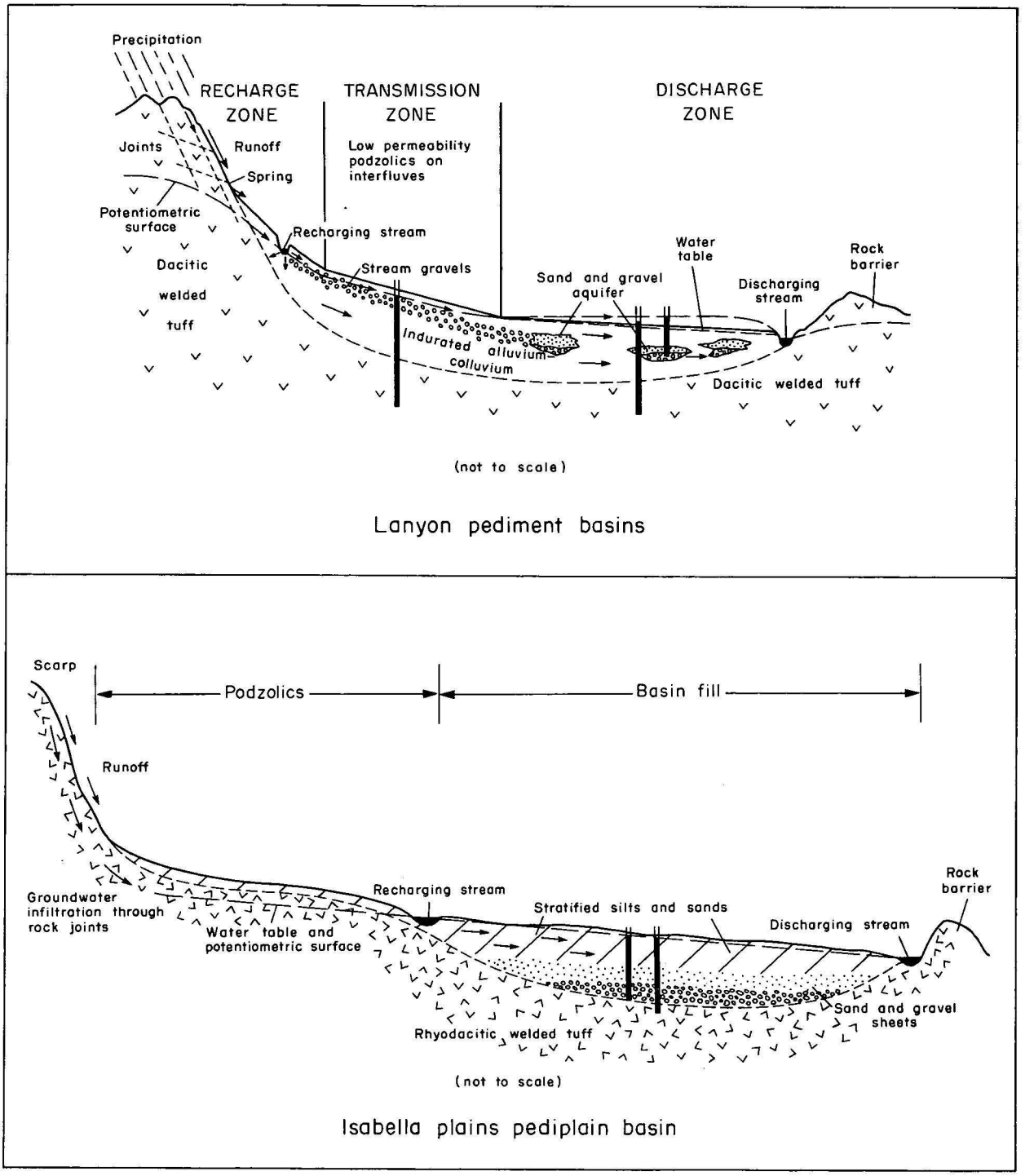

Figure 12. Cross-sections of alluvial aquifers

Drainage problems

Soil drainage problems are present in the pediment basins where restriction of lateral groundwater movement causes water to emerge at the surface as perennial springs and soaks. The potentiometric surface is above ground level in the worst affected areas and extensive remedial drainage works are required to develop such areas. Detailed investigations of the larger seepage areas have been undertaken at Lanyon and Isabella Plains. These investigations have included auger drilling and soil sampling to define the aquifer systems (shown diagrammatically in Figure 12) and hence the most suitable locations for drainage channels. Permeability of the aquifers was determined by pump tests to enable optimum drain spacing to be determined. At Isabella Plains, the construction of preliminary drainage channels in 1974 reduced the potentiometric surface by 2-3 m (Fig. 15). Other areas where remedial works will be needed are Woolshed Creek and Freshford on the western side of the Murrumbidgee Valley.

Seepages associated with small colluvial aquifers are common on hillslopes throughout Tuggeranong and have led to difficult construction conditions in the first residential areas to be developed at Kambah.

Figure 13. **Stratified alluvium exposed in drainage channel, Isabella Plains**

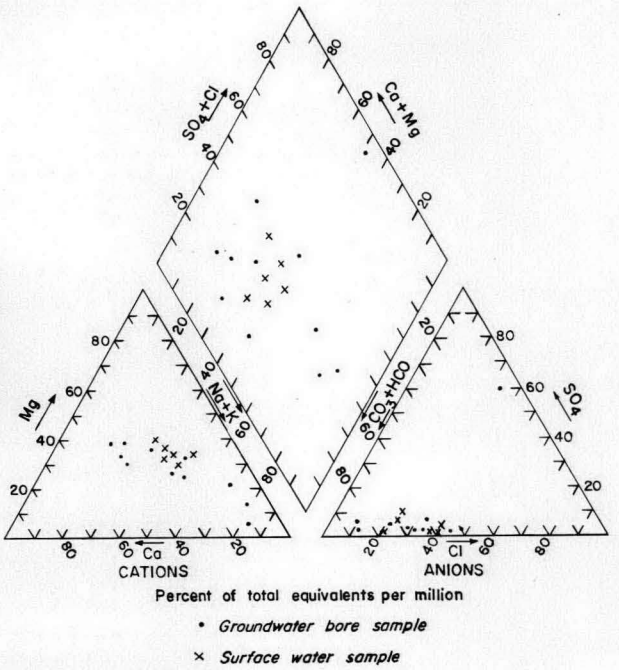

Figure 14. **Chemical composition of groundwater**

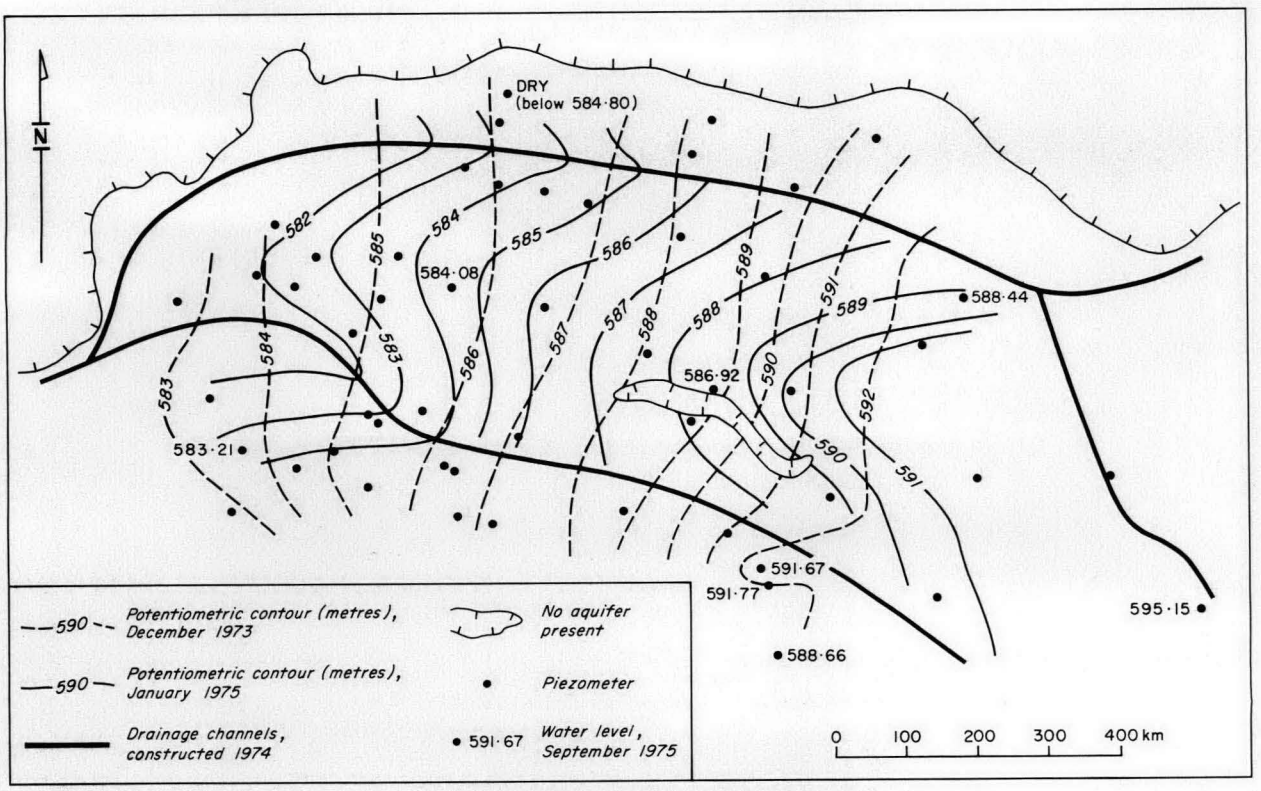

Figure 15. **Isabella Plains potentiometric levels, 1973-75**

Foundation and excavation conditions

Foundation and excavation conditions at Tuggeranong are shown in Figure 16. These conditions have been assessed from the geological and soils mapping and from the 59 auger holes sunk; representative visual auger logs are included in Figure 17. A more detailed investigation was made in the Town Centre area which is largely underlain by irregularly weathered rhyodacite and rhyolite (Fig. 18). Ten drill holes were sunk and nine seismic traverses surveyed to determine conditions for large buildings here; representative visual drill logs and seismic sections are shown on Figure 19.

Foundation conditions are expected to be satisfactory in most areas for single-storey structures. Some thick clay soils

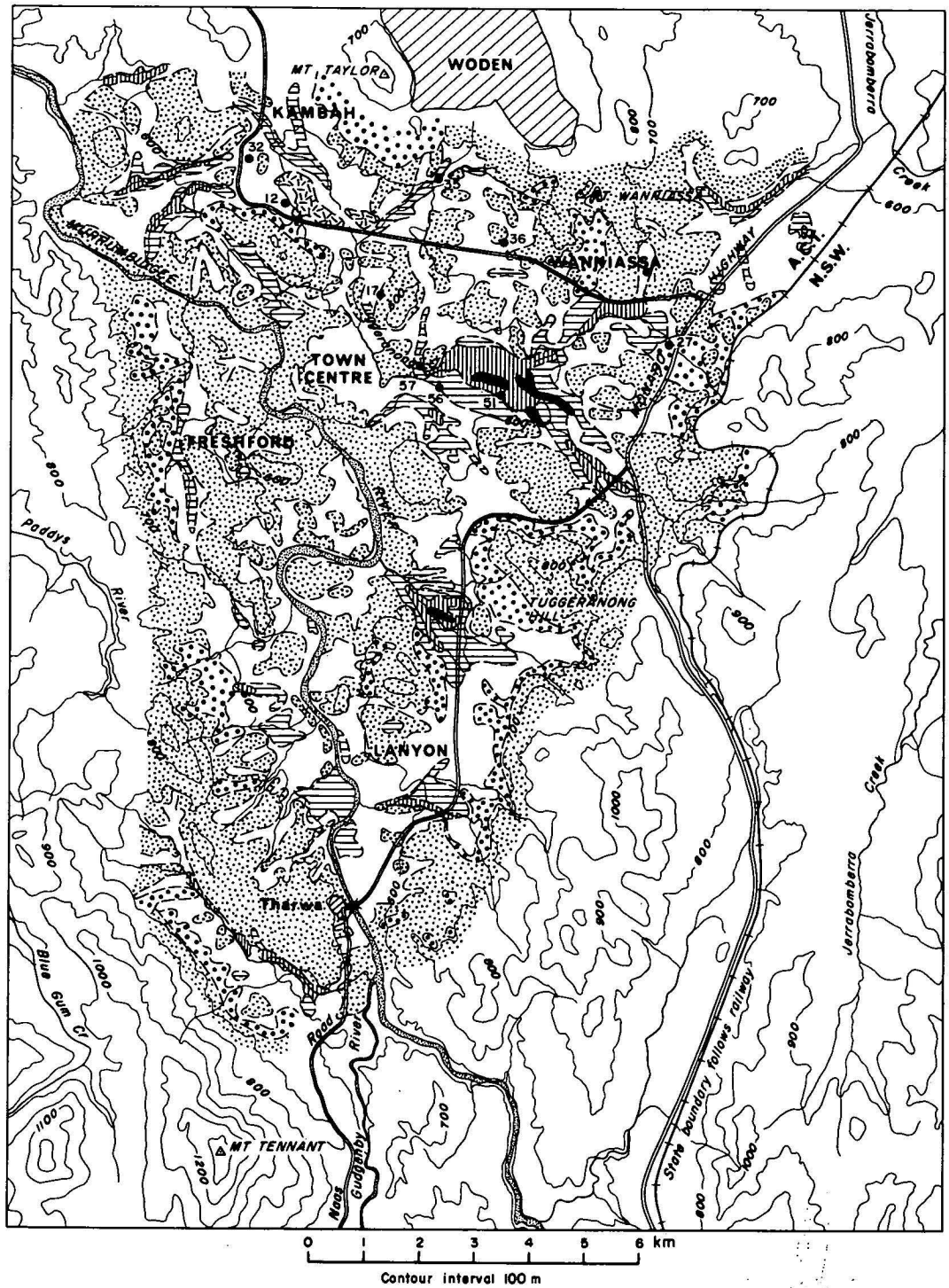

Excavation by blasting
Strong foundations at surface

Excavation by scraping and ripping
Strong foundations below 2 metres

Excavation by ripping and blasting
Strong foundations below 2 metres

Excavation by scraping
Strong foundations below 3 metres

Auger hole

Excavation by scraping
Strong foundations at
variable depths below 3 metres

Excavation by scraping
Requires seepage control
Strong foundations below 5 metres

Excavation by scraping
Requires seepage control
Strong foundations at
variable depths below 5 metres

Figure 16. Foundation and excavation conditions

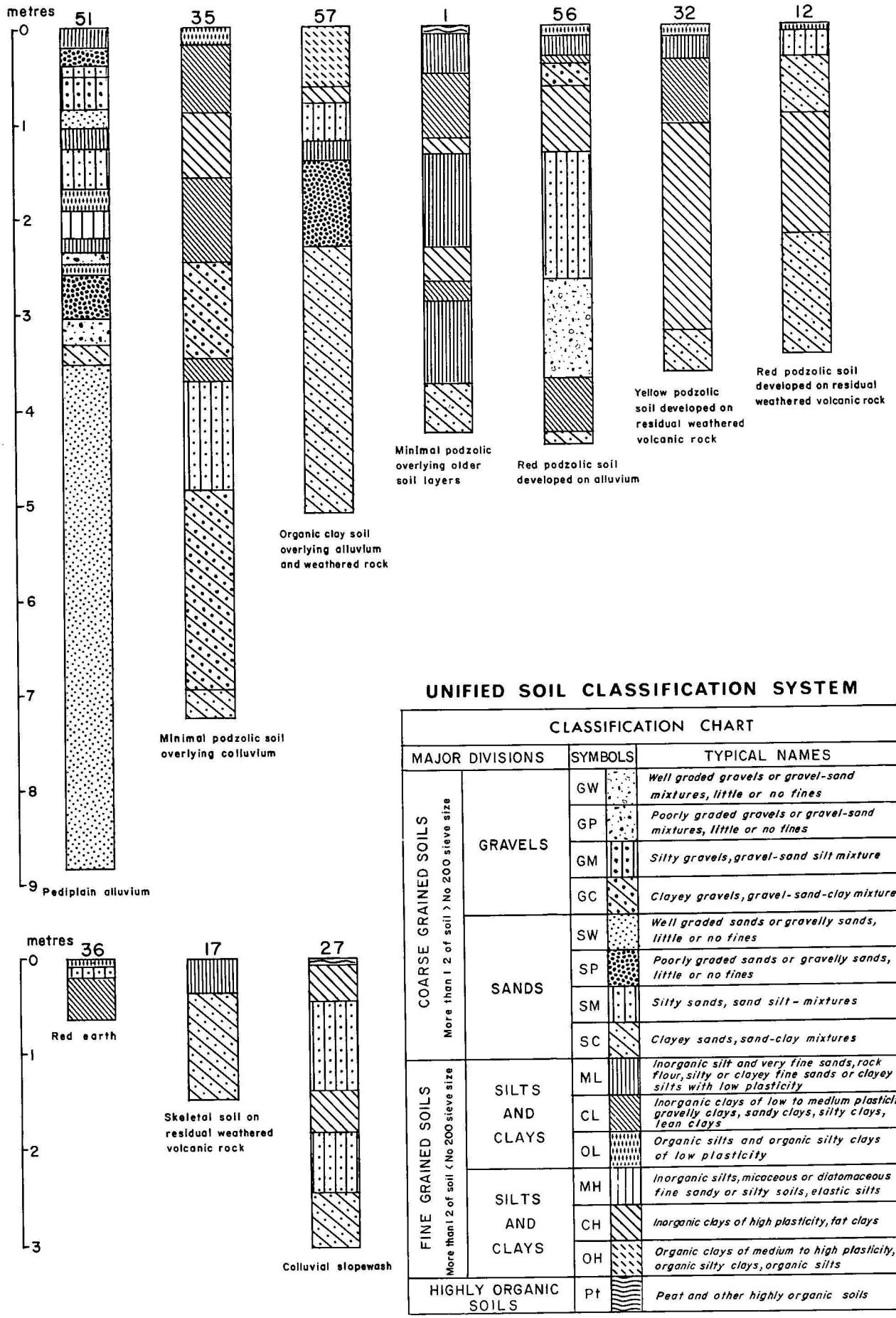

UNIFIED SOIL CLASSIFICATION SYSTEM

CLASSIFICATION CHART				
MAJOR DIVISIONS			SYMBOLS	TYPICAL NAMES
COARSE GRAINED SOILS More than 1/2 of soil > No 200 sieve size	GRAVELS		GW	*Well graded gravels or gravel-sand mixtures, little or no fines*
			GP	*Poorly graded gravels or gravel-sand mixtures, little or no fines*
			GM	*Silty gravels, gravel-sand silt mixture*
			GC	*Clayey gravels, gravel-sand-clay mixture*
	SANDS		SW	*Well graded sands or gravelly sands, little or no fines*
			SP	*Poorly graded sands or gravelly sands, little or no fines*
			SM	*Silty sands, sand silt - mixtures*
			SC	*Clayey sands, sand-clay mixtures*
FINE GRAINED SOILS More than 1/2 of soil < No 200 sieve size	SILTS AND CLAYS		ML	*Inorganic silt and very fine sands, rock flour, silty or clayey fine sands or clayey silts with low plasticity*
			CL	*Inorganic clays of low to medium plasticity, gravelly clays, sandy clays, silty clays, lean clays*
			OL	*Organic silts and organic silty clays of low plasticity*
	SILTS AND CLAYS		MH	*Inorganic silts, micaceous or diatomaceous fine sandy or silty soils, elastic silts*
			CH	*Inorganic clays of high plasticity, fat clays*
			OH	*Organic clays of medium to high plasticity, organic silty clays, organic silts*
HIGHLY ORGANIC SOILS			Pt	*Peat and other highly organic soils*

Figure 17. Logs of auger holes

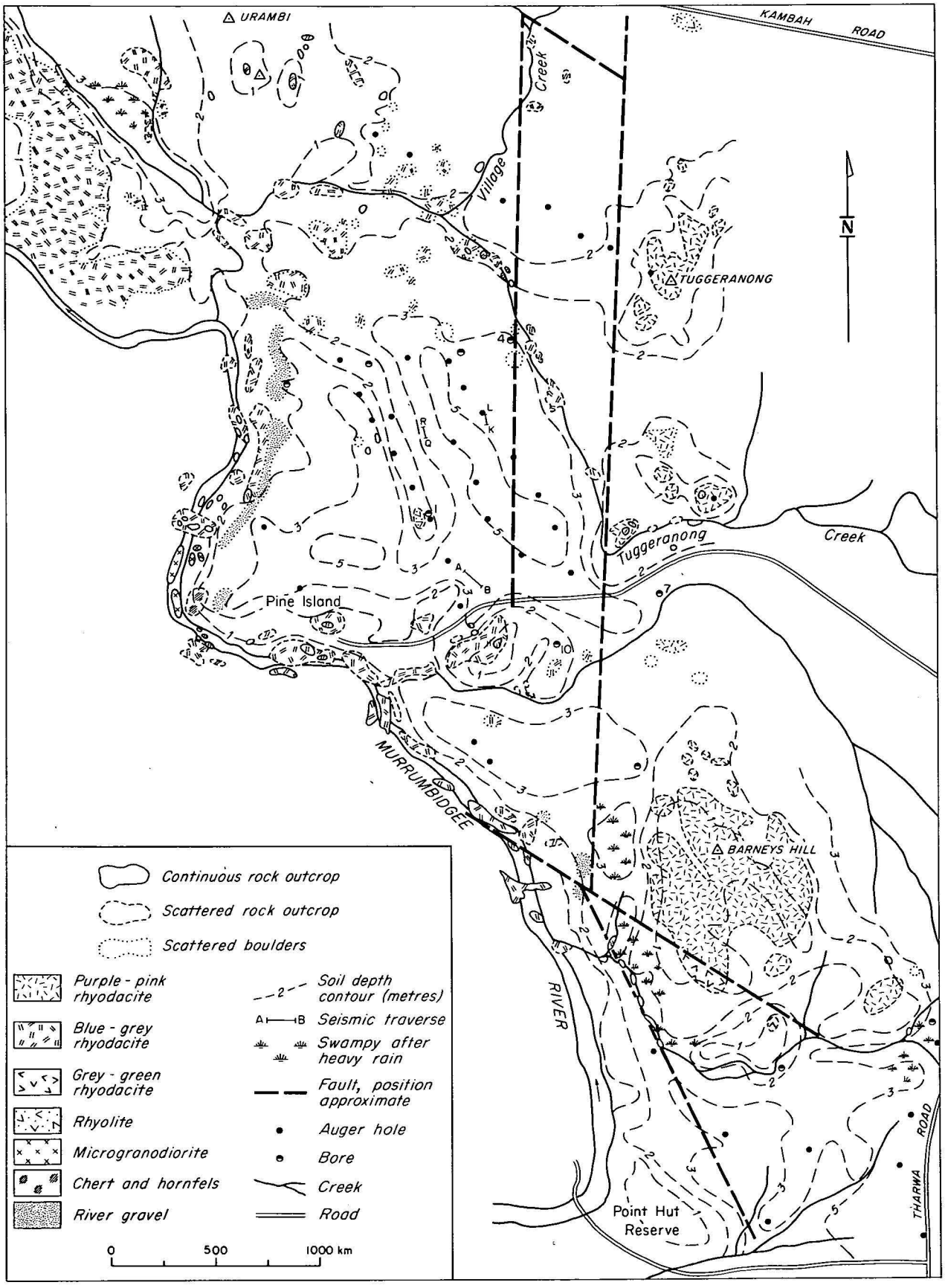

Figure 18. Tuggeranong town centre geology

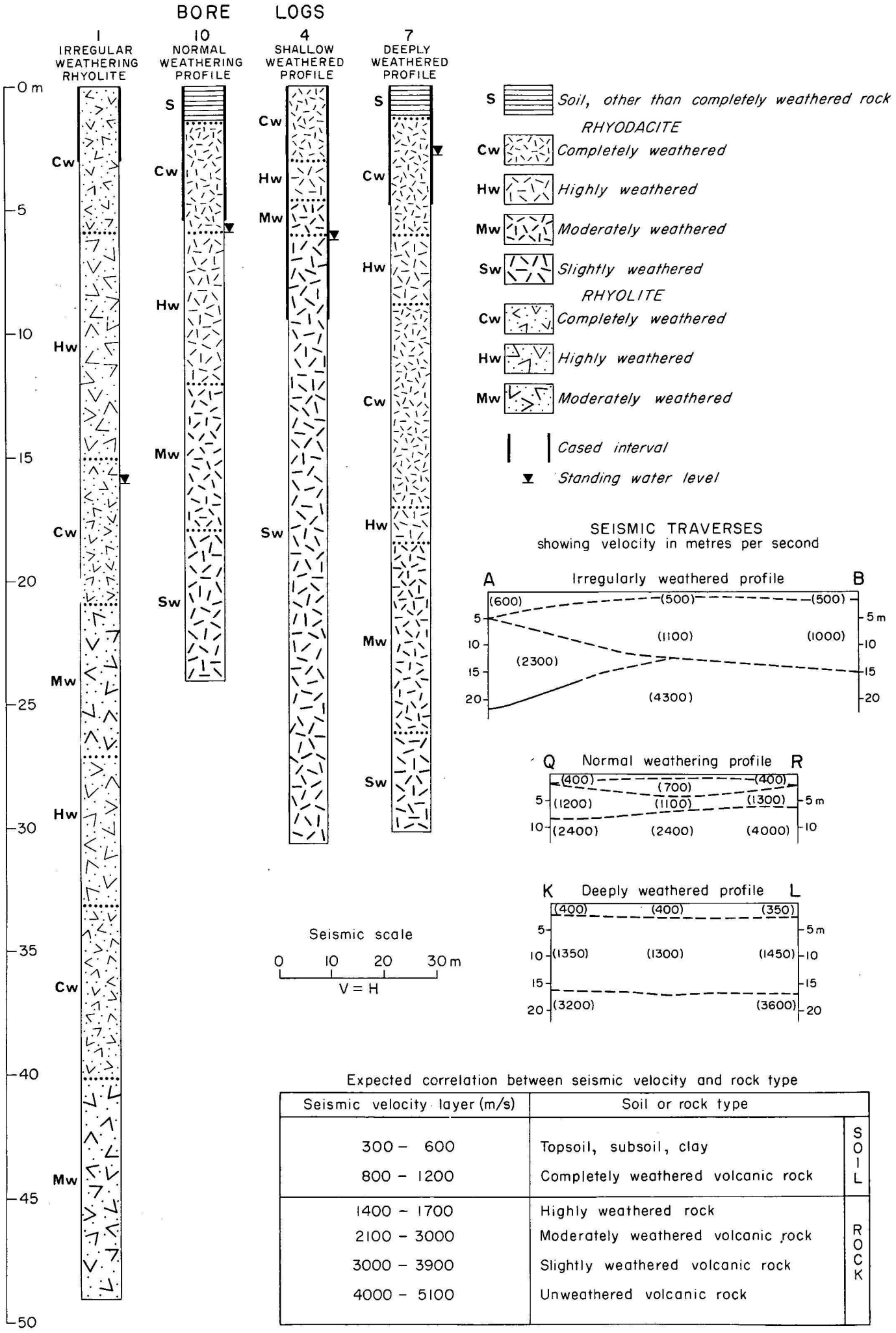

Expected correlation between seismic velocity and rock type

Seismic velocity layer (m/s)	Soil or rock type	
300 – 600	Topsoil, subsoil, clay	SOIL
800 – 1200	Completely weathered volcanic rock	
1400 – 1700	Highly weathered rock	ROCK
2100 – 3000	Moderately weathered volcanic rock	
3000 – 3900	Slightly weathered volcanic rock	
4000 – 5100	Unweathered volcanic rock	

Figure 19. Tuggeranong town centre subsurface conditions

in poorly drained areas may cause detrimental differential foundation movement and special investigation is recommended. Detailed site investigations for large structures founded on irregularly weathered rocks will be required; however no major constraints to building in the Town Centre area are foreseen and large buildings will probably be founded within 5-10 m of the surface on highly to moderately weathered rock. Deep weathering is known to occur in association with major fault zones; consequently, additional investigations are being undertaken of foundation conditions in the Murrumbidgee Fault zone (Fig. 3) which traverses the proposed western suburbs of Tuggeranong, and is up to 400 m wide.

Deep excavation conditions are difficult to predict because of the irregular weathering profiles characteristic for volcanic rocks throughout the region. The irregular weathering profiles commonly contain hard boulders of slightly weathered rock embedded in a matrix of softer, extremely weathered rock; the boulders may range in size from 0.3-3 m. Areas which have scattered rock outcrop at the surface are commonly underlain by irregularly weathered rock, whereas more continuous outcrop at the surface generally indicates that an area is underlain by fresh rock close to the surface and that excavation will be difficult. Areas which are topographically flat and devoid of outcrop normally have deeper, more uniform weathering and easier excavation conditions.

The soil thicknesses (Fig. 9) can be used as a guide for shallow excavation conditions. Some mapping units, for example, the lower pediplain alluvium, may however overlie the colluvium and podzolic soils of older, partly dissected land surfaces rather than weathered rock.

The foundation and excavation conditions map (Fig. 16) has been used by the town planners for computer-based land evaluation studies. Where the mapping has been sufficiently detailed, it can be used by engineers and contractors in assessing the ease of excavation for roads and services.

Resources

Natural resources in the Tuggeranong area are shown in Figure 20. There are no known occurrences of metallic minerals in the area.

Deposits of sand in the beds of the Murrumbidgee and Gudgenby Rivers have been worked in the past as a source of supply for Canberra. Investigations of additional sand reserves have been carried out by the Commonwealth Department of Works (1972) and Coffey and Hollingsworth Pty Ltd (1973). Sand is transported rapidly by the river and replenishment of depleted deposits could occur.

Alluvial terraces in the Murrumbidgee Valley between Tharwa and Point Hut may contain substantial reserves of sand and/or topsoil. These deposits all require investigation by drilling in order to assess their value as a resource before the land is pre-empted for other uses. Minor deposits of fine-grained red aeolian sand are present at Lanyon and Pine Island.

Several possible quarry sites for crushed rock aggregate are indicated on Figure 20. Most of those within the urban area are likely to be rejected on environmental grounds. Possible sources outside Tuggeranong include a site near Mugga Road to the northeast, and other sites near Royalla to the southeast. More detailed investigations will be needed to ensure an adequate supply of rock aggregate as the new town develops.

A number of geological investigations of resources in the area have been undertaken for land acquisition and compensation claims. Some additional investigations have been undertaken for land use planning purposes. In places triple land use may be possible, with extraction of resources

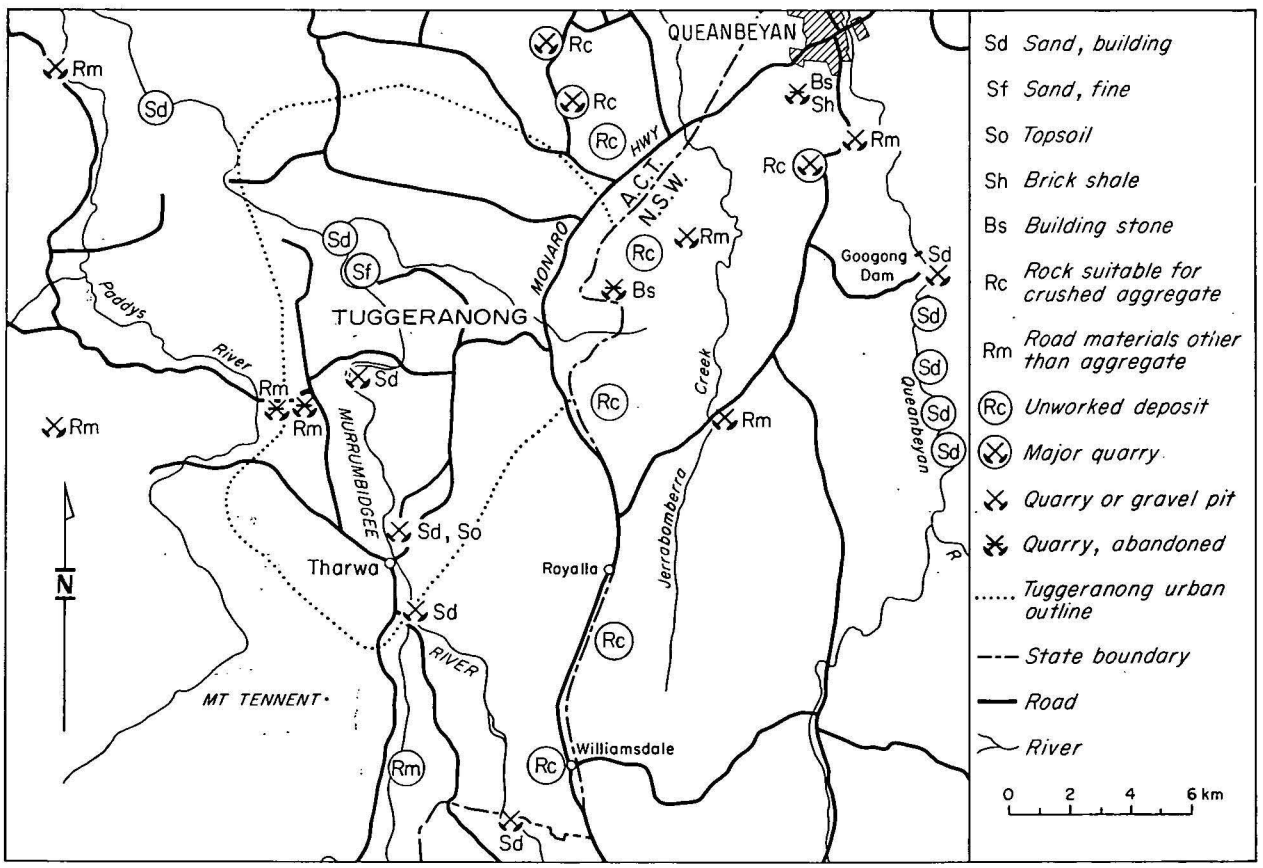

Figure 20. Resources

followed by use of the land for waste disposal, followed eventually by reclamation for building or parkland. The scarcity of some resources in the ACT area and the severe environmental constraints on their extraction, lead to difficult problems of balancing the high cost of haulage against the detrimental effects of local extraction.

Environmental considerations

Some additional environmental geology considerations in various aspects of planning are described below.

Refuse disposal sites

Optimum conditions for solid waste disposal sites are found in well-drained areas with a deep, moderately permeable soil profile and a low water table. Sites should not be liable to flooding and must be located so that pollution of groundwater and surface water courses is minimised. The most likely locations are in the lower pediment podzolics not far from the foot of the surrounding hills, and in deeply weathered volcanic rock profiles. In some cases the excavated weathered material could be used for gravel pavement construction.

Present refuse disposal planning strategy in Canberra indicates that a major site will need to be developed shortly in or near Tuggeranong. There are no obvious sites in Tuggeranong that fulfil the required conditions; therefore, detailed investigations are being undertaken of several alternative sites in the surrounding area.

Sewer lines

The sewerage system in Tuggeranong is planned to include several feeder sewers into a main trunk sewer gravitating north to a treatment plant on the Molonglo River. Geological investigations have been made of several alternative routes for the sewer lines with particular emphasis on determining the feasibility of using tunnels, which are environmentally desirable, rather than cuts which are more economic in areas of low cover.

Stormwater drainage

The stormwater drainage system in Tuggeranong is planned to include several retention ponds to alleviate pollution of the Murrumbidgee River by urban stormwater runoff. The proposed lake in the town centre will also serve this purpose in addition to its ornamental and recreational uses; geological investigations of the site have been made (Purcell & Goldsmith, 1975).

Geological monuments

Some of the rock outcrops in the Murrumbidgee River are of considerable geological interest and recommendations have been made that they should be preserved as geological monuments. These outcrops include a volcanic complex exposed in the river banks downstream from Pine Island (Figs. 6, 7), and a sequence of well exposed agglomerate breccia downstream from Point Hut Crossing. Future road cuts of geological interest should be preserved rather than covered up.

Geological constraints in planning

The main geological constraints to urban development planning are:

1. The volcanic rocks which occur in much of Tuggeranong are weathered to variable depths and detailed foundation investigations will be necessary on sites where large structures are planned.
2. Geological hazards include possible seismicity associated with the Murrumbidgee Fault; possible boulder slides on steep hill slopes; and flooding and erosion by the Murrumbidgee River.
3. Groundwater seepage problems. The large pediment basins at Isabella Plains, Lanyon, Freshford and Woolshed Creek will require remedial drainage works. There are, in addition, extensive areas of colluvium containing lenticular aquifers that will cause springs and seepages in excavations, and possible instability in road cuts.
4. Supplies of topsoil, sand, and gravel are limited in the ACT and it may be desirable to exploit the deposits in the Murrumbidgee Valley before using the land for other purposes.
5. Supplies of rock aggregate will probably have to be sought outside the Tuggeranong development area. Suitable locations for quarries are known in adjacent areas.

References

CLEARY, J. R. 1967—The seismicity of the Gunning and surrounding areas, 1958-61. *Journal of the Geological Society of Australia*, **14**, 23-29.

COFFEY & HOLLINGSWORTH PTY LTD., 1973—Report on the survey of sand resources in the Gudenby and Murrumbidgee Rivers, Angle Crossing area, ACT Report **4750/1** to Commonwealth Department of Works.

COMMONWEALTH DEPARTMENT OF WORKS, 1971—Supplementary report on flood levels and recreational lake development on the Murrumbidgee River at Tuggeranong, July 1971.

COMMONWEALTH DEPARTMENT OF WORKS, 1972—Report on sand quantities in the Murrumbidgee and Gudgenby River in Tuggeranong, April 1972.

DEPARTMENT OF FORESTRY, AUSTRALIAN NATIONAL UNIVERSITY, 1970—An ecological and physiographic survey of the proposed Tuggeranong city area and surrounds, May 1970.

GARDNER, D. E., 1968—Preliminary notes on the geology of the Tuggeranong urban development area, ACT. *Bureau of Mineral Resources, Australia—Record* **1968/75** (unpublished).

JACKSON, M. J., 1970—Engineering geology of the Tuggeranong West urban development area, ACT. *Bureau of Mineral Resources, Australia—Record* **1970/68** (unpublished).

MENDUM, J. R., 1975—Geological investigation of Tuggeranong damsite, Murrumbidgee River, ACT, 1968. *Bureau of Mineral Resources, Australia—Record* **1975/38** (unpublished).

PETTIFER, G. R., 1974—Tuggeranong urban development area, seismic reflection and resistivity surveys, ACT, 1971-2. *Bureau of Mineral Resources, Australia—Record* **1974/3** (unpublished).

PURCELL, D. C., & GOLDSMITH, R., 1975—Tuggeranong town centre water feature, ACT: preliminary geological investigations, 1973-5. *Bureau of Mineral Resources, Australia—Record* **1975/55** (unpublished).

ROSSITER, A. G., 1971—Preliminary notes on the geology of the Village Creek area. *Bureau of Mineral Resources, Australia—Record* **1971/11** (unpublished).

VANDEN BROEK, P. H., 1973—Engineering geology of Tuggeranong town centre, stage 1, ACT. *Bureau of Mineral Resources, Australia—Record* **1973/100** (unpublished).

VANDEN BROEK, P. H., 1974—Engineering geology of Tuggeranong town centre, ACT. *Bureau of Mineral Resources, Australia—Record* **1974/184** (unpublished).

VAN DIJK, D. C., 1959—Soil features in relation to erosional history in the vicinity of Canberra. *CSIRO—Soil Publication* **13.**

WESTERMAN, H. L., 1973—Engineering the environment—the present state of urban planning. *Institute of Engineers of Australia—Publication* **73/2**, 24-31.

Numerical techniques applied to the geochemistry of some estuarine sediments from Broad Sound, Queensland

Wayne Mayo

Q-mode factor analysis classified the estuarine samples from Broad Sound into two main geologically distinct groups representing intertidal and supratidal deposition. This classification was supported statistically by stepwise discriminant analysis, and mathematically by Q-technique canonical correlation analysis. Analysis of variance was useful in identifying significant error with some of the measured variables, and proving the stability of the pH and Eh readings over time.

Using R-mode factor analysis, with the associated correlation coefficients, and stepwise regression analysis, the various processes controlling the concentration of P_2O_5, Cu, Pb and Zn, in the supratidal and intertidal sediments are identified. Although Cu, Pb, and Zn are mainly deposited in both supratidal and intertidal zones adsorbed onto iron hydroxide colloids, the three trace elements (but especially Pb) are released with decreasing pH and Eh in the intertidal zone and form metal sulphides or metallo-organic complexes. The reduced iron is also redeposited as iron sulphide. Under supratidal oxidizing conditions the Cu and Zn remain attached to the iron colloids but Pb is released with increasing acidity.

The absorption of P_2O_5 on clay particles increases with acidity in the intertidal zone, but P_2O_5 is mainly associated with organic carbon in the supratidal sediments.

Introduction

Broad Sound is an estuarine complex on the sub-tropical central Queensland coast. The estuarine water is vertically mixed, with no evidence of salinity stratification—resulting from a combination of shallow water, vigorous wave activity, and a tidal range of up to 10 m. The average annual rainfall and evaporation in the region are approximately 100 cm and 170 cm respectively, most of the rainfall occurring from December to March. Consequently, runoff from the catchment into Broad Sound is negligible for most of the year.

As part of a general study of the sedimentology and geochemistry of Holocene sediments at Broad Sound (Cook & Mayo, in prep.) a set of samples was collected in 1971 with the specific aim of determining the geological processes controlling the concentrations of P_2O_5, Cu, Pb, and Zn. Samples were collected from the open intertidal, mangrove swamp and supratidal flat environments.

Variables which reflect important sedimentary processes and represent the different sediment fractions were measured on these sediments; these were pH, Eh, grainsize mean and standard deviation, carbonate carbon, organic carbon, and iron. The data were analysed using a series of mathematical and statistical techniques to (1) classify the sediments into separate groups reflecting a distinct set of geological processes, (2) carry out detailed error analysis of the data, and (3) determine the interrelations between the variables within each classified group of samples, so that the processes controlling the concentrations of the above trace elements could be identified.

Deposition environments

Of the three depositional environments sampled within the Broad Sound estuarine complex, the open intertidal environment lies within the intertidal zone (within the normal tidal range) and includes three sedimentary facies: the gravel facies, which is predominantly relict (Cook & Mayo, in press); the sand facies, forming extensive sand sheets and ridges; and the mud facies, which is adjacent to the mangrove swamp environment. The boundary of the mud facies and the mangrove swamp marks the upper limit of the open intertidal environment.

The mangrove swamp environment extends from the upper part of the intertidal zone into the supratidal zone (above the normal high-tide level, but inundated by spring tides about once a month) and consists predominantly of mud. Intertidal channels extend through the mangrove swamp to the supratidal mudflats and again mud is dominant in these channels. The supratidal flat environment lies between coastal grassland and the mangrove swamp environment. The sediment deposited in this environment is mainly mud with generally a higher proportion of clay than the mangrove swamp sediment.

Sampling

Nine east-west lines intersecting the intertidal-supratidal boundary of the Herbert Creek estuary were randomly selected (Fig. 1). Twenty-seven sampling localities were specified by randomly selecting one position in the open intertidal, mangrove swamp and supratidal mudflat environments along each of these lines (and one additional open intertidal locality was selected on one of these lines (Fig. 1)). This sampling strategy gave 8 open intertidal (6 mud, 1 gravel and 1 sand), 9 mangrove swamp (7 supratidal and 2 intertidal) and 7 supratidal flat sampling localities, as well as two sampling localities in intertidal mangrove channels cutting through the supratidal zone. In addition, the sediment at two of the localities sampled represented mangrove deposits buried beneath supratidal flat deposits. Three samples were taken at every locality to enable detailed error analysis of the data.

Samples in the intertidal zone were collected at the surface; and the supratidal zone samples were collected 20-25 cm below the surface, where the sediment was always sufficiently moist for Eh and pH readings to be taken. Repeat pH and Eh readings were taken over a 9-hour period in the intertidal zone, and a period of a month in the supratidal zone, to test for the required stability over time of the pH and Eh readings at these depths in the two zones.

Analytical techniques

The grainsize mean and standard deviation parameters (statistical moment measures) were determined by sieving the gravel fraction (> 2 mm), using a settling tube with the sand fraction, and pipetting the mud (< .063 mm) to 9 phi; any mud remaining was extrapolated to 14 phi. Organic carbon was determined using the method described by Bush (1970). The Bush method was found to be unreliable for carbonate carbon, and this was determined at the Australian Mineral Development Laboratories (AMDEL) using gravimetric analysis. AMDEL also determined Cu, Pb, Zn

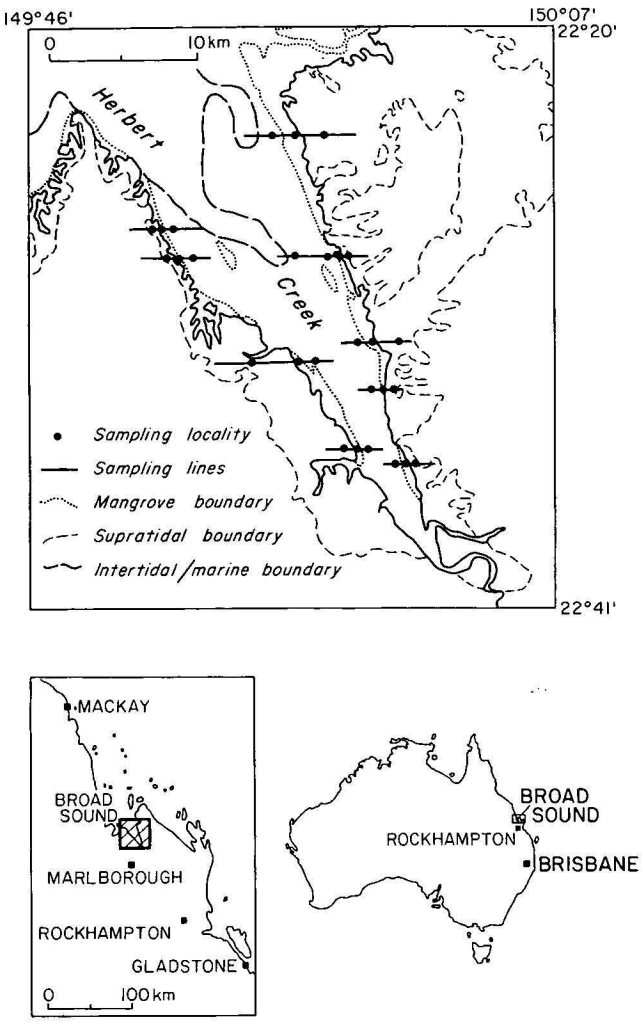

Figure 1. Locality maps, showing sample positions

and Fe using atomic absorption spectrophotometry, and P_2O_5 using the molybdenum blue colorimetric method.

The variables pH and Eh were measured using combined electrodes with a portable Metrohm meter; the electrodes were pushed 1 to 2 cm into the sediment at the depth of sampling. Despite calibration of the meter for pH readings and a check on a standard Eh solution (the Eh reading varied from 270 to 290 mV during the study using a solution with a known value of 267 mV), the accuracy of the readings may be affected by direct contact with sediment particles. Cook (1973) discusses this when comparing *in situ* pH and Eh readings with those measured on extracted pore fluids. Nevertheless, even though the absolute values may not be accurate, relative differences are expected to be meaningful.

Three values for each of the eleven variables were obtained on one sample from five of the sampling localities so that any significant analytical error associated with the variables measured could be detected.

Computer programs

GRSIZE (Mayo, 1972) was used to analyse the grainsize results and ANOVA 1 (Mayo & Long, in prep.) carried out the one-way analysis of variance for error analysis. The three programs, CABFAC (Klovan & Imbrie, 1971), BMD07M (Dixon, 1971) and CLUSTER (Bonham-Carter, 1967) were used to classify the samples with Q-mode factor analysis, stepwise discriminant analysis (as well as Q-technique canonical correlation), and Q-mode cluster analysis respectively. BMD03M (R-mode factor analysis), BMD02R (stepwise regression analysis) and BMD06M (R-technique canonical correlation), all originally documented by Dixon (1971), were employed in unravelling the interrelations between the variables within each group of classified samples.

Documentations of the above programs together with interpretative details for geological data are given by Mayo & Long (in prep.). This paper demonstrates the practical use of the above techniques and additional discussions of the application of these techniques to geological problems are given in Mayo (in prep.).

Except for the error analysis, where values from individual samples are used, the numerical techniques use values representing each locality. These values are obtained by averaging the three sample values of each variable at each locality.

Percent of range transformation is used with the Q-mode factor and cluster analyses so that each variable has an equal weighting. This transformation of the data is also used with the R-technique canonical correlation so that the algebraic size of the canonical coefficients can be compared.

Numerical sample classification

Q-mode factor analysis classification

The first three varimax factors from the Q-mode factor analysis (Manson & Imbrie, 1964) explain 95.0 percent of the variation in the 11 variables measured on each of the 28 samples. The inclusion of an extra factor only increases the amount of variance explained by 1.43 percent and does not change the important variables (indicated by the factor scores in Table 1) in the analysis. Therefore, assuming each factor represents a set of distinct geological processes, three factors adequately represent all the geological processes affecting these samples.

The relative effect of these factors on each sample is shown in Figure 2, which is a triangular plot of the three varimax factor loadings for each sample, normalized so that the loadings sum to 1.0. This triangular plot gives a true spatial representation of the relation between all the samples as there are no loadings of opposite sign in each of the factors (Table 1) and the communality (sum of squares of the factor loadings) for each sample is high, except for

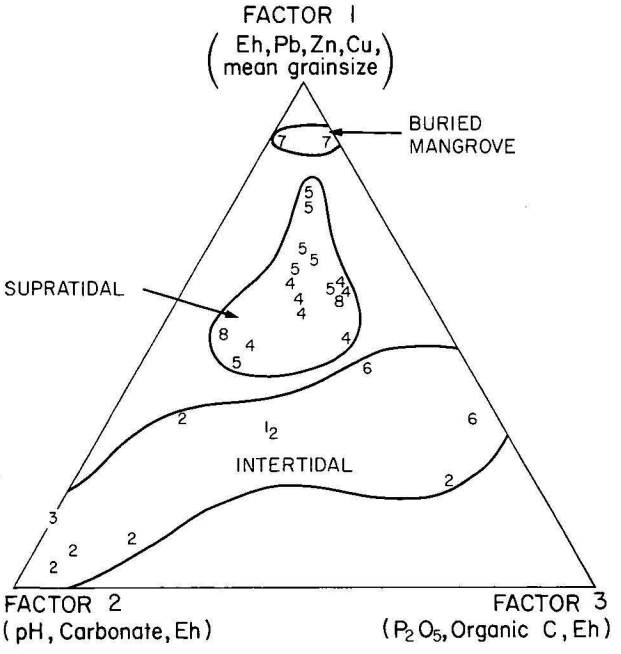

Figure 2. Triangular plot of three normalized factor loadings from the Q-mode factor analysis

Normalized varimax factor loadings					
Locality Number	*Environment (Fig. 2)*	*Communality*	*1*	*2*	*3*
002	6	.9700	.3318	—.0427	.6236
003	2	.9218	.1926	—.1528	.6546
005	6	.9807	.4290	—.1774	.3936
011	2	.9702	.0902	—.7514	.1584
017	2	.9570	.3009	—.4062	.2930
018	1	.6702	.3041	—.4073	.2885
023	2	.9872	.0657	—.8658	.0685
025	2	.9559	.3371	—.5459	.1170
026	2	.9822	.0348	—.9159	.0492
028	3	.8873	.1267	—.8732	.0001
001	5	.9684	.5914	—.1533	.2552
004	5	.9792	.6699	—.1719	.1582
006	5	.9523	.7744	—.1122	.1134
007	8	.9797	.5673	—.1582	.2746
008	4	.9873	.6051	—.2207	.1741
009	5	.9865	.6452	—.1638	.1911
010	5	.9647	.7624	—.1149	.1227
012	4	.9935	.4719	—.3594	.1687
013	4	.9580	.5493	—.2283	.2223
016	4	.9687	.5990	—.1437	.2573
019	8	.9154	.4954	—.3935	.1110
020	4	.9619	.4893	—.1730	.3377
021	5	.9922	.6276	—.2058	.1666
022	4	.9706	.5895	—.1454	.2651
024	5	.9549	.4413	—.3975	.1611
027	4	.9848	.5685	—.2251	.2064
014	7	.9276	.8833	—.0114	.1053
015	7	.8684	.8787	—.1098	.0114
Scaled varimax factor scores					
Grainsize { *Mean*		1	1.081	—.450	.561
Grainsize { *St. Dev*		2	.859	—.264	.616
P_2O_5		3	—.112	—.316	1.696
pH		4	—.090	—2.175	.580
Eh		5	1.809	—1.509	—1.514
Organic C		6	.085	.352	1.643
Carbonate		7	—.960	—1.737	.828
Cu		8	1.151	.398	.890
Pb		9	1.247	.400	.487
Zn		10	1.233	.379	.501
Fe		11	.688	.129	.367

Table 1. Normalized factor loadings and scaled factor scores from the Q-mode factor analysis

sample 018. The communality reflects the amount of representation by the factors of each variable with a maximum value of 1.0 for complete representation, and is used to normalize the factor loadings. Therefore, the communality values in Table 1 indicate that the three normalized factors represent each sample well, except for 018 which has about 33 percent of the information from the measured variables unrepresented in the triangular plot.

Three separate sample groups are apparent in Figure 2. The major subdivision reflects the different depositional conditions in the intertidal and supratidal zones, with the 10 samples from the intertidal zone and 14 from the supratidal zone being grouped separately. The two mangrove channel samples also plotted with the supratidal group, indicating the sediment in these channels is probably derived from the surrounding supratidal deposits. The two buried mangrove samples plotted separately as a third minor group. Because of the lack of true representation of sample 018 in the classification plot (Fig. 2), this sample (the only intertidal gravel sample) will be removed when the results of the intertidal group are analysed.

Geological interpretation of factor analysis classification

The geological interpretations of the three factors which affect this sample classification are aided by the factor scores (Table 1). These factor scores indicate the variables which are important contributors to each of the factors. The variables with an absolute factor score value greater than 1.0 were taken as the important variables for each factor and these variables are shown in Figure 2 with the corresponding factor. Interpretations from these factor scores are further aided by the comparison of the mean values of the variables between the three sample groups (Table 2).

Finer grainsize, with associated higher Cu, Pb, Zn and Fe, and lower carbonate, distinguish the supratidal group from the intertidal samples. The differing grainsize of the intertidal and supratidal sediments is shown in Figure 3 using the grainsize frequency distribution of a typical sample from each group. In addition, slightly acid and oxidizing conditions in the supratidal zone contrast with the alkaline and reducing conditions in the intertidal deposits (assuming absolute values are meaningful). The buried mangrove samples are separated from the supratidal group because of lower pH, P_2O_5, and carbonate; and higher grainsize standard deviation.

The extremely low average pH values of the buried mangrove samples (Table 2)—the lowest pH value measured being 3.5—were considered too low to be due to organic acids and are probably due to oxidation of Fe sulphide, originally deposited under the intertidal reducing conditions (Table 2) to form sulphuric acid. This reaction which follows an increase in Eh and is catalyzed biologically in the sediment, is considered by Krauskopf (1967) to approximate to

$$2FeS_2 + 15/2O_2 + 4H_2O \longrightarrow Fe_2O_3 + 4SO_4^{2-} + 8H^+$$

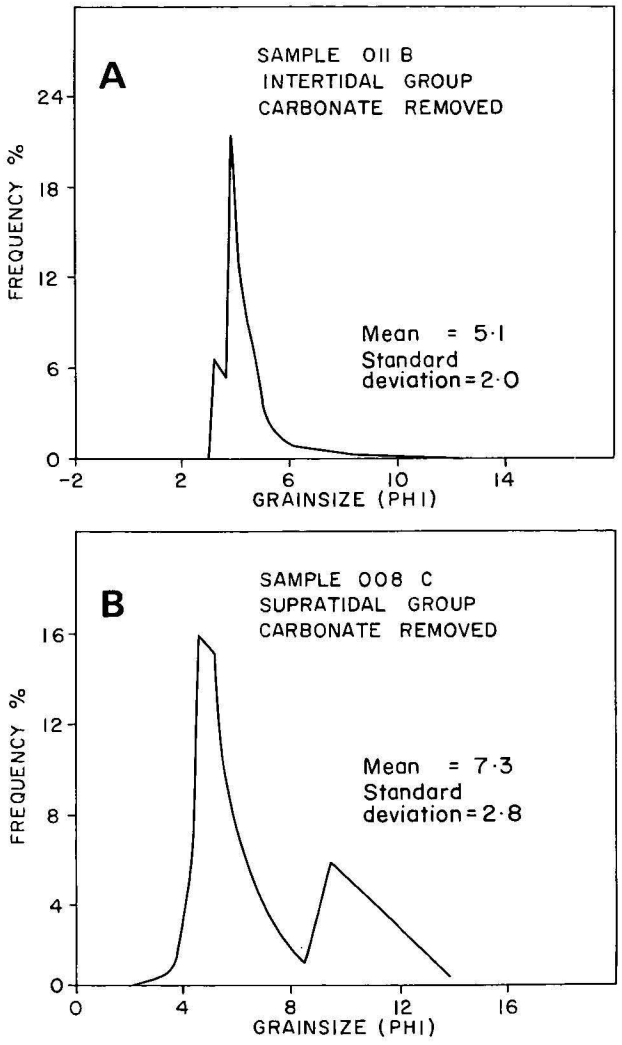

Figure 3. Typical grainsize frequency distributions for the intertidal and supratidal groups

VARIABLES		*CLASSIFIED GROUP (Number of samples)*		
		Intertidal (9)	*Supratidal (16)*	*Buried Mangrove (2)*
Grainsize	*Mean (phi)*	5.60* (1.45)	7.59 (.728)	7.21 (1.56)
	Standard deviation (phi units)	2.15 (.775)	2.53** (.201)	3.20 (.609)
	P_2O_5 (ppm)	632* (129)	761** (172)	400 (4.71)
	pH	7.30* (.494)	6.99** (.208)	4.39 (.260)
	Eh (mV)	—27.4* (220)	250** (19.2)	307 (18.9)
	Organic C (%)	.833 (.676)	.882 (.212)	.934 (.655)
	Carbonate (%)	31.7* (16.7)	12.8** (6.5)	.18 (.061)
	Cu (ppm)	8.26* (4.53)	13.6 (2.78)	11.7 (5.19)
	Pb (ppm)	8.91* (3.77)	15.5 (4.56)	17.0 (7.07)
	Zn (ppm)	24.5* (13.2)	51.3 (9.34)	42.2 (14.8)
	Fe (%)	1.36* (.772)	2.85 (.491)	2.38 (.401)

Table 2. Mean and Standard deviation values of the variables in each sample group

The standard deviation values are in parentheses. * Significant difference between the intertidal and supratidal groups. ** Significant difference between the buried mangrove and supratidal groups. Tests are of the difference between the means using a one-sided Student's t test at the 95% level (Hoel, 1962) but any differences between the sample variances are ignored.

With the regressive accumulation of sediments along the Herbert Creek shoreline (Burgis, 1972), the intertidal mangrove reducing conditions under which these samples were deposited reverted to oxidizing supratidal conditions causing this change from sulphide to sulphate. Observed Fe oxide pseudomorphs after mangrove-organic material present in the sand fraction of the buried mangrove samples supports this suggested cause of the pH reduction. The low P_2O_5 values of these buried mangrove samples (Table 2) indicate that processes favouring the adsorption of phosphate by clays under low pH conditions (Stumm & Morgan, 1970) are not dominant within these sediments.

Summarizing, Q-mode factor analysis classifies the estuarine samples into three groups, representing intertidal depositional conditions, supratidal depositional conditions and a change from intertidal to supratidal environmental conditions.

Statistical and mathematical check of factor analysis classification

Factor analysis has no supporting statistical theory, and multiple discriminant analysis (Anderson, 1958) was used to test the factor analysis sample classification statistically. Discriminant analysis tests for differences between previously classified sample groups, so the three groups from the factor analysis were used in the analysis (and with the same 11 variables). The assumption of normality of variables in the discriminant analysis could not be tested owing to the small number of samples.

The matrix of F distribution values used to test for differences between each pair of sample groups is shown in Table 3. As all these values are greater than the 99.5 percent critical value for the F distribution with (3, 23) degrees of freedom (5.58), each of the sample groups is significantly different from the others. Therefore, the factor analysis classification is supported statistically by the multiple discriminant analysis. This classification was also tested statistically by using the Mahalanobis Generalized Distance, D^2, which is a measure of the distance between two points within any number of dimensions. By determining the D^2 of each individual sample from each of the three groups (Dixon, 1970) and using this as a chi-square variable, each individual sample may be classified statistically into the appropriate group. The results of this theoretical classification are shown in Table 3, and again the factor analysis classification is corroborated as each individual sample is classified as in the original factor analysis grouping.

Q-technique canonical correlation analysis (Rao, 1952; Lee, 1969) was also applied to the original Q-mode factor analysis sample classification. The two canonical vectors, corresponding to the two canonical correlations, explain

(a) *F distribution values from the stepwise discriminant analysis (3, 23 degrees of freedom)*

	Intertidal	*Supratidal*
Supratidal	50.22	
Buried Mangrove	130.64	99.97

F(3, 23) at the 99.5% level = 5.58

(b) *Mahalanobis' Generalized Distance theoretical sample classification*
Number of samples classified into each group:

GROUP	*Intertidal*	*Supratidal*	*Buried Mangrove*
Intertidal	10	0	0
Supratidal	0	16	0
Buried Mangrove	0	0	2

(c) *Q-Technique Canonical Correlation*

Eigenvalues

17.11	4.66	0.00

Cumulative proportion of total variance

.786	1.000	1.000

Canonical correlations

.972	.907	0.0

Table 3. Stepwise discriminant analysis and Q-technique canonical correlation results

100 percent of the total variance in the original data (Table 3) and therefore the plot of the first (and only) two canonical variables (Fig. 4) fully represents the configuration of the sample groups. As in Figure 2, samples from the three previously classified groups plot as distinct population in Figure 4.

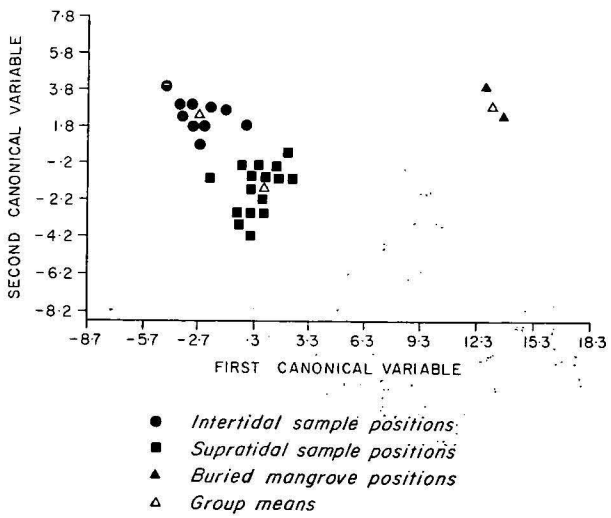

Figure 4. Plot of the two canonical variables from the Q-technique canonical correlation analysis

Therefore, both the stepwise discriminant analysis and the Q-technique canonical correlation analysis support the original Q-mode factor analysis. Although the discriminant and canonical correlation analysis require prior sample grouping they were able to confirm the differences between the sample groups classified by the factor analysis.

Q-mode cluster analysis may also be used for sample classification and does not require prior grouping of the samples. As a comparison with the factor analysis classification, a Q-mode cluster analysis was carried out using an unweighted group-average clustering strategy (Bonham-Carter, 1967) to produce a dendrogram from which the sample classification is determined. The dendrogram for the estuarine samples is given in Figure 5 with the environment of each sample, as well as the factor analysis group classification, indicated.

Except for the buried mangrove samples and two intertidal samples the sample grouping on Figure 5 agrees with that on Figure 2. These differences are probably due mainly to the less than two-dimensional representation of the relation between the samples in the dendrogram, compared to the three-directional (sample positions are determined by movement in three directions) representation with the Q-mode factor analysis triangular plot. In fact, the amount of information excluded from the dendrogram is not known—in contrast with the factor and canonical correlation analysis. It should also be noted that the split between the supratidal and intertidal groups cannot be obtained from the dendrogram by separating the clusters at one level of similarity.

In summary, the sample classification into three groups using the Q-mode factor analysis triangular plot was based on 95 percent of the available information and was supported by the Q-technique canonical correlation analysis, and corroborated statistically by the stepwise discriminant analysis. The interrelations between the variables within these separate sample groups may now be studied in detail. This effort spent on obtaining a meaningful sample classification was considered necessary to ensure that interrelations between the variables relate to distinct geological populations (as represented by the classified sample groups) and do not simply reflect differences between the populations.

The geological reasons for the separate classification of the buried mangrove group have been discussed above. As only two samples represent this group, the following discussions will concentrate on the intertidal and supratidal groups.

Error analysis

One-way analysis of variance (Ehrenfeld & Littauer, 1964) tests several means of a variable simultaneously. When used for error analysis, no significant difference between groups of values measured on repeat samples indicates that the variation within localities masks that between localities; similarly, no significant difference between groups of repeat analyses on individual samples indicates that the analytical error is greater than the variations between localities.

Table 4 lists the final F distribution values from the one-way analysis of variance of the triplicate sampling at each locality for both the intertidal and supratidal groups, and of the triplicate analytical results on one sample from five different localities. An F-value greater than the selected critical value (generally the 95 percent value) indicates significant difference between the groups of repeat values and suggests no significant error. No significant analytical error was apparent for each of the 11 variables measured on the estuarine samples.

The repeat sampling results for both the supratidal and intertidal groups show that the grainsize mean and standard deviation values for the supratidal sediments do not vary significantly throughout those sediments when compared to the local variation of these two variables. All other variables do vary significantly within both groups of sediments. Because any interpretations based on the grainsize mean and standard deviation variables in the supratidal sediments would have to be made with reservation, the percentage of clay of the repeat samples was also tested using one-way analysis of variance. The F distribution value for the analysis of variance of the clay values was 2.91, indicating significant differences in the clay values between

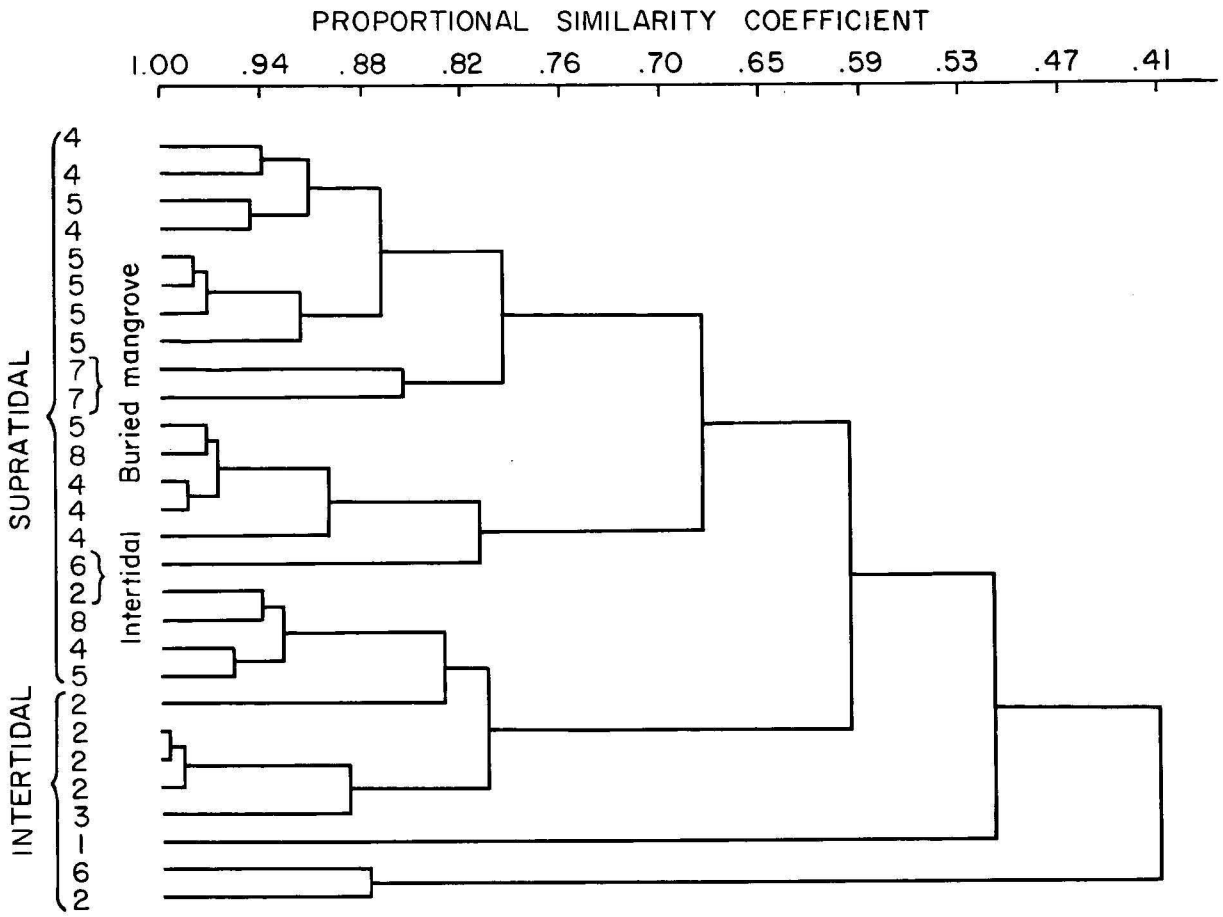

Figure 5. Q-mode cluster analysis dendogram

Variable		Total Error (triplicate sampling) Intertidal group F(9, 20)	Total Error (triplicate sampling) Supratidal group F(15, 32)	Analytical error (triplicate analysis) F(4, 10)
Grainsize	Mean	171.2	.74*	30.8
	Standard deviation	54.9	1.28*	101.5
P_2O_5		17.5	4.96	17.9
pH		34.7	4.73	368.1
Eh		26.8	2.01	73.8
Organic C		16.7	2.72	11.4
Carbonate		39.8	4.52	340.5
Cu		28.0	6.34	73.5
Pb		11.1	3.09	5.4
Zn		201.4	10.45	71.1
Fe		193.7	12.17	55.7
95% F-dist. critical value		2.39	1.99	3.48

Table 4. One-way analysis of variance results for total and analytical error. * For this variable the hypothesis of equality of means between the localities is accepted. This indicates significant total error with this variable.

localities in the supratidal sediments. Consequently, abundance of clay will be used instead of the grainsize mean and standard deviation variables, to represent the effects of grainsize when analysing the interrelations between the variables in the supratidal sediments.

Analysis of variance was also used to test whether the pH and Eh values were stable just below the sediment-water interface, in the intertidal zone and at the depth of sampling in the supratidal zone. Without stability between normal tides in the intertidal zone, and between spring tides in the supratidal zone, the pH and Eh values measured at the sampling localities could not be associated meaningfully with the other variables measured at these localities. To test this stability in the intertidal zone, triplicate pH and Eh values were taken every 1.5 hours over a 9 hour period in an intertidal mud locality enabling one-way analysis of variance to be used (Table 5). In the supratidal zone, triplicate pH and Eh values were taken at three sampling points at each of three sampling localities on three different days during a period of a month (one before a spring tide, and twice after). This repeat measuring strategy in the supratidal zone enabled two-way analysis of variance with specific day replication (Table 6) to be used to test the pH and Eh stability.

Table 5 shows that the pH values were stable in the intertidal zone, although a 99.5 percent confidence level was required. The Eh values were also stable at the 95 percent level, but the wide range of mean values of the groups of repeat readings indicates the even wider variation within the groups. The wide ranges of Eh values were in fact characteristic of the intertidal mud sediments rather than of all the intertidal deposits. Nevertheless, the results indicate that the pH and Eh values can be used as indicators of the diagenetic conditions in the intertidal sediments.

The rows and columns in the two-way analysis of variance table (Table 6) represent the three different sampling points at each locality and the three different localities respectively. The 'days' source of variance in Table 6 represents the measurement replication on the three days during the month period in the supratidal zone.

The results in Table 6 indicate that in the supratidal zone Eh values vary between sampling points at individual

This analysis is for pH
Test for equality of variances
Chi-square value with 5D.F is 2.665 (therefore, variances equal)
Analysis of variance table

Source of Variance	*Sum of squares*	*Degrees of freedom*	*Mean square*	*F(5, 12)*
Between Groups	.1474	5	.0295	5.44*
Within Groups	.0650	12	.0054	
Total	.2124	17		

* no significant difference at the 99.5%

Group	*Mean*
1	7.20
2	7.33
3	7.40
4	7.15
5	7.17
6	7.27

Least significant difference
L.S.D. for means = .0601* T-value (12.D.F.)
= .118 (95 PCT conf. and Large D.F.)

This analysis is for Eh
Test for equality of variances
Chi-square value with 5D.F. is 4.315 (therefore, variances equal)
Analysis of variance table

Source of Variance	*Sum of squares*	*Degrees of freedom*	*Mean square*	*F(5, 12)*
Between Groups	66027.7778	5	13205.5556	2.07*
Within Groups	76533.3333	12	6377.7778	
Total	142561.1111	17		

* no significant difference at the 95% level

Group	*Mean*
1	156.67
2	50.00
3	36.67
4	60.00
5	—50.00
6	30.00

L.S.D. for means = 65.2062* T-value (12.D.F.)
= 127.804 (95 PCT conf. and Large D.F.)

Notes:

1. Chi-square 95% critical value with 5 degrees of freedom = 11.07

2. F(5, 12) 95% critical value = 3.11
99.5% critical value = 6.07
(test for the equality of variance between the groups which is assumed in the analysis)

Table 5. One-way analysis of variance of pH and Eh values in the intertidal zone.

	pH values				*Eh values*			
Source of Variance	*Sum of Squares*	*Degrees of Freedom*	*Mean Square*	*F-value*	*Sum of Squares*	*Degrees of Freedom*	*Mean Square*	*F-value*
Rows (between samples)	3.44	2	1.718	120.5	5651.9	2	2826.0	11.92
Columns (between localities)	39.03	2	19.513	1368.3	13563.0	2	6781.5	28.61
Interaction (between rows and colums)	17.95	4	5.984	419.6	4503.7	4	1125.9	4.75*
Days	.012	2	.0059	.414*	140.7	2	70.4	.297*
Residual	.929	16	.0143		3792.6	16	237.0	
Total	60.654	26			27651.9	26		

Table 6. Two-way analysis of variance (with replication) of pH and Eh values in the supratidal zone.

*** no significant difference at the 99% level**

localities, and between localities, but that they are stable with time (i.e., the F-value for 'days' is less than the F distribution critical value). As the interaction effects between the rows and columns are significant in relation to the pH results (Table 6) the pH results are not conclusive but nevertheless suggest similar conclusions to those for the Eh results, especially concerning the stability of the readings with time.

Interrelations between variables within the intertidal and supratidal sediments

R-mode factor analysis (Davis, 1973), resulting in an oblique rotated factor matrix, was used to partition the variables into geologically associated groups. Empirical techniques described by Mayo (in prep.) were used to determine the 'ideal' number of mathematical factors to be rotated obliquely as well as the cut-off value for significance of the factor loadings. Four factors were obtained for each of the sample groups with significance levels of the loadings at .44 and .50 for the intertidal and supratidal matrices respectively. These mathematical factors, which may reflect geological processes, 'explain' 97.8 percent of the intertidal data variance and 85.9 percent of the variance of the supratidal sediment data.

Correlation coefficients were used to confirm the relations between the variables with significant loadings in each factor suggested by the sign of the factor loadings. For all tests of significance of the sample correlation coefficients, the normal distribution test (Hoel, 1964) was used at the 95 percent level with the hypothesis that the population correlation coefficient, ϱ, equals zero.

To clarify the associations obtained with the factor analysis, multiple stepwise regression (Draper & Smith, 1966) and R-technique canonical correlation (Cooley & Lohnes, 1971) were used. Regression analysis enables the influence several variables have on one particular variable to be studied whereas R-technique canonical correlation analysis can be used to study the relation between two sets of variables measured on the same samples. The chemical elements P (as P_2O_5), Cu, Pb and Zn were regressed on the remaining non-elemental variables and also on Fe, and were used as one set of variables opposed to the set of remaining variables in the canonical correlation analysis.

Intertidal sediments

The chemical elements in the intertidal sediments were partitioned into three of the four rotated R-mode factors. The variables with significant factor loadings in each of these factors are shown in Table 7 together with the corresponding regression analysis results. In these sediments, increasing phi grainsize values indicates increasing mud content as well as an increasing clay/silt ratio.

The iron control factor (Table 7) suggests that Cu and Zn are associated with Fe in the clay fraction of the sediments. This association could reflect the adsorbtion of Cu and Zn on the surface of iron-rich clays or on ferric hydroxide colloids deposited with the clay fraction. The dominance of Fe in the regression equations for Cu and Zn indicates that perhaps the ferric hydroxide colloidal adsorption is the main process reflected in this factor. Adsorption of trace elements on hydrous ferric oxides is certainly an important process for distributing these elements within sediments (Stumm & Morgan, 1970), and Goldberg (1954) noted that the levels of trace elements in the ocean sediments depend on the Fe or Mn content of the sediments. In addition, ferric hydroxide colloids may either be positively or negatively charged depending on the presence of excess H^+ or OH^- (Krauskopf, 1967), and in the alkaline estuarine environment would be expected to attract trace element cations.

In contrast, the diagenesis factor (Table 7) points to the concentration of Pb (in association with organic carbon in the fine-grained fraction of the sediments), with decreasing pH and Eh. It must be emphasised that all the correlation coefficients of Cu, Pb and Zn with both Fe and organic carbon are significant at the 95 percent level, but the factor analysis separated Pb into a separate factor because of the relatively low correlation of Pb with Fe and the relatively high correlation of Pb with organic carbon (Table 8). With

A. Fe Control factor

Mean grainsize, Cu, Zn, Fe/Carbonate
(Carbonate loading has opposite sign)

Relevant regressions:
Fe = Mean grainsize (79.9%), −carbonate (18.1%)
Cu = Fe (93.6%). Mean grainsize (3.4%),
—Grainsize standard deviation (1.5%)
Zn = Fe (92.6%),—pH (6.0%), Mean grainsize (0.9%)

B. pH Control Factor

P_2O_5
Relevant regression:
P_2O_5 = —pH (60.7%)

C. Diagenesis Factor

Mean grainsize (phi), Pb, Organic carbon/pH, Eh
(pH and Eh loadings have opposite sign to the other variables)

Relevant regression:
Pb = —Eh (90.7%),—Carbonate (4.5%)

Notes:
1. **Variables shown within one factor with significant loadings of the same sign are positively correlated (95% level) and those with opposite signs are negatively correlated (95% level). (Except for mean grainsize and carbonate in Factor A which are uncorrelated).**
2. **The dependent variable in each regression equation is shown to the left of the = and the independent variables (with the appropriate sign of the coefficient) to the right. The independent variables are entered using the appropriate F distribution value (Mayo & Long, in press) at the 95% level.**
3. **The percentage after each regression independent variable indicates its contribution in the prediction of the dependent variable.**

Table 7. Summary of the R-mode factor analysis and stepwise regression results for the intertidal sediments

increasing acidity and decreasing Eh, metal ions adsorbed to hydrous iron oxides would be released (Stumm & Morgan, 1970). Therefore, the diagenesis factor could be reflecting the subsequent formation of metallo-organic complexes with these released ions—with an emphasis on Pb ions—or alternatively the deposition of metal sulphides under aerobic conditions in the presence of organic material. The significant correlation of Fe and Eh (−.690),

(a) INTERTIDAL

	Cu	*Pb*	*Zn*	P_2O_5
Fe	.968	.763	.962	.615
Organic C	.831	.912	.837	.638
pH	—.854	—.895	—.941	—.779
Eh	—.854	—.952	—.800	—.453
Mean grainsize (phi)	.948	.733	.959	.773

The limiting absolute value for significance of the correlation coefficents at the 95% level (under Ho: ϱ = 0.0) is .664

(b) SUPRATIDAL

	Cu	*Pb*	*Zn*	P_2O_5
Fe	.829	.392	.884	.347
Organic C	.214	.297	.105	.501
pH	—.184	—.745	—.126	—.079
Eh	.314	.228	.476	.023
Clay	.583	.344	.653	.076

The limiting absolute value for significance of the correlation coefficients of the 95% level (Under Ho: ϱ = 0.0) is .496.

Table 8. Correlation coefficients within the intertidal and supratidal sediments

and of Fe and organic carbon (.748) also suggests the deposition of iron sulphides after the reduction of the iron hydroxides. This possibility was suggested earlier from the extremely low pH values measured in the buried intertidal mangrove sediments.

P_2O_5 represents the only significant loading in the pH control factor, which was so named because of the associated regression equation which reflects increasing concentration of P_2O_5 with increasing acidity. Increasing adsorption of phosphate on clay particles with decreasing pH has been noted in laboratory studies (Stumm & Morgan, 1970), where the maximum adsorption of phosphate on kaolinite, for example, occurred at a pH of about 3. Although this process was not confirmed by the P_2O_5 values in the buried mangrove samples, it could be operating within the intertidal sediments. This interpretation is supported by the correlation coefficients of P_2O_5 with mean grainsize and pH (Table 8), which have the largest absolute values when compared to the coefficients of the other variables with P_2O_5.

The R-technique canonical correlation results for the intertidal sediments (Table 9) show that the first canonical correlation is significant—using the chi-square test, which is made under the hypothesis that the two sets of variables are unrelated. The high redundancy values, reflecting how much each set of variables 'explains' the other set, indicate for this canonical correlation that the geological processes reflected in the independent set of variables (Set 2) are also controlling most of the changes in the chemical elements (Set 1). Despite this, the significant canonical coefficients (using a cut-off value of .40 for significance) only emphasise the relations between P_2O_5 and Zn in one set, and mean grainsize, pH, Eh and organic carbon in the other. With the intertidal results then, this canonical structure is not a substitute for the combination of factor analysis and regression analysis.

(a) Chi-square tests with successive canonical pairs removed (The first pair is removed first followed by the second)

No. of pairs Removed	*Chi-square value*	*Degrees of freedom*	*95 percent chi-square critical value*
0	64.67	28	41.3
1	6.89	18	28.9

Using this test only the first canonical correlation is significant:
Canonical correlation 1:1.000

(b) Redundancy Tests

Canonical correlation
Redundancy of set 1 given set 2 = .783
Redundancy of set 2 given set 1 = .696

(c) Canonical Coefficients

Canonical correlation 1

SET 1			*SET 2*	
Variable	*Coefficient*		*Variable*	*Coefficient*
P_2O_5	.428	*Grainsize*	*Mean*	.642
Cu	.200		*Standard deviation*	—.194
Pb	.012	*pH*		—.639
Zn	.448	*Eh*		.671
		Organic C		.533
		Carbonate		.000
		Fe		.000

Table 9. R-technique canonical correlation results for the intertidal sediments

Supratidal sediments

A summary of the three factors which include the chemical elements, together with the associated regression results, for the supratidal sediments is given in Table 10. P_2O_5 is associated with organic carbon and is probably adsorbed on the surface of fine-grained organic particles derived from the mangrove swamps. As shown by the regression summary in Table 10, organic carbon is a poor predictor of P_2O_5—other processes not reflected in the variables measured also influence the level of P_2O_5 in the supratidal sediments. Nevertheless, the relation between P_2O_5 and clay observed in the intertidal sediments is not evident in the supratidal sediments (Table 8); perhaps subaerial weathering and diagenesis at the depth of sampling have affected this association in the supratidal zone.

Under the oxidising conditions in the supratidal zone Cu and Zn remain adsorbed to hydrous ferric oxide colloids in contrast to the suggested release of these elements under intertidal conditions. The Fe control factor (Table 10) suggests the association of Cu and Zn with the clay fraction as well as the iron colloids, but, as in the intertidal zone, the regression results indicate the dominant process is sorbtion on iron hydroxides. The different relations between the trace elements and Eh in the intertidal and the supratidal sediments support the suggested contrasting geological processes in these two zones. Significant negative correlation coefficients between the trace elements (including Fe) and Eh reflect the suggested sulphide deposition (or organic carbon complexing) in the intertidal sediments. In contrast, Eh is included in the regression equation for Fe (Table 10) with a positive coefficient, and the correlation coefficients of the trace elements with Eh are positive (although not significant at the 95 percent level) with the supratidal results reflecting the suggested deposition of ferric hydroxides with adsorbed trace elements under oxidizing conditions.

A. Fe Control Factor

Clay, Cu, Zn, Fe
Relevant regressions:
Cu = Fe (68.7%)
Zn = Fe (78.1%)
Fe = Clay (41.9%), Eh (21.5%)

B. pH Control Factor

Organic carbon, Pb/pH
(pH loading has opposite sign)
Relevant regression:
Pb = —pH (55.5%), —Carbonate (13.4%)

C. Organic Carbon Control Factor

P_2O_5, Organic carbon, Carbonate
Relevant regression:
P_2O_5 = Organic carbon (25.1%)

Table 10. Summary of the R-mode factor analysis and stepwise regression results for the supratidal sediments

Notes:
The note accompanying Table 7 also apply to this table except that, (1) organic carbon and Pb in Factor B are not significantly correlated; (2) organic carbon and pH in Factor B are negatively correlated at the 90% level; (3) organic carbon and carbonate in Factor C are not significantly correlated; and (4) P_2O_5 and carbonate in Factor C are positively correlated at the 90% level.

Despite the inclusion of organic carbon with Pb in the pH control factor (Table 10), there is no significant correlation between organic carbon and Pb (Table 8), and those two variables are included in the same factor because of their negative correlation with pH. The regression equation for pH (Table 10) also shows that increasing concentrations of Pb in the supratidal deposits depend mainly on increasing

(a) Chi-square tests with successive canonical pairs removed (the first pair is removed first followed by the second and so on)

No. of pairs removed	*Chi-square value*	*Degrees of freedom*	*95 percent chi-square critical value*
0	66.28	28	41.3
1	36.80	18	28.9
2	15.41	10	18.3
3	6.36	4	9.5

The first two canonical correlations are significant using this chi-square test:
Canonical correlation 1 : .981
Canonical correlation 2 : .952

(b) Redundancy Tests

Canonical correlation 1
Redundancy of Set 1 given Set 2 = .192
Redundancy of Set 2 given Set 1 = .093

Canonical correlation 2
Redundancy of Set 1 given Set 2 = .457
Redundancy of Set 2 given Set 1 = .245

(c) Canonical coefficients

SET 1		*Canonical Correlation*	*SET 2*	
Variable	*Coefficient*		*Variable*	*Coefficient*
P_2O_5	—.226		*Clay*	.232
Cu	.476		*pH*	—.329
Pb	.338		*Eh*	.139
Zn	.418		*Organic C*	—.056
			Carbonate	—.464
			Fe	.414

Table 11. R-technique canonical correlation results for the supratidal sediments

acidity. The lack of significant positive correlation between Pb and the other variables makes interpretation of the geological process controlling the Pb concentration difficult. Perhaps the Pb ions are preferentially released from the iron oxides under acidic conditions, as was noted in the intertidal zone, but the process of local redeposition of the Pb is not clear.

The R-mode canonical structure (Table 11) also reflects these relations between the variables in the supratidal deposits. Although the first two canonical correlations were statistically significant using the chi-square test, the redundancy measures indicated that the second pair of canonical vectors were much more important for representing the relations between the two sets of variables (Table 11). The significant canonical coefficients (> .30) for the second canonical correlation emphasise the relation between both Cu and Zn, and Fe, as well as the relation between Pb, and pH and carbonate. Nevertheless, this canonical structure is really no substitute for the details obtained from the combination of factor and regression analyses.

Conclusions

Q-mode factor analysis was found to be useful for classifying the Broad Sound estuarine sediments into two main groups—the intertidal and the supratidal groups —each representing a distinct set of geological processes. Stepwise discriminant analysis supported this classification statistically, and Q-technique canonical correlation analysis confirmed it mathematically. Q-mode cluster analysis was not as useful as factor analysis for classifying this set of sediments.

One-way analysis of variance showed that there was no significant error in the analytical procedures for each variable measured on the sediments. This technique also indicated the need to replace the grainsize mean and standard deviation variables with the supratidal results by the clay variable because the former two grainsize parameters did not vary significantly throughout the supratidal sediments. Analysis of variance showed further that the pH and Eh values were stable over the daily tidal cycle in the intertidal zone, and over the monthly spring tidal cycle in the supratidal zone; thus enabling these two variables to be used with confidence in the analysis.

Using R-mode factor analysis together with the associated correlation coefficients and multiple stepwise regression results, interpretations of the dominant processes controlling P_2O_5, Cu, Pb and Zn within the supratidal and intertidal sediments were possible. The factor analysis partitioned associated sets of variables within the two sediment types, and the interrelations between the variables were clarified by the relevant correlation coefficients and regression equations. R-mode canonical correlation analysis was found not to be a substitute for the above numerical techniques.

The general increase in Cu, Pb, Zn, Fe, and organic carbon concentrations with increasing clay content and decreasing pH and Eh in the intertidal sediments, results in a set of significant correlation coefficients between most of these variables. Nevertheless, R-mode factor analysis grouped the chemical elements, enabling certain important geological processes to be isolated from the obviously complex set of interrelated processes affecting the sediments in the intertidal zone. This factor analysis and the corresponding regression analyses suggest intertidal deposition of ferric hydroxide colloids with attached Cu, Pb, and Zn as well as clay particles with adsorbed P_2O_5. With decreasing pH more P_2O_5 is adsorbed on the clay particles and with decreasing pH and Eh the metal ions are released and form metal sulphides or metallo-organic complexes. The formation of iron sulphides in the intertidal zone is also suggested by the very low pH values measured in the buried intertidal mangrove sediments which are assumed to have been deposited originally under reducing conditions, but are now subject to supratidal oxidizing conditions.

The association of P_2O_5 with organic carbon in the supratidal sediments is in contrast to the P_2O_5 association with clay particles in the intertidal zone, and the difference may be due to the diagenetic effects and the subaerial weathering in the supratidal zone. Although the processes controlling Pb concentrations in the supratidal sediments are not clear, Cu and Zn adsorption on ferric hydroxide colloids appears to be the main process controlling the concentrations of these two elements in the supratidal zone. When these colloids are deposited in the supratidal oxidizing conditions the redox reactions of the Cu, Zn and Fe observed in the intertidal zone do not occur.

Acknowledgement

The illustrations were drawn by the general draughting section of the geological drawing office, BMR. Mr C. Maddin's help in collecting samples and measuring pH and Eh values, often under very uncomfortable conditions, was greatly appreciated.

References

ANDERSON, T. W., 1958—INTRODUCTION TO MULTIVARIATE STATISTICAL ANALYSIS. *Wiley, New York.*

BONHAM-CARTER, G. F., 1967—FORTRAN IV program for Q-mode cluster analysis of non-quantitative data using IBM 7090/7094 computers. *Kansas Geological Survey—Computer Contribution* **4.**

BURGIS, W. A., 1972—Cainozoic history of the Peninsula east of Broad Sound, Queensland. *Bureau of Mineral Resources, Australia—Record* **172.**

BUSH, P. R., 1970—A rapid method for the determination of carbonate carbon and organic carbon. *Chemical Geology,* **6,** 59-62.

COOK, P. J., 1973—Supratidal environment and geochemistry of some recent dolomite concretions, Broad Sound, Queensland, Australia. *Journal of Sedimentary Petrology,* **43,** 998-1011.

COOK, P. J. & MAYO, W., in prep.—Sedimentology and Holocene history of a tropical estuary (Broad Sound, Queensland). *Bureau of Mineral Resources, Australia—Bulletin* **170.**

COOK, P. J. & MAYO, W., in prep.—Geochemistry of a tropical estuary (Broad Sound, Queensland). *Bureau of Mineral Resources, Australia—Bulletin* **170.**

COOLEY, W. W., & LOHNES, P. R., 1971—MULTIVARIATE DATA ANALYSIS. *Wiley, New York.*

DAVIS, J. C., 1973—STATISTICS AND DATA ANALYSIS IN GEOLOGY. *Wiley, New York.*

DIXON, W. J., Editor, 1971—BIOMEDICAL COMPUTER PROGRAMS. *University of California Press, Berkeley.*

DRAPER, N. R., & SMITH, H. 1966—APPLIED REGRESSION ANALYSIS. *Wiley, New York.*

EHRENFELDS, S., & LITTAUER, S., 1964—INTRODUCTION TO STATISTICAL MEASUREMENT. *McGraw-Hill, New York.*

GOLDBERG, E. D., 1954—Marine Geochemistry 1. Chemical Scavengers of the Sea. *Journal of Geology,* **62,** 249-265.

HOEL, P. G., 1964—INTRODUCTION TO MATHEMATICAL STATISTICS. *Wiley, New York.*

KLOVAN, J. E., & IMBRIE, J., 1971—An algorithm and Fortran IV program for large-scale Q-mode factor analysis and calculation of factor scores. *Mathematical Geology,* **3,** 61-68.

KRAUSKOPF, K. B., 1967—INTRODUCTION TO GEOCHEMISTRY. *McGraw-Hill, New York.*

LEE, P. J., 1969—Fortran IV programs for canonical correlation and canonical trend-surface analysis. *Kansas Geological Survey, Computer Contribution* **32.**

MANSON, V., & IMBRIE, J., 1964—Fortran program for factor and vector analysis of geological data using an IBM 7090 or 7094/1401 Computer System. *Kansas University—Special Publication* **13.**

MAYO, W., 1972—A computer program for calculating statistical parameters of grainsize distributions derived from various analytical methods. *Bureau of Mineral Resources Australia—Record* **1972/140** (unpublished).

MAYO, W., in prep.—The application of numerical techniques. *In* COOK, P. J. & MAYO, W. Geochemistry of a tropical estuary (Broad Sound, Queensland). *Bureau of Mineral Resources, Australia—Bulletin* **170.**

MAYO, W., & LONG, K. A., in prep.—Documentation of BMR Geological Branch Computer Programs. *Bureau of Mineral Resources, Australia—Report.*

RAO, C. R., 1952—ADVANCED STATISTICAL MODELS IN BIOMETRIC RESEARCH. *Wiley, New York.*

STUMM, W., & MORGAN, J. J., 1970—AQUATIC CHEMISTRY. *Wiley, New York.*

Mesozoic outcrops on the lower continental slope off Exmouth, Western Australia

N. F. Exon and J. B. Willcox

Seismic reflection profiles over the southwestern margin of the Exmouth Plateau, which have been tentatively tied to the Northwest Shelf stratigraphic sequence, indicate that rocks of probable Permian to Early Tertiary age form bedrock on the lower continental slope and probably crop out in places. Water depths range from 1400 to 4000 m. It is surmised that the rocks present include pre-Late Jurassic fluvial, deltaic and shallow marine sandstone, siltstone and shale; Late Jurassic to Neocomian deltaic sandstone, siltstone and shale; mid Cretaceous shallow marine shale; Late Cretaceous shelf limestone and Cainozoic foraminiferal ooze.

The Exmouth Plateau is cut by normal faults which are predominantly downthrown oceanwards and trend north-northeasterly across most of the area, except near the southwestern margin where they trend northwesterly. Faulting occurred primarily in the Middle to Late Jurassic and led to formation of the northwestern and northern margins by seafloor spreading. A major anticline, which parallels the southwestern margin, has one limb truncated by the lower continental slope, probably resulting in older rocks cropping out in places. Deep Sea Drilling Project results on the Cuvier Abyssal Plain indicate that the southwestern margin formed in the Late Cretaceous, either as a transcurrent fault associated with seafloor spreading or by collapse along normal faults.

Sampling of outcrops along the southwestern margin would enable the sequence to be dated more reliably and this would permit the theories of geological evolution and favourable petroleum potential of the Exmouth Plateau to be tested.

Seismic reflection profiles on the Exmouth Plateau and adjacent areas off Western Australia (Fig. 1) show that rocks of varying ages form bedrock along the southwestern margin of the Plateau (Fig. 2), where water depths exceed 1400 m (Exon, Willcox & Petkovic, 1975). This paper documents these occurrences and discusses their significance and their geological setting within the Exmouth Plateau area.

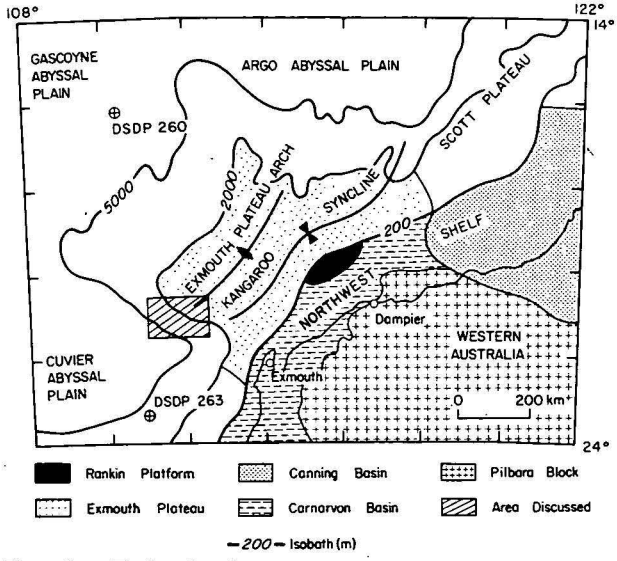

Figure 1. Regional setting

The seismic profiles were obtained as part of contract surveys conducted for the Bureau of Mineral Resources (BMR Continental Margin Survey, 1970-73) and Esso Exploration Ltd. (Indian Ocean, Offshore Western Australia E71A Survey, 1972). Their location is plotted in Figure 3, and typical profiles are illustrated in Figures 4 and 5. These data, together with seismic profiles recorded by Gulf Research and Development Company (Gulfrex Survey, 1973) and Shell Development (Australia) Pty Ltd (Petrel Survey, 1971), have been used to provide tentative ties between the Exmouth Plateau and the Northwest Shelf (Exon *et al.*, 1975).

Distribution of bedrock

Bedrock, which probably ranges from Permian to Early Tertiary in age, is distributed over 10 000 km² of the southwestern margin of the Exmouth Plateau. It is mapped in Figure 2, which also shows bathymetry. The location of the seismic profiles from which all the information has been derived is shown in Figure 3. The navigation during the seismic surveys was imprecise, with errors in position of up to 2 km. The depth of water above the bedrock ranges from 1400 to 4000 m, averaging about 2000 m.

The seismic profiles indicate that along the southwestern margin the older rocks have been folded into a marginal anticline, which parallels the lower continental slope, and are about 500 m above their regional level on the southwestern part of the Plateau. The lower continental slope truncates the southwestern limb of this anticline, so that the older rocks apparently crop out on the sea-bed (Figs. 3, 4, & 5). A veneer of Tertiary to Recent sediment may overlie the older rocks but it is not visible on the seismic profiles. In places it may have been stripped by gravity sliding and current action on the slope. The thickness of any sediment veneer cannot be determined from the existing profiles since the broad pulse generated by the seismic source has obliterated the structure of the uppermost 50 m of the sedimentary section. A zone of slumped sediments, which occurs on the lower part of the slope in water depths of about 3000 to 4800 m, obscures the deep structure in that area.

Evidence for age and lithology

Evidence for the age and lithology of the various units comes largely from an interpretation of seismic profiles extending across the Exmouth Plateau (Exon *et al.*, 1975) from the Northwest Shelf, 220 km distant, where the stratigraphic sequence and its structural characteristics have been described by Thomas & Smith (1974), and Powell (1976). The characteristics and ages of reflectors and seismic intervals reported in detail by Exon *et al.* (*op cit.*) are summarized in Tables 1 & 2. Only four of the seven major reflectors mapped on the Exmouth Plateau have been identified on its southwestern margin.

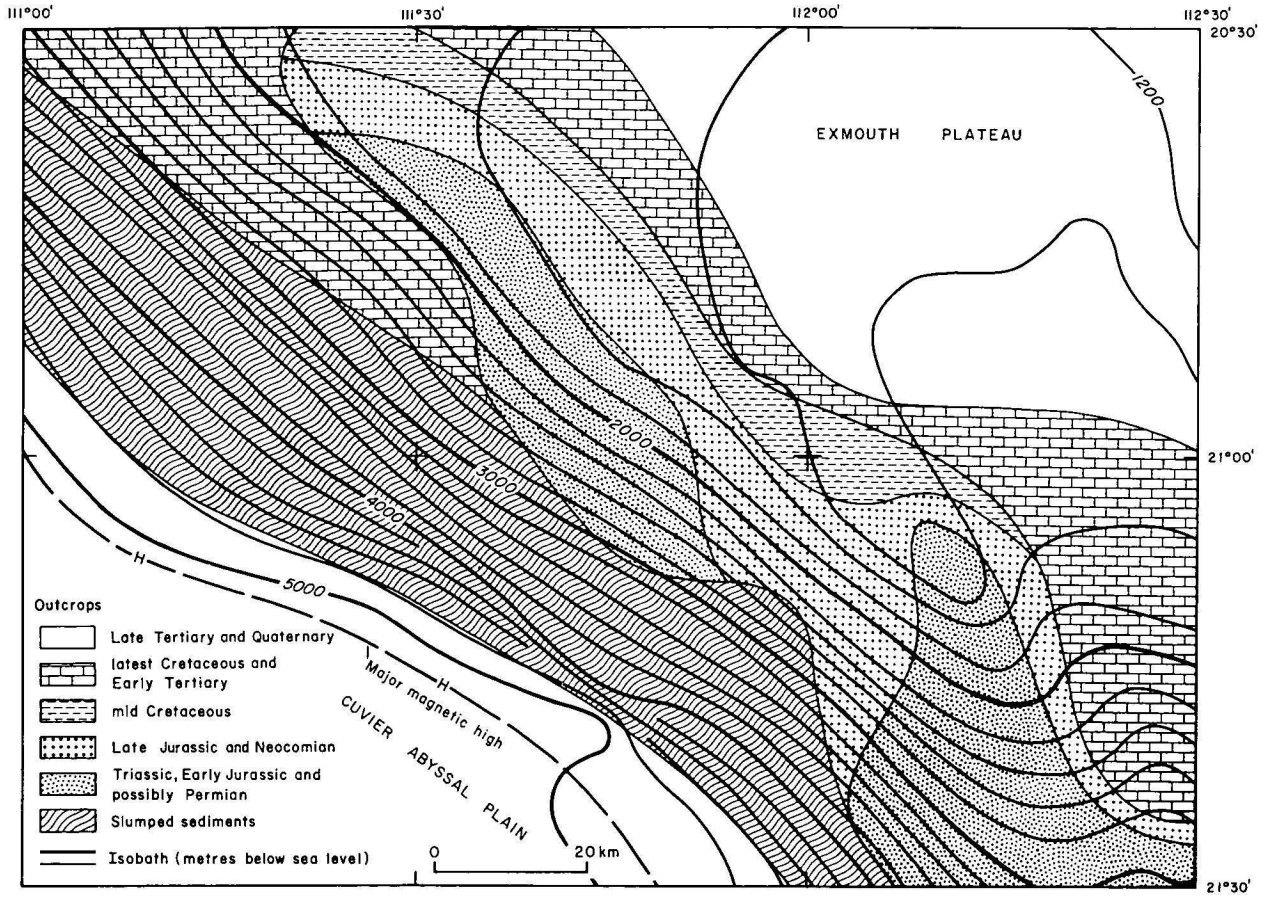

Figure 2. Outcrop and bathymetric map

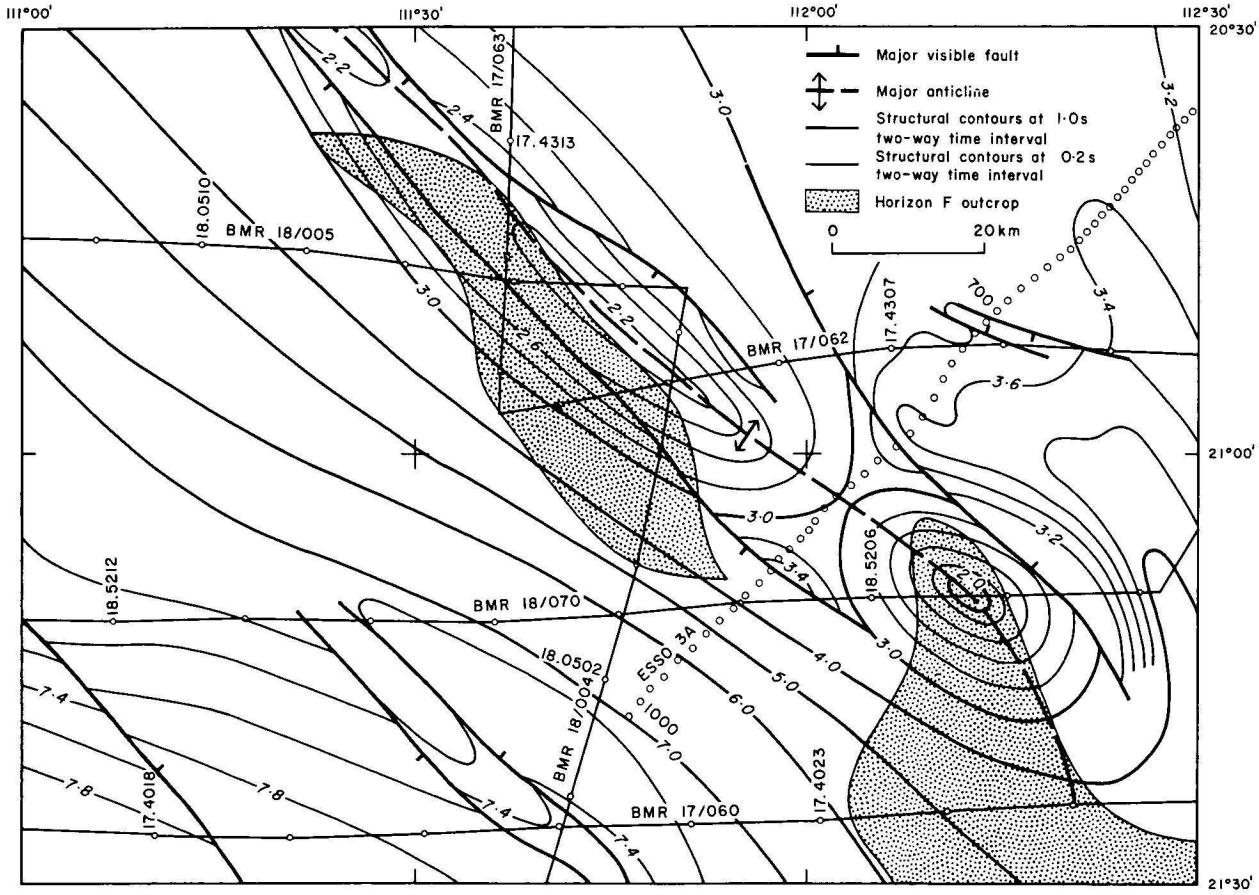

Figure 3. Structural contour map of Horizon F (showing location of tracks)

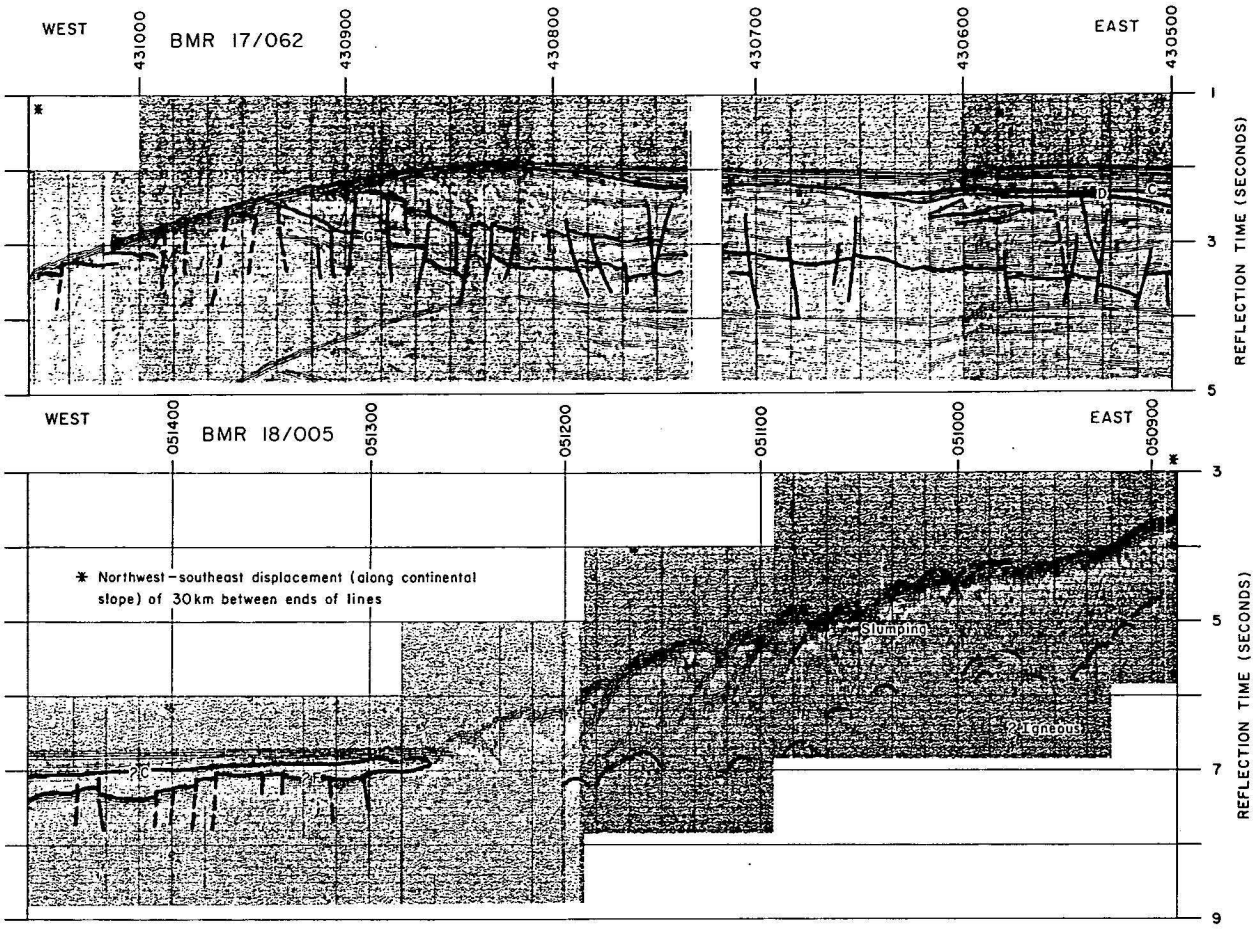

Figure 4. Seismic profile and interpretation: BMR 17/062 and 18/005

basis of the Deep Sea Drilling Project (DSDP) results for holes 260 and 263, Veevers, Heirtzler *et al.* (1974) and Exon *et al* (*op. cit.*) believe that the northern and northwestern margins of the Exmouth Plateau formed in the Late Jurassic (Callovian), and that the southwestern margin formed in the Late Cretaceous. Thus, it seems probable that at least some of the faults which affect the bedrock on the lower continental slope along the southwestern margin are of Cretaceous age, and are directly related to formation of that margin. It is also possible that major Cretaceous faults are obscured by the zone of slumped sediment and that the igneous bodies on BMR 17/060 are associated with faults of this age.

According to Veevers & Heirtzler (1974), and Exon *et al.* (*op. cit.*), the Exmouth Plateau was bounded by a landmass to the south and west until late Mesozoic times. During the Permian, Triassic and Jurassic, fluvial, deltaic and shallow marine detrital sediments were laid down over much of the Carnarvon Basin, including the Exmouth Plateau, and probably over the southwestern landmass. During the Middle to Late Jurassic a period of rifting gave rise to extensive systems of normal faults. In the Late Jurassic (Callovian) the landmass to the west drifted away northwestwards, and the northwestern and northern margins of the Exmouth Plateau were formed. Deltaic and shallow marine detrital sedimentation continued through into the Cretaceous. The southwestern margin and the embryonic Cuvier Abyssal Plain formed in the Late Cretaceous. The Exmouth Plateau itself subsided steadily from about this time and Late Cretaceous and Cainozoic carbonates were deposited upon it.

If the southwestern landmass was carried away to the northwest by seafloor spreading, as proposed by Veevers & Heirtzler, a relatively narrow strip of continental material must have been removed along transcurrent faults which bounded the southwestern margin of the Exmouth Plateau and the northeastern margin of the Wallaby Plateau. The presence of pre-Late Cretaceous sediments beneath the Cuvier Abyssal Plain is suggested by seismic horizons which have similar acoustic characteristics to Horizons C and F on the plateau, and is proven in DSDP 263 by shallow marine sediments overlying acoustic basement which are equivalent to the Winning Group (Table 2). Thus, it is possible that the eastern part of the Cuvier Abyssal Plain is floored by subsided continental crust, and that the southwestern margin of the Exmouth Plateau is structured by normal rather than transcurrent (or transform) faults.

Significance of outcrops

Seismic profiles connecting the virtually unsampled Exmouth Plateau with the extensively drilled and stratigraphically well-documented Rankin Platform of the Northwest Shelf (Fig. 1) have enabled Exon *et al.* (*op. cit.*) to make tentative correlations of the seismic intervals on the plateau with the shelf sequence. Because the crest of the plateau is 220 km from the Rankin Platform considerable doubts about the plateau geology must remain until stratigraphic drilling is undertaken. However, probable outcrops along the southwestern margin appear to correspond with much of the section seen on seismic profiles over the plateau, and are considerably closer to the plateau crest than is the Rankin Platform. Representative samples from

The unconformities bounding a number of the stratigraphic intervals retain their character from the continental shelf out onto the plateau. They are assumed to be roughly synchronous throughout their extent, except for the Horizon F unconformity, which may become slightly older westwards. This unconformity appears to define a rift-basin, which in a gross sense formed by sequential normal faulting from west to east, as a result of breakup of Gondwanaland in the Late Jurassic. This led to formation of the northern and northwestern margins of the Exmouth Plateau. The acoustic character of many of the seismic intervals varies little from shelf to plateau and this is interpreted to indicate similar lithologies in the two areas. The Mesozoic sequence of the Exmouth Plateau is probably similar to that in the adjacent part of the Carnarvon Basin.

Horizon	*Characteristics*	*Suggested age*
C	Strong reflector at base of well stratified zone. Mild angular unconformity	Late Cretaceous: Turonian and Coniacian hiatus.
D	Reflector marking the top of a zone of northerly prograding sediments.	Early Cretaceous: Late Neocomian.
F	Strong angular unconformity marking top of faulted blocks. top of faulted blocks.	Late Triassic to late Middle Jurassic.
G	A strong reflector which generally parallels Horizon F.	Permian or early Triassic.
Basement = I	Envelope of diffraction patterns	

Table 1. Seismic horizons

Geological setting

The Exmouth Plateau is underlain by up to 10 000 m of Phanerozoic strata, most of which have been extensively faulted and warped into a major arch and syncline, which lie 220 and 100 km respectively northwest of the Rankin Platform (Fig. 1). Seismic Horizons C and D generally parallel the seabed and are little disturbed, whereas Horizons F and G are affected by numerous antithetic faults which trend north-northeasterly over most of the area, except near the southwestern margin where the dominant trend is northwesterly.

The southwestern margin is formed by northwesterly-trending faults which have average individual throws of about 100 m (Figs. 4 & 5); there is a total downthrow of 2000 to 3000 m to the southwest. A large northwesterly-trending anticline (Fig. 3) lies just beyond the edge of the plateau proper, beneath the lower continental slope, and Horizons F and G are downthrown to both the northeast and southwest along numerous parallel normal faults within this structure. The anticline has two major culminations on Horizon F, at depths of 1400 and 1600 m, with respective closures of 700 and 600 m (assuming interval velocities shown in Table 3, derived in Exon *et al.*, 1975). In the southeast there is a syncline parallel to the anticline with its axis about 4400 m below sea level.

Horizon	*Sea level*	*Sea bed*	*C*	*D*	*F*	*G*	*I*
Velocity (m/s)	1500	2300	2500	3500	3500	4000	

Table 3. Seismic interval velocities

A zone of slumped sediment is interpreted on the deepest half of the lower continental slope (Fig. 2). On the seismic profiles it is characterized by numerous diffractions and generally by absence of bedding (Fig. 5), and may have been attributed to crystalline rocks if it were not for the relatively low amplitude, long wavelength, magnetic anomalies with which it is associated. The magnetic anomalies suggest a sediment thickness ranging from about 500 to 1500 m. The slumped sequence appears to be laterally continuous with undeformed Jurassic and Cretaceous sediments.

Igneous bodies, which penetrate the younger sedimentary section, are observed near the foot of the lower continental rise on line BMR 17/060 (for location see Fig. 3), and the deepest one of these is associated with a major magnetic high which extends northwestwards along the edge of the Cuvier Abyssal Plain (Fig. 2).

The acoustic characteristics of the sedimentary section beneath the Cuvier Abyssal Plain reveal similar structures to those on the plateau, with undisturbed sediments overlying normally faulted sediments. Assuming the interval velocities shown in Table 3, more than 1700 m of pre-Upper Jurassic sediments may be present, below 1000 m of younger material (Figs. 4 & 5).

On the Exmouth Plateau as a whole, the main episode of faulting, which gave rise to the north-northeasterly-trending faults, post-dates Horizon F and generally pre-dates most of the sediment within the interval D-F, indicating that it is of Middle to Late Jurassic age. On the southwestern margin, the northwesterly-trending faults appear to truncate the north-northeasterly-trending faults, although there is no obvious age difference from the seismic data. The similar ages for these two sets of faults is unexpected, since on the

Interval (see Fig. 2)	*Approximate thickness on SW margin (m)*	*Dominant sediment type (inferred)*	*Northwest Shelf equivalent*
Late Tertiary and Quaternary	200	Foraminiferal ooze	
Latest Cretaceous and Early Tertiary	500	Foraminiferal ooze resting on shelf limestone	Toolonga Calcilutite-Giralia Calcarenite
Mid Cretaceous	200	Shallow marine shale	Winning Group
Late Jurassic and Neocomian	1500	Deltaic sandstone, siltstone and shale	Dingo Claystone-Barrow Group
Triassic to Middle Jurassic, and possibly Permian	3000+	Fluvial, deltaic, and prodeltaic sandstone, siltstone and shale.	Locker Shale-Mungaroo Beds

Table 2. Mapped intervals and sediment types

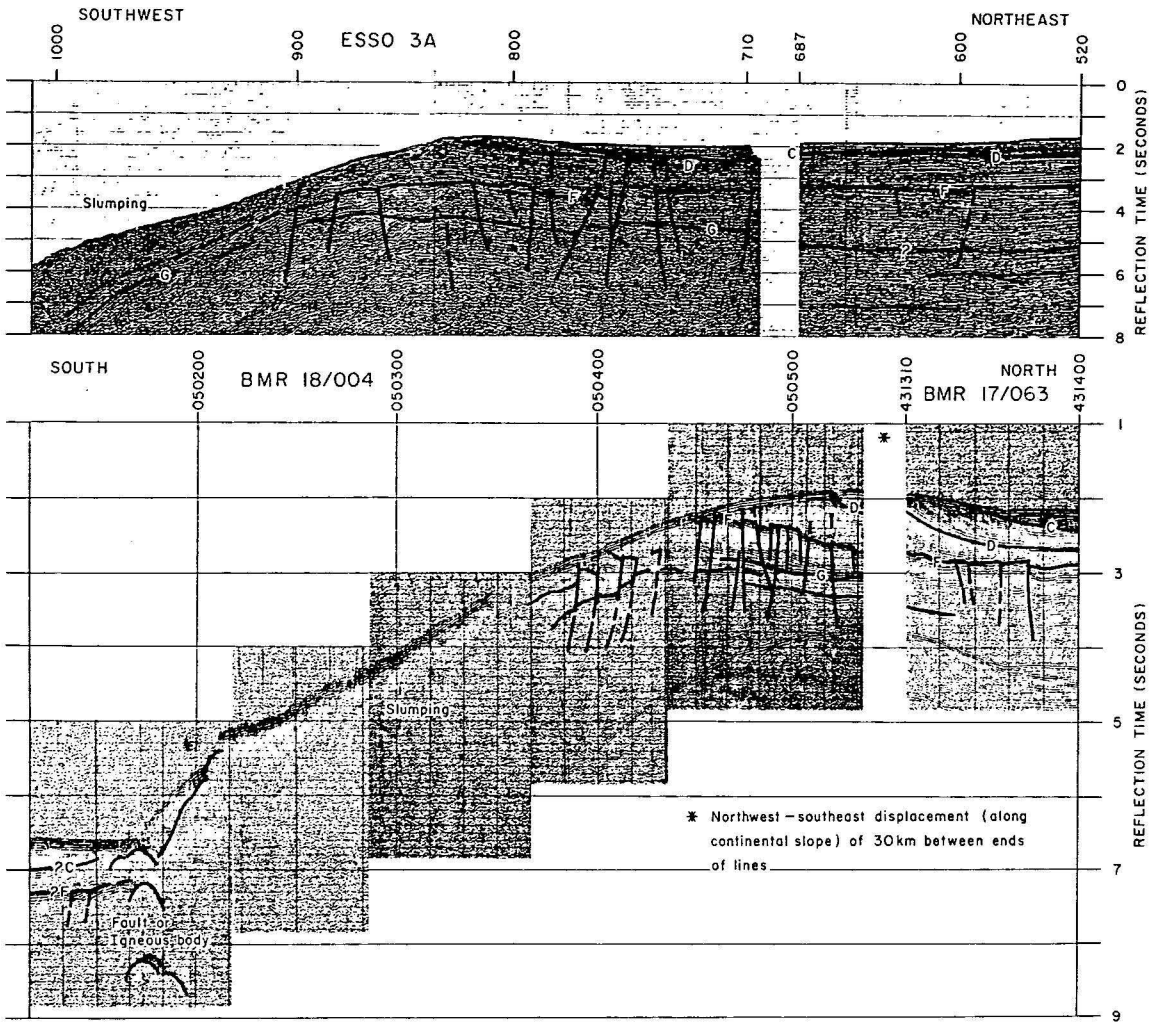

Figure 5. Seismic and magnetic profiles and interpretation: Esso 3A, BMR 18/004 and 17/063

the outcrops of older rocks on the lower continental slope would enable the various sequences to be dated, and lithological and palaeogeographic evidence could be added to the structural information revealed by the seismic profiles. This would enable testing of the theories of geological development of the margin, and the plateau as a whole, outlined by Veevers & Heirtzler (*op. cit.*), and Exon *et al.* (*op. cit.*), as well as theories that assign considerable petroleum potential to the large structures and thick sequence of the Exmouth Plateau (Willcox & Exon, 1976).

Sampling sites could be selected primarily by means of a precision depth recorder with a high frequency (ca. 3.5 KHz) sound pulse. This should give a penetration of 20 to 100 m (Damuth, 1975) and a resolution of a few metres, and enable the thickness of the young sediment overburden to be determined. A conventional seismic system could be used to make a structural comparison between the site and profiles used in the planning stage, and should enable each site to be related to the stratigraphic column. Possible sampling methods might include dredging, coring or drilling.

Acknowledgement

The drafting of figures for this text was carried out by L. Hollands of the BMR geophysical drawing office.

References

DAMUTH, J. E., 1974—Echo character of the western equatorial Atlantic floor and its relationship to the dispersal and distribution of terrigenous sediments. *Marine Geology* **18,** 17-45.

EXON, N. F., WILLCOX, J. B., & PETKOVIC, P., 1975—A preliminary report on the regional geology of the Exmouth Plateau. *Bureau of Mineral Resources, Australia—Record* **1975/158.**

POWELL, D. E., 1976—The geological evolution and hydrocarbon potential of the continental margin off northwest Australia. *APEA Journal.* **16,** 13-23.

THOMAS, B. M., & SMITH, D. N., 1974—A summary of the petroleum geology of the Carnarvon Basin. *APEA Journal.* **14,** 66-76.

VEEVERS, J. J., HEIRTZLER, J. R., *et al.*, 1973—Deep Sea Drilling Project, Leg 27 in the eastern Indian Ocean. *Geotimes* **18,** 16-17.

VEEVERS, J. J., & HEIRTZLER, J. R., 1974—Tectonic and palaeographic synthesis of Leg 27: *in* VEEVERS, J. J., HEIRTZLER, J. R., *et al.* Intitial Report of the Deep Sea Drilling Project, 27, 1049-1054, Washington, U.S. Government Printing Office.

WILLCOX, J. B., & EXON, N. F., 1976—The regional geology of the Exmouth Plateau. *APEA Journal,* **16,** 1-11.

The nature and origin of beach ridges, western Cape York Peninsula, Queensland

J. Smart

Two sets of beach ridges are known from the western side of Cape York Peninsula. The older set are thought to be late Pleistocene. They rest on a basement of older fan deposits and are regarded as a regressive sequence of barrier islands.

The younger ridges represents a progradational sequence post-dating the Holocene transgression. The earliest formed ridge, which is poorly developed, formed as a chenier. It was followed by a barrier island complex whose development lasted until about 3000 years B.P. Subsequently, there was rapid progradation and the development of two sets of chenier-type beach ridges, the younger of which is locally discordant to the ridges of the barrier island complex. These ridges rest on a marine sand and mud unit which appears continuous with a similar unit mapped offshore.

The Pleistocene ridges consist of quartzose sand, with negligible carbonate, while the Holocene ridges consist of quartzose sand, shell sand and shells. They show a progressive leaching with age.

Introduction

Extensive beach ridges border the southern and eastern margins of the Gulf of Carpentaria; they extend from the Roper River in Arnhem Land to Cape York, are patchily developed between the Roper River and Gove, and are also present on the Wellesley, Pellew and Wessel Islands and Groote Eylandt. The beach ridges on the Queensland coast of the Gulf have been examined by many workers and have been mapped by field parties of the Bureau of Mineral Resources (BMR) and the Geological Survey of Queensland (GSQ) between 1969 and 1973 (Doutch *et al.*, 1970, 1972, 1973). Smart (1976) reported the results of systematic drilling and levelling of beach ridges on the west coast of Cape York Peninsula from August to October 1973 and this paper summarizes the results. The purpose of the study was to elucidate the stratigraphy of the beach ridge complexes and to provide information on the late Pleistocene-Holocene geological history of the area, particularly in terms of sea-level changes. The results of C^{14} dating of shells from this and adjacent areas are also discussed and the history of beach-ridge formation in the region briefly reviewed.

Previous investigations

Twidale (1956) briefly described the beach ridges along the southern shore of the Gulf, between the Leichhardt and Gilbert Rivers. He divided the ridges into two groups: an older series of three ridges, whose formation was followed by a younger series of two ridges after a drop in sea level of about 6 m. The ridges were all considered to be formed as offshore bars, analogous to a present day feature. Twidale attributed the emergence to eustacy and said that the coastline displayed features characteristic of emergence. In 1966, Twidale presented a C^{14} date of 3320 ± 125 years B.P. for shells from the youngest beach ridge at Karumba and suggested that its emergence may be related to a eustatic fall in sea level during the Holocene (Twidale, 1966).

In the area south of Archer Bay, Valentin (1961) noted the two ages of beach ridges. He regarded the older ridges as having formed partly from many parallel dunes blown together by wind action and partly as old individual dunes.

Whitehouse (1963) discussed the beach ridges on the west side of Cape York Peninsula in a general review of sandhills in Queensland. He reported augering showing that the youngest ridges at Edward River Mission rested on marine muds and he postulated a sequence of beach ridges in three zones: firstly, young ridges with sharp profiles along the coast, secondly a series of older ridges having a more subdued relief with some incipient claypan development and finally an area, many kilometres wide, of sand with abundant claypans. The first two series are recognized in this paper as Holocene and Pleistocene beach ridge sequences respectively, but the area of sand with claypans is underlain by fluvial sediments. The claypans developed during an arid period in the late Pleistocene (Grimes & Doutch, in prep.).

Doutch *et al.* (1972) discussed the morphology and origin of the beach ridges in the area between latitudes 15° and 17°S. They presented a conjectural cross section of the ridge sequence which subsequent work (Smart, 1976) has shown to require revision.

Grimes (1974) described the beach ridges along the southwestern coast of the Gulf of Carpentaria in Queensland, and briefly discussed the results of C^{14} dating of ridges at Edward River Mission on Cape York Peninsula. He did not distinguish different ages of ridges on his maps, but his Figures 6 and 7 can be interpreted as showing two sets of ridges. Geological mapping in the area (Powell & Smart, in press; Smart, in press, a & b; Grimes, in press) has recognized two sets of beach ridges on the west coast of Cape York Peninsula, of Holocene and Pleistocene (?) age respectively. Whitaker & Gibson (in press) show similar features on the Charlotte Plain on the east coast of the Peninsula, and Gibson (1975) reported on an auger hole drilled through one of the younger ridges on that coast.

Beach-ridge nomenclature

The nomenclature of beach ridges has been unsystematic and confusing in the past. Two terms have been applied to beach ridges—bar or barrier, and chenier, but the distinction between them has not always been made clear. Todd (1968) made the distinction between ridges of barrier island origin and those of chenier origin, while Leblanc (1972) and Busch (1974) summarised the geometry and stratigraphy of the two types (Fig. 2). Essentially, the chenier is a sand body resting on coastal sediment associated with the progradation of the coastline, while the barrier island is a thick sand body which rests on basement, with its seaward margin underlain by marine sand and mud.

Cheniers

The original description of the chenier plains of Louisiana was by Howe *et al.* (1935) who wrote, 'Rising slightly above the surrounding marshes, several long, narrow, sandy ridges run roughly parallel to the coast of southwestern Louisiana and form the most conspicuous topographic features of the region. Sharply localized, well drained and fertile, they support naturally luxuriant

vegetation cover . . . the ridges have been called cheniers by their Creole inhabitants.' Price (1955) used the term chenier plain for this type of coastal feature and described cheniers as 'shallow-based, perched, sandy ridges resting on clay'. Subsequent work, including extensive drilling (Byrne *et al.* 1959; Gould & McFarlane, 1959; Bernard *et al.* 1959; Coleman, 1966), has revealed the stratigraphy of the beach ridge sequence in detail. The typical chenier does not rest on swamp mud as assumed by some (Russell & Howe, 1935; Tanner, 1961), but on a firm base of marine sand and silty clay. Todd (1968) distinguishes cheniers from barrier islands and he noted that the near-shore gradient of the seabed was twice as steep where barrier islands had developed as where cheniers had developed; otherwise conditions were similar.

Todd (1968) suggests that three conditions are necessary for the formation of cheniers:

(1) Stability or fall of sea level;
(2) a variable supply of sediment from rivers;
(3) effective longshore currents.

However if the supply of sediment is fairly constant, the classical chenier plain will not develop, and in its place a continuous sequence of sand ridges overlying muddy sediments will form, for example Figure 4C. Ridges of this nature are similar in genesis to cheniers and quite distinct from barrier island ridges. They are referred to in this paper as chenier-type ridges. Cheniers tend to form on coasts of high sediment supply, near major rivers.

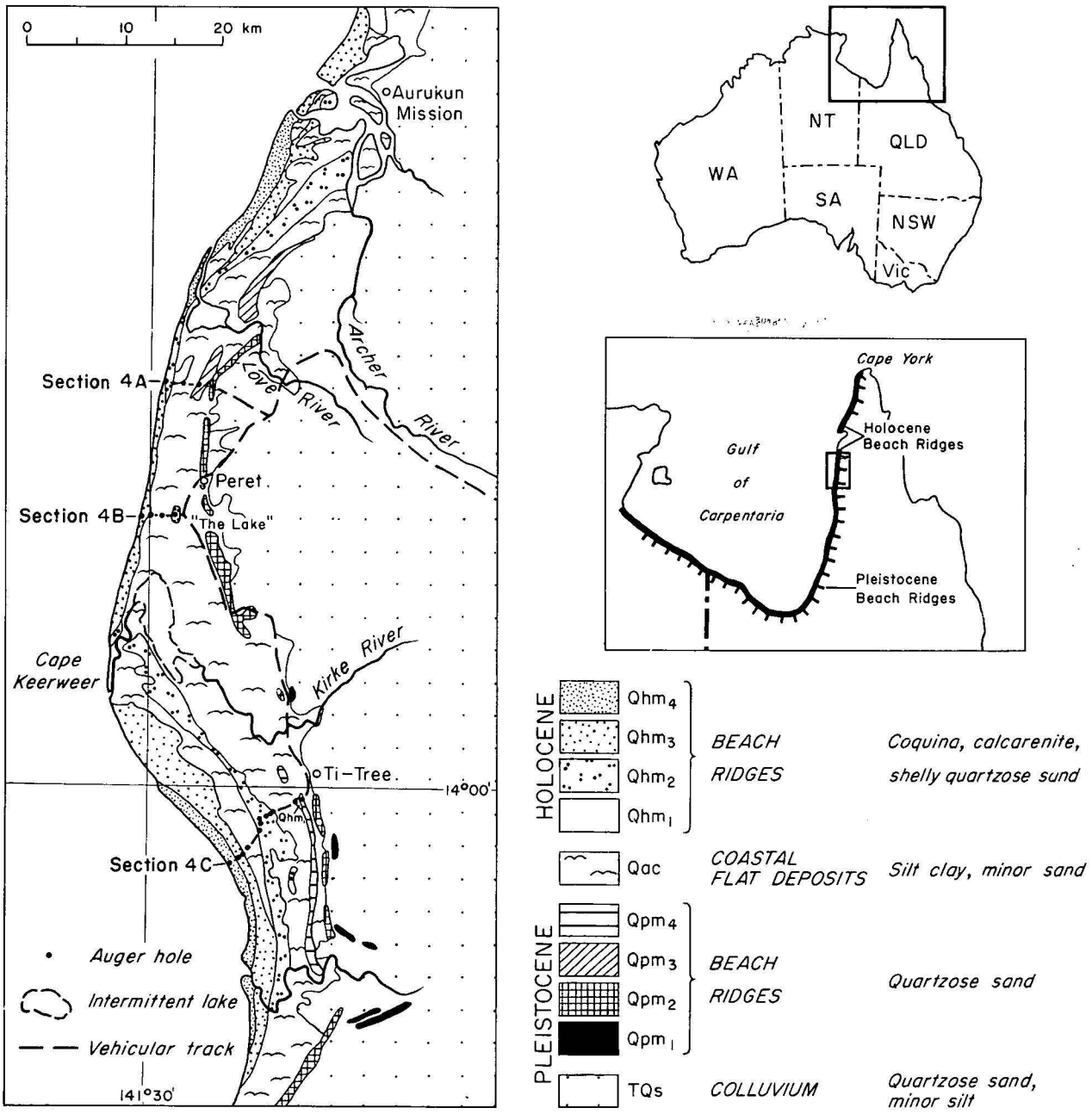

Figure 1. Locality map showing beach ridge distribution and location of sections

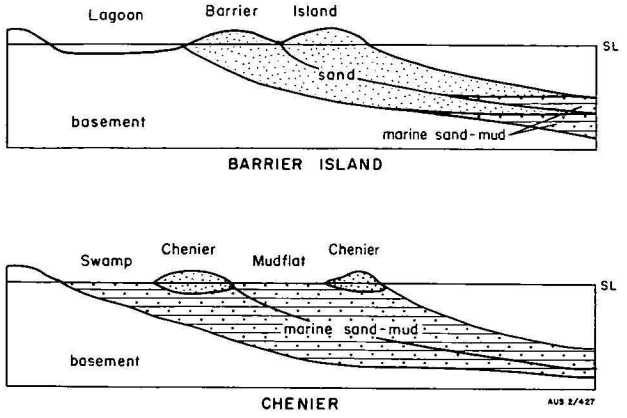

Figure 2. Diagrammatic cross sections of chenier and barrier island beach ridges, based on Leblanc (1972)

Barrier-island ridges

Barrier islands are well described in the literature, particularly those from the Gulf of Mexico and the Atlantic coast of the U.S.A. and their essential features are well known. They tend to be much larger than cheniers; generally up to three times thicker, and commonly tens of miles in length (Leblanc, 1972). As noted above, Todd (1968) showed that seabed gradients are much steeper off a barrier island than a chenier coast. Barrier islands appear to form on coasts where there is a limited supply of sediment, so that progradation is slow relative to a coast with cheniers. This allows a thorough sorting of sediment and the accumulation of a large, thick sand body.

General description

The results of the 1973 drilling are summarized as beach-ridge sections in Figure 4 and detailed logs are presented by Smart (1976). C^{14} dating results are shown in Table 1. The beach-ridge sections show that there is a group of ridges near the coast and more subdued ridges inland. These correspond to the younger (Qhm) and older (Qpm) ridges noted by previous workers. The map symbols Qhm and Qpm are used in this paper with appropriate suffixes to indicate the different sets of ridges.

Pleistocene beach ridges

Distribution

The older group of ridges has been mapped along the western coast of Cape York Peninsula as far south as latitude 15°. South of this, the older ridges have been recognized along the coast as far as the Northern Territory border (Needham & Doutch, 1973a, b: Ingram, 1973; Grimes, 1974) and can be recognized beyond on air photographs as far as the Roper River area.

Morphology

The older group comprises low, rounded ridges, which are covered by tall trees and contain, in a few places, deflation features (clay pans and minor blow outs) (Fig. 3). Air-photo interpretation suggests the presence of four sets of ridges within the older sequence, all of which can be traced over most of the coast. In this paper they have been mapped out, within the survey area, as Qpm_1, Qpm_2, Qpm_3 and Qpm_4 from the oldest to the youngest (Fig. 1).

The Qpm_1 ridges are poorly preserved as low, linear, sand ridges whose trends are generally discordant to the Qpm_2 and Qpm_3 ridges. No ridges of this group have been levelled but their crests appear similar in height to the Qpm_2 group.

The intermediate set, Qpm_2, is the best preserved set in the survey area and appears to be best preserved elsewhere on the coast. The crests of the Qpm_2 ridges are approximately 5 m above sea level but it is unlikely that this is their original height. They are present over all the survey area south of the Love River.

Witin the survey area, the Qpm_3 ridges are recognized only west of Don Yard, where they lie slightly discordant to the Qpm_2 ridges. Claypans characterize the Qpm_3 ridges but there are only a few deflation features on the other Pleistocene ridges. The present elevation of the Qpm_3 ridge crests is about 2 m above sea level.

The youngest of the group, Qpm_4, has a less degraded appearance than the older ridges although its crest lies at about the same elevation, about 3.5 m above sea level. Vegetation cover is similar to that on the older ridges except that there are fewer large trees.

The Qpm_4 ridges are present only in the south of the survey area (Fig. 1), and have been mapped both as Qpm (Smart, in press, b) and Qhm (Grimes, in press) in the recent 1:250 000 geological maps, as their affinities are less certain than those of the other ridges. However, the drilling and levelling data (Fig. 4) suggests their formation at a higher sea level than present and so they are probably part of the older group.

A possible explanation for the restriction of deflation features to the Qpm_3 ridges is that deflation occurred immediately after the formation of the Qpm_3 ridges and before deposition of the Qpm_4 ridges. If the previous climate had been more humid and the Qpm_1 and Qpm_2 ridges had developed a thick vegetation cover, they would have been little affected by the deflation episode. However no arid period has so far been established in that part of the Pleistocene.

Lithology and relationships

The Pleistocene beach ridges consist of slightly clayey quartzose sand, with local traces of shell material at depth. The sand is generally yellow or brown, locally red-brown, and is sub-horizontally bedded. A soil profile about 0.5-1.0 m thick is present on top of the ridges but no old soil layers or humic material have been encountered in drilling.

The oldest ridges (Qpm_1) have not been drilled, but photo-interpretation suggests they rest on the sequence of Pliocene-Pleistocene alluvial fan deposits in the survey area. Sections across the other ridges are shown in Figures 4A and 4C. The Qpm_2 ridges rest on the Pliocene-Pleistocene fan deposits (TQa), their bases being up to 1.5 m above present sea level. Qpm_4 ridges also rest on fan deposits (Fig. 4C); their bases are about 1.5 m above present sea level on the landward side, but the seaward side has not been drilled.

The Pleistocene ridges in the survey area are all of the barrier-island type, resting on a basement of older fan deposits.

Age

Negligible carbonate material has been recovered from the Qpm_1, Qpm_2, Qpm_3 and Qpm_4 ridges, and C^{14} dates have not been obtained. However the age of the ridges is almost certainly beyond the limit of radio-carbon dating. Consideration of late Pleistocene history in the region and comparison with other coastal features dated in eastern Australia by Marshall (1975) suggests an age of about 120 000 years B.P. for the group. The maximum age is probably younger than 170 000 years B.P., as Jongsma (1974) found a eustatic low of —200 before 170 000 years B.P., and the fan deposits on which the ridges rest postdate this sea level low.

Sea levels

The Pleistocene beach ridges formed at a sea level slightly higher than present. The exact height above present sea level is uncertain. B. G. Thom (pers. comm.) suggests a high of 4-6 m for 120 000 years B.P. in S.E. Australia, and other authors suggest highs of the same order elsewhere (e.g Chappell, 1974), but evidence of strand lines around the Jardine River and the Charlotte Plain indicates a higher stand, perhaps as much as 15 m. (H. F. Doutch, pers. comm.) The Pleistocene beach ridges appear to have formed during regression from this sea-level high.

Holocene beach ridges

Distribution

The Holocene ridges are present along most of the coast in the survey area. They can be traced on airphotos northwards as far as the mouth of the Jardine River, and are also present on the Torres Strait Islands and in New Guinea. Southwards they are present around the coast to the Roper River area and there is some patchy development further north.

Morphology

The Holocene ridges show fairly sharp relief, have a cover of small trees, shrubs or grass, and lack deflation features. Airphoto interpretation shows the presence of four sets of ridges, the younger three of which can be traced over most of the west coast of Cape York. The oldest is poorly preserved and can be recognized in only a few places. Within the survey area, the ridges have been mapped out as Qhm_1, Qhm_2, Qhm_3 and Qhm_4, from oldest to youngest (Fig. 1).

The Qhm_1 ridges are low and broad, and have crests, about 2 m above sea level, but they may have been higher originally, the loss in height being due to leaching. The Qhm_2 ridges are extensive and are present along most of the survey area as well as farther north and south. They are 3-4 m above sea level in the Cape Keerweer area, but 5-6 m

Figure 3. Air photograph, Kendal River area. RC9 Series, 1969; HOLROYD Run 2, Photo 46

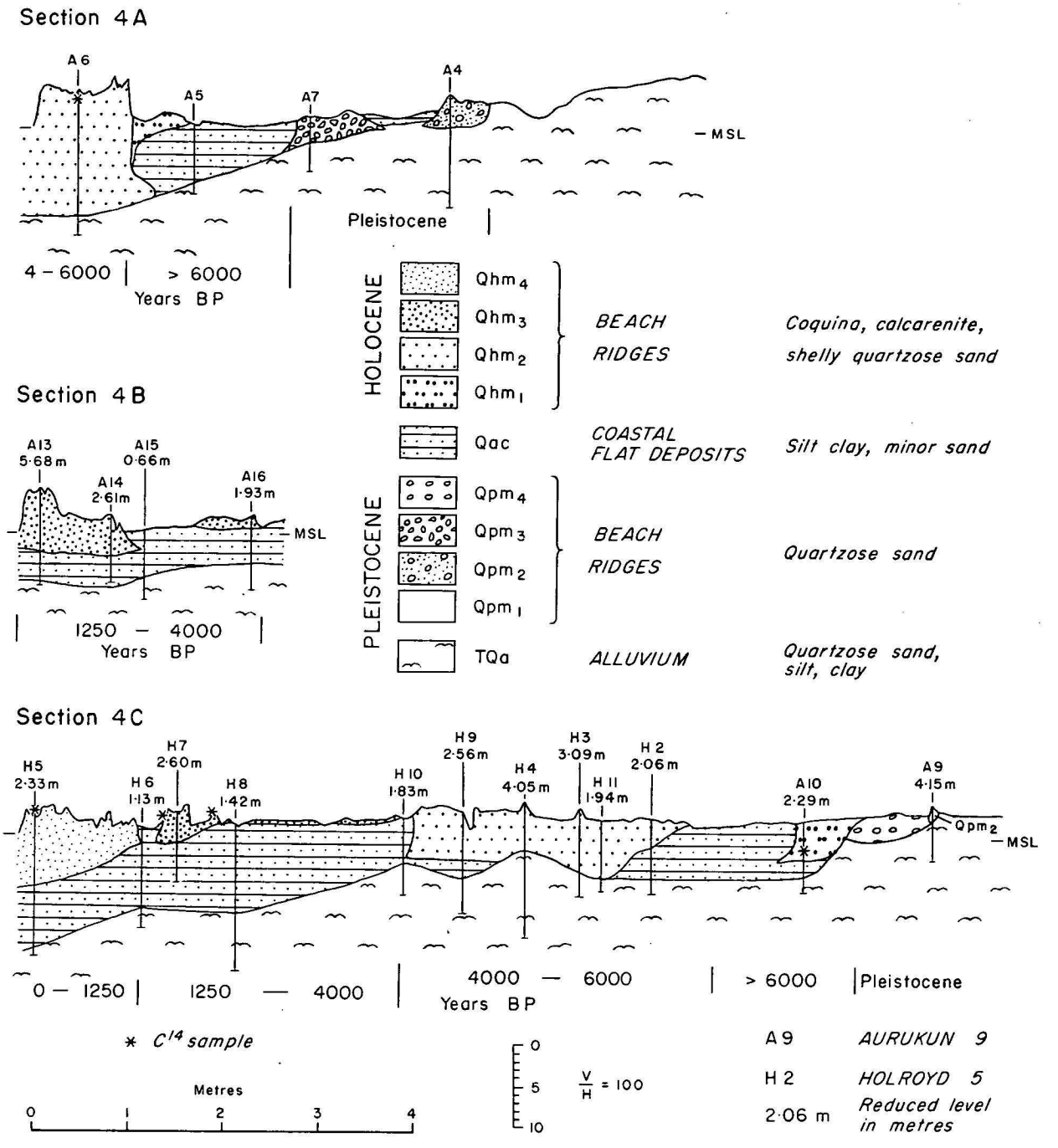

Figure 4. Cross sections of beach ridges. Locations shown on Figure 1. Detailed drill logs were presented by Smart (1976)

high farther north, west of Don Yard. The latter are the highest ridges in the survey area. The Qhm_2 ridges have sharper relief than the Qhm_1 ridges, but the relief is not quite so sharp as that of the younger ridges. In several areas fresh-water lagoons have developed in the swales (e.g. Bull Yard Swamp).

The Qhm_3 ridges are extensive and show a marked discordance with the Qhm_2 ridges just north of Cape Keerweer (Fig. 1). They are asymmetric, about 5 m above sea level on the seaward side, and about 2 m on the landward side. Their morphology is slightly sharper than that of the Qhm_1 ridges. Southwest of Don Yard, the Qhm_3 series appears to merge with and slightly overlap the Qhm_2 series.

The vegetation on the Holocene (Qhm) group of ridges is more dense than that on the Pleistocene ridges; the Qhm_1 and Qhm_2 ridges have small trees or large shrubs and the younger ridges have a cover of shrubs only. The ridges nearest to the coast are generally grassed and have few shrubs. On all the Holocene ridges, the trees and shrubs tend to be best developed on the ridge crests, and the intervening swales have a grass cover. Other workers have noted that crests are initially vegetated preferentially to swales, and Bird (1960) suggests that this is due to the lower salinity of the crests (due to more rapid leaching). Russell (1948) noted that the crests of cheniers in Louisiana had better developed soils than the flanks.

The Qhm_4 ridges are present only in the north and south of the survey area. The ridges are about 5 m above sea level and well defined with sharp ridge crests. They appear to be still forming.

Sample No.		Beach Ridge	Lab. No.	Location		Age	Remarks
72797020		Qhm_2	SU 185	13°53′S;	141°23′E	4130 ± 80	
72797025		Qhm_4	SU 202	13°23′S;	141°38′E	1110 ± 85	
72797026		Qhm_4	SU 203	13°23′S;	141°38′E	910 ± 70	
72797011	A	Qhm_2	SU 201A	13°25′S;	141°41′E	5330 ± 85	bivalves
	B		SU 201B			4430 ± 85	gastropods
72797023		Qhm_2	NSW 156	13°51½′S;	141°29′E	4060 ± 100	bivalves
72797506		Qhm_2	NSW 158	13°37′S;	141°30½′E	3350 ± 400	bivalves
73797510		Qhm_1	NSW 159	14°00½′S;	141°38½′E	3500 ± 500	
72796243		Qhm_3	SU 197A	14°54′S;	141°37′E	1350 ± 75	bivalves) present
			B			470 ± 80	gastropods) beach
72796244		Qhm_4	SU 198A	14°54′S;	141°37′E	750 ± 70	bivalves
			B			980 ± 75	gastropods
72796245		Qhm_4	SU 199	14°54′S;	141°37′E	995 ± 75	
72796246		Qhm_2	SU 200	14°54′S;	141°37′E	3935 ± 85	
73797110	A	Qhm_3	NSW 120	14°04′S;	141°35′E	1780 ± 70	
73797111	A	Qhm_3	NSW 121	14°03′S;	141°36′E	2600 ± 80	
(Holroyd)			SU 427			2580 ± 115	
73797110	A	Qhm_3	SU 429	14°04′S;	141°35′E	1760 ± 95	bivalves
(Holroyd)	B		SU 430			1700 ± 100	gastropods
	C		SU 431			1790 ± 100	bivalves
	D		SU 432			2510 ± 140	
73797111	B	Qhm_3	SU 428	14°03′S;	141°36′E	2150 ± 100	
7379108		Qhm_4	NSW 157	14°04′S;	141°34½′E	500 ± 80	bivalves
70795047			SU 183	16°42′S;	141°15′E	5630 ± 120	
70795050			SU 184	16°42′S;	141°12′E	820 ± 70	

Table 1. Radio-carbon dating

NSW—University of New South Wales, SU—University of Sydney

Lithology and relationships

The younger (Qhm) ridges consist of slightly clayey, quartzose sand, with some shell sand and whole shells. Shell material is abundant in the Qhm_4 and Qhm_3 ridges (> 50% in Qhm_4) but less so in the older ridges of this group, which generally have no carbonate in the upper part (discussed below). On the ridge tops, a soil profile up to 0.5 m thick is present; its thickness increases with the age of the ridges. The bedding within the ridges is sub-horizontal; no cross bedding has been observed.

The Qhm_2 ridges rest on TQa (Fig. 4A, 4C), and their bases are up to 10 m below present sea level. The partly contiguous Qhm_1 ridges appear to rest on muddy silt and sand (Qac). The Qhm_4 and Qhm_3 ridges rest on muddy silt and sand (Qac) as noted by Whitehouse (1963). The base of the Qhm_4 ridges are 4-5 m below sea level but those of the Qhm_4 ridges range from 3 m below to 1 m above sea level.

The Qhm_1 ridges appear to rest on sandy mud and may represent a chenier-type ridge sequence which failed to develop fully because it was superseded by the development of a barrier island, the Qhm_2 ridges. The latter fit the barrier island model of Leblanc (1972) very well, being thick sand bodies, formed mainly below sea level, resting on 'basement' and locally having their seaward margin resting on sandy mud.

The Qhm_3 and Qhm_4 ridges are chenier-type ridges, relatively thin sand bodies, resting on sandy mud. They do not form a classical chenier plain, as ridge development has been almost continuous throughout the latter part of the Holocene, probably due to a fairly constant supply of sediment (cf. Todd, 1968).

Age

Results of C^{14} dating are presented in Table 1 and are summarized below. The Qhm_1 ridges have not been dated directly, but by comparison with the Qhm_2 ridges, a minimum age of about 6500 years B.P. seems likely. E. G. Rhodes (pers. comm.) has obtained an age of 6440 years B.P. for the most inland ridge north of Edward River. The latter date, combined with dates of marine sediments, led Smart (in prep.) to suggest the sea reached its present level at about 6500 to 7000 years B.P. The Qhm_2 ridges have ages of between 4130 and 4330 years B.P. in the survey area, and slightly older farther south (5630 years B.P.), so that a time span of 4000-6000 years B.P. seems probable. The time represented by the erosion between Qhm_2 and Qhm_3 sequences north of Cape Keerweer is uncertain. Ages for the Qhm_3 ridges go back to 2500 years B.P. in the survey area, but this specimen appears to be in the middle of the sequence. A specimen from the landward side of the sequence at Edward River Mission gave an age of 3935 years B.P. The youngest ages are about 1250 years B.P., giving a time span of 1250 to about 4000 years B.P., which suggests probable continuity of deposition without a break. The absence of Qhm_2 ridges between Cape Keerweer and Don Yard may have been due to erosion contemporaneous with beach-ridge formation to the south, or more likely, to non-deposition. The youngest ridges, $Qhm_4$1, have given ages between 1110 and 500 years B.P., which fits well with the ages of the Qhm_3 ridges.

The ages obtained for the Holocene ridges generally form a logical sequence, oldest inland and progressively younger seawards, which suggests that the ages are reliable. However, the age obtained for the Qhm_1 ridge west of Ti-Tree is younger than those obtained from the Qhm_2 ridges elsewhere. The sample was shell fragments, of mixed species, picked out of drill cuttings, from a level below the present water table. It is therefore suggested that the date is unreliable because of the mixture of material and the probability of contamination by younger carbonate.

It should be realized that the dates obtained are those of the death of the organism and that there may be a time lag between this and the incorporation of the shell in a beach ridge. In addition, reworking of a pre-existing ridge will lead to the incorporation of shells much older than the ridge itself. However, the logical sequence of ages obtained, from 500 years B.P. to over 6000 years B.P. suggests that these effects have not been significant in this area.

A sequence of Late Pleistocene and Holocene beach ridges is known elsewhere in Australia and is present along much of the southeast coast of the continent (e.g. Bird, 1965; Langford-Smith & Thom, 1969; Cook & Polack, 1973). Cook & Polack compared ages of individual ridges at Broad Sound on the east coast of Queensland with ages of Holocene beach ridges from other parts of the world and could find no direct correlation.

The rapid progradation of the coast after about 4 000 years B.P. (Qhm_3 and Qhm_4 sets) corresponds in time to increasing aridity in the Atherton Tableland to the southeast (Kershaw & Nix, in prep.) and the greater aridity, if present in the Peninsula, may have caused a higher rate of erosion and consequent supply of sediment.

Leaching

The removal of carbonate from beach ridges by leaching is a common process and has been severally reported (e.g. Salisbury, 1925; Russell, 1948; Bird, 1965). Salisbury (1925) showed that the carbonate content of sand dunes dropped from over 6 percent to zero in less than 300 years in a cool wet climate. Bird (1965) reports a steady reduction of soil pH with age and a consequence change of plant species on beach ridges in Victoria. Smart (1976) described a costean into a Holocene ridge (Qhm_3) west of The Lake which showed a cemented horizon at the dry season water table. He concluded that the cementation was due to the precipitation at the water table of carbonate leached from the upper part of the profile. If the process continued, the final profile would be a leached zone devoid of carbonate, over a hard pan of carbonate-cemented sand and shells (a 'groundwater podzol' of Stephens, 1962).

The bed of the Gulf of Carpentaria adjacent to the Holocene beach ridges is underlain by a shelly sandy mud (mapped as Qcm by Smart, in press, a, b) and the sand and shells of the Holocene ridges were derived by the winnowing of this by wave action. Similarly, the Pleistocene ridges had an analogous offshore provenance in the calcareous sandy clay which has subsequently been indurated during the late Pleistocene (Smart, *op. cit.*). However, the Pleistocene ridges are now essentially devoid of carbonate although their original composition was presumably similar to that of the Holocene ridges. It is therefore inferred that they have undergone leaching since their formation. Pleistocene ridges in South Australia contain abundant carbonate (P. J. Cook, pers. comm.), but the present rainfall in that area is less than half that of the survey area, and average temperatures are lower.

The Holocene ridges show a decline in carbonate content landwards, and an increasing depth of leaching. Drilling in 1973 showed a relatively low carbonate content in Qhm_1 and Qhm_2 ridges, but no indurated horizons were detected. The groundwater podzolization process has not proceeded to finality in the survey area; the reason is uncertain.

Sea levels

It is difficult to infer from the section of a beach ridge the sea level at which it was actually formed. Some chenier-type ridges have most of their volume above sea level, while others have a considerable volume below it (e.g. Fig. 4C); similarly with the barrier island ridges (Fig. 4A, 4C). In addition, leaching of carbonate may greatly reduce the volume of the ridge. It is not possible in this area to find evidence for or against a slightly higher sea level in the early Holocene as postulated by others in northern Queensland (e.g. Hopley, 1968, 1971). However, most workers do not accept a worldwide Holocene sea level high (e.g. Thom *et al.*, 1969, 1972).

Conclusions

1. The Pleistocene beach ridges formed as a series of barrier island complexes during a sea level high of at least 4-5 metres above present. By comparison with ridges in southeast Australia their age is probably around 120 000 years B.P. Subsequently sea level dropped, and was below the present level until the Holocene transgression.
2. The sea reached its present level or slightly higher about 6500-7000 years B.P., and small localized ridges developed (Qhm_1) associated with fairly rapid progradation of the coast. The transgression corresponds in time to the great increase in rainfall noted by Kershaw (1975).
3. From about 6000 to 4000 years B.P., a barrier island complex (Qhm_2) developed, but was probably absent in the central part of the area. Lagoonal sediments accumulated landward of the complex.
4. There was an increase in sediment supply and rapid progradation of the coast (over 6 km at Cape Keerweer) from about 4000 years B.P. to the present and chenier-type ridges developed in two sets (Qhm_3 and Qhm_4).

Acknowledgements

I wish to thank the Aurukun Aboriginal Council for permission to work in the Reserve and also the people and staff of the Mission for their co-operation and assistance during the survey; in particular the late Mr K. Steiler, former cattle manager at Peret, and his wife who provided unstinted help throughout the survey.

Thanks are also due to D. Hoops and his survey party from Department of Services and Property who carried out the levelling, D. L. Gibson who logged many of the holes, and the remainder of the field party, in particular D. B. Gourlay.

I also thank H. F. Doutch for useful discussion of Late Cainozoic geology and P. J. Cook for his valuable comments on the manuscript. The figures were drawn by A. J. Retter of the geological drawing office, BMR.

References

BERNARD, H. A., MAJOR, L. F., Jr. & PARROT, B. S., 1959—The Galveston barrier island and environs: a model for predicting reservoir occurrence and trend. *Gulf Coast Association of Geological Societies Transactions*, **9**, 221-224.

BIRD, E. C. F., 1960—The formation of sand beach ridges. *Australian Journal of Science*, **22**, 349-50.

BIRD, E. C. F., 1965—The evolution of sandy barrier formations on the East Gippsland coast. *Proceedings of the Royal Society of Victoria*, **79**.

BUSCH, D. A., 1974—Stratigraphic traps in Sandstones —exploration techniques. *American Association Petroleum Geologists. Memoir* **21**.

BYRNE, J. V., LEROY, D. C., & RILEY, C. M., 1959—The chenier plain and its stratigraphy, southwestern Louisiana. *Gulf Coast Association of Geological Societies Transactions*, **9**, 1-23.

CHAPPELL, J., 1974—Geology of coral terraces, Huon Peninsula, New Guinea: a study of Quaternary tectonic movements and sea-level changes. *Bulletin of the Geological Society of America*, **85**, 553-570.

COLEMAN, J. N., 1966—Recent coastal sedimentation, central Louisana coast. *Louisiana State University. Coastal Studies Institute Technical Report*, **29**.

COOK, P. J., & POLACH, H. A., 1973—A chenier sequence at Broad Sound, Queensland and evidence against a Holocene high sea level. *Marine Geology*, **14**, 253-268.

DOUTCH, H. F., in prep.—Late Cainozoic tectonics and geomorphology of southern New Guinea and Cape York Peninsula. *Bureau of Mineral Resources, Australia—Record* (unpublished).

DOUTCH, H. F., INGRAM, J. A., SMART, J., & GRIMES, K. G., 1970—Progress report on the geology of the southern Carpentaria Basin, 1969. *Bureau of Mineral Resources, Australia—Record* **1970/39** (unpublished).

DOUTCH, H. F., SMART, J., GRIMES, K. G., NEEDHAM, R. S., & SIMPSON, C. J., 1972—Progress report on the geology of the Central Carpentaria Basin, 1970. *Bureau of Mineral Resources, Australia—Record* **1972/64** (unpublished).

DOUTCH, H. F., SMART, J., GRIMES, K. G., GIBSON, D. L., & POWELL, B. S., 1973—Progress report on the geology of the Carpentaria Basin in Cape York Peninsula. *Bureau of Mineral Resources, Australia—Record* **1973/187** (unpublished).

GIBSON, D. L., 1975—Auger drilling, Cape York Peninsula, 1974. *Bureau of Mineral Resources, Australia—Record* **1975/11** (unpublished).

GOULD, H. R., & MCFARLANE, E., 1959—Geologic history of the chenier plain, southwestern Louisiana. *Gulf Coast Association of Geological Societies Transactions*, **9**, 261-270.

GRIMES, K. G., 1974—Mesozoic and Cainozoic geology of the Lawn Hill, Westmoreland, Mornington and Cape Van Dieman 1:250 000 Sheet areas, Queensland. *Bureau of Mineral Resources, Australia—Record* **1974/106** (unpublished).

GRIMES, K. G., in press—Holroyd, Queensland—1:250 000 Geological Series. *Bureau of Mineral Resources, Australia—Exploratory Notes.* **SD/54-11.**

GRIMES, K. G., & DOUTCH, H. F., in prep.—Late Cainozoic fluviatile deposits from the Carpentaria Plains, north Queensland. *Geological Survey of Queensland—Report.*

HOPLEY, D., 1968—Morphology of Curacao Island spit, North Queensland. *Australian Journal of Science*, **31**, 122-123.

HOPLEY, D., 1971—The origin and significance of North Queensland Island spits. *Geomorphology*, **15**, 371-389.

HOWE, H. V., RUSSELL, R. J., MCGUIRT, J. H., CRAFT, B. C., & STEPHENSON, M. B., 1935—Reports on the geology of Cameron and Vermilion Parishes. *Louisiana Geological Survey Bulletin*, **6.**

INGRAM, J. A., 1973—Burketown, Queensland—1:250 000 Geological Series. *Bureau of Mineral Resources, Australia—Explanatory Notes.*

JONGSMA, D., 1974—Marine geology of the Arafura Sea. *Bureau of Mineral Resources, Australia—Bulletin* **157.**

KERSHAW, A. P., 1975—Late Quaternary vegetation and climate in northeastern Australia. *Quaternary Studies. Royal Society of New Zealand.*

KERSHAW, A. P., & NIX, H. A. in prep.—The regional significance of late Quaternary vegetation changes in northeastern Queensland, Australia.

LANGFORD-SMITH, T., & THOM, B. G., 1969—New South Wales coastal geomorphology. *In* PACKHAM, G. H., (Editor), GEOLOGY OF NEW SOUTH WALES. *Journal of the Geological Society of Australia* **16(1).**

LEBLANC, R. S., 1972—Geometry of sandstone reservoir bodies. *American Association of Petroleum Geologists Memoir* **18**, 133-190.

MARSHALL, J. F., 1975—Uranium series dating of corals from the south west Pacific. *M.Sc. Thesis, Australian National University.* (unpublished).

NEEDHAM, R. S., & DOUTCH, H. F., 1973a—Galbraith, Queensland—1:250 000 Geological Series. *Bureau of Mineral Resources, Australia—Explanatory Notes.* **SE/54-3.**

NEEDHAM, R. S., & DOUTCH, H. F., 1973b—Rutland Plains, Queensland—1:250 000 Geological Series. *Bureau of Mineral Resources, Australia—Explanatory Notes.* **SD/54-15.**

POWELL, B. S., & SMART, J., in press—Jardine River and Orford Bay, Queensland—1:250 000 Geological Series. *Bureau of Mineral Resources, Australia—Explanatory Notes.* **SD/54-15, 16.**

PRICE, W. A., 1955—Environment and formation of the chenier plain. *Quarternaria*, **2**, 75-86.

RUSSELL, R. J., 1948—The coast of Louisiana. *Societe Belge de Geologie, de Palaeontologie et d'Hydrologie.*

RUSSELL, R. J., & HOWE, H. F., 1935—Cheniers of southwestern Louisiana. *Geographical Review* **25**, 449-61.

SALISBURY, E. J., 1925—Note on the edaphic succession in some dune soils with special reference to the time factor. *Journal of Ecology*, **13**, 322-8.

SMART, J., 1976—Auger drilling of beach ridge complexes, western Cape York Peninsula, 1973. *Bureau of Mineral Resources, Australia—Record* **1976/16** (unpublished).

SMART, J., in press (a)—Weipa, Queensland—1:250 000 Geological Series. *Bureau of Mineral Resources, Australia—Explanatory Notes.* **SD/54-3.**

SMART, J., in press (b)—Aurukun, Qld,—1:250 000 Geological Series. *Bureau of Mineral Resources, Australia—Explanatory Notes. 5054-7.*

SMART, J., in prep.—Late Pleistocene sea-level changes, Gulf of Carpentaria.

STEPHENS, C. G., 1962—A MANUAL OF AUSTRALIAN SOILS. 3rd Edition *Commonwealth Scientific and Industrial Research Organisation*, Melbourne.

TANNER, W. F., 1961—Offshore shoals in areas of energy deficit. *Journal of Sedimentary Petrology*, **31**, 87-95.

THOM, B. G., HAILS, J. R., MARTIN, A. R. H., & PHIPPS, C. V. G., 1969—Post-glacial sea levels in eastern Australia. *Marine Geology*, 161-168.

THOM, B. G., HAILS, J. R., MARTIN, A. R. H. & PHIPPS, C. V. G., 1972—Post-glacial sea levels in eastern Australia—a reply. *Marine Geology*, **12**, 223-242.

TODD, T. W., 1968—Dynamic diverisons: influences of longshore current—tidal flow interaction on chenier and barrier island plains. *Journal of Sedimentary Petrology*, **38**, 734-746.

TWIDALE, C. R., 1956—A reconnaissance survey of the coastline of the Leichardt-Gilbert area of northwest Queensland. *Australia Geographer* **6**, 14-20.

TWIDALE, C. R., 1966—Geomorphology of the Leichardt-Gilbert area, northwest Queensland. *Commonwealth Scientific and Industrial Research Organization, Land Research Series* **16.**

VALENTIN, H., 1961—The central west coast of Cape York Peninsula. *Australian Geographer* **8**, 65-72.

WHITAKER, W. G., & GIBSON, D. L. in press—Ebagoola, Queensland—1:250 000 Geological Series. *Bureau of Mineral Resources, Australia—Explanatory Notes*, **SD/54-12.**

WHITEHOUSE, F. W., 1963—The sand hills of Queensland, coastal and desert. *Queensland Naturalist*, **17**, 1-10.

BMR J. Aust. Geol. Geophys., 1 (1976), 219-230

The Late Triassic molluscs, conodonts, and brachiopods of the Kuta Formation, Papua New Guinea

*S. K. Skwarko, Robert, S. Nicoll and K. S. W. Campbell**

The Kuta Formation is mainly a limestone deposit which crops out on the flanks of the Kubor Anticline in the Central Highlands of Papua New Guinea. It has been variously regarded as Cainozoic, Permian and Permo-Triassic in age, but is now positively dated as late Norian or Rhaetian (Late Triassic) on the basic of conodonts, molluscs and brachiopods. The Kuta Formation is thus the youngest known Triassic formation in Papua New Guinea. Interpretation of the local stratigraphy is simplified by this dating. It is now apparent that the marine Triassic sedimentation in Papua New Guinea commenced no later than the Anisian (Middle Triassic) and continued, probably uninterrupted, until Rhaetian time.

The fossils identified and described include the conodont *Misikella posthernsteini* Kozur & Mock, 1974, the ammonite *Arcestes (Arcestes)* cf. *sundaicus*, Welter, 1914, and some bivalves. The brachiopods *Clavigera*, *Zugmeyerella*, *Sinucosta*, *Robinsonella*, *?Hagabirhynchia* are equally important in dating the assemblage, but will be described in detail separately.

All the more closely identified fossils have a Tethyan Provincial aspect except *Clavigera* which was previously known only from New Zealand and New Caledonia.

Introduction

In the course of the regional mapping of the Kubor Anticline in the central highlands of New Guinea in 1968 and 1970 the Kuta Formation was sampled in a number of places with the hope of obtaining a more definite and accurate dating than had hitherto been possible. The preliminary palaeontological study of the collected fauna was not successful, as the contained corals proved to be too poorly preserved for identification, brachiopods seemed indicative of either Permian or Triassic age, the foraminifera were long ranging genera, and the bivalves were too few and fragmentary for identification and dating. The resulting general consensus was that the limestone straddled the Permo-Triassic boundary (Bain, Mackenzie & Ryburn, 1975).

In the present study the additional brachiopods and molluscs have been examined and 14 samples processed for conodonts in an attempt to establish the age of the formation more precisely. Nicoll is responsible for identification of the conodonts, Skwarko for the cephalopods and bivalves, and Campbell for the brachiopods. The stratigraphic section of the paper is the work of Skwarko and Nicoll.

Acknowledgements

Many of the samples were collected by J. H. C. Bain, D. E. Mackenzie, and R. J. Ryburn, of BMR; we wish to thank them for discussions concerning the field and stratigraphic relationships of rock units around the Kubor Anticline. J. D. Campbell (Univ. Otago, New Zealand) has been most helpful with comments on the *Clavigera* specimens. Sincere thanks are due to Dr. Y. Bando of Kagawa University, Japan, for his helpful comments on the identity of the ammonites; Professor J. A. Grant-Mackie of the University of Auckland, New Zealand, for the exhaustive discussion regarding the likely phylogeny of one of the more enigmatic bivalves; and Dr. K. Nakazawa, of Kyoto University, Japan, for his comments on the bivalves. The text-figures were drawn in the general draughting section of the geological drawing office, BMR.

* **K. S. W. Campbell, Department of Geology, Australian National Universtiy, P.O. Box 4, Canberra, ACT 2600**

The Kuta Formation

The Kuta Formation consists of a suite of marine arkose, limestone, and shale outcropping in the central highlands of Papua New Guinea (Fig. 1). Its description below is largely based on Bain *et al.* (1970, unpublished; 1975).

The formation is 30 to 250 m thick and mainly consists of hard, buff to dark grey, massive, crystalline, coarse to fine-grained limestone. In places the limestone appears to grade laterally into calcareous breccia containing fragments of metamorphic rocks. The limestone rests on, and in places grades laterally into, a coarse, calcareous arkose, which in turn unconformably overlies the Kubor Granodiorite or the Omung Metamorphics. The formation is overlain by either the Late Jurassic Maril Shale or the Early Cretaceous Kondaku Tuff.

The presence in places of molluscs, brachiopods, corals, bryozoans, and crinoids, as well as the existence of the coarse basal arkose, points to a shallow-water environment of deposition, and Bain *et al.* (1975, p. 18-20) concluded that the limestone was deposited as fringing reefs on granitic wash and breccia derived from the adjacent Palaeozoic basement.

The Kuta Formation has been little disturbed since its deposition, and where observed is only slightly folded.

Age of the Kuta Formation

Bain *et al.* (1970, 1975), and Bain & Mackenzie (1974a, 1974b), have discussed in some detail earlier evidence pertaining to the age of the Kuta Formation, and this information is only briefly reviewed here.

The age has been the subject of much controversy. Limestone was first collected by N. H. Fisher, in 1937, from exposures overlying the Kubor Granodiorite near Kuta village, and a Miocene age was ascribed to these samples (Glaessner *et al.*, 1950). Glaessner identified foraminifera from new samples obtained from the Kuta area and dated the unit as Permian. These specimens and others identified later by Belford (Bain *et al.*, 1975) belong to long-ranging genera and do not necessarily indicate a Permian age for the Kuta Formation. Rickwood (1955, p. 69-70) used the name Kuta Group for limestone and calcareous arkose exposed east of Kuta Village, and identified several macrofossils, mostly brachiopods, from the unit. He thought the age to be Permian but noted that the macrofauna differed from described Permian faunas from either Australia or Timor. Rickwood's brachiopod identifications are discussed below.

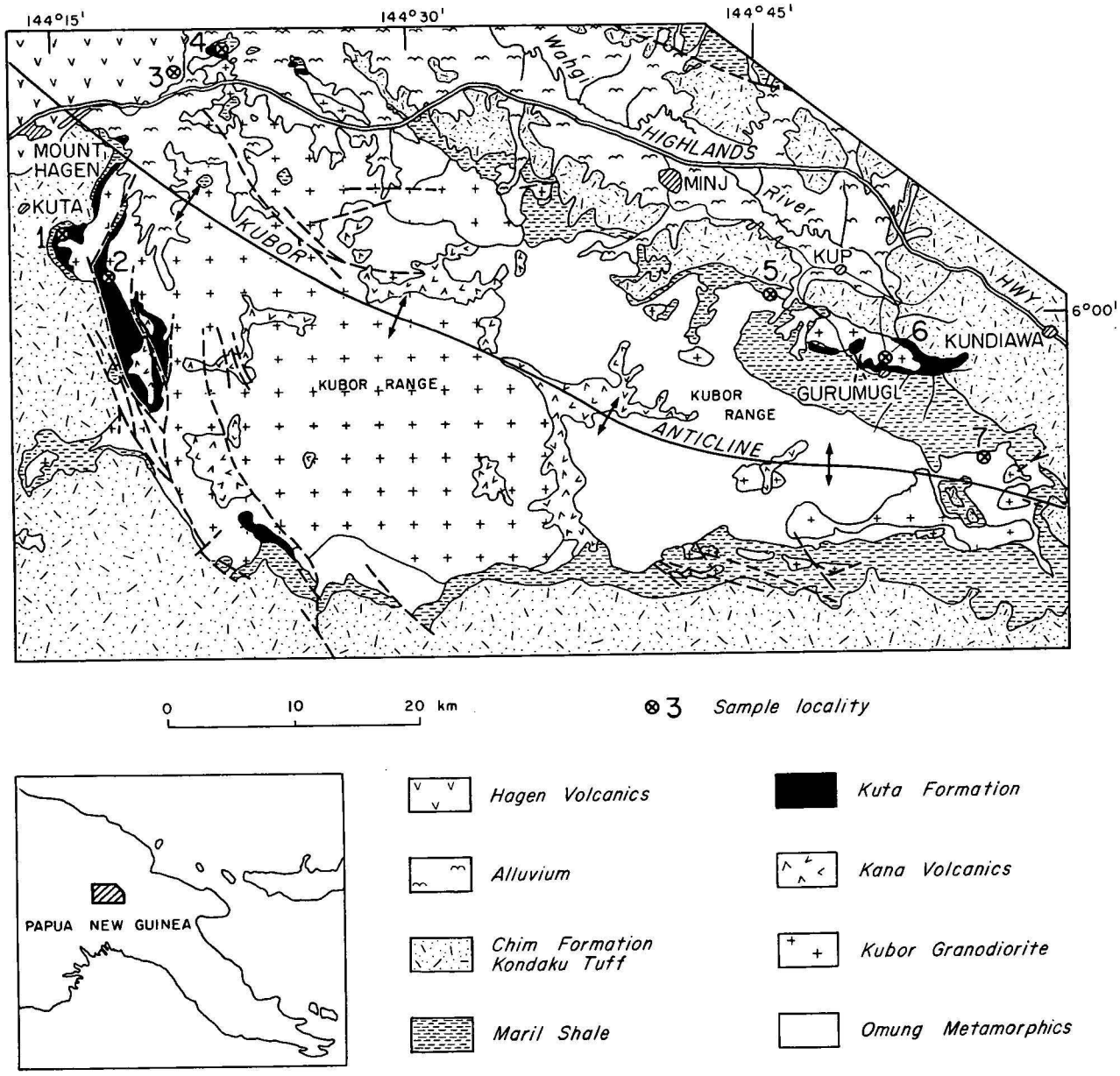

Figure 1. Generalised geologic map of the Kubor Anticline, showing collecting localities. Simplified from Bain & MacKenzie (1974, 1975).

Later collections of macrofossils from the Kuta were cursorily examined by workers at BMR and the Australian National University, who concluded that the fauna probably came from close to the Permian-Triassic boundary (Bain *et al.*, 1970, p. 15).

The recent discovery of the conodont *Misikella posthernsteini* (as *Neospathodus hernsteini* in Bain *et al.*, 1975) was the first indication of a late Norian or a Rhaetian age for at least part of the formation. This age was then confirmed by the recognition of *Arcestes* cf. *A. sundaicus*, a species originally described from Norian-Rhaetian strata of Timor. The athyroid brachiopod *Clavigera* represented by a species comparable with specimens from the late Norian-Rhaetian of New Zealand and New Caledonia offers further support. Finally the age is consistent with the occurrence of brachiopod genera known from farther afield, particularly *Zugmeyerella, Robinsonella, ?Hagabirhynchia* and *Sinucosta*. *Canadospira* and *Stolzenburgiella* suggest slightly greater ages (Carnian and Anisian respectively) but these genera are known from a very limited number of occurrences elsewhere, and their ranges must be greater than previously realised.

Regional geology

The re-evaluation of the age of the Kuta Formation changes the previous interpretation of Permian and Triassic lithostratigraphic relationships in the Kubor Anticline. Figure 2 shows the revised stratigraphic column based on field observation (Bain *et al.*, 1975) and the present palaeontological determinations.

The Omung Metamorphics are regionally metamorphosed, non-calcareous sediments believed to have been deposited in a deep-water marine environment (Bain *et al.*, 1975, p. 16). The metamorphics were later intruded by the Kubor Granodiorite. Page (1971) dated the Kubor Granodiorite as either 244 (Rb-Sr) or 220 m.y. (K-Ar), that is either Late Permian or Early-Middle Triassic, the former being preferred.

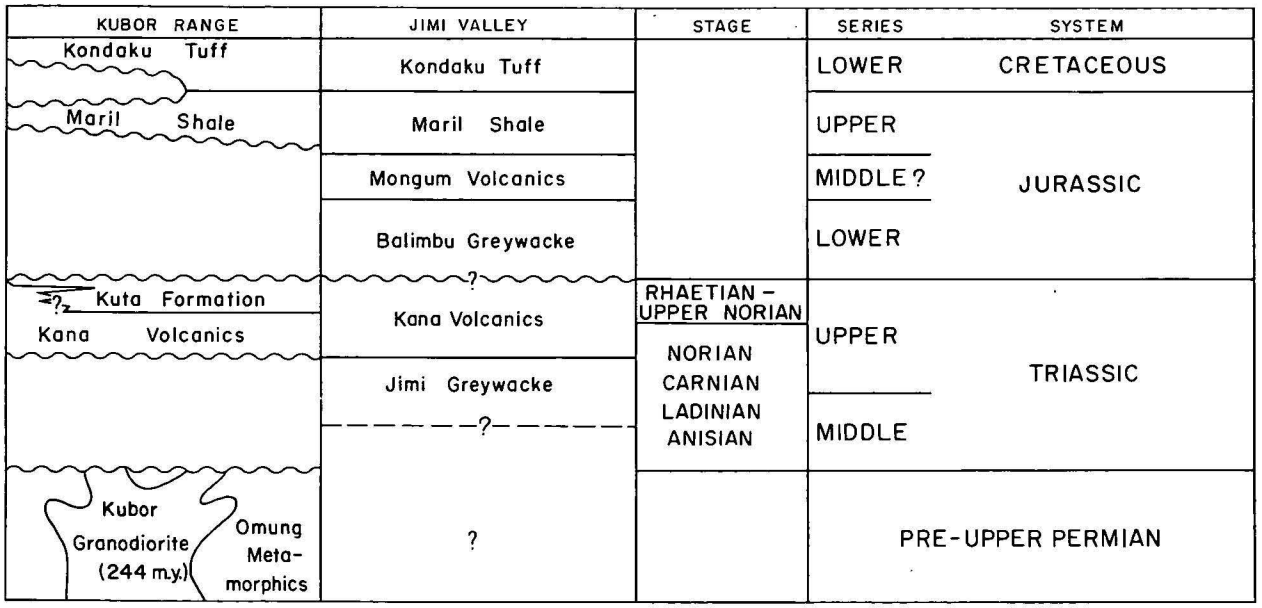

Figure 2. Stratigraphic correlation of Upper Palaeozoic and Lower Mesozoic units in the Kubor Range and Jimi Valley.

Following the intrusion of the Kubor Granodiorite the area was uplifted and subjected to erosion. By the Late Triassic, sedimentation had recommenced in the Jimi Valley area, to the north of the Kubor Anticline, with the deposition of the Jimi Greywacke, followed by the Kana Volcanics. These units were both considered by Skwarko (1967, p. 46) to be Late Triassic (Carnian-Norian) on the basis of macrofossils. The Jimi Greywacke is absent from the Kubor Range but there are remnants of the volcanic rock, up to 700 m thick, on the crest of the Kubor Anticline (Bain *et al.*, 1975). Lithologically these volcanics are similar to the Kana Volcanics but there has been no palaeontological age established for them in the Kubor Range.

On the palaeontological evidence the Kuta Formation is the youngest Triassic (Late Norian-Rhaetian) unit in the area. In the Kubor Range the Kuta Formation rests on a variety of stratigraphic and lithologic units, usually either the Kubor Granodiorite or the Omung Metamorphics. In a few areas it rests on a thin basalt which may be equivalent to the Kana Volcanics, but it has not been found overlying any of the thick volcanic sequences.

Previously the Kana Volcanics were thought to be younger than the Kuta Formation. However this was based on the presumed Permian age of the Kuta Formation. As it has been shown here that the Kuta Formation is, at least in part, younger than the Kana Volcanics, the relationship of these units in the Kubor Anticline is reversed.

In the Kubor Range the Kuta Formation and Kana Volcanics are both unconformably overlain by either Upper Jurassic or Cretaceous units. This depositional break, from latest Upper Triassic to Upper Jurassic probably represents a period of uplift and erosion in the Kubor Range area but Lower Jurassic units are present to the north. The erosion of both the Kuta Formation and Kana Volcanics during that period may help to explain their patchy distribution in the area.

Triassic palaeogeography

Until thirteen years ago no marine deposits of early Mesozoic age were known in Papua New Guinea. Today, following a series of discoveries of fossil assemblages, relatively extensive marine Triassic sedimentary rocks are known from the central part of the country.

There is still no evidence for inundation in the Early Triassic. The oldest known sediments are the Anisian (Middle Triassic) Yuat Formation, at least 600 m thick, on the Yuat River in the Central Highlands. The massive black shale contains some fine silty bands and rare beds of calcareous feldspathic sandstone. The presence of coaly fragments, carbonaceous lenses, small pieces of bone and a rich molluscan fauna (Skwarko, 1973a; Skwarko & Kummel, 1974) together with the absence of graded bedding, indicates a shallow-water environment of deposition (Dow *et al.*, 1972, p. 19).

The next youngest stratigraphic unit is the Carnian-Norian Jimi Greywacke; although probably present at the top of the Yuat River section it is more widespread in the Jimi River area, where it exceeds 800 m in thickness and from where it was first reported and its fauna described (Skwarko, 1963, 1967; Dow & Dekker, 1964, pp. 10-12). The Jimi Greywacke is an indurated fine to medium-grained greywacke and siltstone, commonly micaceous and calcareous, with coarse beds that are generally carbonaceous; there are minor beds of shale and feldspathic sandstone. Cross-bedding and ripple marks have been observed in places. The conformably overlying Kana Volcanics, of similar age, vary in thickness from 200 to 3000 m and consist mainly of interbedded feldspathic arenite and tuffaceous siltstone; massive dacite conglomerate and minor beds of quartz sandstone and calcarenite occur throughout (Dow & Dekker, 1964, pp. 10-12). The Kana Volcanics were deposited in shallow-water; and the Jimi Greywacke in somewhat deeper water.

The recent discovery of Ladinian or Ladino-Carnian Halobiidae in the general outcrop area of the Jimi Greywacke (Skwarko, 1973b) suggests uninterrupted sedimentation between the Anisian and Carnian-Norian. The Norian-Rhaetian age of the Kuta Formation further extends the duration of the Triassic seas in Papua New Guinea. Although the sediments, namely limestone and arkose, are quite different from the older Triassic sediments in the Central Highlands, they, together with their associated fossils, give evidence of shallow-water marine conditions (see Fig. 3).

Apart from the definitely Triassic units discussed above, there are others which may have been formed at least partly in the Triassic time. In this category are the '?Mesozoic-

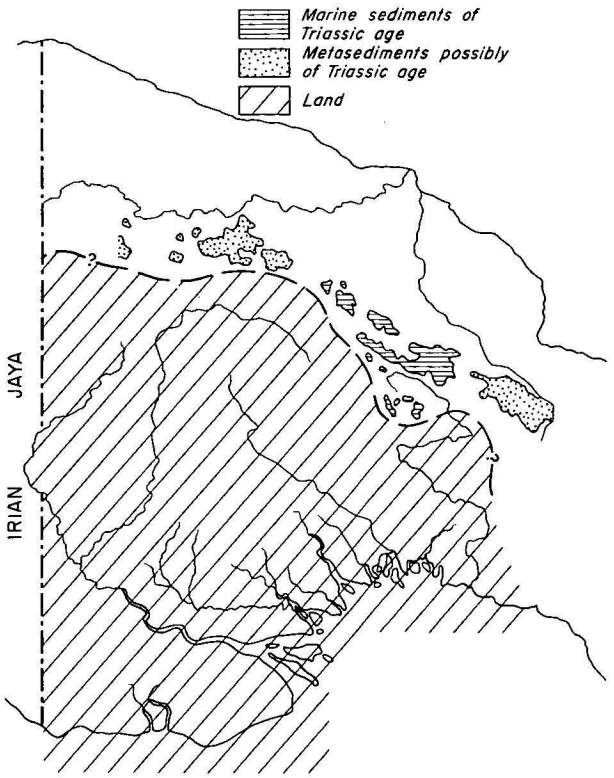

Figure 3. Distribution of Triassic sediments in Papua New Guinea and location of the Triassic shoreline.

Early Tertiary' Ambunti Metamorphics in the South Sepik region, the 'Mesozoic' Bena Bena Formation on the Markham and Karimui 1:250 000 Sheet areas, and the 'Mesozoic' Owen Stanley Metamorphics which extend through most of the length of peninsular Papua.

Figure 3 is an attempt to put the above data in the form of a palaeogeographic map. The coastline of the Triassic landmass is placed south of the Ambunti Metamorphics in the west, the known shallow-water marine sediments in the centre, and the Bena Bena and Goroka Formations as well as the Owen Stanley Metamorphics in the east. The generalizations and the assumptions of such a presentation are obvious, given the paucity of critical data.

Faunal analysis and systematic palaeontology

Details of the conodont, molluscan, and brachiopod elements of the Kuta Formation are given in the following section. All specimens are deposited in the Commonwealth Palaeontologic Collection (CPC) at the Bureau of Mineral Resources, Canberra. Sample locality information is given in Table 1.

Conodont fauna

Only two conodonts were recovered and both are assigned to *Misikella posthernsteini* Kozur & Mock. In Europe *M. posthernsteini* occurs in strata assigned to the *Rhabdoceras suessi* and *Choristoceras marshi* Ammonoid Zones (Kozur & Mock, 1974), which correspond to the Upper Norian Substage and the Rhaetian Stage of the Upper Triassic (Sweet *et al.*, 1971).

The references by McTavish (1975, p. 486) and Bain *et al* (1975, p. 20) to *Neospathodus hernsteini* from the Kuta Formation are to the specimens now assigned to *M. posthernsteini.*

The scarcity of conodonts in the Kuta Formation is probably a reflection of the reduced diversity, and probably also low abundance, of conodonts in the latest Triassic, just prior to their extinction. Rhaetian conodont faunas appear to be impoverished in Europe and absent in North America (Sweet *et al.*, 1971, p. 459). In the Gondwana Region the youngest previously recorded conodont faunas, from New Zealand and India (McTavish, 1975), are from the Upper Norian Substage. McTavish (1975, p. 486) believes the Indian fauna, originally considered Rhaetian by Sahni & Prakash (1973, p. 218) on the presence of *N. hernsteini,* is probably Late Norian. Neither the Indian nor New Zealand conodont faunas contain any elements in common with the Kuta fauna.

Systematics

Genus MISIKELLA Kozur & Mock, 1974

Type species: Spathognathodus hernsteini Mosher, 1967; MISIKELLA POSTHERNSTEINI Kozur & Mock, 1974 Fig. 4 A-H.

1968 *Neospathodus lanceolatus* Mosher (part) p. 930, pl. 115, Fig. 7 only.

1974 *Misikella posthernsteini* Kozur & Mock, p. 247, Figs. 1-4.

Material studied: 2 specimens, CPC 16562 (locality 6, sample PNG-1), 16563 (loc. 6, PNG-0).

Description: A spathognathodoform element with laterally expanded basal cavity and reduced number of oral denticles. The element is slightly bowed laterally with left and right forms. The two specimens recovered have 4 and 3 denticles respectively. The denticles are laterally compressed with sharp margins that are fused to near their tips. The anterior denticles are posteriorly inclined and the upper part of the posterior-most denticle is bent sharply backward and away from the adjacent denticle. The anterior margin is sharp-edged rather than rounded.

The basal cavity is deeply excavated but it cannot be determined if the cavity extended into the denticles. The margin of the basal cavity of specimen CPC 16562 (Fig. 4, A-D) is flared outward near the base, except near the anterior end where the cavity margins narrow abruptly. The other specimen (CPC 16563, Fig. 4, E-H) is only slightly flared at the base. The posterior margin of the element is folded into the basal cavity and a prominent groove, very broad at the base, extends upward to the inflection point of the posterior denticle. The margins of this groove are rounded at the base but become sharp upward. The groove fades out as the posterior denticle becomes prominent.

Remarks: Misikella posthernsteini probably developed from *M. hernsteini* by a reduction in the number of denticles and the in-folding of the posterior margin. Mosher (1968, p. 930) mentions forms with flattened posterior margins and few denticles, which are probably transitional between *M. hernsteini* and *M. posthernsteini,* but gives no indication of their stratigraphic distribution.

The lack of other types of conodont element could indicate that the spathognathodoform morphology was the only surviving element in the conodont organism. However, the recovery of so few specimens more probably implies that conodonts were sparse in the study area and other elements were missed in sampling.

Map Locality	*Sample Number (a)*	*Locality data*	*Fossils studied (b)*	*Weight processed (c)*
	20 NG 2688A	Extensive outcrop, type area of the Kuta Fm, 10.4 km	Bi	12.3 kg
1	20 NG 2688B	SSE of Mount Hagen township, 3.5 km E of Kuta village	Bi	5.3 kg
	20 NG 2688C		Bi	12.9 kg
	20 NG 2688D	Grid ref. RAMU 1:250 000-196344; 5°55′S, 144°15′15″E	B	3.1 kg
2	116	Head of Pagum Ck, 12.5 km SSW of Korn. Sample 117 lies stratigraphically higher than 116 Collected by Rickwood	B	—
	117	Grid ref. RAMU 1:250 000-199341; 5°56′S, 144°17′E	B	—
3	20 NG 1319A	Small outcrop north of the Highlands Hwy, 12 km ENE of Mount Hagen township Grid ref. RAMU 1:250 000-205351; 5°49′25″S, 144°20′E		4.0 kg
4	20 NG 1377	Small outcrop north of the Highlands Hwy, 16 km ENE of Mount Hagen township	Bi	2.1 kg
	20 NG 1377A	Grid ref. RAMU 1:250 000-208357; 5°48′20″S, 144°22′E	B	2.0 kg
5	C 26/27	Rickwood sample, exact locality unknown, labelled NORMANZ LS, probably equates to BMR field locality 20 NG 0573; 10 km SE of MINJ township, vicinity of Dek village Grid ref. RAMU 1:250 000-251338; 5°58′40″S, 144°45′05″E	B	—
6	21 NG 0664	Samples from outcrop forming ridges north and northeast	B	2.0 kg
	21 NG 0665	of Gurumugl village, 13 km W of Kundiawa	B	—
	PNG-0	Samples PNG0 to 3 collected by Skwarko & Brown, 1972	B, Co	1.5 kg
	PNG-1		B, C, Co	4.8 kg
	PNG-2	Grid ref. KARIMUI 1:250 000-261332; 6°02′S, 144°50′25″E	C	6.7 kg
	PNG-3		C	4.0 kg
7	21 NG 0660	Sample may be either Kuta Fm or Maril Shale, from side of village road, 11 km SSW of Kundiawa Grid ref. KARIMUI 1:250 000-269325; 6°06′S, 144°54′50″E		2.0 kg
Not located	164	Rickwood locality 164, no data available	B	—
	None	Sample located only as 'Triassic Hills S of Mt Hagen', probably from the vicinity of locality 1 above		1.8 kg

Table 1. Collecting localities

(a) 20 NG and 21 NG samples were collected by BMR field parties during regional mapping.
(b) indicates fossil groups recovered and included in this paper. B—brachiopod, Bi—bivalve, C—cephalopod, Co—conodont.
(c) weight of samples processed for conodonts.

Molluscan fauna

Cephalopoda

Superfamily ARCESTACEAE Mojsisovics, 1875
Family ARCESTIDAE Mojsisovics, 1875

The available specimens, all incomplete, appear to belong to the Arcestidae, one of the six families of Middle and Late Triassic ammonites included in the Arcestaceae. Joannitidae can be distinguished by the overall curvature of the suture and its greater number of elements, as well as by the presence of bifurcating saddles; the Sphingitidae have a much wider umbilicus; the Cladiscitidae have more flattened whorl sides and venter; the Megaphyllitidae and generally larger Nathorstitidae both have ceratitic sutures with phylloid saddles—multisellate in the latter. In the context of this paper the relative size of the former is not significant, and the sharp venter of the Nathostitidae, although one more differentiating feature, can safely be omitted for ease of expression. The relationship of our specimens to the Arcestidae is clearly established through the presence of a modified peristome, and a straight ammonitic suture with both lobes and saddles triangular in shape, in combination with pronounced involution, considerable inflation, and a complexly subdivided ammonitic suture with a dividend ventral lobe and a series of lateral lobes decreasing in size towards the umbilicus. There is no specimen in the collection with a complete body chamber.

Genus ARCESTES Suess, 1865

Type species: Ammonites galeiformis Hauer, 1865 (pro *Am. glaeatus* Hauer, 1864; non von Buch); SD Mojsisovics, 1893.

There are six subgenera of *Arcestes*, a cosmopolitan genus of the Anisian-Rhaetian times. Our specimens lack the discoidal cross-section and rather complicated umbilicus cf. *Stenarcestes* Mojsisovics, 1895, the radial ribbing or ridging on the body chambers of both *Ptycharcestes* Mojsisovics, 1893, and *Anisarcestes* Kittl, 1908, and the constrictions and flared ribs on the phragmocone and body chamber of *Pararcestes* and *Proarcestes* Mojsisovics, 1893. They are consequently referred to the *Arcestes* s. str.

ARCESTES (ARCESTES) cf. SUNDAICUS Welter, 1914
Figs. 5, 6, 7, 8, G, H, L, 9A, E, G, H,

Material: Only five ammonites have been collected from the Kuta Formation. They are incompletely preserved, and from three geographically close sites. Diagnostic features which can be observed in one specimen generally cannot be observed in the others because of the unsatisfactory preservation. Four of the specimens are considered to represent the same species, but I have preferred to describe them individually, thereby showing clearly which specimen contributed which diagnostic features to the overall description.

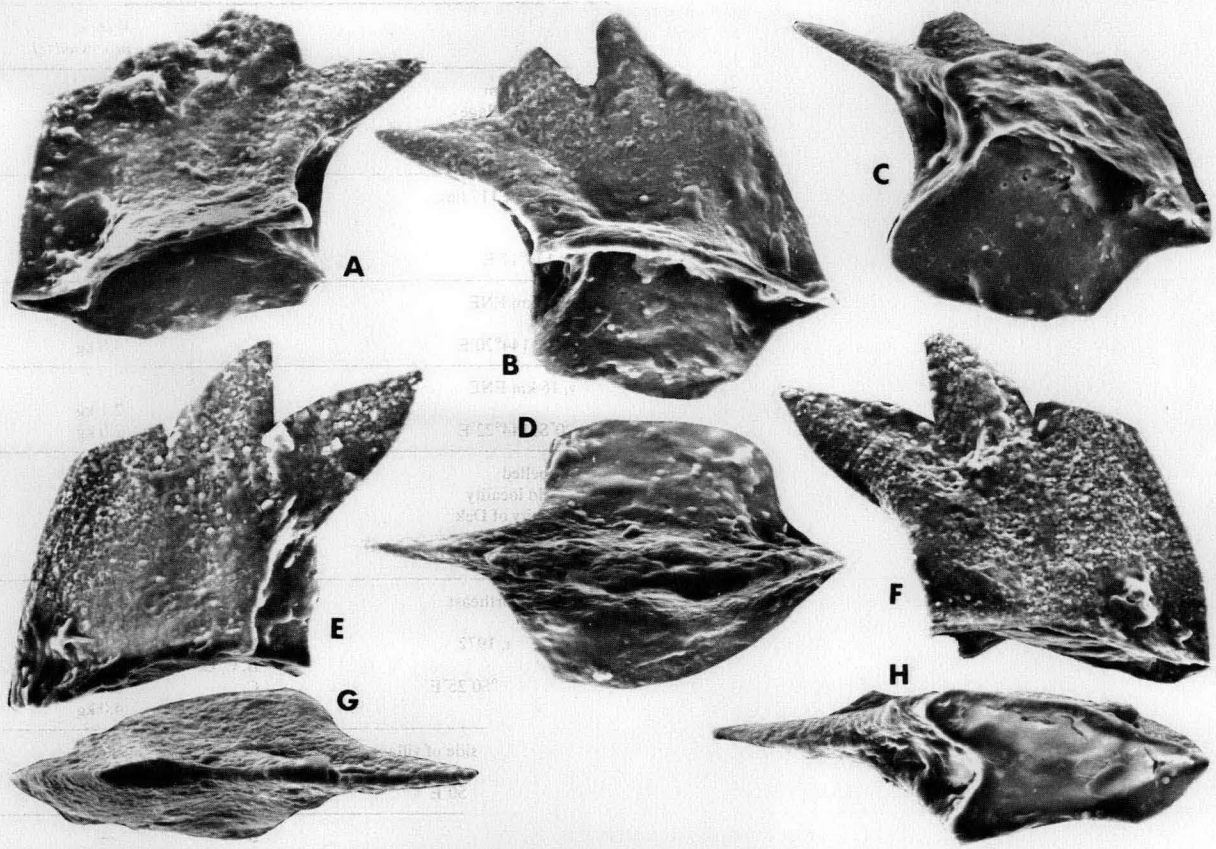

Figure 4. *Misikella posthernsteini* **Kozur & Mock. A-D left lateral, right lateral, aboral, and oral views of specimen CPC 16562; E-H, left lateral, right lateral, oral and aboral views of specimen CPC 16563. All specimens 200X**

Specimen CPC 15757 (loc. 6, PNG-2)—Figs. 9A, E, G

This, the most nearly complete specimen in the collection, is about 190 mm high and 110 mm across its widest part. It is involute with a completely smooth exterior. The body whorl is long and spindle-shaped in cross-section; the earlier whorls have a much more spheroidal cross-section. The shape of the peristome is unknown. the umbilicus is deep but with a narrow opening only about 18 mm across, its size reduced somewhat by a callus growing off at least a part of the umbilical shoulder. Inside the conch the umbilicus broadens somewhat before finally tapering off.

The sutures are complex ammonitic and closely spaced, and seem to be similar to that illustrated for CPC 15758 (Fig. 5).

Specimen CPC 15758 (loc. 6, PNG-2)—Figs 5, 8H, L

The presence of the suture pattern over the whole surface of this incomplete conch, together with the globose cross-sectional shape of the whorls, suggests that it is an internal whorl of a much larger shell. The surface is smooth.

Specimen CPC 15759 (loc. 6, PNG-1)—Figs 6, 8G

This is the only specimen in the collection with a complex mature suture pattern, some of which it is possible to reproduce (Fig. 6). In addition this is the only specimen which has constrictions, shallow though they may be: one of the phragmocone, and another on the body chamber not far from the line of the last suture.

When compared with CPC 15757 this specimen seems to be larger, with a larger umbilicus, and with possibly a more globose portion of the shell ventral to the umbilicus.

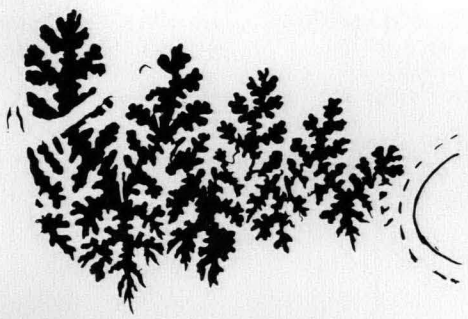

Figure 5. Suture line of specimen CPC 15758—*Arcestes (Arcestes)* cf. *sundaicus*.

Figure 6. Suture line of specimen CPC 15759—*Arcestes (Arcestes)* cf. *sundaicus*

Specimen CPC 15760 (loc. 6, PNG-2)—Fig. 9H

This fragment of a large specimen comes from the distal-most portion of the body chamber and gives an insight into the shape of the aperture.

The margin of the aperture, i.e. the peristome, is complexly flexed (Fig. 7), but only portions of it are preserved and can be traced. As the chamber is followed toward the aperture, its dorsolateral wall maintains or even increases a little its inflation, before plunging steeply inwards while the ventrolateral part of the body wall becomes broadly but only slightly invaginated before swelling outward into two dome-like areas one on each side of the venter; a long, depressed strip with a fairly prominent linear median ridge precedes and parallels the peristome (Fig. 7).

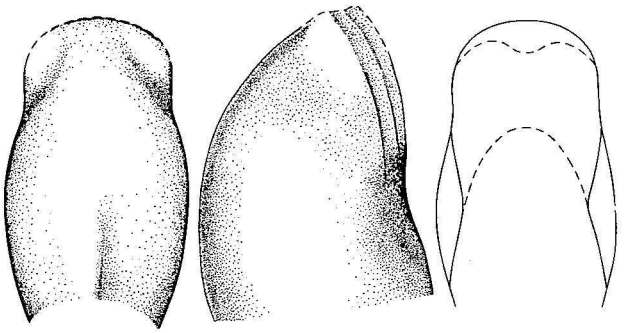

Figure 7. The body whorl and aperture shape of *A.* cf. *sundaicus* as reconstructed mainly from specimen CPC 15760. Because of the poor preservation of this specimen some structures may have been misrepresented. The sharpness of the keel shown on the left hand side figure may be a result of crushing

Discussion: Close similarity of the suture patterns and of the cross-sectional shape of the inner whorls leaves little doubt that specimens CPC 15757 and 15758 are conspecific. On comparison of these with CPC 15759 the similarity is, at first glance, not as obvious. This is because of the presence in CPC 15759 of constrictions on both phragmocone and body whorl, and because of the greater complexity of its suture pattern. However, the constrictions are extremely shallow and weakly defined, which implies that in this species the tendency towards formation of these structures is not very strong; from this it follows that within the range of intra-specific variation one could expect some specimens altogether free from constrictions. Regarding the differences in the suture patterns it is stressed that in both CPC 15757 and 15758 the sutures are on the immature part of the conch. In CPC 15759 on the other hand, it is the most mature set of sutures available for study and comparison, and these would be expected to be more complicated. All three specimens, CPC 15757-9, are thought to represent a single species.

Dr Y. Bando (pers. comm.), though agreeing with the identification of specimens CPC 15757 and CPC 15759 suggests that specimens CPC 15758 and CPC 15761 may in fact be a new species, the large size of their umbilicus making them comparable to the ammonite referred to by Welter (1914, pl. 29, fig. 20) as *Arcestes* sp. nov. ind. ex aff. *rothpletzi* Welter. Though Fig. G on Plate 9 of this paper shows that the umbilicus on the inner whorls of *A.* cf. *sundaicus*—and specimens CPC 15758 and CPC 15761 are such inner whorls—is in fact larger than on the last whorl where its size is reduced by a callus, Bando's valuable observation may indeed be correct.

CPC 15760, though a large specimen, represents in fact a small portion of the complete shell. It is a part of the most distal portion of the conch, and in our collection it shows the shape of the peristome. This specimen may well belong to the same species as those discussed above, but it is so incomplete that without additional material it will never be possible to verify its identification.

Comparison with other species: The great number of species of *Arcestes* s. str. already described, many of them in old literature, as well as the fragmentary nature of the available material seemingly makes identification not only difficult but also questionable. However,the large size of our mature specimens in itself eliminates most species from consideration, and the complex shape of the peristome also helps to narrow the field to but a few species of which *A.* (*A.*) *sundaicus*, described by Welter (1914) from undifferentiated Norian-Rhaetian strata of Timor, seems to be the most closely related. *A. sundaicus* is so far unknown beyond Timor, so its presence in the Kuta Formation cannot be used for dating more closely than 'Norian-Rhaetian'.

ARCESTES sp. indet.
(Fig. 8C, D)

Specimen CPC 15761: (loc. 6, PNG-3)

This small specimen almost certainly represents an inside portion of a larger shell. Its surface is covered by suture patterns of simple ammonitic type, having at least 8 elements and there is one moderately well preserved constriction. Its cross-section is compressed, and the inflation is much less than could be expected by comparison with the cross-section of the inner whorls of specimen CPC 15757. It is suggested that specimen CPC 15761 represents a species distinct from that represented by other specimens in the collection.

The evidence that CPC 15761 probably belongs to a different species from those above is fairly convincing and seen in the apparently greater involution of its whorls and their lesser inflation.

Bivalvia

In the Kuta Formation the bivalves are poorly represented. Specimens are few and fragmentary; their preservation allows only limited insight into external morphology, and no opportunity to study the hinge and other internal structures. The material illustrated and discussed here has been chosen mainly to complete the presentation of the fossil record. All identifications are tentative.

Family PECTINIDAE Rafinesque, 1815
CHLAMYS Group
Genus CHLAMYS Roding, 1798

Type species: Pecten islandicus Muller, 1776; SD Herrmannsen, 1847

CHLAMYS? sp. nov.
(Fig. 8A, B, E, F)

Material studied: At least five fragments. CPC 15764, 15766, 16909, 15765 (all loc. 1, 20NG2688C).

Description: Shell large, auriculate and orthocline, with unequally inflated valves, and with well defined and inflated umbo on convex valve bordered at least on one side with umbonal ridge. Both valves radially striated with regularly spaced primary riblets, their thickness increasing gradually and evenly distally; interspaces somewhat narrower than riblets. Secondary riblets, originating away from umbo are somewhat thinner than primary ones, few in number and irregularly arranged.

Remarks: In the course of discussions with Professor J. A. Grant-Mackie and Dr K. Nakazawa regarding the possible identity of this enigmatic bivalve a number of

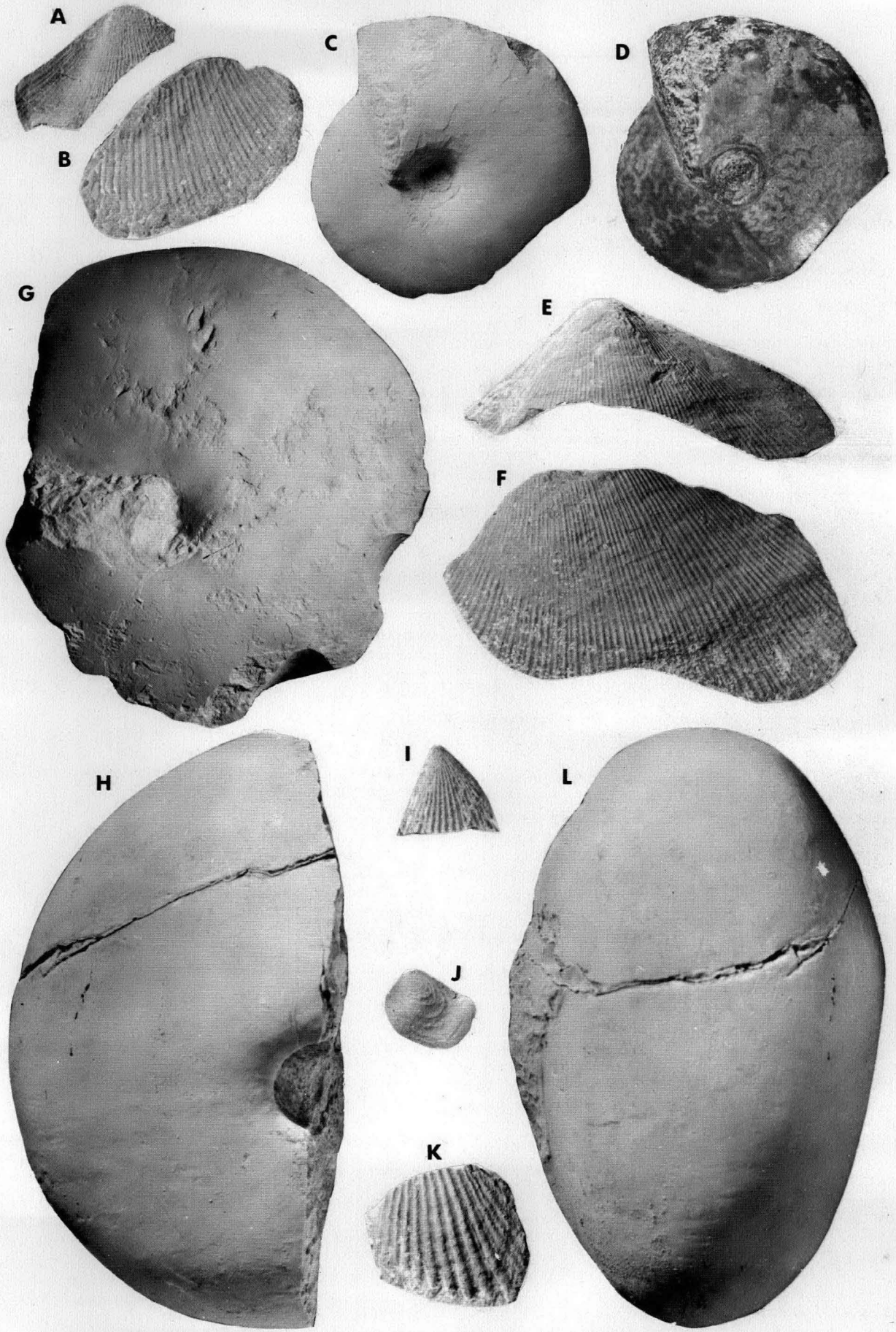

Figure 8. All specimens of natural size, coated with ammonium chloride and photographed in lateral view unless otherwise noted. A, B, E, F, *Chlamys?* sp. nov. A, fragment of proximal part of shell, external view, CPC 15764 (loc. 1, 20NG2688C); B, fragment of distal margin of shell, external view, CPC 15766 (loc. 1, 20NG2688C); E, incomplete proximal part of shell, external view, locality 20NG2688g. CPC 16909 (loc. 1, 20NG2688C); F, large fragment of medium part of inflated valve, external view, CPC 15765 (loc. 1, 20NG2688C). C, D, *Arcestes* sp. indet. Juvenile specimen in lateral view, coated with ammonium chloride, and bare showing suture pattern. CPC 15761 (loc. 6, PNG-3). G, H, L, *Arcestes (A.)* cf. *sundaicus* Welter, 1914. G, incomplete mature specimen, x 0.5, CPC 15759 (loc. 6, PNG-1); H, L, immature part of conch in lateral and ventral views, CPC 15758 (loc. 6 PNG-2); I, K, *Limea?* sp. Two fragments probably of same specimen, CPC 15763 (loc. 1, 20NG2688); J, *'Ostrea'* sp. Probably immature specimen, CPC 15762 (loc. 1, 20NG2688).

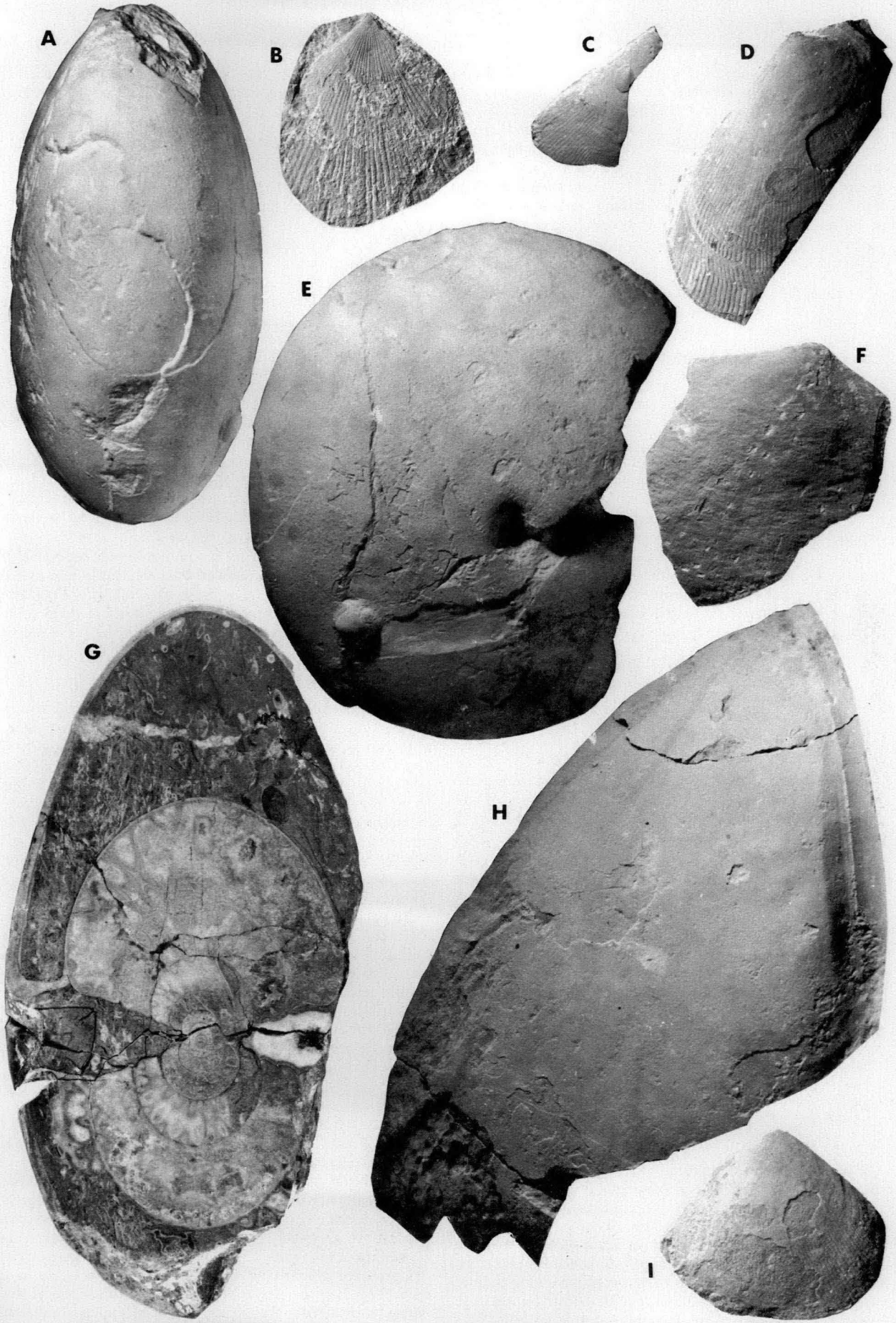

Figure 9. All specimens of natural size, coated with ammonium chloride and photographed in lateral view unless otherwise noted. A, E, G, H, *Arcestes (A.)* cf. *sundaicus* Welter, 1914. A, E, plaster copy of specimen in ventral and lateral view, x 0.5, CPC 15757 (loc. 6, PNG-2); G, cross-section of specimen cut along line shown in 5, x 0.7, CPC 15757 (loc. 6, PNG-2); H, portion of distal-most part of shell showing detail of structure of aperture, x 0.9, CPC 15760 (loc. 6, PNG-2). B, *Pecten* s.l., left valve, CPC 15768 (loc. 4, 20NG1377). C, D, F, I, *Plagiostoma* sp. C, young left valve incomplete posteroventrally, CPC 15770 (loc. 1, 20NG2688A); D, mature left valve incomplete posteroventrally, CPC 15771 (loc. 1, 20NG2688A); F, distally incomplete, weakly ornamented left valve, CPC 15767 (loc. 1, 20NG2688B); I, incomplete valve, CPC 15769 (loc. 1, 20NG2688B).

genera have been considered, including *Monotis, Limatula, Plagiostoma, Leptochondria, Eopecten, Eumorphotis* and *Chlamys*. In referring it to *Chlamys* I follow Nakazawa's suggestion, as its resemblance to the much smaller *C. (Praechlamys) inaequialternans* (Parona, 1889) from the middle Carnian of Southern Alps is indeed striking. In fact its similarity to the also smaller *C. (P.) inconspicua* (Bittner, 1901) seems to be hardly less striking, and I think that additional material, should it become available, will confirm the shell as a large new species of *Chlamys (Praechlamys)*.

Family AVICULOPECTINIDAE Meek & Hayden, 1864
AVICULOPECTINIDAE? indet.
(Fig. 9B)

Material studied: one specimen—CPC 15768 (loc. 4, 20NG 1377)

There is only one incomplete valve in the collection. It is 40 mm high, with a pointed right-angle umbo, and is radially striated with low flat riblets which increase in breadth very gradually distally bifurcating in the process. The interspaces are linear and shallow. The auricle bears riblets similar to those on the main body of the valve.

Remarks: This specimen is either a right valve of an Aviculopectinid—as suggested by the bifurcating ribs and presence of radial riblets on the ear (Nakazawa, pers. comm.) or a left valve of a member of the *Pecten* group. The material in hand does not allow to establish the relationship between this specimen and the five specimens referred to *Chlamys (Praechlamys)*? sp. nov. above.

Family LIMIDAE Rafinesque, 1815
Genus PLAGIOSTOMA J. Sowerby, 1814

Type Species: Plagiostoma giganteum J. Sowerby, 1814

PLAGIOSTOMA sp.
(Fig. 9C, D, F, I)

Material studied: One ventrally and two posteriorly and ventrally incomplete left valves, one of them juvenile; one proximally incomplete right valve. CPC 15770 and 15771 (both loc. 1, 20NG2688A) and CPC 15767 and 15769 (both loc. 1, 20NG 2688B).

Description: Shell about 60 mm long and probably about 55 mm high, weakly to moderately inflated, with weak ornamentation over most of shell surface. Posterior auricle long, with shell margin beneath it initially flexed inwards then broadly convex. Anterior umbonal margin broadly and gently concave. Surface of valve—apart from beak area—ornamented with fine, shallow, somewhat sinuous flat riblets which increase in breadth very gradually distally; riblets separated by linear interspaces, and periodically somewhat offset by growth-rugae.

Genus LIMEA? Bronn, 1831

Type species: Ostrea strigilata Brocchi, 1814

LIMEA? sp.
(Fig. 7I, K)

Two fragments which probably belong to the one and the same valve (CPC 15763) are strongly ribbed with costae which radiate from a narrow and pointed umbo, gradually and evenly increasing in breadth distally. The ribs are robust and U-shaped (inversed) in cross-section; they are separated from each other by deep interspaces of about the same width as the ribs. Two interspaces have longitudinal threads in the middle along their length. In what appears to be the posterior part of the shell the ribs are reduced in size and relief, and seem to be more closely spaced.

Remarks: The preservation of the valve does not allow to determine whether it is an internal cast or an external mould; if an internal cast than the ribs are preserved less angular in cross-section than they should be, and the shell is probably *Pseudolimea*.

Family OSTREIDAE Rafinesque, 1815
'OSTREA' sp.
(Fig. 8J)

Material studied: One specimen—CPC 15762 (loc. 1, 20NG 2688).

The valve is probably that of a small oyster. It has a narrow sharp umbo and is concentrically ribbed with unevenly spaced growth-rugae. The strongly flexed surface reduces the likelihood of its being *Posidonia* or *Claraia*. A somewhat similar oyster has been described from the Triassic of Timor (Welter, 1914).

Brachiopod fauna

In the present study I have had access to the collection reported on by Rickwood (1955) and subsequent material collected by Bain *et al.* (1970) and by Brown and Skwarko in 1972. Much of the Rickwood material was calcined so that the specimens could be extracted with greater ease. Nevertheless it has still proved suitable for sectioning, and by further breaking up some of the blocks more genera have been obtained.

The Rickwood specimens are unnumbered, but some of them are in the original labelled boxes so that it is possible to refer to the individuals he used. The following notes are based on these specimens, supplemented where possible by others from the same collection and from the more recent collections.

Systematic notes

Terebratuloids. Several small terebratuloids are known from a number of localities. There are at least three different genera represented, one of which has dental lamellae and a short septalium supported on a septum that extends about one-third the length of the valve. It is this form that was referred to *Dielasma* cf. *elongatum* (Schlotheim) by Rickwood (1955). The calcite infilling has prevented preparation of the loop, and so generic identification is not yet possible. The form of the shell and the umbonal characteristics suggest that it is a species of *Zeilleria* Bayle.

Among the larger terebratuloids is the form referred to by Rickwood as *Dielasma* cf. *itaitubense* (Derby), a Brazilian Carboniferous species with strong dental lamellae and a long sessile septalium, whose loop is unknown. The New Guinea specimens also have dental lamellae but the inner hinge plates meet the floor of the valve separately at least towards the front of the narrow spetalium. The loop is short and lacks a median plate, and the crural points are high. The specimens probably belong to a new genus.

Spiriferoids.

Canadospira sp.

Several isolated pedicle and brachial valves are referred to this genus. They have the general form, smooth fold and sinus, simple sub-rounded lateral plicae, high cardinal area, dental lamellae, ventral median septum, dorsal median septum supporting the cardinal process, coarse punctation, and finely pustulose surface of the type species *C. canadensis* (Logan). It has not been possible to confirm the presence of denticle grooves on the ventral cardinal area. The form of the shell, the number and size of the plicae, and the orientation and height of the cardinal area are also variable, as in the type species (see Logan, 1967).

According to Dagis (1974) the genus is known only from the Carnian in far eastern USSR and Arctic Canada.

Specimens of this species were referred to *Spiriferina* sp. by Rickwood.

Spiriferinid *indet*

A smooth coarsely punctate brachial valve with a high smooth fold and a parasulcate commissure is included here. The length of the hinge is unknown, but it is probably brachythyrid. It has similar contours to *Laballa* Moisseiev, but without a pedicle valve definite identification is impossible.

Zugmayerella sp.

Two pedicle valves and at least one brachial valve are placed in this genus. The characteristic internal structures of the pedicle valve and the denticle grooves on the cardinal area have been observed. Pedicle and brachial valves are separated, and since *Canadospira* occurs at the same locality it is not possible to be sure of the assignment of all the broken brachial valves.

This genus is known from the Norian-Rhaetian of Tethys and far-eastern USSR.

Specimens were identified as *Spiriferina* by Rickwood.

Sinucosta sp.

Three isolated pedicle valves, a broken specimen with the two valves together, and about ten isolated brachial valves are assigned to this genus. They have the separated dental lamellae and medium septum in the pedicle valve, and the long and widely divergent crural plates characteristic of the genus. The ventral cardinal area is too high and the sinus a little too deep for them to be referred to *S. emmrichi* (Suess). The genus is widespread in the Middle-Late Triassic of Tethys and extends into the Lias in Europe. The greatest similarities are with Norian-Rhaetian species.

It was an isolated brachial valve of this species that was referred to *Streptorhynchus* cf. *pyramidalis* King by Rickwood.

Athyroids.

Clavigera sp.

Several specimens of isolated valves and three with valves together clearly belong to this genus. The identification has been confirmed by Dr J. D. Campbell of Otago University, who notes that they are similar to young specimens of *Clavigera* from the New Zealand Otamitan and Otapirian (late Norian-Rhaetian). The genus occurs in a similar stratigraphic position in New Caledonia.

Stolzenburgiella n. sp.

Two almost complete individuals and many broken isolated valves probably belong to this genus. The doubt in the identification comes from the lack of data on the internal structure of the type and only known species, *S. bukowskii* Bittner, from the Anisian of the Dinaride Alps.

Rhynchonelloids. There are at least four genera of rhynchonelloids in the faunas.

Costirhynchia sp.

This genus can be confidently identified. It is known from the Middle and Late Triassic of the Alps, Carpathians, Caucasus and China (Dagis, 1974).

Robinsonella sp.

Several specimens of this genus are present. It comes from the Norian and Rhaetian of the Alps, Balkans and Caucasus (Dagis, 1974).

Among the others is a representative of the Praecyclothyridinae Makridin, that is similar in many respects to *Hagabirhynchia* Jeffries. This whole subfamily is restricted to the Late Triassic, and *Hagabirhynchia* is from the Norian of Oman, the Himalaya and Indonesia.

Strophomenoids.

Thecidacean indet.

The single valve in the Rickwood collection that was referred to *Marginifera* is a wide straight-hinged form with a sharply reflexed margin. The shell structure is coarsely fibrous—definitely not pseudo-punctate. It cannot be a productacean. On the other hand, although the shell structure is compatible with a thecidacean assignment, the specimen is unusually large for a member of that group, and the shell form is different from any genus as presently assigned to it. Proper identification awaits the discovery of the other valve and the internal structure.

Age

There is no guarantee that the sampling localities are all on the same stratigraphic level. Consequently the faunas are listed separately.

Locality 2 (Fig. 1, table 1)—Rickwood's loc. 116.

Species represented:

?*Zeilleria* sp.
Large Terebratuloid ('*D. cf. itaitubense*')
Canadospira sp.
Zugmeyerella sp.
Sinucosta sp.

Age: *Zugmeyerella* indicates a Norian-Rhaetian age and the species of *Sinucosta* is similar to Norian-Rhaetian species in Tethys. *Canadospira*, on the other hand, is known only from the Carnian, though it is recorded from only a few localities. The age is clearly Late Triassic with a Norian-Rhaetian restriction preferred.

Locality 2 (Fig. 1, Table 1)—Rickwood's loc. 117

Species represented:

?*Zugmeyerella* sp.
Clavigera sp.
Thecidacean indet

Age: The significance of *Clavigera* is discussed below.

Rickwood's locality 164 (locality not located, Table 1):

Species represented:

Large Terebratuloid ('*D. cf. itaitubense*')
Stolzenburgiella sp.

Locality 5 (Fig. 1, Table 1)—Rickwood's loc. C26/7

Species represented:

Rhychonelloids indet.
Robinsonella sp.
Sinucosta sp.

Age: The *Robinsonella* and *Sinucosta* both indicate Norian-Rhaetian age.

Locality 6 (Fig. 1, Table 1)—samples PNG-0, PNG-1

Species represented:

Clavigera sp.
Spiriferinid indet.
Large Terebratuloid ('*D. cf. itaitubense*')
Costirhynchia sp.
?*Hagabirhynchia* sp.

Age: *Clavigera* sp. being closely comparable with late Norian-Rhaetian species in New Zealand and New Caledonia, is regarded as most significant. *Costirhynchia* is consistent with this age, and *Hagabirhynchia* supports a Norian assignment.

Locality 1 (Fig. 1, Table 1)—sample 20NG 2688D

Species represented:

Calvigera sp.

Age: Late Norian-Rhaetian

Localities 4, 6 (Fig. 1, Table 1)—samples 20NG 1377A, 21NG 0664, 21NG 0665

Species represented:

Stolzenburgiella sp.

Age: Middle-Late Triassic. Since this genus is known only from the Anisian overseas it is difficult to know how to date these occurrences. The only known species is *S. bukowskii,* so further discoveries are bound to extend the generic range. The fact that it occurs at Locality 164 with the same large terebratuloid as occurs with *Clavigera* elsewhere in the Kuta Limestone, suggests that a Norian-Rhaetian age is not impossible.

Apart from *Clavigera* which is only known from the Maorian Province, and *Canadospira* from the far eastern USSR and Canada, all the brachiopod genera identified are from the Tethyan Province. Most of them are from the European or Middle Eastern part of the province, but their apparent absence farther east is probably due to a lack of study of the faunas in south east Asia.

References

BAIN, J. H. C., & MACKENZIE, D. E., 1974a—Ramu, Papua New Guinea, 1:250 000 Geological Series. *Bureau of Mineral Resources, Australia—Explanatory Notes* **SB/55-5.**

BAIN, J. H. C., & MACKENZIE, D. E., 1974b—Karimui, Papua New Guinea 1:250 000 Geological Series. *Bureau of Mineral Resources, Australia—Explanatory Notes* **SB/55-9.**

BAIN, J. H. C., MACKENZIE, D. E., & RYBURN, R. J., 1970—Geology of the Kubor Anticline—central highlands of New Guinea. *Bureau of Mineral Resources, Australia—Record* **1970/79** (unpublished).

BAIN, J. H. C., MACKENZIE, D. E., & RYBURN, R. J., 1975—Geology of the Kubor Anticline, central highlands of Papua New Guinea. *Bureau of Mineral Resources, Australia—Bulletin* **155.**

DAGIS, A. S., 1974—Triassic brachiopods (morphology, classification, phylogeny, stratigraphical significance and biogeography). *Trudy Instituta Geologii i Geofiziki Sibirskoe Otdelenie Akademiya Nauk SSSR,* 214, 388p. *Nauka Press, Novosibirsk.*

DOW, D. B., SMIT, J. A. J., BAIN, J. H. C., & RYBURN, R. J., 1972—Geology of the south Sepik region, New Guinea. *Bureau of Mineral Resources, Australia—Bulletin* **133.**

DOW, D. B., & DEKKER, F. E., 1964—The geology of the Bismarck Mountains, New Guinea. *Bureau of Mineral Resources, Australia—Report* **76.**

GLAESSNER, M. F., LLEWELLYN, K. M. & STANLEY, G. A. V., 1950—Fossiliferous rocks of Permian age from the Territory of New Guinea. *Australian Journal of Science,* **13,** 24-25.

KOZUR, HEINZ & MOCK, RUDOLF, 1974—*Misikella posthernsteini* n. sp., die jungste. Conodontenart der tethyalen Trias. *Casopis pro mineralogii a geologii,* **19,** 245-250.

LOGAN, A., 1967—Middle & Upper Triassic spiriferinid Brachiopods from the Canadian Arctic Archipelago. *Geological Survey of Canada—Bulletin* **155,** 1-37.

MCMILLAN, N. J., & MALONE, E. J., 1960—The geology of the eastern central highlands of New Guinea. *Bureau of Mineral Resources, Australia—Report* **48.**

MCTAVISH, R. V., 1975—Triassic Conodonts and Gondwana stratigraphy; *in* K. S. W. CAMPBELL (Editor), GONDWANA GEOLOGY; papers from the 3rd Gondwana Symposium, 481-490, *Australian National University Press, Canberra.*

MOSHER, L. C., 1968—Triassic conodonts from western North America and Europe and their correlation. *Journal of Palaeontology,* **42,** 895-946.

PAGE, R. W., 1971—The geochronology of igneous rocks in the New Guinea region. *Ph.D. thesis, Australian National University.* (unpublished).

RICKWOOD, F. K., 1955—The geology of the western highlands of New Guinea. *Journal of the Geological Society of Australia,* **2,** 63-82.

SAHNI, ASHOK & PRAKASH, INDRA, 1973—Rhaetic conodonts from the Niti Pass Region, Painkhanda, Kumaun Himalayas. *Current Science (India)* **42,** 218.

SKWARKO, S. K., 1973a—Middle and Upper Triassic Mollusca from Yuat River, eastern New Guinea. *Bureau of Mineral Resources,* Australia—Bulletin **126,** 27-50.

SKWARKO, S. K., & KUMMEL, B., 1974—Marine Triassic Mollusca from Yuat River, eastern New Guinea. *Bureau of Mineral Resources, Australia—Bulletin* **126,** 27-50.

SKWARKO, S. K., 1973b—On the discovery of Halobiidae (Bivalvia, Triassic) in New Guinea. *Bureau of Mineral Resources, Australia—Bulletin* **126,** 51-54.

SKWARKO, S. K., & KUMMEL, B., 1974—Marine Triassic Mollusca of Australia and Papua New Guinea. *Bureau of Mineral Resources, Australia—Bulletin* **150,** 1-18.

SWEET, W. C., MOSHER, L. C., CLARK, D. L., COLLINSON, J. W., HASENMUELLER, W. A., 1971—Conodont—Biostratigraphy of the Triassic; *in* W. C. SWEET & S. M. BERGSTRAM (Editors), *Symposium on Conodont Biostratigraphy. Geological Society of America—Memoir* **127,** 441-465.

WELTER, O. A., 1914—Die obertriadischen ammoniten und nautiliden von Timor. *Palaeontologie von Timor*—(Stuttgart), **1,** 1-252, 36 pls.

BMR J. Aust. Geol. Geophys. 1 (1976), 231-240

The evolution of One Tree Reef, Southern Great Barrier Reef, Queensland

Peter J. Davies, B. M. Radke, and C. R. Robison

One Tree Reef is one of fourteen reefs in the Capricorn Group, southern Great Barrier Reef. The reef has an asymmetrical triangular shape, 5.5 km long and 3 km wide, with a small coral shingle cay on the south-eastern corner. One Treef Reef evolved from a karst carbonate platform, now 10 to 25 m below sea level, but emergent during the last sea-level low before 9600-9000 years B.P. With rising sea level, vertical organic accretion was dominant, although there was some lateral accretion on the higher southeastern corner. By 4400 years B.P. the reef grew up into the influence of the present wind-induced southeasterly wave regime. Present reef shape approximates a bow of a ship facing into wind, with the resultant wave refraction and diffraction producing a symmetrical energy pattern which has influenced the present sediment pattern. This pattern is symmetrical about a lagoonal axis of interaction of wave fronts. Present lagoonal sedimentation is controlled by flood tide and swash or wave surge transport, swash sorting and slack water periods when sediment in suspension is deposited.

Introduction

In 1843, H.M.S. Fly carried J. Beete Jukes to his first encounter with a coral reef. He named it One Tree Island because of an upstanding mass of *Pandanus* and *Pisonia* in the middle of the cay. Steers (1938) visited the reefs of the Capricorn and Bunker Group during the geographical expedition to the Great Barrier Reef in 1936, and concluded that One Tree Reef was by far the most interesting reef in the province.

One Tree Reef is one of fourteen reefs in the Capricorn Group, which together with the Bunker Group, forms the southern Great Barrier Reef Province (Fig. 1). Reefs of the Capricorn Group lie approximately 90 km east of Rockhampton, Queensland, and are aligned along two topographic highs (Fig. 1), with One Tree Reef south-southeast of the intersection of the two highs at Latitude 23°30′S, Longitude 152°06′E.

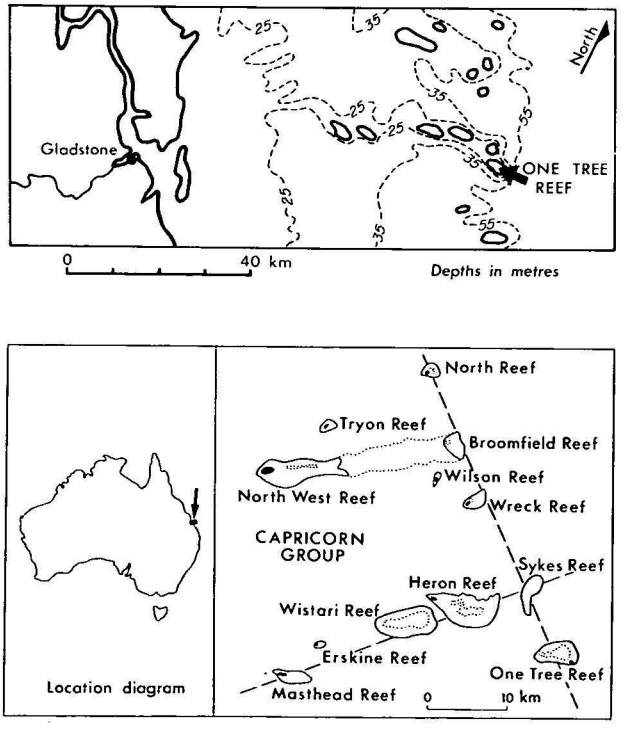

Figure 1. Generalized bathymetry in the Capricorn Group area, and the position of the Capricorn Reefs in relation to the major topographic highs (dashed lines)

This contribution results from a multidisciplinary approach to reef studies sponsored by the Australian Museum, encompassing marine biology, reef energetics, coral calcification and reef development. As a result of this approach more is known about process interaction and systems input at One Tree than at any other reef in the Great Barrier Reef. This paper is an analysis of reef physiography and sedimentation, presented with an appraisal of meteorologic and oceanographic factors which have influenced the evolution of this reef.

Meteorologic and oceanographic factors

The regional climate is subtropical with distinct winter and summer seasons and wind patterns.

Winds

An appraisal of dominant wind patterns has been made from a complete record of 13 years of basic data collected at Heron Island, 19 km to the west of One Tree Reef. Because of the close proximity to the study area and the long record we assume that these data are applicable to One Tree Reef. Wind directions are grouped into octants and within each of these, histograms of wind strengths, based on the Beaufort Scale, are plotted. The percentage of total winds for each octant is shown as well as the percentage of calms (Fig. 2). Throughout the year, predominant winds are from the southeast quarter, and winds from all westerly directions form only a minor component of the annual wind pattern. Major differences between summer and winter wind patterns are the east-northeast component in summer and the south-southwest component in winter. The period August to December is consistently calmer (average winds force 3) than the winter period (average winds force 4). The summer tendency is for infrequent very strong winds, whereas the winter winds are consistently strong.

Swell

Limited data (US Navy Hydrographic Office, 1950) show predominant east-southeast swell directions affecting the southern Great Barrier Reef.

Ocean currents

Little is known of the near-surface ocean currents in this area. Wyrtki (1960) suggests that the southern Great Barrier Reef is affected predominantly by southerly moving currents. However, Woodhead (1970) concluded from a

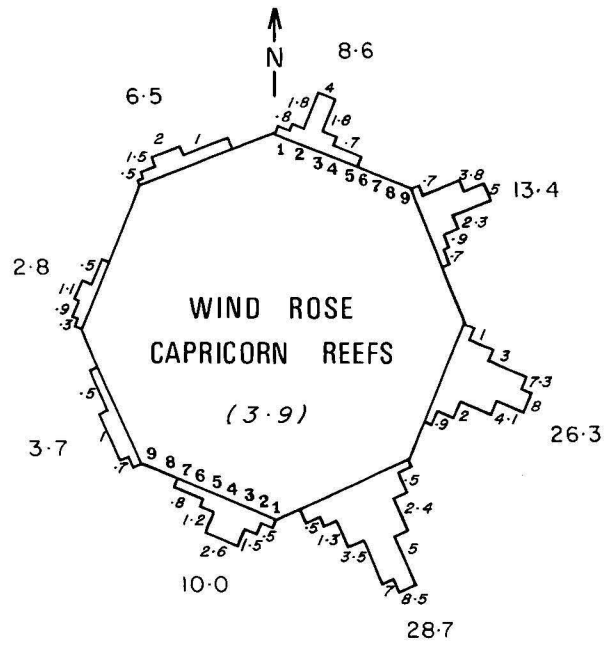

3·4 *Total winds in octant (%)*
(3·9) *Calms (%)*
8·5 *Sub-total for wind velocity range (%)*
7 *Beaufort scale of wind velocity*

Figure 2. Wind rose data for Heron Island compiled from thirteen years of observations

float release program that a northerly current was dominant, at least in the spring.

Tides

The tides are mesotidal on the springs (tidal range of 2.0 m) and microtidal on some neaps (tidal range of 0.8 m). The average tidal range is 1.5 m, classifying One Tree Reef overall as a mesotidal region. Outside the reef, tidal currents set generally to the west on a flood tide, and to the east on an ebb tide. Tidal current velocities of 100 cm/sec (2 knots) are common between the islands in the Capricorn Group.

The reef crest and coralgal rim is continuous around the main lagoon (Fig. 3), and the drainage level of this crest is a few centimetres above the mean water level for the area. A consequence of the ponded lagoon level is prolific coral-algal growth higher in the lagoon than mean low water. As a result, the lagoon holds a constant water level for approximately half of each tidal cycle and this enclosed lagoonal water mass is affected by a flood tide only in the last three hours of the rise, at which time water quickly enters the lagoon from the southeast. On the ebb tide, drainage from the lagoonal water mass is only in the first 2.5 hours until the algal rim/reef crest is emergent. Drainage is to the northwest, and there is no significant flow over the south and east margins at this time. The lagoon therefore experiences a slack water period of 6½ hours during each tidal cycle. An extrapolation of oxygen and carbon dioxide concentrations in the lagoon water mass (Kinsey, pers. comm. 1975) implies only a 25 percent volume exchange in the lagoon water mass with each tidal cycle.

Physiographic zonation of the reef

Physiographic zonation of reefs has been described by many workers (Braithwaite 1971; Mergner 1971; Pichon 1971, 1974). At One Tree, most zones are recognized, but some are better developed and are more distinct than others.

Reef platform

The simplified bathymetric chart of the Capricorn Group (Fig. 1) shows the reef situated on a platform at a depth of around 25 m. Many workers have shown that a carbonate sequence in excess of 200 m occurs in the subsurface in this region (Richards & Hill, 1942; Maxwell 1962, 1973; Palmieri 1971; Lloyd 1973). Such a limestone sequence, exposed during the Wisconsin glacial low is likely to have undergone extensive subaerial erosion prior to the Holocene submergence, resulting in the formation of a karst surface. Davies (1974) identified such a surface at a depth of 20 m below Heron Island (Fig. 1). Purdy (1974) demonstrated the presence of a pre-Holocene karst surface beneath reefs in British Honduras. It is likely therefore that the reef platform at One Tree is a karst surface at a depth of approximately —20 m.

Fore-reef slope

The geomorphic characteristics of the fore-reef slope vary along each side of the Reef. On the south side, the slope is generally quite steep from the low-tide level to a depth of 10 m, below which it steepens to a vertical cliff down to 25 m. Corals are sparse on the cliff and only gorgonians have been observed growing out from the face. The northern fore-reef slope has an irregular surface due to some deep channels (7-15 m) and large, isolated coral colonies. Further down this slope, the surface is extremely irregular, with caves, crevices and coral pinnacles standing 5 m high in a water depth of 12-14 m, but overall the slope of this fore-reef area is gentle. The eastern and southeastern slopes are characteristically weather sides, as seen on many reefs. These slopes are gentle due to the extensive accumulation of coral debris.

Reef front

The reef front is a maze of coral gardens and pinnacles, dominated by branching and plate-like forms of *Acropora*. Prominent spur and groove structures occur on the southern and southeastern reef fronts. Individual spurs are up to 20 m long and the grooves up to 2-3 m deep and 5-10 m wide.

Coralgal rim

The coralgal rim is the most elevated part of the reef exposed at low tide and is smooth and compact. It generally comprises encrusting coralline algae such as *Porolithon* forming individual nodules, intergrown nodules and a porous meshwork. This coralgal rim is best developed around the southern and western sides of the First Lagoon (Fig. 3). It is only 25-40 m wide, compared with 500 m width on some reefs. On the south side, little detritus accumulates on its surface, while on the southeastern and northern side, permanent and semi-permanent detrital accumulations are common and are composed predominantly of *Acropora* sticks with a little molluscan debris. Stabilization of these deposits has occurred at Long Bank, and First, Second and Third Banks (Fig. 3). The accumulation and destruction of ephemeral banks on the southeastern edge of the reef has occurred during a single storm.

On the western margin of First Lagoon, the inner side of the coralgal rim is a vertical wall, extending to a depth of 10 m. This effectively separates First Lagoon from the western margin of the reef front.

Reef flat

The reef flat is divisible into a living coral zone nearest the coralgal rim, merging into a dominantly dead coral zone nearest the lagoon. Along the southern reef flat, a zone of prolific subtidal coral (40 percent bottom cover and 0.8 m deep) is dominated by circular patches (1-5 m diameter) of *Porites andrewsi* growing on a sandy bottom. The densest growth occurs to the lee of the algal rim, and becomes sparser towards the lagoon. Wind-rows, with identical parallel linearity to the spurs and grooves, occur in the dense coral zone.

Along the southern and southeastern corner of the island, a broad area 0.5 km wide, is composed of broken, algal-encrusted coral rubble, cemented into an indurated potholed platform. On both the northern and southern sides of the island, this indurated platform is dissected by gutters, 3-4 m deep. The northern gutter appears prominently on the air photo (Fig. 4).

Subtidal sand sheets

Subtidal sand sheets occur on both the southern and northeastern sides of First Lagoon. Both sheets are approximately 0.5 km wide, and clearly appear to be prograding into the lagoon. The sand-engulfed outlines of previous lagoonal patch reefs are visible within the southern sand sheet (Fig. 5). First and Second Lagoons are partly separated by a lobe of this southern sand sheet.

Lagoons

One Tree Reef has three lagoons of which the largest, First Lagoon, is the central lagoon and occupies an area of approximately 10 km^2. Is is triangular in shape with an apex projecting southeast. This lagoon is shallow at the southern end but deepens progressively to a depth of 10-

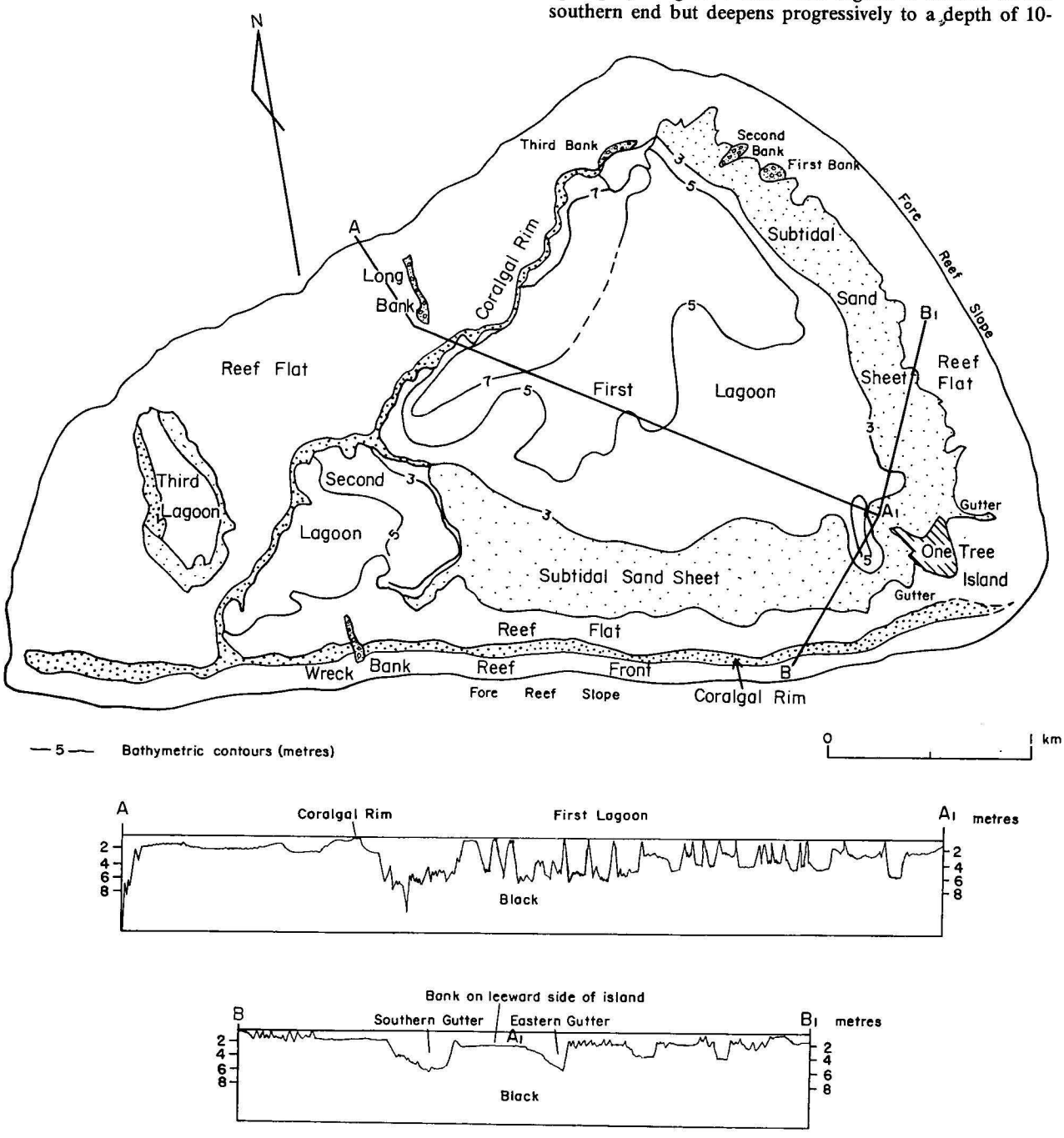

Figure 3. Principal morphological and sedimentological features of One Tree Reef. The positions of echo profiles are indicated.

Figure 4. Oblique aerial photograph of One Tree Island and adjacent gutters

12 m along the coralgal rim on the northwestern margin (Fig. 3). It may be of some consequence that the depth of the deepest part of the lagoon is similar to the depth of the top of the cliff along the southern reef front. Numerous patch reefs of varying forms are contained within the lagoon; the smaller patch reefs are linear, or reticulate, and occur mainly on the south side of the lagoon, while larger, wider circular patch reefs or micro-atolls (70 m diameter) occur randomly distributed throughout the lagoon. At the deeper western end, coral-cover over a sand bottom is approximately 10-15 percent. In each tidal cycle the First Lagoon is isolated from the open ocean for about 6½ hours when its level is higher than the surrounding ocean. Corals and algae have grown vertically to this ponded level and form a 'piecrust' or flat top surface. Patch reefs of all types decrease in number towards the deeper end of First Lagoon (Fig. 5). The smaller Second and Third Lagoons are shown in Figure 3.

Sediment distribution

The entire reef is composed of autochthonous carbonate sediments with only a minute siliceous skeletal component.

The most prominent area of sediment accumulation is the island itself which measures 0.3 km by 0.2 km; its highest point is 1.5 m above mean high water springs. It is composed almost entirely of pebbly shingle dominated by *Acropora* sticks (Fig. 6). Minor sand-size detritus has accumulated only in the intertidal zone on the leeward side of the island. Storm ridges along the windward eastern and southern sides testify to the combined action of spring tides and strong winds.

Ephemeral shingle banks (Fig. 3), mostly composed of *Acropora* rubble, are prominent features of the wide eastern reef flat. These banks, with dimensions 200 m by 30 m and 1 m high can be formed in a single southeasterly storm and may be destroyed just as quickly. More permanent shingle

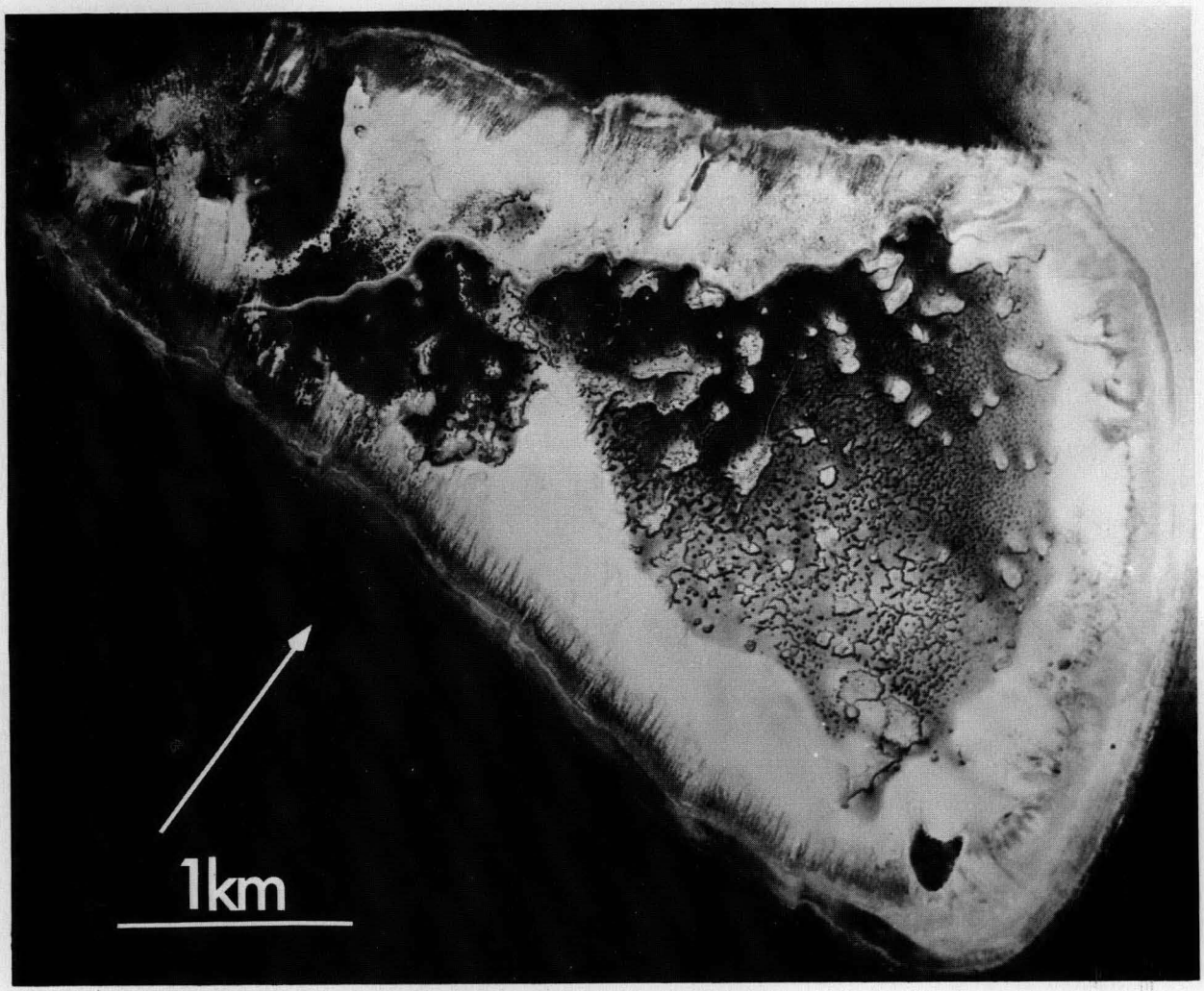

Figure 5. Air photograph of One Tree Reef.

Figure 6. Intertidal coral shingle, One Tree Island.

banks occur further west along the northeastern reef flat. Four of these, First, Second, Third and Long Banks are subaerially exposed except on the highest spring tides.

The lagoonal sediment characteristics and grain-size distributions are based on 82 grab samples from First Lagoon. Quantitative grain-size and grain type determinations were made and the sediment granulometry, subdivided into gravel, very coarse sand, fine to coarse sand, and mud is shown in Figure 7. Each of these is discussed in turn.

Gravel comprises a maximum of 20 percent of the sediment along the southern reef flat but decreases to 5-10 percent towards the lagoon. Near the southern part of the cay and on the eastern reef flat, gravel is the major sediment component. A lobe of sediment comprising 10 percent gravel extends between First and Second Lagoons, while a patch occurs to the west of the coralgal wall close to Long Bank. Gravel is almost everywhere composed of mixtures of coral, coralline algal, pelecypod, foraminiferal, and crustacean debris. In the lee of the island gravel is composed almost entirely of pelecypod fragments.

Very coarse sand comprises up to 30 percent of the sediment and has a wider distribution than gravel. The arcuate distribution around the southern and eastern margins of First Lagoon is significant, as is the lobe dividing First and Second Lagoons. The percentage of very coarse sand decreases across the sand sheets towards the lagoon proper. Predictably, a very coarse sand component accompanies the gravel on the western side of the coralgal ridge, to the southeast of Long Bank. The very coarse sand component is most abundant immediately to the southwest and north of the cay, especially in the region of the gutters, where 20-30 percent is common. Generally this fraction is composed of coralline algae, pelecypods, corals, foraminifera, gastropods, echinoderms and crustaceans; the coralline algae dominating in the highest energy environments, and foraminifera such as *Baculogypsina* forming an important fraction in the moderate energy areas bordering the First Lagoon.

Over most of the lagoon, sediments have a dominant coarse to fine sand fraction—especially in the lee of the island, in the eastern central First Lagoon, and in the lobe separating First and Second Lagoons. While the sediments of First Lagoon are composed primarily of coarse to fine sand, there is a noticeable decrease towards the reef margins, especially in the gutters and near the southern reef flat. The coarse to fine sand fraction comprises coral,

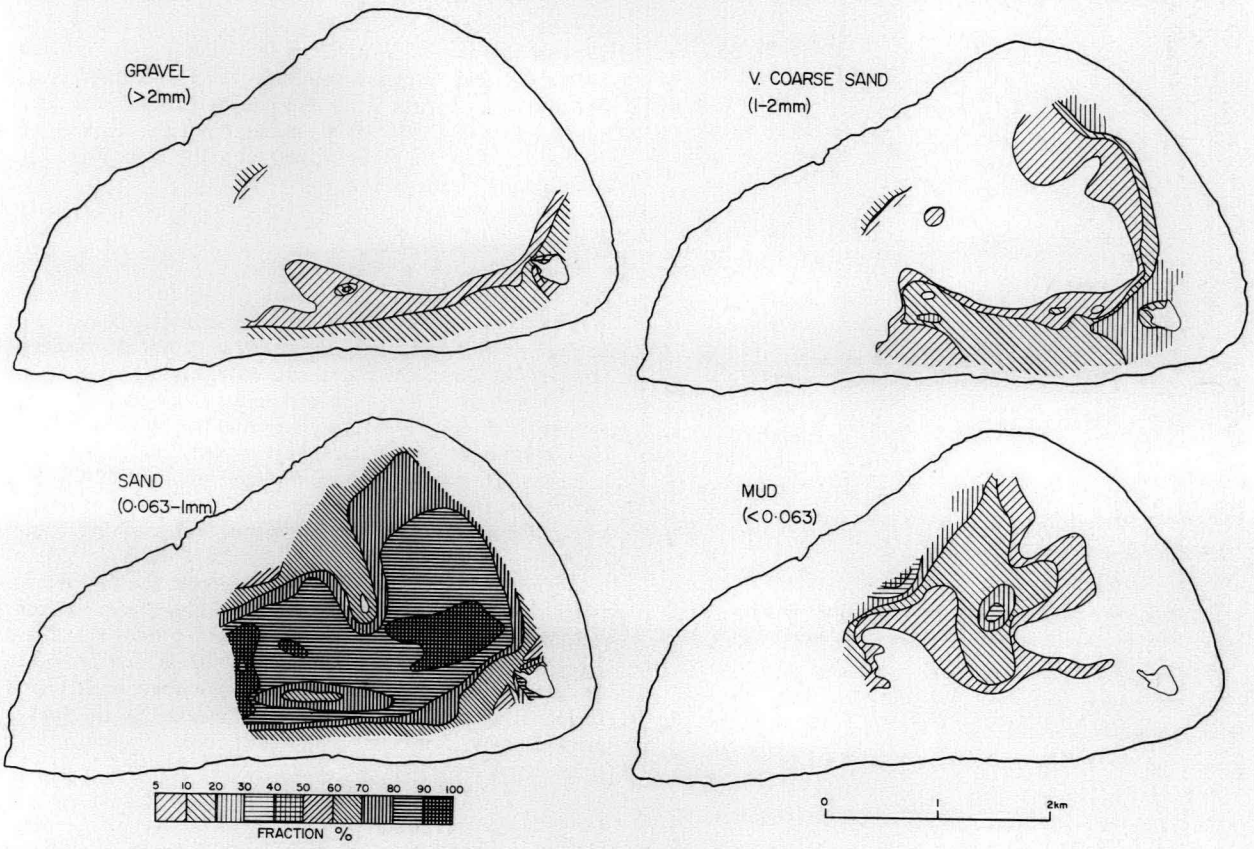

Figure 7. Sediment granulometry of First Lagoon.

coralline algal (principally *Halimeda*), foraminiferal, mollusc, echinoid, gorgonacean schlerite, sponge and crustacean detritus. Coral fragments dominate this fraction except in the outer higher energy zones bordering the sand sheets where algae are prominent. Gross foraminiferal morphology is apparently controlled by water depth and wave energy in the lagoon; the robust *Baculogypsina* dominates moderate energy zones, while *Miliolids* are abundant in the deeper quieter lagoonal areas.

Carbonate mud constitutes between 5 percent and 50 percent of the total sediment. The distribution of the mud is symmetrical about a northwest to southeast axis down First Lagoon, and maximum abundance (50%) is in the middle of the lagoon and against the eastern wall of the coralgal rim. Mud is entirely restricted to the lagoon proper.

Reef growth, sedimentation, and the wave regime

The effects of wind and resultant waves are significant factors influencing reef development. To predict and explain the observed reef morphology and sediment patterns a model of wave interactions on a reef platform is presented. This model is based on three assumptions

1. The growth platform is outlined by the southern and eastern reef crests. This is borne out by the position of One Tree in relation to the general bathymetry (Fig. 1).
2. Wave orthogonals result from the combined effects of the easterly swell and the wind direction prior to interaction with the reef platform.

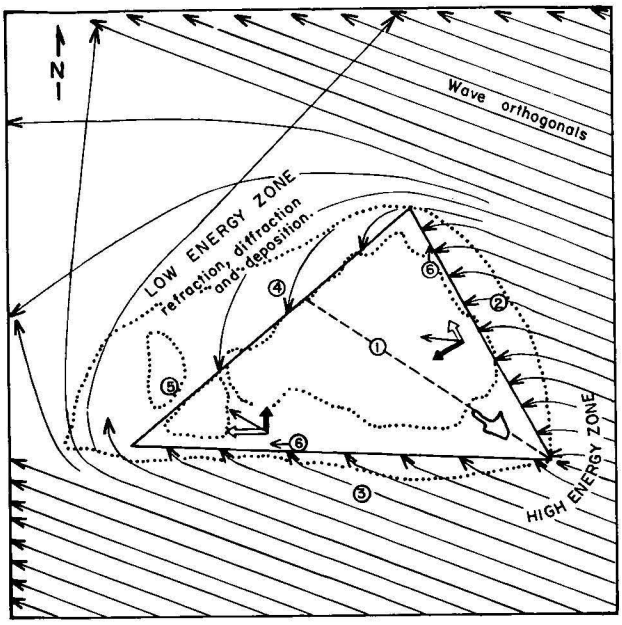

Figure 8. Model of wave patterns affecting One Tree Reef in east-southeasterly weather

3. The present wind patterns have been fairly consistent for at least the last 4 400 years B.P. Flint (1971, p. 244-250), concludes in fact that prevailing wind directions have been consistent during most of the Pleistocene.

The model of the probable effects of such prevailing winds and swell on reef morphology and reef growth is shown in Figure 8. Using wave orthogonals, the directions of maximum wave energy can be shown for typical east-southeasterly weather. The model uses an asymmetrical triangular base which approximates the part of the present reef outlined by the northeast and southern windward edges and the coralgal rim at the leeward margin of the first lagoon. The asymmetrical platform shape has resulted from the shape of the original growth platform, modified by the effects of summer easterly winds and the easterly Pacific swell truncating growth along the northeast reef edge.

The effect of the platform on approaching ocean waves will be to induce wave refraction on windward margins, and wave diffraction and standing wave formation in lee situations. A principal effect of wave refraction on windward surf zones is the developments of two relative components of wave energy—longshore movement, and swash or wave surge. Angles of refraction and diffraction (Fig. 8) were calculated from tables (U.S. Army Corps of Engineers Beach Erosion Board, 1971) within the limitations of the accuracy of the bathymetric information around the reef. In this case maximum waves that developed in east-southeasterly winds of a mean velocity of between 10 to 15 knots were considered.

The density of orthogonals is proportional to, and thus illustrates, the relative intensity of wave energy around the reef. There are three significant features evident in this model. Firstly, the wave refraction shows a dominance of longshore water movement over swash on the southern edge of the reef, while swash predominates over longshore currents along the northeast margin (Fig. 8). Secondly, at the leeward end of the reef, a low energy zone of wave diffraction and resultant standing wave formation exists. Thirdly, the platform is bisected by an axis of wave front interactions. The effects of these factors on the dynamics of the model, and the comparisons with the One Tree Reef situation are discussed in turn.

Wave refraction effects

The northeastern windward side (Fig. 8) is typified by almost perpendicular wave approaches and a greater density of wave orthogonals than the southern side. Vector analysis of these data shows a greater expenditure of energy as swash on the northeastern side, while similar calculations show longshore currents predominant over swash on the southern side (Fig. 8). Morphology and the known sediment characteristics of these zones support this model. The high northeastern side of the reef, the ephemeral rubble banks, and the gutters, have resulted from the action of swash, while the shingle spit on the western side of the island indicates the extent to which swash from the northeastern side penetrates across the lagoon. The most obvious depositional feature of the southern side is the sand sheet adjacent to the reef flat. However the dominant longshore movement of sediment, combined with flood tide effects have produced the tongue of sand which now separates First and Second Lagoons, as well as the asymmetry evident in the longer southern side of the reef compared to the northeastern edge where longshore effects are less significant.

Low energy leeward zone

The model predicts refraction and diffraction of waves around the northwestern corner of the reefs (Fig. 8),

generating a weak longshore component to the southwest, while little refraction and only a small degree of diffraction occurs around the southwestern corner. The result of these two effects is a low energy shadow zone in the lee of the southwestern corner with resultant minimal transport and sediment accumulation. Where interference of components of the same wave trains occur, standing waves develop between the interference of the opposing wave fronts, producing parallel alternating very low energy and high energy zones. As a result, the deep Third Lagoon occupies the zone of low energy around the southwestern corner, and the alteration of rubble banks, deeper coral-rich areas and sand sheets on the lee side are indicative of standing wave effects.

The lagoonal axis

The theoretical position of the axis of interaction of waves from the south and east, is shown in Fig. 8; energy conditions decrease both towards the line, and down the line from east to west. This axis is the probable eventual meeting line of prograding sand sheets from the south and northeast, but does not represent the deepest part of the lagoon. The bilaterally symmetrical distribution of sediments in First Lagoon (Fig. 7) is genetically related to this energy pattern. The decrease in grain size away from the southern and northeastern margins, and also from east to west is in agreement with the energy model. A major question arising however from this discussion is what are the principal factors effecting lagoonal sedimentation.

Controls of lagoonal sedimentation

The main body of the lagoon is a zone where swell, ocean wave, and longshore current effects are excluded for half of the tidal cycle. Sediment derived from the reef edge and reef flat is transported into the lagoon as a prograding shoal of poorly sorted sand material. Resorting and redistribution of such material within the lagoon may result from wind stress on the water surface and wind-induced wave motion from tidal currents, and from swash over the reef, especially in storms.

The development of wind-stress currents would be inhibited by the short fetch over the lagoon and the well developed coral patch reefs, so that such currents would be of little use as sediment sorters. However, wind stress may induce short-period waves of up to 0.3-1.0 m, in height in the lagoon, which may agitate sediment into suspension. Using mathematical wave relationships (U.S. Army Coastal Engineering Research Center, 1966) to relate wave size and bottom velocity in such a lagoonal situation (Fig. 9B), the probable lagoonal grain-size distribution of sediment moved by wind-induced waves is shown in Fig, 9C, and directly related to a simplified SE to NW profile along the lagoonal axis. By applying grain size velocity threshold data (U.S. Army Coastal Engineering Research Center, 1966), energy fences for various grain sizes may be plotted (Fig. 9C). It can be seen that no large grain size variations due to transporation by wind-induced wave motion are likely to occur in an open lagoon, let alone one with a large number of patch reefs. This conclusion is in agreement with our own observations, and those of Kinsey (1972, p. 22) that 'at slack water, the water surface is protected from severe wind effects by the slightly exposed piecrust which prevents any extreme development of surface chop'. The absence of appreciable water mixing is also borne out by oxygen and temperature data from the lagoon (Kinsey, 1972, Table 1).

The unlikely transport of coarse sediment by surface wind stress and wave motion leaves only two alternatives as dominant processes in lagoonal sediment transport—swash and tidal currents. The effects of swash are restricted to the lagoon margins so that most sediment sorting must be by tidal currents. On the rising tide, the predominant direction of water movement is initially from east to west through the gutters on either side of the island (Figs 3, 4), and then from all directions. However, because of the height of the algal rim, water enters the lagoon for only the last three hours of the rising tide, and does so rapidly. A similar situation exists on the falling tide, water leaving the lagoon for only three hours, in a direction from southeast to northwest, over the algal rim. We consider that maximum lagoonal sedimentation of suspended matter occurs during the six hour period of isolation from the ocean, the sediment having been transported by the tidal currents. Therefore, in the lagoon, the sediment distribution pattern is a result of a combination of processes:

1. Sand sheet progradation, towards the axis of the lagoon due dominantly to swash and flood-tide currents.

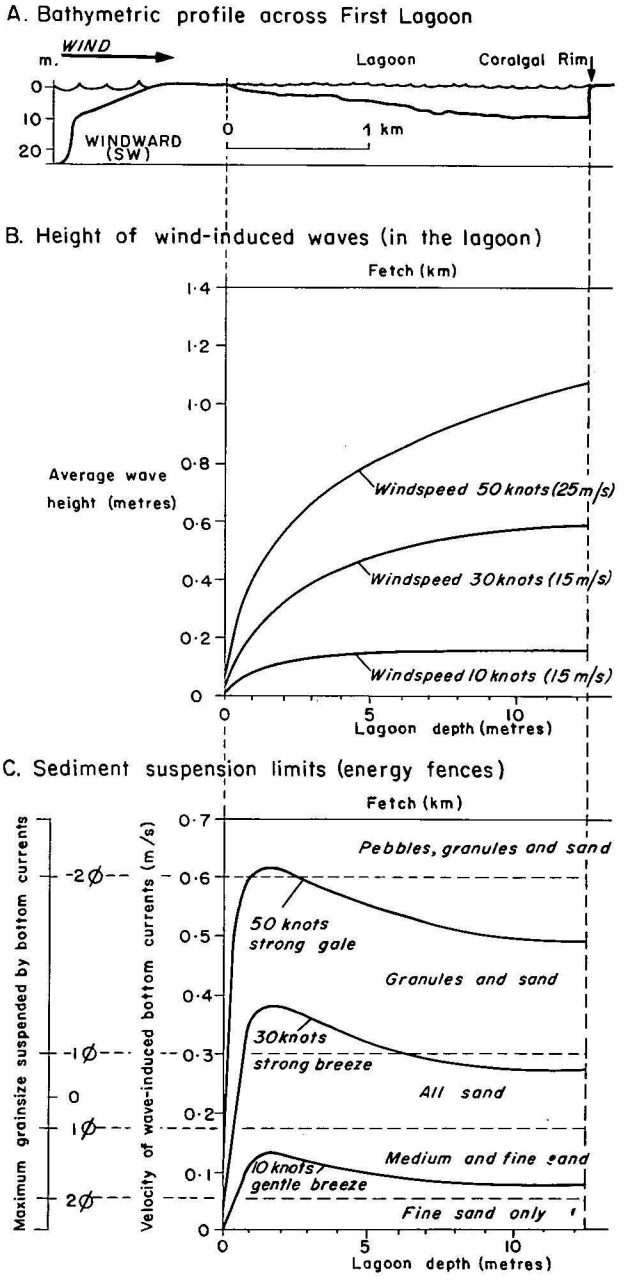

Figure 9. **A. Bathymetric profile of First Lagoon.**
B. Height of wind induced waves in the lagoon.
C. Sediment suspension limits (energy fences).

2. Some probable resuspension by residual swash effects. This and the above processes transport sediment to the lagoon.
3. Re-suspension of finer sediment by tidal and wave-induced currents, especially during a falling tide, and transport of such material by tidal currents to the deep western end of the lagoon.
4. Settling of sediment during the six hours of each tidal cycle when the lagoon water mass is isolated from the open ocean.

Growth of One Tree Reef

To explain the growth of reefs, it is imperative to consider how far morphological features reflect modern conditions and to what extent they are inherited from Pleistocene features. Little attention has so far been given by researchers to the effects of reef growth rates and sea level changes on reef morphology, factors which must surely be reckoned with. Our study at One Tree has shown that a satisfactory theory of reef growth can be made only after studies of past and present growth rates and their relation to sea level; and after studies of the present-day relations between growth rate, shedding rate and the wave regime.

Growth rates

Authoritative statements regarding the growth rates of coral reefs are few and far between. Estimates by Sargent & Austin (1949), Odum & Odum (1955), and Chave *et al.* (1973), have been drastically revised by Kinsey (1972) working at One Tree Reef, Smith (1973) working at Eniwetak, and the Limer Expedition Team (1976) working at Lizard Island, all of whom agree that windward reef flats calcify at a rate of 4.0 Kg m^2 $year^{-1}$. This translates into a potential vertical growth rate of 3 mm $year^{-1}$.

Chappell & Polach (1976) conclude that in New Guinea, maximum growth rates of up to 4 mm $year^{-1}$ may have occurred between 8000-6000 years B.P. It is not clear from Chappell and Polach's data whether they mean net, gross or community growth rate, but the close similarity between their figures, the recent One Tree Island and Lizard Island data, and the Eniwetak data of Smith (1973) suggests that growth rates may not have varied greatly during the Holocene.

The history of the Holocene transgression is poorly known in the Great Barrier Reef Province. However the recently published sea level curve for southeast Australia (Thom & Chappell, 1975) is probably applicable in general, if not in detail. These authors concluded that sea level was at approximately —20 to —25 m, at 9000 to 9600 B.P., and around its present level at 6200 years B.P. At the present day steady sea level, it is likely that little or none of the vertical growth potential (≃3 mm $year^{-1}$) can be realized and that accrued material must represent lateral growth and progradation. However, during the period of the Holocene transgression when the early reef was submerged by a sea rising at a rate of from about 10 mm $year^{-1}$ (25 m below present sea level) to about 6 mm $year^{-1}$ (Thom & Chappell, 1975), it is likely that growth would be predominantly vertical at a rate similar to the maximum potential exhibited by the active perimeter zones i.e. 3 mm $year^{-1}$. Protection offered by the increasing water cover would have

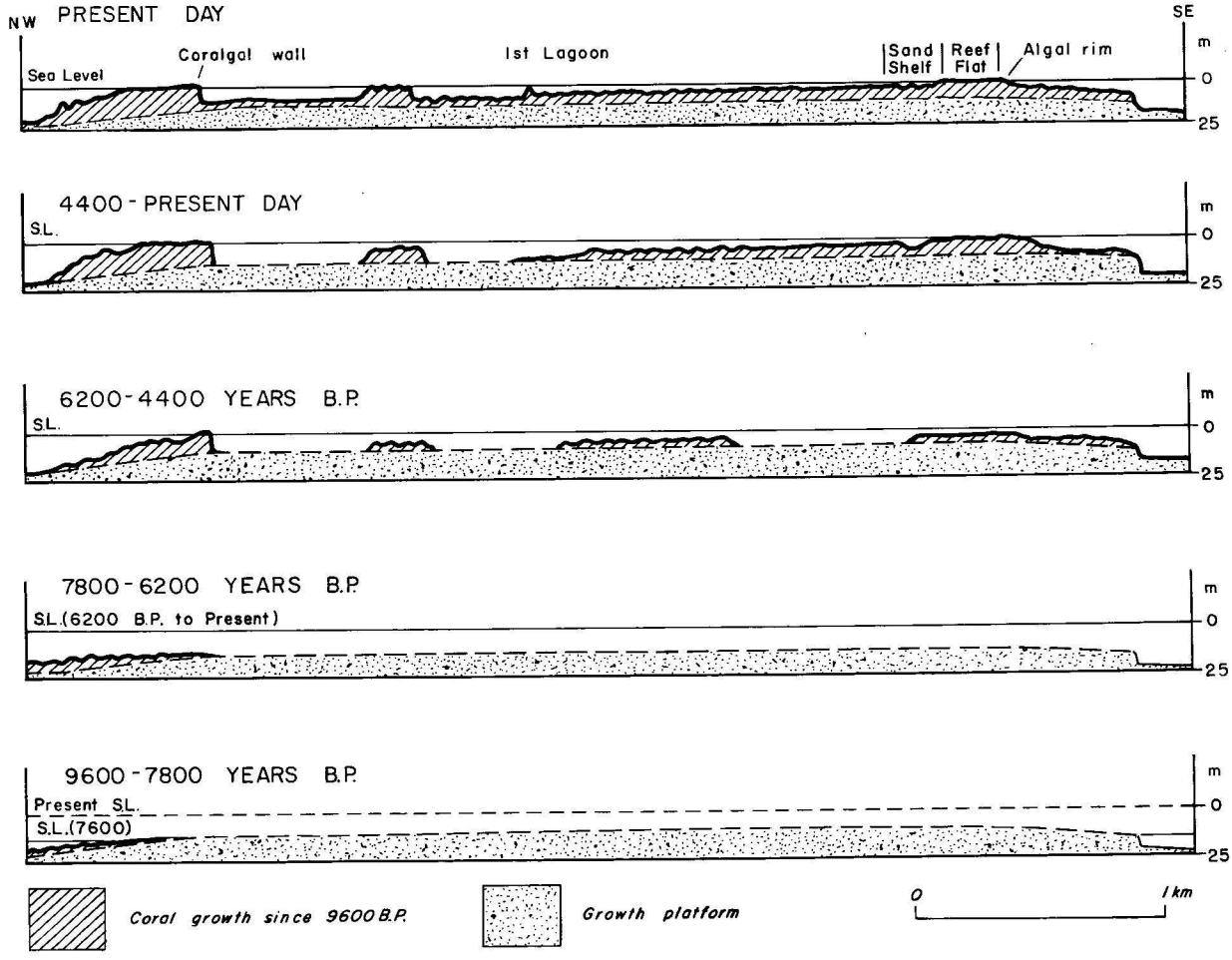

Figure 10. Evolution of One Tree Reef since 9600 BP. The dark line is the top of the growing reef.

reduced lateral transfer to a minimum, until such time as the vertical growth stopped or slowed near the sea surface. Considering the curve of Thom & Chappell (1975), this would have occurred only 1000 years ago for growth from a substrate at —25 m, about 4400 years for growth from a substrate at —10 m, and about 5500 years ago for growth from a substate at —5 m.

The growth platform

We suggest that the Holocene growth of One Tree Reef is founded on a platform, a section across which is shown in Fig. 10. The cliff from —10 to —25 m which outlines the southern side, could only have formed prior to 9600 B.P. (Thom & Chappell, 1975) during emergence, or perhaps earlier; in any case before Holocene reef growth. The top of the cliff must therefore have formed a surface at least 10-15 m higher than that indicated by the regional bathymetric map. Its lateral extent is speculative, but the —10 m maximum depth of First Lagoon is thought not to be coincidental, and implies a —10 m platform extending at least as far as the western end of First Lagoon, after which a general westerly slope down to —20 to —25 m is indicated by the slope of the present surface in this direction. Based on this interpretation (Fig. 10a) and applying the data of Kinsey (1972) and Thom & Chappell (1975) the likely development of One Tree Reef may be traced (Fig. 10).

a. Between 9600-7800 B.P., sea level rose from around the —20 to —25 m platform to —10 m. Very little coral growth occurred on the south side of the reef because of the declivity of the cliff. However growth almost certainly would have occurred on the gentler northern lee slope. In this time interval, maximum growth of 5 m would have accreted on this surface.
b. Between 7800 and 6200 B.P., sea level rose to the present level. Reef growth began on the —10 m platform where the optimum site for coral growth would have been on the platform margins. Vertical growth was dominant around the western margin at the junction between the —10 m platform and the north-western slope as lateral spread would have given little advantage for coral colonies gaining shallow water. In contrast, the absence of a contemporary vertical wall on the south side, implies that the —10 m platform may have sloped gently upwards, allowing coral to colonize upslope towards shallow water where, in this time interval, 5 m of growth could have accumulated. The thickest part of the reef (10 m) would have been on the northwest slope leading down to the platform at —20 m to —25 m.
c. Since 6200 B.P. reef growth was probably vertical. Coral growing off the —10 m platform reached sea level by 4400 B.P., after which continued growth of the reef would have resulted in lateral accretion and reef modification. This date limits the amount of accretion and modification possible, and it is also probable that at this time the island formed as a consequence of the reef growth up into the sphere of direct influence of surface conditions.

Acknowledgements

The authors wish to express their thanks to the Authorities of the Australian Museum for permission to use the facilities at One Tree Island for this study.

We gratefully acknowledge the support and assistance given in the field by Miss Katarina Lundgren and Mr Ted Chilvers.

We thank Mr J. N. Casey for his encouragement with this study, and we are indebted to the technical staff of the marine geology section, for the preparation and grain-size analysis of the sediment samples; the illustrations were drawn by the general draughting section of the geological drawing office, BMR.

References

BRAITHWAITE, C. J. R., 1971. Seychelles Reefs: Structure and development; *in Regional variation in Indian Ocean Coral Reefs. Zoological Society of London Symposium*, **28**, 39-63.

CHAPPELL, J., & POLACH, H. A., 1976. Holocene sea level change and coral reef growth at Huon Peninsula, Papua New Guinea. *Bulletin of the Geological Society of America*, **87**, 235-240.

CHAVE, K. E., SMITH, S. V., & ROY, K. J., 1972. Carbonate production by coral reefs. *Marine Geology*, **12**, 123-140.

DAVIES, P. J., 1974. Sub-surface solution unconformities at Heron Island, Great Barrier Reef. *Proceedings of the Second International Symposium on Coral Reefs*, **2**, 573-578.

FLINT, R. F., 1971. GLACIAL AND QUATERNARY GEOLOGY. *New York, John Wiley.*

KINSEY, D. W., 1972. Preliminary observations on community metabolism and primary productivity of the psuedo-atoll reef at One Tree Island, Great Barrier Reef. *Proceedings of Symposium on Corals and Coral Reefs*, 1969, *Marine Biological Association of India*, 13-22.

LIMER EXPEDITION TEAM. Metabolic processes of Coral Reef communities at Lizard Island, Queensland. *Search* (in press).

LLOYD, A. R., 1973. Foraminifera of the Great Barrier Reef bores; *in* JONES, O. A., & ENDEAN, R. (Editors), BIOLOGY AND GEOLOGY OF CORAL REEFS, **1**, 347-366, *Academic Press, New York.*

MAXWELL, W. G., 1962. Lithification of carbonate sediments, in the Heron Island Reef, Great Barrier Reef. *Journal of the Geological Society of Australia*, **8**, 217-238.

MAXWELL, W. G., 1973. Geomorphology of eastern Queensland in relation to the Great Barrier Reef; *in* JONES, O. A., and ENDEAN, R. (Editors), BIOLOGY AND GEOLOGY OF CORAL REEFS, **1**, 233-272, *Academic Press, New York.*

MERGNER, H., 1971. Structure, ecology and zonation of Red Sea reefs (in comparison with South Indian and Jamaican reefs). *Zoological Society of London Symposia*, **28**, 141-161.

ODUM, H. T., & ODUM, E. P., 1955. Trophic structure and productivity of a windward coral reef community on Eniwetok Atoll. *Ecological Monographs* **25**, 291-320.

PALMIERI, V., 1971. Tertiary subsurface biostratigraphy of the Capricorn Basin. *Geological Survey of Queensland—Report* **52**, 1-18.

PICHON, M., 1974. Dynamics of benthic communities in the coral reefs of Tulear (Madagascar): Succession and transformation of the biotopes through reef tract evolution. *Proceedings of the Second International Coral Reef Symposium*, **2**, 55-68.

PICHON, M., 1971. Comparative study of the main features of some coral reefs of Madagascar, La Reunion and Mauritius, *in* STODDART, D., & YONGE, C. M. (Editors), *Symposia of the Zoological Society of London*, **28**, 185-215.

PURDY, E. G., 1974. Reef configurations: cause and effect, *in* LAPORTE, L. F., (Editor), *Society of Economic Paleontologists and Mineralogists, Special Publications*, **13**, 9-76.

RICHARDS, H. S., & HILL, D., 1942. Great Barrier Reef Bores, 1926 and 1937. Descriptions, Analyses and Interpretations. *Report of the Great Barrier Reef Committee*, **5**, 1-122.

SARGENT, M. C., & AUSTIN, T. S., 1949. Organic productivity of an atoll. *Transactions of the American Geophysical Union*, **30**, 245-249.

SMITH, S. V., 1973. Carbon dioxide dynamics: A record of organic carbon production, respiration and calcification on the Eniwetok windward reef flat community. *Limnology and Oceanography*, **18**, 106-120.

STEERS, J. A., 1938. Detailed notes on the islands surveyed and examined by the Geographical Expedition to the Great Barrier Reef in 1936. *Great Barrier Reef Committee—Report*, **4**, 51-104.

THOM, B. G., & CHAPPELL, J., 1975. Holocene sea levels relative to Australia. *Search*, **3**, 90-93.

U.S. ARMY CORPS OF ENGINEERS BEACH EROSION BOARD, 1971. Coastal Engineering. *Technical Report*, **4**, *United States Department of the Interior.*

U.S. NAVY HYDROGRAPHIC OFFICE, 1950. Atlas of sea and swell charts, northwestern Pacific Ocean, southwestern Pacific Ocean. *Hydrographic Office Publications* **799 C-E.**

U.S. ARMY COASTAL ENGINEERING RESEARCH CENTER, 1966. Shore protection, planning and design. *Technical Report* **4**, (3rd edition).

WOODHEAD, P. M. J., 1970. Sea-surface circulation in the southern region of the Great Barrier Reef, Spring 1966. *Australian Journal of Marine and Freshwater Research*, **21.**

WYRTKI, K., 1960. The surface circulation in the Coral and Tasman Sea, *CSIRO, Division of Fisheries and Oceanography, Technical Papers*, **8**, 1-44.

Resistivity methods in the search for groundwater, Cape York Peninsula, Queensland

G. R. Pettifer and J. Smart

On the western side of Cape York Peninsula, north Queensland (Fig. 1), in the Weipa-Aurukum area, surface water supplies are seasonal, and mining and pastoral development relies on the availability of groundwater. Artesian water is obtainable from the Mesozoic sandstone units of the Carpentaria Basin throughout the area, but the water is slightly saline (1000 ppm total dissolved salts) and unacceptably high in fluorine (around 15 ppm). Domestic and stock water is taken almost entirely from shallow aquifers within the late Cretaceous or early Tertiary Bulimba Formation, which underlies most of the area and supplies all the domestic and some of the processing water at Weipa and the domestic and irrigation water at Aurukun Mission. Because of the variable permeability of the Bulimba Formation pattern drilling is expensive for groundwater investigations on a large scale; in the area studied drilling alone had a 1 in 35 success rate. There is a need for a cheap reconnaissance geophysical method to locate favourable areas for drilling.

The purpose of this note is to describe a resistivity traversing technique, supported by drilling, which was developed in a detailed geophysical and geological study (Pettifer *et al.*, 1976) of a test area between Weipa and Aurukum, and to outline some interesting aspects of the use of resistivity methods in this type of environment.

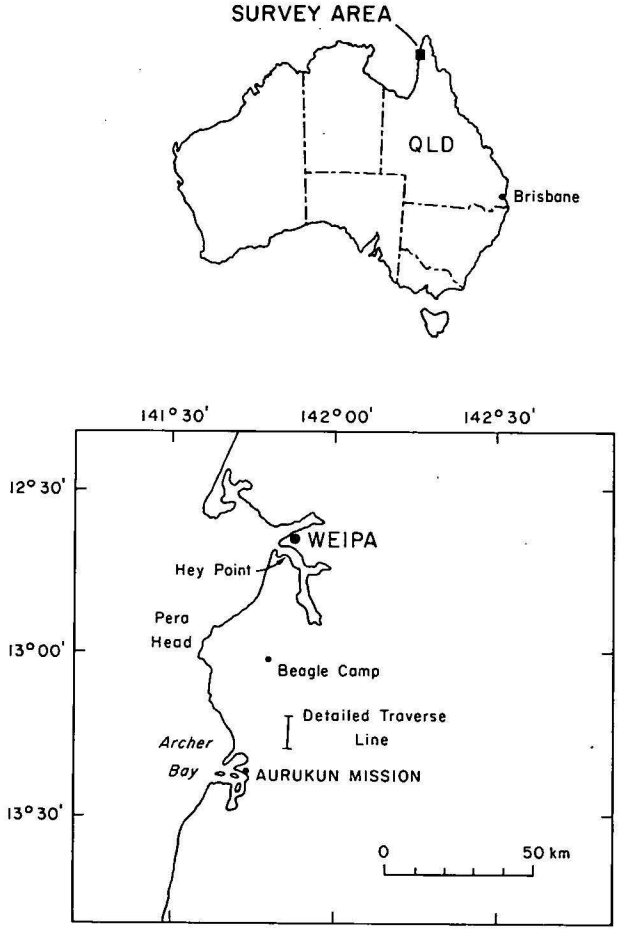

Figure 1. Locality Map

Geology

The geological sequence consists of 20-30 metres of lateritized Bulimba Formation overlying slightly weathered siltstones and sandstones of the Mesozoic Rolling Downs Group (Figure 2). For details see Smart (in press, b).

The Bulimba Formation underlies an area of about 120 000 km² on the west coast of the Peninsula for a distance of 650 kms. The formation was deposited as an alluvial fan by streams flowing from a provenance area to the east, and it is the east-west trending ancient channel deposits that are the most permeable aquifers. The unit is mainly sandy clay and clayey sand, with minor clean sand and gravel. There is little consolidation within the area studied.

The Bulimba Formation was originally feldspathic almost everywhere, the feldspar grains being associated with quartz of similar grainsize. Lateritic weathering has subsequently converted the feldspar to kaolin and has developed bauxite several metres thick at the surface.

The volume changes due to the lateritic weathering have produced numerous vugs and fissures within the formation. This effect, combined with the inter-granular pore space, produces a relatively high permeability in many areas (Smart, in press, a). However, bore development in such areas causes a collapse of the vugs and the kaolin pseudomorphs break down to soft clay, releasing quartz of silt to fine-grained sand grainsize originally present as inclusions within the feldspar clasts (Edwards, 1957, 1958; Smart in press, a). This reduces the permeability of the formation by decreasing the sorting and causes problems of abrasion in pumps and other equipment.

Smart (*in* Doutch *et al.*, 1973, and in press a & b) pointed out that drilling had suggested the presence of east-trending permeable bodies, and considered that these probably represented old stream channels within the formation. Hydrological investigations had suggested that the permeable bodies were large and abundant in the Weipa Peninsula but smaller and less common elsewhere. The location of these by drilling alone is obviously expensive and the resistivity method appeared to offer a possible solution although previous attempts (Coffey & Hollingsworth, 1971) had been unsuccessful. Previous hydrological investigations in the area are reviewed by Pettifer *et al.*, (1976).

Objectives

The geophysical investigation had two main objectives; firstly to define both the vertical and lateral changes in resistivity in the Bulimba Formation by surface geophysical methods and borehole logging, and secondly to determine an economical reconnaissance geophysical traversing technique to reduce the need for expensive pattern drilling

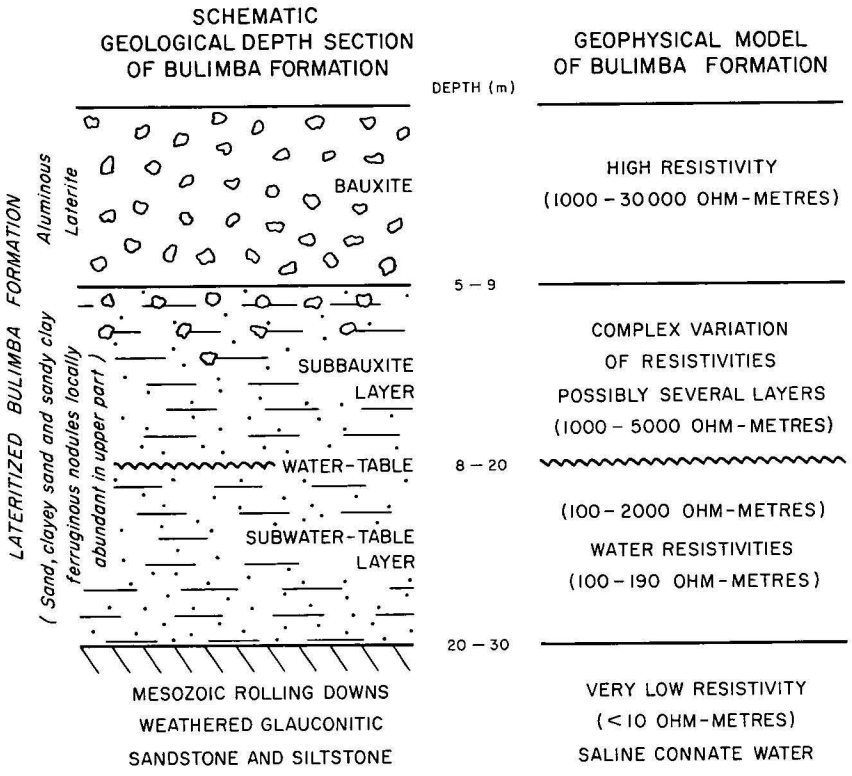

Figure 2. Models of the Bulimba Formation

over the large areas involved. To achieve these objectives an 8 km north-south test traverse was chosen and several resistivity traversing and sounding techniques were tried.

In September-October 1974, a combined party from the Engineering Geophysics Group and the Geological Branch of the Bureau of Mineral Resources investigated in detail an area about 70 km south of Weipa on the road between Aurukun Mission and Beagle Camp (Fig. 1).

Resistivity sounding and traversing

Six principal resistivity methods were used in the investigation:

(1) Resistivity sounding (half-Schlumberger configuration).
(2) Frequency domain IP sounding (half-Schlumberger configuration 0.3, 3Hz).
(3) Alfano sounding (down-hole current electrode).
(4) Resistivity borehole logging (single point and four electrode Wenner array (a = 0.5 m).
(5) VLF resistivity traversing (Radiohm principle, 10 m intervals).
(6) Conventional resistivity traversing/half Schlumberger configuration

$(AB/_2 = 50\ m, \frac{MN}{2} = 10\ m, 20$ metre intervals)

/Wenner configuration (a = 10 m, 10 m intervals)

Using methods 1-5, the first objective was partly realized in the sense that an understanding of the general relations of lithology, permeability, and resistivity of the Bulimba Formation was obtained. However, surface geophysical methods were unable to reliably and economically quantify the resistivity variations both with depth and laterally beneath the surface bauxite layer.

The second objective was successfully achieved using resistivity traversing with the half-Schlumberger configuration at an electrode separation large enough to penetrate the high and variable-resistivity bauxite layer.

Resistivity of the sediments of the Bulimba Formation

Figure 2 shows the relation between the typical geological depth section of the Bulimba Formation and its geophysical model.

The principal feature of the model is the high-resistivity surface bauxite layer (1000-30 000 ohm-metres) and the low-resistivity basal layer (<10 ohm-metres) of the upper Rolling Downs Group. The intermediate layers are herein referred to as the sub-bauxite zone (1000-5000 ohm-metres) and the sub-water-table zone (100-2000 ohm-metres). Water resistivities are high (100-300 ohm-metres) and this reflects the low ionic contents of waters in bauxite-covered areas (Evans, 1965).

The model as shown in Figure 2 was used as a basis for planning the geophysical investigation. As the investigation proceeded it became obvious that with the high clay content of the Bulimba Formation and the complex structure of the clay in the sediments, no simple relations existed between sediment resistivity, porosity, and clay content. The investigation revealed, however, a general inverse relation between resistivity and permeability below the water-table.

Particular points of interest arising from the study of the relation between resistivity and the lithology are

(i) The importance of resistivity changes laterally within the Bulimba Formation and to a lesser extent in the Rolling Downs Group. The large changes of resistivity within the bauxite and sub-bauxite layers tend to mask the more interesting smaller changes of resistivity beneath the water-table.

(ii) The kaolin clay is virtually inert in its electrical properties in the presence of groundwaters of low ion concentration.

(iii) The investigation tends to confirm that there is no relation between subsurface permeability and bauxite grade or thickness on a detailed scale. Resistivity variations within the pisolitic bauxite bear no simple relation to bauxite characteristics either.

In attempting to define the distribution of resistivity and electrical properties in the Bulimba Formation (with

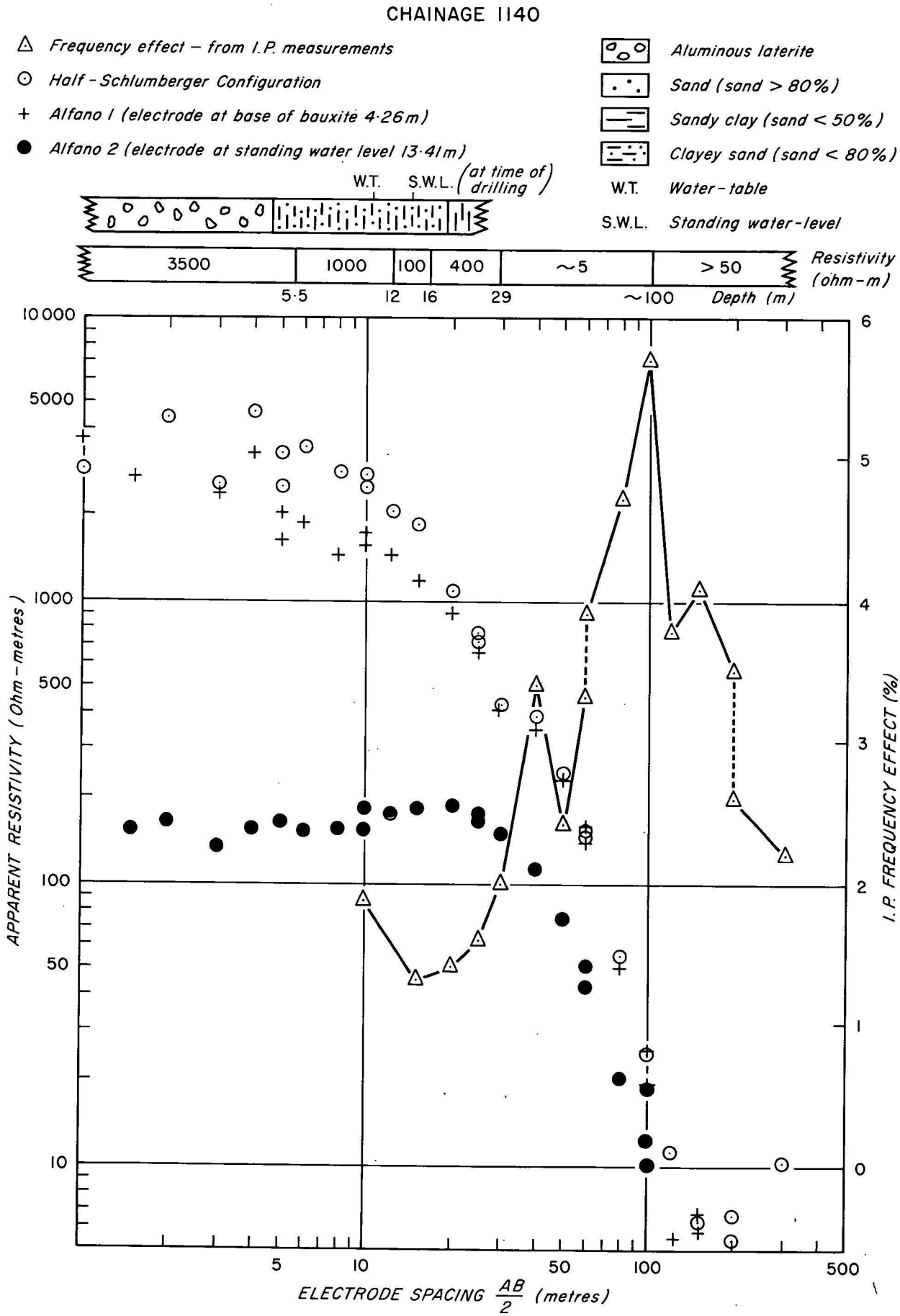

Figure 3. Resistivity depth probe at borehole H8

sounding, logging and traversing methods) several difficulties were encountered and are discussed below.

Resistivity sounding methods

Conventional resistivity soundings. The half-Schlumberger configuration, with one mobile current electrode and a fixed remote return electrode, was used to reduce problems of electrode contact in this high surface resistivity environment. The interpretation of sounding curves for large resistivity contrasts between surface and basal layers suffers from the well known suppression of the influence of intermediate layers (Keller & Frischknecht, 1966). The intermediate layers appear as small inflections in the descending branch of the resistivity sounding curve. Lateral resistivity changes, particularly in the bauxite and sub-bauxite layers, often produced scatter in the data which masked the effect of the sub-bauxite layer. A typical sounding curve is shown in Figure 3 with the interpretation and auger-hole log. The interpretation is derived mainly from resistivity logging data and Alfano sounding data and is far more detailed than could be expected from conventional sounding data alone.

The resistivity sounding method was found to be an unreliable and uneconomical investigation technique for widespread water search because of difficulties of interpretation and rapid lateral changes of resistivity which invalidated correlating the interpretation of a sounding any distance from a sounding location. Although this is also a major limitation with drilling, it is considered that drilling and resistivity logging is the only reliable technique of obtaining information on resistivity and lithology on a detailed scale.

Alfano sounding method. To overcome problems of interpretation of the intermediate layer resistivity in conventional soundings the Alfano sounding method (Alfano, 1962) was employed. The method utilizes a down-hole current electrode, a remote return electrode, and a moving receiving dipole. The down-hole current electrode is placed in the intermediate layer and the sounding graph is asymptotic at small electrode spacings to a resistivity related to the intermediate layer resistivity. Figure 3 shows a typical field example of two Alfano soundings and the conventional sounding at the same position. The Alfano sounding with an electrode at the water-table (Alfano 2) identifies a 100-ohm-metre layer at this depth. The interpretation is complicated by a 400-ohm-metre layer beneath this however. The Alfano sounding with an electrode at the base of the bauxite (Alfano 1) shows little evidence of the decrease in resistivity at the base of the bauxite.

These examples illustrate firstly, that the Alfano technique can provide data on the sub-water-table resistivity by placement of an electrode in the water-table; however, this is obviously economically unviable, except where hole collapse beneath the water-table prevents conventional logging. Secondly, the change of resistivity with depth beneath the water-table limits the value of the Alfano method. The method would be more useful in an environment where the intermediate layer resistivity is more uniform both with depth and laterally.

Frequency domain IP sounding

Induced Polarization (IP) sounding was tried to determine the IP properties of the Bulimba Formation. Figure 3 shows a frequency-domain IP sounding using the half-Schlumberger configuration. The IP sounding curve is dominated by the large frequency effect of the finely disseminated pyrite and carbonaceous material in the shales of the Rolling Downs Group. The sounding curve shows low IP values at small electrode spacings, indicating very small IP effects in the Bulimba Formation. This illustrates the low IP effects of kaolin clays (Vacquier *et al.*, 1957) in the low concentrations of metallic cation and slight acidity of the groundwaters prevalent in bauxite areas. For these reasons the IP method was found to be unsuitable as a technique for shallow groundwater investigations in this environment.

Traversing methods

The resistivity traversing methods, particularly Wenner and VLF traversing, indicated that the lateral changes of resistivity and hence permeability, were equally important as the vertical changes. It was in the traversing techniques that a suitable reconnaissance method to locate drilling sites was found.

Location of permeable sand bodies by resistivity traversing. A successful reconnaissance technique was found to be half-Schlumberger configuration (AB/2 = 50 m, MN/2 = 10 m). Figure 4 shows the traversing and drilling results for the test traverse. From correlation with the conventional depth sounding results the traversing data reflects variations in the transverse resistance (Kunetz, 1966) of the Bulimba Formation.

The electrode separations for the half-Schlumberger traversing must be carefully chosen to overcome effects of bauxite resistivity variation. In the test area a minimum value of AB/2 = 50 m was required. The principal use of depth probes is envisaged as defining a suitable traversing electrode separation in a particular area, and also to provide spot measurement of transverse resistances for correlation with the traversing data.

Potential aquifers in the Bulimba Formation are principally the high-permeability unconfined sand bodies lying below the water-table. These zones are characterized by a localized higher water-table and, because of the higher permeability, generally lower resistivities than the surrounding relatively impermeable sediments. The localized thickening of the low-resistivity sub-water-table layer and particularly the accompanying thinning of the high-resistivity sub-bauxite layers results, then, in a localized decrease in the transverse resistance of the Bulimba Formation over the unconfined permeable sand bodies. Regional variations in transverse resistance of the Bulimba Formation occur and are attributable to regional thinning of the formation or of the surface bauxite layer. In Figure 4, thinning of the Bulimba Formation to the north is reflected in the decreasing values of resistivity from chainages 6500 to 8000. Two localized resistivity lows at chainages 1930 m and 5800 m in this figure reflect the presence of two major permeable sand bodies. Figure 5 shows a detailed cross-section of the sand body at borehole H10 (chainage 5800 m).

Two confined sand bodies were located by drilling at chainages 2700 m and 3850 m (Fig. 4); because there is no rise in the water-table at these locations they are not identified by localized resistivity lows in the traversing data. Such data can thus only detect a potential aquifer where it is locally unconfined.

Resistivity traversing, covering 5 to 6 km per day with a 5-man team, plus follow-up drilling is estimated to be between one-third to one-tenth of the cost of pattern drilling at 100-m intervals. Based on the statistics of occurrence of the two confined sand bodies in the test area, a cost of about $3 800 per sand body is estimated for location by drilling alone. Aquifer testing may further reject many of these sand bodies. A minimum survey area of 100 km^2 is thus suggested for any reasonable chance of suitable aquifers being found. The expense of pattern drilling would be

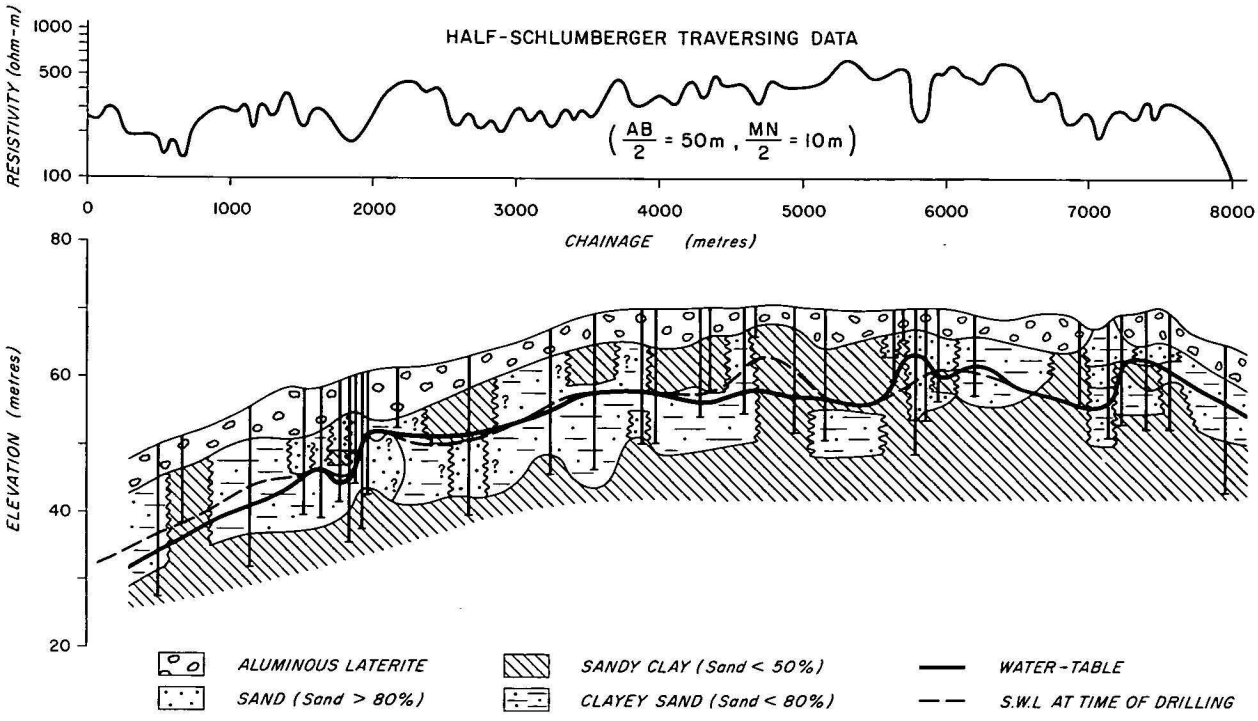

Figure 4. Geological section, and pole-dipole resistivity data, along traverse line

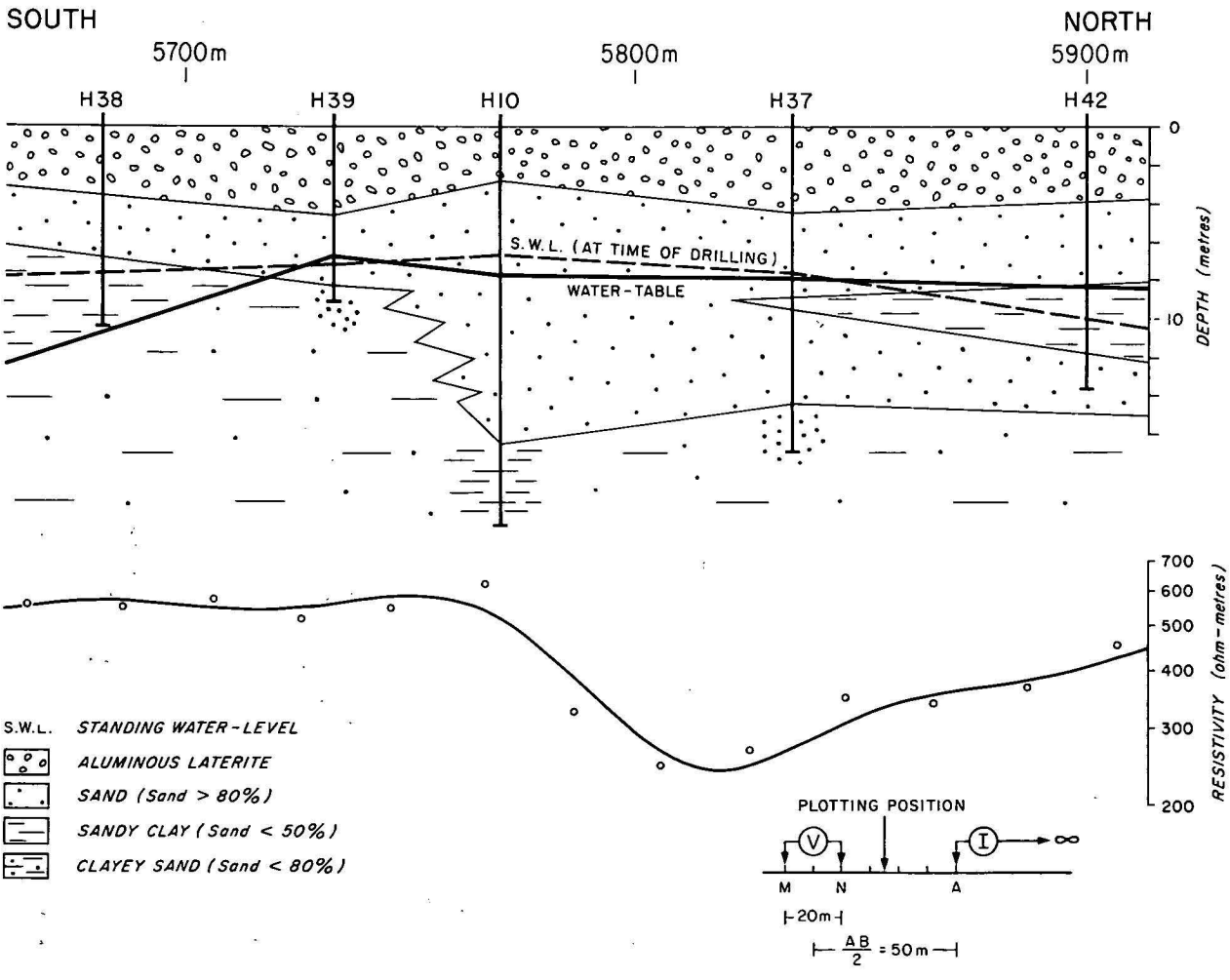

Figure 5. Detailed section between boreholes H38 and H42

considerable in such an area and the reduction of costs using the traversing—follow-up drilling approach is an extremely attractive proposition.

Conclusions

Resistivity traversing with drilling, electrical logging and Alfano soundings has given a clearer picture of the resistivity of the Bulimba Formation. Electrical soundings have been shown to be suitable for production work in groundwater search and drilling and electrical logging is preferred. The sand bodies discovered have been drilled in detail and their geometry has been better defined than is possible with resistivity methods.

An economical traversing technique using the half-Schlumberger configuration has been proven in the test area. The traversing electrode spacings must be chosen carefully to overcome surface bauxite variations. Initial resistivity soundings will provide data for choice of suitable electrode spacings.

For production work on large groundwater search projects in this area, half-Schlumberger traversing with auger drilling and electrical logging follow up is envisaged as the main approach. Considerable saving in costs over pattern drilling can be achieved over the large areas to be investigated.

Acknowledgements

The authors wish to thank the staff of Aurukun Associates and the people of Aurukun for their generous assistance during the field investigations.

References

ALFANO, L., 1962—Geoelectrical prospecting with underground electrodes. *Geophysical Prospecting* **10,** 290-303.

COFFEY & HOLLINGSWORTH, 1971—Comalco Limited shallow aquifer investigation Weipa, North Queensland (unpublished Company Report).

DOUTCH, H. F., SMART, J., GRIMES, K. G., GIBSON, P. L. & POWELL, B. S., 1973—Progress report on the geology of the Carpentaria Basin in Cape York Peninsula. *Bureau of Mineral Resources, Australia—Record.* **1973/187** (unpublished).

DOUTCH, H. F., SMART, J. & GRIMES, K. G., in prep.—Geology of the Carpentaria and Karumba Basins, Queensland. *Bureau of Mineral Resources, Australia—Bulletin.*

EDWARDS, A. B., 1957—Quartz and heavy minerals in Weipa bauxite. *CSIRO Mineragraphic Investigations Report* **749.**

EDWARDS, A. B., 1958—Quartz and heavy minerals in bauxite of Weipa N. 10 000/W. 15 000 Pit. *CSIRO Mineragraphic Investigations Report* **750.**

EVANS, H. J., 1965—Bauxite deposits of Weipa in geology of Australian ore-deposits. *8th Commonwealth Mining and Metallurgy Conference* **1,** 396-401.

KELLER, G. V., & FRISCHKNECHT, F. C., 1966—ELECTRICAL METHODS IN GEOPHYSICAL PROSPECTING. *Pergamon Press, Oxford.*

KUNETZ, G., 1966—Principles of direct current resistivity prospecting. *Geoexploration Monographs* **1** *(1), Geopublication Associates Gebrüder—Börntraeger-Berlin-Nikolasee.*

PETTIFER, G. R., SMART, J., MCDOWELL, M. I., HORSFALL, C. L., GIBSON, D. L., & IDNURM, M., 1976—Cape York Peninsula geophysical and geological groundwater survey, Queensland, 1974. *Bureau of Mineral Resources, Australia—Record* **1976/3** (unpublished).

SMART, J., in press (a)—Weipa, Queensland—1:250 000 Geological series. *Bureau of Mineral Resources, Australia—Explanatory Notes* **SD54/3.**

SMART, J., in press (b)—Aurukun, Qld.—1:250 000 Geological series. *Bureau of Mineral Resources, Australia—Explanatory Notes* **SD54/7.**

VACQUIER, V., HOMES, C. R., KINTZINGER, P. R., & LAVERGNE, M., 1957—Prospecting for groundwater by induced polarization. *Geophysics,* **22,** 660-87.

BMR J. Aust. Geol. Geophys., 1 (1976) 246-247

Scuba-operated coring device

P. J. Davies and D. B. Stewart

The geologist's traditional tool has been the hammer, while marine geologists have substituted grab samplers and corers. None of these devices is totally satisfactory for studying modern coral reefs. The hammer may be used for sampling beach rocks and intermittently exposed reef rock, while grabs and corers have their use in sampling unconsolidated lagoonal sediment. However, 95 percent of a coral reef is inaccessible to the geologist using these means.

The importance of scuba investigations of reefs has been borne out by studies on The Great Barrier Reef, the results from which indicate the necessity for collection of rock samples while observations are being made. The futility of wielding a hammer effectively underwater has therefore prompted the design and development of a hand-operated pneumatically powered drill, at present capable of providing a 20 mm by 300 mm core in water depths down to 20-30 m. The instrument is composed of three parts—a rotary pistol drill, an impact attachment, and a rotary core cutter (Fig. 1).

A commercially available Japanese URYU type UD-60-07 drill was selected on the basis of its weight, size and characteristics. It has an integral gearbox, no load speed of 700 rpm, an average air consumption of 0.5 m^3/min, an operating pressure of 0.6 MPa, and an output power of 2 kW.

The impact attachment is a German Bosch Type S30 impact tool which connects directly to the rotary output spindle of the URYU drill and provides ten impacts per revolution of the core cutter. The impact tool consists of a pair of axially serrated meshing wheels which give impact loading only when the operator applies a positive force with the pistol drill.

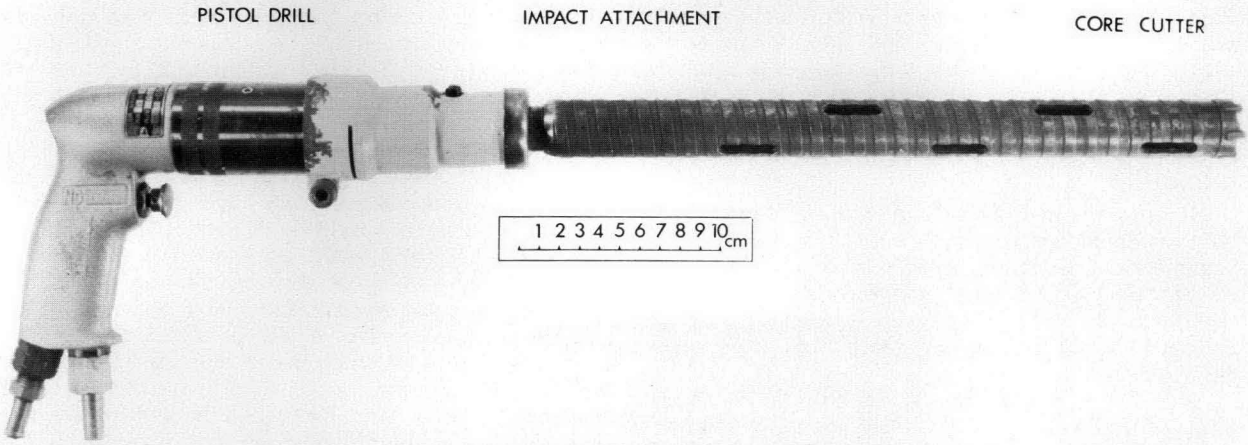

Fig. 1 The major components of the coring device

A Bosch, tungsten carbide-tipped, core cutter of outside diameter 30 mm, internal diameter of 21 mm, and six cutting teeth, was modified by extending its length to 300 mm. Further modifications include a spiral groove around the external surface, and longitudinal slots through the body, both of which facilitate the easy removal of cuttings during coring, and prevent the core cutter seizing in the hole, or the core. No centring hole is necessary for initiation of a drill hole.

The drill is driven by compressed air, chosen because of its inherent safety. Principal considerations in selecting the mode of air supply were restrictions of weight and space in the types of small boats normally used around coral reefs. For these reasons, petrol-driven compressors were discarded in favour of industrial air cylinders pressurized to 13.8 MPa, with a free air capacity of 6.8 m^3. A cylinder of compressed air gives 10 minutes of coring time. The air is first reduced in pressure through an oxygen regulator and then fed underwater to the drill via 30 m of 9.5 mm bore rubber hose. The pressure drop in the supply hose is approximately 24 kPa. In shallow water depths, the exhaust air can be bled underwater.

The equipment was successfully tested at Lizard Island in September 1975. The impact drilling attachment proved absolutely essential. Without it, coring would have been virtually impossible, because no appreciable positive push can be applied by an unsupported diver against a rock outcrop underwater. During underwater operations, the gearbox and impact attachment were filled with grease, and plastic tape was bound around parts highly susceptible to corrosion. At water depths of 4-7 m, three 300 mm cores can be drilled in ten minutes, i.e. from one air cylinder. Two modifications have been considered and partially implemented. First a waterproof housing has been built around the gearbox and a carbon face seal used to protect the output spindle. Secondly, it is proposed to replace the impact attachment with a free-piston air-powered vibrator for a 1 m core depth capability. Thought has also been given to the problems of exhaust during deeper water sampling, where an exhaust hose to the surface will be necessary.

The instrument can be operated underwater by one diver although it is more economical in time and energy if the operation is divided between two divers, one operating the drill, the other logging and storing the core. In this way, vertical or horizontal sequences can be sampled rapidly.

BMR J. Aust. Geol. Geophys., 1 (1976) 247-248

The Registry of Stratigraphic Names

E. K. Carter and K. Modrak*

A registry of stratigraphic names was started in BMR in 1949. In 1976 the Stratigraphic Names Index alone contains over 20 000 entries.

The central registry now includes the following indexes:

Author Index. All references to the geology of Australia, some nearby islands, and Papua New Guinea are indexed regardless of whether they contain stratigraphic names. The bibliographic reference, together with any stratigraphic names used, are recorded.

Stratigraphic Name Index. The heading of each card includes the State or Territory in which the unit occurs. Listed on each card are bibliographic references, with a brief comment on the nature of each reference: e.g., mention, description, definition. Fresh information is added to each card as it is extracted from the literature.

Sheet Area Index. In this index author cards are filed under 1:250 000 map Sheet areas (Australian Map Grid). The Sheet areas are arranged serially within each State or Territory.

Basin Index. Relevant bibliographic reference cards are filed under basin name.

Subject Index. Bibliographic references are filed under subjects. Until recently the Australian National Geological Index (ANGI) Thesaurus was used for classification; but the Australian Mineral Foundation (AMF) Thesaurus has now been developed, and will be followed.

PNG Bibliographic Index. The bibliography of

* **E. K. Carter is the Convenor of the Stratigraphic Nomenclature Committee of the Geological Society of Australia; and also has responsibility for the work of the Registry of Stratigraphic Names in BMR.**

Papua New Guinea, begun by G. A. V. Stanley, is being maintained.

Reserved Name Index. Reserved, as yet unpublished, names are filed alphabetically by geographic term. Each card also records for whom the name was reserved, the date of reservation, and any other information available.

Definition Card Index. A recently started index contains definitions approved by State or Territory Subcommittees of the Stratigraphic Nomenclature Committee of the Geological Society of Australia (GSA). Such definitions have no status until published. They are arranged lexicographically under each State by the name of the unit defined.

Among other indexes that are available is the Author Index of Fascicule 5h of the International Stratigraphic Lexicon. The central registry has been much involved in the preparation of material for publication in the parts of Fascicule 5 (Australia) of Volume 6 of the International Stratigraphic Lexicon. Fascicule 5h, in press in Paris, is an index volume for Australia as a whole, listing names published up to 1968.

The functions of the Stratigraphic Index are linked to the administration, by the GSA, of the Australian Code of Stratigraphic Nomenclature.

The procedure adopted by the GSA for the establishment of new stratigraphic units is as follows. Before publication (a) an author should submit the name(s) of the proposed unit that he wishes to use to the Convenor of the Stratigraphic Nomenclature Committee* for the Registry Staff to check whether it is available. If it is, the name will be reserved. (b) the proposed definition of the unit should then be submitted for approval, preferably on the definition card supplied, to the Divisional Stratigraphic Nomenclature Subcommittee of the State (or Territory) in which the type section occurs. At present the Territories Subcommittee in Canberra covers all Commonwealth territory units (including the Northern Territory). (c) The Subcommittee satisfies itself that the proposed definition is in accord with the provisions of the Australian Code of Stratigraphic Nomenclature and, where appropriate, approves the definition. It is not the function of the Subcommittee, or through it the Registry, to check on the accuracy of an author's work. It does, however, endeavour to ensure that new names are not erected when suitable names have been published, and attempts to ensure that neither synonyms nor homonyms arise where more than one geologist is working in an area. When a definition is approved the author is informed and the approved definition lodged with the registry. All who have a hand in the preparation of publications should ensure that stratigraphic names have been checked with the Registry prior to publication.

It follows from the foregoing that input to the various indexes comes not only from all the publications—texts and maps—received by the BMR Library; but also in the form of requests by authors for the reservation of names, and from Stratigraphic Nomenclature Subcommittees of the GSA—mainly as approved definitions of units.

In addition to an involvement with the International Stratigraphic Lexicon output from the central Registry includes Variation Lists, Deletions Lists and responses to enquiries. Copies of some of the index cards are supplied to State Geological Surveys in accordance with their wishes.

The bimonthly **Variations List** is distributed widely in Australia. It contains names reserved by each State (Territory) with details of variations or deletions: reserved names for each State that have recently been published, for whom the name was reserved, by whom it was published, the reference and a short comment on the nature of the reference (e.g. defined, description only, map reference only); other names, i.e. names published without prior reservation, the reference and a short comment on the nature of the reference; names of published definitions of units, with the reference.

Proposed stratigraphic names are reserved for a period of five years. In line with this, a **Deletions List** of names to be taken off the reserved list is distributed once a year. Only those names for which retention is requested are retained for a further five years.

The Registry welcomes visitors, to whom any information presently on the cards can be made available. Until such time as the various indexes are automated information cannot however, be made available in any other manner; it is also unlikely that until such time any further volumes of the International Stratigraphic Lexicon will be produced. A study of the feasibility of converting the information in the various indexes to computer-retrieval form has started but is hampered by a lack of staff. While the type of information undoubtedly lends itself to automatic handling, conversion of the existing data would be a large task.

BMR J. Aust. Geol. Geophys., 1 (1976) 248-250

Tentative correlation of onshore and lacustrine stratigraphy, Lake Frome area

*R. A. Callen**

The purpose of this discussion is to relate the informal lacustrine units, A, B & C of Draper & Jensen (1976) to the broader Cainozoic stratigraphy of the area. The Cainozoic stratigraphy used follows Callen & Tedford (in press), being a slightly modified version of that shown on the published Frome 1:250 000 geological map (sheet SH54.10).

The Cainozoic stratigraphy of the Lake Frome area is presented in the accompanying figure. The schematic cross-section depicts facies relationships in the various units and their spacial distribution, whilst the inset shows the rock units placed in time sequence, broadly differentiated into environment.

Sections 8, 9 and 14 in this discussion are, respectively, sections 4, 5 and 8 of Callen & Tedford (*in press*). Section 14 in this appendix is therefore the type section for the

* **South Australian Department of Mines, P.O. Box 151, Eastwood, S.A. 5063**

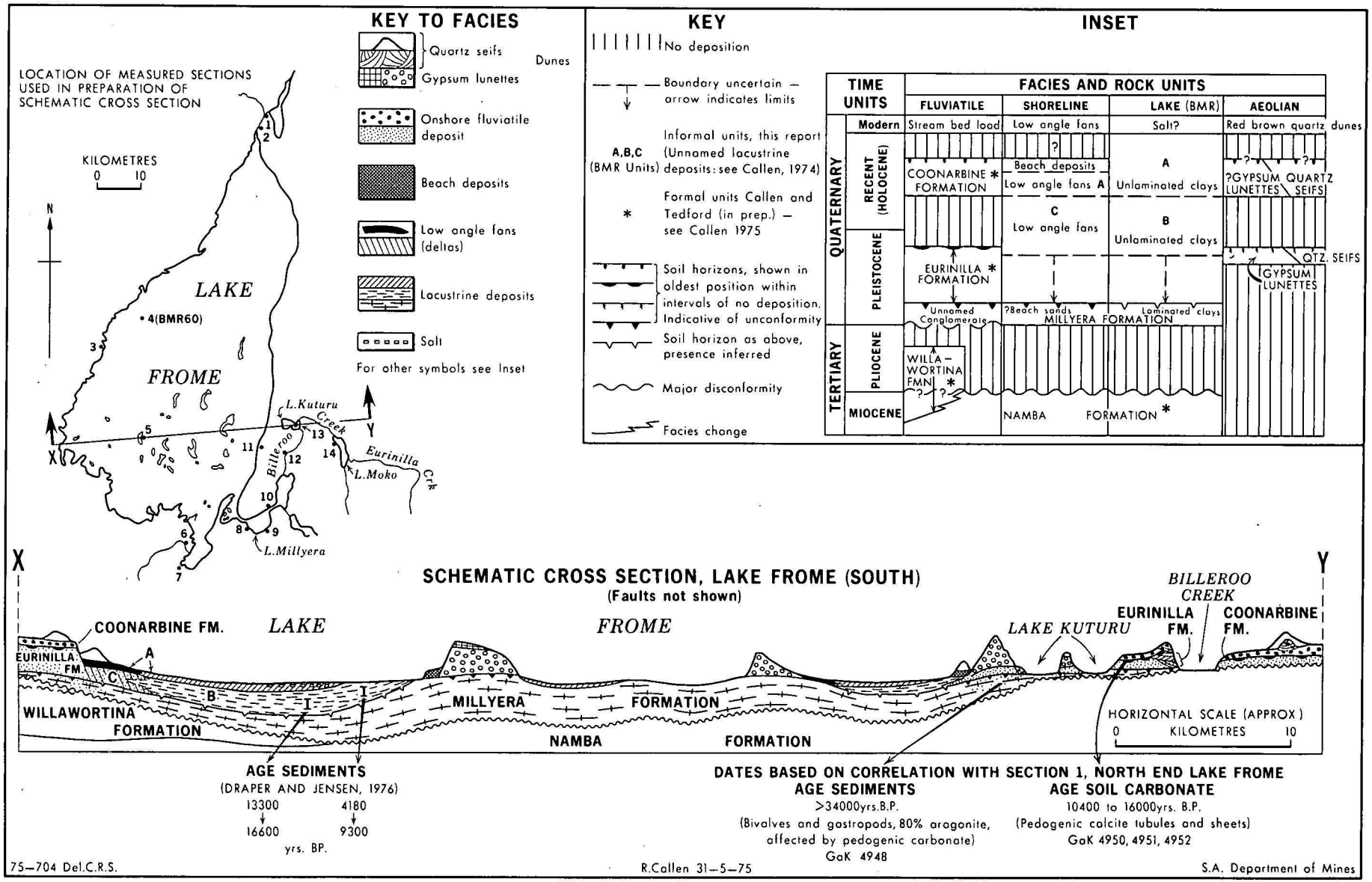
KEY TO FACIES
Quartz seifs
Gypsum lunettes
Dunes
Onshore fluviatile deposit
Beach deposits
Low angle fans (deltas)
Lacustrine deposits
Salt
For other symbols see Inset
LOCATION OF MEASURED SECTIONS USED IN PREPARATION OF SCHEMATIC CROSS SECTION
KILOMETRES 0 10
N
LAKE
FROME
4(BMR60)
L.Kuturu
Billeroo Creek
Eurinilla Crk
L.Moko
L.Millyera
KEY
No deposition
Boundary uncertain — arrow indicates limits
A,B,C (BMR Units)
Informal units, this report (Unnamed lacustrine deposits: see Callen, 1974)
*
Formal units Callen and Tedford (in prep.) — see Callen 1975
Soil horizons, shown in oldest position within intervals of no deposition. Indicative of unconformity
Soil horizon as above, presence inferred
Major disconformity
Facies change
INSET
TIME UNITS
FACIES AND ROCK UNITS
FLUVIATILE
SHORELINE
LAKE (BMR)
AEOLIAN
QUATERNARY
TERTIARY
Modern
RECENT (HOLOCENE)
PLEISTOCENE
PLIOCENE
MIOCENE
Stream bed load
Low angle fans
Salt?
Red brown quartz dunes
COONARBINE * FORMATION
Beach deposits
Low angle fans A
A
Unlaminated clays
?GYPSUM QUARTZ LUNETTES
SEIFS
C
Low angle fans
B
Unlaminated clays
QTZ. SEIFS
EURINILLA * FORMATION
GYPSUM LUNETTES
Unnamed Conglomerate
?Beach sands
MILLYERA FORMATION
Laminated clays
WILLA – WORTINA FMN *
NAMBA
FORMATION *
SCHEMATIC CROSS SECTION, LAKE FROME (SOUTH)
(Faults not shown)
X
Y
COONARBINE FM.
LAKE
FROME
BILLEROO CREEK
EURINILLA FM.
COONARBINE FM.
LAKE KUTURU
EURINILLA FM.
A
C
B
WILLAWORTINA FORMATION
MILLYERA
FORMATION
NAMBA
FORMATION
HORIZONTAL SCALE (APPROX)
0 KILOMETRES 10
AGE SEDIMENTS
(DRAPER AND JENSEN, 1976)
13300
16600
4180
9300
yrs. BP.
DATES BASED ON CORRELATION WITH SECTION 1, NORTH END LAKE FROME
AGE SEDIMENTS
>34000yrs.B.P.
(Bivalves and gastropods, 80% aragonite, affected by pedogenic carbonate)
GaK 4948
AGE SOIL CARBONATE
10400 to 16000yrs. B.P.
(Pedogenic calcite tubules and sheets)
GaK 4950, 4951, 4952
75—704 Del.C.R.S.
R.Callen 31—5—75
S.A. Department of Mines

Rock unit	*Code No.*	*Sample*	*Age, B.P. (years before 1950)*	*Material*
Millyera Formation-shell layer	GaK-4948	Inorganic carbonate CALDI/3882/1A (dated by Process B)	35 200 ± 1200	Shell 80% aragonite
Base Eurinilla Formation	GaK-4949	Inorganic carbonate CALDI/3882/1B	>33 400	pedogenic carbonate around shell moulds (calcite)
Top Eurinilla Formation	GaK-4950	Inorganic carbonate # 1	14 360 ± 310	soil carbonate
	GaK-4951	Inorganic carbonate # 2	10 760 ± 190	soil carbonate
	GaK-4952	Inorganic carbonate # 3	16 090 ± 370	soil carbonate
Base Eurinilla Formation	GaK-4953	Inorganic carbonate # 5	26 340 ± 1230	Pedogenic carbonate and shell (calcite)

Table 1. C^{14} dates—Lake Frome area

Coonarbine and Eurinilla Formations, section 12 is the type section for the Millyera Formation, and section 13 is a supplementary section for both units.

The interpretation is subject to revision as new evidence becomes available, and cannot be fully resolved until further dating of onshore material has been accomplished. Three C14 dates (GaK4950-4952) were determined from a soil developed on the Eurinilla Formation before the Coonarbine Formation was laid down. They were derived from soft calcite cylindroids and sheets from three separate horizons at increasing depths within the top 30 cm of the Eurinilla Formation at locality 2 (see Figure 1). The site was chosen so as to avoid some of the problems described by Williams & Polach (1971, p. 3076-3080).

The calculation of age is based on Libby's half life of C^{14} of 5570 years, and the indicated errors are the years corresponding to the standard deviations (one sigma) of beta rays counting statistical errors. Indicated limit of age of GaK-4949 corresponds to the C^{14} activity of three sigma.

The dates correspond approximately in time with the formation of the Motpena Paleosol (Williams & Polach, *op. cit.*), overlapping deposition of Draper & Jensen's units B and C. This suggests deposition was proceeding in the lake at the same time as soil formed on adjacent inactive floodplains. Thus sediment seems to have bypassed the floodplains: it may have been derived from incision of alluvial fans near the ranges. However, a date of 12 500 ± 170 years B.P. (ANU222), determined by Williams & Polach from charcoal at the top of an uneroded alluvial fan at the exit of Mount Chambers Gorge (the eastern edge of the Flinders Ranges), indicates that at least some fan deposition was occurring.

There is some indication of a slowing of the rate of deposition in unit B at about 7000-12 000 years B.P., considering Draper & Jensen's dates in their entirety. Similarly, three dates on carbonate from near section 5 in the bed of Lake Frome (charophytes, ostracods, N1913-1916, *pers. comm.* J. M. Bowler, 1974, Department of Biogeography and Geomorphology, Australian National University) suggest a similar slowing of sedimentation at this time. This corresponds to the period before transgression of the sands of the upper part of unit C. This time interval is a period of alluviation in Williams & Polach's scheme.

Similarly the younger period of sedimentation (approximately 3900-5500 years B.P.) corresponds to part of Williams & Polach's period of fan dissection and soil formation (Nacoona Paleosol). The Coonarbine Formation is thought to be equivalent to member 1 of the Thomson Creek Formation in the type section, though it has been mapped elsewhere to include some younger material, possibly equivalent to member 2. This younger material has been dated from carbon and egg shell at 2-3000 years B.P. (*pers. comm.* 1975, R. H. Tedford, American Museum of Natural History, New York) in the Lake Callabonna region.

Thus onshore and lacustrine sedimentation are somewhat out of phase, suggesting fan deposition occurs when little sediment is accumulating in the lake, and lake deposition when the fans are being eroded. However, much more dating needs to be done before this can be firmly established. The role of reaction relaxation and lag (Allen, 1974) on such long term sedimentary processes needs to be established before events can be correlated with climatic changes.

References

ALLEN, J. R. L., 1974—Reaction, relaxation and log in natural sedimentary systems: general principles, examples and lessons. *Earth Science Reviews*, **10**, 263-342.

CALLEN, R. A., 1974—Geology of the FROME 1:250 000 geological map and adjacent regions. *South Australian Department of Mines—Report Book*, **74/25**, (unpublished).

CALLEN, R. A., 1974—Geology of the Frome 1:250 000 geological rock units and depositional environments, Lake Frome area, South Australia. *Transactions of the Royal Society of South Australia.*

DRAPER, J. J. & JENSEN, A. R., 1976—The geochemistry of Lake Frome, a playa lake in South Australia. *BMR Journal of Australian Geology and Geophysics*, 1, 83-104.

WILLIAMS, G. E. & POLACH, H. A., 1971—Radiocarbon dating of arid-zone calcareous paleosols. *Bulletin of the Geological Society of America*, **82**, 3069-3086.

Fifth BMR Symposium*

The 5th BMR Symposium was held in Canberra on the 28th and 29th April 1976, and was opened by the Minister for National Resources, the Rt. Hon. J. D. Anthony. These annual symposia stress work of relevance to industry. The program included results of completed projects, of work in progress, and some more general topics.

Abstracts of the talks presented are given below.

Some insights into old and new zinc mineralization at Dugald River and Squirrel Hills, and uranium at Mary Kathleen, Queensland

G. M. Derrick

Stratigraphic relations between the Dugald River ore zone and the adjacent Knapdale Quartzite are much debated. Recent mapping by BMR and GSQ suggests that the lode occurs in the upper Corella Formation, which is overlain to the west by a constantly west-facing block of Knapdale Quartzite; this in turn is overlain by, and grades into, cupriferous scapolitic metasiltstone and limestone assigned to the White Blow Formation. No faulting is evident along the Knapdale Quartzite/White Blow Formation boundary, but farther west the White Blow Formation is probably faulted against pyrrhotitic limestone of the upper Corella Formation.

At the Lady Clayre mine, 8 km southwest of Dugald River, a thin stromatolite-bearing sequence is faulted against the Knapdale Quartzite. It contains a thin bed of branched columnar stromatolites, overlain by a domed biostromal bed, and is considered to be part of the upper Corella Formation. Domed brecciated quartzitic rocks which flank the Dugald River lode to the east are thought to be a part of this sequence.

The likely presence of stromatolites in the vicinity of the Dugald River lode adds further weight to the suggested correlation of Dugald River with the Deighton Pass sequence, 60 km to the south-southwest. Both sequences are essentially transgressive, and display stromatolitic carbonate zones which grade seawards (?) into Zn-bearing black pyrrhotitic and graphitic shale and limestone deposited in the more rapidly subsiding parts of the depositional basin. In both areas the mineralized beds are overlapped by regressive fluvial arenites, which are succeeded by silt, limestone, and shale of a second cycle of transgression.

Copper mineralization in both areas occurs in fine arenite-siltstone-limestone facies landwards of the Zn-bearing black shales. Base metal may have been derived by erosion of basement areas, but the Renfro model, in which metal-charged terrestrial waters mix with saline and sulphate-enriched seawater, and precipitate metals in the presence of H_2S derived from algae, may be applicable.

The presence of copper in scapolitic siltstone above the Knapdale Quartzite suggests that similar transitional facies in the White Blow Formation at Deighton Pass should be examined for this metal.

In 1971, Amoco Minerals discovered zinc mineralisation in the Soldiers Cap Group, at Squirrel Hills southeast of Cloncurry. It occurs in at least four stratabound zones which extend discontinuously for over 50 km along strike. The country rocks are metamorphosed shale, greywacke, siltstone, feldspathic arenite, and basalt of the Llewellyn Creek Formation and Mount Norna Quartzite; they are intruded by granite, aplite, and pegmatite, and are metamorphosed to at least high-amphibolite grade.

The lode horizons contain iron-rich sphalerite in a gangue of garnet 'sandstone' and 'quartzite', skarn, and gahnite-bearing quartzite, and closely resemble Broken Hill mineralization. Previous comparisons between the Willyama and Cloncurry Complexes based on the supposed similarity of the major Mount Isa and Broken Hill Ag-Pb-Zn deposits have foundered because of a 200 m.y. age difference between the deposits. However, the Soldiers Cap Group zinc mineralization now provides at least circumstantial evidence that the eastern part of the Cloncurry Complex is a continuation of the Broken Hill sequence.

Features common to both Soldiers Cap and Broken Hill mineralization are:

1. Lode horizons contain gahnite and garnet 'sandstone/quartzite', skarn, magnetite, and apatite.
2. Upper lode levels are Zn-rich, whereas the lower levels are enriched in Cu and pyrrhotite.
3. Sphalerite is iron-rich.
4. Country rocks are of similar composition. Basalt, shale, siltstone and feldspathic quartzite at Squirrel Hills are compositionally similar to amphibolite, feldspathic gneiss, and quartzite at Broken Hill.
5. Sequences are metamorphosed in the low-pressure intermediate facies series.
6. Ages of the two deposits are similar, between 1650 and 1780 m.y., the older age being closer to the likely age of sedimentation.

Differences between the two areas include lower lead values and a slightly lower grade of metamorphism at Squirrel Hills, but these features probably reflect a geological continuum in the original depositional basin and depth of burial, respectively.

The Mary Kathleen uranium deposit is contained in west-dipping middle Proterozoic calcareous, dolomitic, and alkali-rich metasediments of the Corella Formation. These rocks have been thermally metamorphosed to pyroxene and hornblende-hornfels grade by the nearby Burstall Granite, and they are intruded by a swarm of rhyolitic and microgranitic dykes associated with this granite.

On textural grounds the allanite-uraninite skarn mineralization is related to fluids associated with these dykes. This is supported by the high uranium content of the dykes (12 ppm average) compared to that in Burstall Granite (7 ppm), calcareous metasediments (3.5 ppm), quartzite (1 ppm), and basic rocks (1 to 3 ppm).

The uranium-rich fluids travelled in a westerly direction away from the Burstall Granite and rhyolitic dykes, down a falling temperature gradient. Some enrichment of fluids by collecting of uranium from metasediments may have occurred.

These fluids were impeded in most places by a chemically inert barrier of quartzite, but breached this barrier on the eastern side of the Mary Kathleen orebody, and intersected a sequence containing permeable lenses of conglomerate, within which the broadly stratabound orebody was deposited.

Similar orebodies could be expected in the vicinity of other permeable zones stratigraphically above quartzite and adjacent to fractures and acid dykes, but such sites appear to have been removed by faulting and erosion. However, fractured areas of the quartzite hanging wall (i.e. the eastern side of the quartzite), in the vicinity of rhyolite dykes, could also be sites of economic uranium mineralization at depth.

Copper prospects in the Mount Isa and Westmoreland areas

A. G. Rossiter

Geochemical work by the BMR since 1973 has shown promising indications of copper mineralization at two localities—one near Mount Isa, the other in the Westmoreland area.

The first prospect is 12 km WNW of Mary Kathleen. An ironstone outcrop, discovered in the course of regional geological mapping in 1972, was considered sufficiently interesting for geochemical and geophysical work to be carried out in the area during the following year. The geochemical investigation consisted of a detailed stream-sediment survey followed by soil sampling on a geometric grid. A small copper anomaly occurs in the vicinity of the original ironstone, but a much more

*** The sixth BMR Symposium will be held at the Australian Academy of Science Building, Canberra, on 3-4 May, 1977**

promising anomalous zone, also associated with ironstone outcrops, lies some 200 metres to the west. Here a soil anomaly 600 metres long and up to 100 metres wide has been outlined. A peak copper value of 950 ppm in the anomalous zone compares with background levels of less than 60 ppm elsewhere. Ironstone samples contain as much as 0.5 percent copper. No elements apart from copper appear to be significantly enriched in the area. The prospect is situated at the intersection of two faults in calcareous siltstone of the Lower Proterozoic Corella Formation—a very favourable geological environment for copper mineralization.

The second prospect is in the Westmoreland area just west of the Queensland-Northern Territory border, about 400 km NNW of Mt Isa. A stream-sediment anomaly delineated in 1975 during regional sampling of the Seigal 1:100 000 Sheet area was followed up by more detailed stream-sediment work and a reconnaissance soil survey. A soil anomaly exceeding 2 km in diameter has been outlined. The maximum copper value found so far is 1180 ppm—this compares with regional background levels of less than 60 ppm. Copper appears to form a halo around a core rich in lead, lithium, niobium, rubidium, thorium, uranium, and yttrium. Arsenic, beryllium, bismuth, tin, and tungsten are enriched in the area, but it is not yet known whether there is any zoning of these elements. The anomaly occurs in high-level granite and acid volcanics of Carpentarian age. The geological environment, large apparent size, and elemental zoning of the mineralization suggest that it may be of the 'porphyry' type.

Pay versus Non-pay Kimberlites

John Ferguson

About 88 percent of natural diamonds are derived directly from kimberlite, the remainder from detrital deposits. Diamond can be an accessory mineral in kimberlite; if present the concentration is less than 1 ppm. World-wide distribution of kimberlites indicates that they are virtually restricted to the older (1500 m.y.) continental cratonic areas, and that the diamondiferous kimberlites are concentrated in the even older and thicker nuclei of these stable platforms. Kimberlites range in age from Precambrian to cretaceous, and possibly even younger; this spread of ages may be present in single provinces.

Kimberlite emplacement is confined to areas of anorogenesis, and related to large-scale uplift and distension; in some cases there is an association with major rifting. Structures in the upper crust control the localization of individual intrusives. Kimberlites most commonly occur as diatremes or dykes; rare sills are known. The diatremes have conical shapes and result from explosive breakthrough from kimberlite fissure feeders at depths 2 to 3 km below surface.

Kimberlite is an ultramafic alkaline rock recognized more commonly by its associated suite of xenoliths (mostly garnet lherzolite, peridotites, pyroxenites, and eclogites) and xenocrysts (mostly Mg-rich ilmenite, pyrope-rich garnet, chrome-diopside and phlogopite) rather than by the matrix minerals. The latter comprise olivine (Fo_{90}) and lesser amounts of dolomite, calcite, ilmenite, perovskite, rutile, spinels, magnetite, phlogopite, and apatite. Owing to the rapid emplacement of kimberlites, the mineral assemblage has not had time to equilibrate to crustal conditions, thereby maintaining an upper-mantle facies assemblage. Kimberlites probably form at depths ranging from 100 to 250 km, so that the first essential requirement for the presence of diamond would be that they originate at depths below about 150 km—that is, within the diamond stability field for the projected continental geotherm. In that the site of kimberlite generation is thought to be close to the lithosphere-asthenosphere boundary—that is, within the low-velocity zone—it is important, from a prospecting viewpoint, to select target areas for pay kimberlites where the palaeo-low-velocity zone exceeded depths of 150 km ±. A study of the mineral assemblages in some xenoliths allows estimates of equilibration temperatures and pressures to be made. For this P-T estimate it is necessary that the equilibrated rock contains the assemblage Ca-rich pyroxene + Ca-poor pyroxene + garnet. The equilibration temperature is estimated from the diopside solvus, and with this knowledge it is possible to estimate the equilibration pressure from the Al_2O_3 content of enstatite. Using this pyroxene geotherm, it has been found that old stable cratonic areas more than 1500 m.y. old provide the necessary conditions for the generation of kimberlites within the diamond stability field. Additional useful mineralogical parameters for determining the favourability of kimberlites for diamonds can be gleaned from the composition of garnets and ilmenites. High Mg and Cr, and low Ca contents in garnets; and high Mg and Ti contents in ilmenites reflect diamond-facies assemblages. The intergrowth of diopside$_{ss}$ and magnesite$_{ss}$ is an additional indication of an assemblage originating within the diamond facies regime.

Economic mineralization associated with carbonatites

John Ferguson

Carbonatites are primary igneous rocks containing one or more of the following principal minerals: calcite, magnesiodolomite, ankerite and/or siderite. The most common minor minerals are sodic pyroxenes and amphiboles, apatite, magnetite, biotite, and alkali feldspars, all of which may reach the proportions of major constituents producing associated rock types. Carbonatites are geochemically identified by strong enrichment in one or more of the following elements: Sr, Ba, La, Ce, and Nb, which can occur in independent minerals or else proxy for other elements in the major and accessory mineral assemblages. In common with feldspathoidal rocks, carbonatites are also enriched in P, F, Zr, Hf, Ti, and Th.

Carbonatites occur in alkaline igneous provinces as independent or composite plugs, dykes, cone-sheets, rarely concordant intrusions; and as effusives. Most typically they occur as central cores to ultramafic alkaline volcanic rocks, and mark the latest phase of explosive igneous activity. Carbonatites range in age from Precambrian to present-day, and are mostly confined to stable continental platforms associated with areas of major uplift, distension, and rifting. Carbonatites are surrounded by metasomatic aureoles (fenites) characterized by the introduction of alkalis. The chemistry of the fenitised rocks suggests that the metasomatising fluids were originally in equilibrium with silicate magmas.

The economic minerals most commonly exploited in carbonatites are apatite, pyrochlore, rare-earth minerals, fluorspar, and barite. By-products of these commercial operations include vermiculite and minerals containing iron, titanium, zirconium, uranium, thorium, and strontium. Copper enrichment in carbonatites is regarded as atypical, despite the large-scale mining of copper at the Palabora carbonatite complex, Transvaal. In order to understand the role of sulphides in carbonatites it is necessary to look at their petrogenesis. As noted, carbonatites are associated in space and time with other alkaline rocks, and are typically found in closest association with the ultramafic alkaline varieties which include kimberlites. Textural evidence within such rock-suites suggest that the carbonatites developed by a process of unmixing or immiscibility with these magmas. Experimental work demonstrates that silicate magmas can dissolve large proportions of CO_2 at. mantle pressures. Once this carbonated magma is brought into low-pressure crustal regimes, the CO_2 enters into a carbonate phase giving rise to carbonatites. The silicate-carbonate fractionation results in the partitioning of the sulphide-rich assemblage into the volatile-rich carbonatitic magma. Providing that this magma is not violently erupted to surface, with attendant loss of the volatile phase, the sulphide assemblage is retained in the carbonatite or in the shattered and fenitised wall-rocks.

Geochemistry and petrography around the Woodlawn Cu-Pb-Zn orebody, NSW

I. B. Lambert
Baas Becking Geobiological Research Laboratory

The Woodlawn ore body, which is being developed by Jododex Australia Pty Ltd, is near Tarago, about 45 km northeast of Canberra. It consists of massive Cu-Pb-Zn sulphide lenses plus stringer and disseminated mineralization.

Chemical, X-ray diffraction and microscopic studies have been carried out on approximately two hundred and fifty representative samples from diamond drill cores at various distances up to several kilometres from the orebody.

These investigations have substantiated the general geological picture evolved during complementary studies by Jododex, the NSW Geological Survey and CSIRO Division of Mineralogy, and further elucidated details of rock distributions, alteration minerals and geochemical anomalies in the Woodlawn area.

The two main rock types in the vicinity of the ore are the felsic volcanics, which are dominant to the south and the west of the ore, and the fine-grained sedimentary rocks, which are most abundant in the immediate vicinity of the ore body and to the north. The sedimentary rocks seem to be mainly derived from the acid volcanics. Dolerite intrusions are common to the north.

There is an extensive aureole of silification, chloritization, sericitization and stringer mineralization around the ore body, in which feldspar and primary ferromagnesian minerals are virtually absent (except in some dolerite intrusions). The main chemical changes within the hydrothermally altered rocks include addition of Si, Mg, Fe, (Mn), Al, (K), Ag, Cd, Zn, Pb, (Bi), Cu, S, (Sn) and depletion of Na and Ca, with the elements in brackets showing less systematic trends.

The aureole of chemical and mineralogical anomalies can be divided into several distinct zones.

Zone 1 occurs in the immediate vicinity of the massive ore. It represents the most intense alteration and may include precipitates from the metal-rich ore-forming solution. It is characterized by abundant stringer mineralization, chlorite schists and cherts, together with altered volcanic and sedimentary rocks. The rock chemistry is dominated by high Mg and Fe values with low SiO_2 in the cherts; the altered volcanics and sediments are chemically intermediate between these extremes. Ca and Na contents of all rocks are very low, as evidence by the absence of plagioclase, and K is somewhat depleted.

Zone II surrounds Zone I. It is a relatively extensive zone of less intense hydrothermal alteration, characterized by less common stringer and disseminated mineralization and a virtual absence of feldspars (except in some basic rocks). There is widespread silicification of the felsic volcanics, whilst Mg contents are significantly higher than in unaltered felsic volcanics and sediments, and tend to increase towards the ore body. Na and Ca are much depleted, but K contents are fairly normal and reflect the abundance of sericitic muscovite.

Zone III, which comprises the volcanic pile to the south of the ore body, evidently was not permeated ubiquitously by hydrothermal solutions. It contains patchy development of chlorite-rich rocks and stringer to disseminated base metal and pyrite mineralization. Elsewhere the felsic volcanics tend to be silicified, but they generally contain albitic feldspar. The chemical features of the rocks in this zone are therefore highly variable.

Outside these zones there is some silicification of the felsic volcanics and other mild chemical changes which can be ascribed largely to deuteric alteration and low grade metamorphism, rather than to mineralization.

We consider that sea water descended into the volcanic pile and was heated and chemically modified to a minor degree as it circulated and ascended to the surface, where it gave rise to Zone II alteration by reaction with the volcanics and sediments. Ore formation and Zone I alteration could have occurred relatively rapidly following mixing of this circulating sea water with highly metalliferous solutions. The latter would be analogous to those which form porphyry copper deposits and could have been generated during sub-volcanic magma fractionation and/or by extensive rock leaching at moderate to high temperatures. Explosive volcanic activity offers a feasible means of 'tapping' the metalliferous solution and enabling rapid ascent of the resultant mixed solution.

The response to geophysical prospecting methods of the Woodlawn orebody, NSW

I. G. Hone

BMR has conducted test surveys over the Woodlawn orebody with transient electromagnetic, magnetic induced polarization and a variety of down-hole geophysical methods. The purpose of this work was to investigate the response of the orebody to recently introduced electrical prospecting methods. Interpretation of the data recorded was greatly assisted by geological information provided by company mapping and drilling.

A semi-regional transient electromagnetic survey was made with the Rusian MPPO-1 equipment and, although affected by cultural noise, the results show a strong anomaly over the orebody. Detailed analyses of the results indicate the attitude of the orebody and its shallow depth.

The magnetic induced polarization survey was carried out using recently developed Scintrex equipment. Anomalies were recorded over the orebody, black pyritic shales, and weakly mineralized dolerites. It was difficult to separate these anomalies on the basis of polarization response alone, but the ore zone was clearly resolved by a zone of high conductance.

The down-hole surveys employed resistance, resistivity, induced polarization, self-potential, gamma-ray and electromagnetic methods. All down-hole surveys provided information on the physical properties of the ore and host rocks. Most methods can be used to assist geological correlation between holes. The resistivity and resistance logs indicate a large contrast in resistivity between the conductive massive sulphides and the resistive country rocks. The self-potential method proved the most successful in indicating the presence of remote mineralization. The down-hole electromagnetic surveys were made with a Turam-type system and recorded anomalous field strength and phase readings when the probe was in or less than ten metres from the orebody.

The survey results show that the Woodlawn orebody has an extremely high conductivity and that the orebody clearly responds to prospecting methods based on conductivity, conductance or self-potential measurements. Of the surface methods used by the Bureau of Mineral Resources the transient electro-magnetic method proved the more cost-effective for semi-regional exploration in this environment. The down-hole surveys indicate that the self-potential method is an effective tool for detecting mineralization away from the hole.

Geophysical surveys of heavy mineral sand deposits, Jerusalem Creek, NSW

N. Sampath

Between May and November 1975 BMR carried out airborne and ground geophysical surveys over heavy mineral sand deposits in the Jerusalem Creek area, New South Wales. The surveys were the first stages of an investigation into the geophysical response of heavy mineral sand deposits and the role of geophysical methods in heavy mineral sand exploration.

The heavy mineral sand deposits at Jerusalem Creek are of the beach-ridge type and occur in several forms and grades. Rutile, zircon and ilmenite are the major constituents of the heavy minerals.

The geophysical methods employed in the surveys were magnetic, radiometric and induced polarization. These methods were selected because of the expected contrasts in the magnetic, radioactivity, and induced polarization characteristics of heavy mineral sand and quartz sand.

The airborne magnetic and gamma-ray spectrometer surveys covered an area of approximately 200 square kilometres of coastal plain centred on Jerusalem Creek. No aeromagnetic anomalies were observed over heavy mineral sand deposits; however the airborne gamma-ray spectrometer data show some correlation with the beach-ridge system. The most distinct radioactivity anomalies correlate with dumps and excavated areas.

On the ground, magnetic, radiometric, and magnetic and electrical induced polarization surveys were carried out over the high-grade Evans West deposit. This deposit was chosen as the site for ground surveys because the detailed geology provided by the extensive development drilling could be used to assist interpretation of the geophysical results. To further assist interpretation of the geophysical survey results, beach sand samples were collected for laboratory measurement of physical properties.

The magnetic induced polarization (MIP) results clearly delineate the orebody but a limited electrical induced polarization (EIP) survey of the deposit was not so successful. EIP traverses over dumps containing different heavy mineral fractions showed that ilmenite was the source of the induced polarization anomalies produced by the heavy mineral sand, a finding supported by subsequent laboratory studies. No magnetic anomalies were observed over the heavy

mineral sand deposit and this result is consistent with laboratory measurements which show a very small susceptibility contrast between heavy mineral sand and quartz sand. Measurements made in the laboratory and in mine workings show that the heavy mineral sand deposits were distinctly radioactive; however owing to the blanketing effects of overburden, no radioactivity anomalies were recorded over unmined ore.

The ground surveys show that the MIP method could be usefully employed as a prospecting tool for high grade heavy mineral sand deposits. Ground magnetic and radiometric methods seem unsuitable for deposits of the Jerusalem Creek type owing to the low susceptibility of the heavy minerals and the blanketing effect of overburden.

Gravity investigation of the geometry of the granitic complexes at Rum Jungle, NT

J. A. Major

In 1974 BMR made a gravity survey on and around the Rum Jungle and Waterhouse granitic complexes, about seventy kilometres south of Darwin. The principal aim of this work was to determine the sze and shape of the granitic bodies.

The investigations indicate that some of the rocks in the complexes have the same density as the surrounding metasediments. Other rocks in the complexes have lower density.

The geometry and density of the granitic complexes were investigated by matching observed gravity profiles with theoretical profiles calculated for models having a uniform density contrast with the surrounding rocks. Mass deficiency calculations were also made to estimate the volume of low density material in the complexes. For both studies, rock densities used were determined from measurements on drill core samples. Results show that the volume of low density material determined from the calculations is consistent with the volume determined by modelling.

Simple modelling indicates that the density discontinuity between the light rocks and the surrounding dense rocks extends no deeper than four kilometres. The most realistic geological interpretation of this model is that the low density material forms a basement at about four kilometres depth which rises to the surface within the complexes. This interpretation agrees with the theory put forward by other workers in the area, that the Archaean rocks were intruded by a low density Middle Proterozoic granite.

Sediments in the trough between the Rum Jungle Complex and the Waterhouse Complex appear to reach a depth of 2½ kilometres. Sediments in the embayment area deepen to the west and contain denser rocks, possibly amphibolite or massive dolomite.

In areas where there is a marked density contrast between the complexes and metasediments, estimates can be made of the contact inclination. These estimates show that the contact invariably slopes outwards from the complexes, a finding which agrees with current geological concepts regarding the emplacement of granite bodies.

The Cahill Formation—host to uranium deposits, Alligator Rivers area, NT

R. S. Needham

The Alligator Rivers Uranium Field of the Northern Territory has proven reserves of about 335 000 tonnes of uranium oxide which is worth about $16 000 million, calculated at likely contract prices for delivery of yellowcake in the early 1980's. The area is amongst the world's greatest uranium fields, and promises to become one of the great mining districts in Australia.

The uranium is contained in the Cahill Formation, a Lower Proterozoic unit confined to the northeastern part of the Pine Creek Geosyncline. It is a time and facies equivalent of the Koolpin and Golden Dyke Formations, which are host to uranium deposits elsewhere in the geosyncline. Lower Proterozoic units of the uranium field are poorly exposed. Clues which led to recognition of the Cahill Formation and its relationship to mineralization were: similar host rock geology of the ore deposits, air-photo trend patterns, scattered but characteristic exposures of silicified carbonate which are confined to the formation, aeromagnetic patterns, and finally the results of drill traverses across the formation in unmineralized areas.

The formation comprises a carbonate-carbonaceous-pelitic lower unit and a more psammitic upper unit, both containing amphibolite-grade schist as the major rock type. The major uranium deposits and prospects are located in the lower carbonate-carbonaceous unit which is correlated with the host rocks of the major ore bodies. The uranium is probably syngenetic, having originally been precipitated under reducing conditions in lagoonal environments adjacent to an ancient granitic land mass. Concentration took place during extensive regional metamorphism and deformation 1800 m.y. ago.

Folding and metamorphism are more intense in the northeast of the area, where the rocks have been granitized and are transitional into a migmatite complex, which is the focus of the 1800 m.y. event. The southwestern margin of the complex is marked by a large overfold, where metasedimentary rock types more resistant to partial melting enable approximate extensions of Cahill Formation in a migmatite terrain to be mapped.

Conventional airborne radiometric techniques are of little use in areas of overburden. Track-etch and emanometer methods are being used in the area, but pattern drilling may soon become the predominant exploration method. Careful selection of areas will be fundamental to successful exploration, and will be based on the distribution pattern and stratigraphy of the Cahill Formation.

A mineralogical and stable isotope investigation of ore genesis in the Golden Dyke Formation, NT

T. H. Donnelly and W. M. B. Roberts

The Golden Dyke Formation is part of the Lower Proterozoic Goodparla Group of sediments. The Formation has been mined principally for gold and uranium. In this study three base metal deposits have been selected for isotopic examination: the Mount Bonnie and Browns deposits approximately 150 km and 80 km south, respectively, from Darwin; and the Woodcutters deposit approximately 8 km east of the Browns deposit, in an attempt to corroborate conclusions based on mineralogical and geological evidence on the genesis of mineral deposits within the Golden Dyke Formation.

Stable isotopes of sulphur, from sulphides separated from both the mineral deposits and unmineralized Goodparla sediments, were used to determine the source of sulphur from which each deposit formed and to carry out temperature studies. Carbonate and carbonaceous-carbon associated with each of the deposits, and carbonate from the unmineralized Coomalie and Celia Dolomite Formations, were isotopically examined (carbon and oxygen) to determine the source of carbonate, chemistry of the formation of the hydrothermal carbonate, and the origin of the hydrothermal solutions associated with each deposit.

Results were obtained which suggested that connate fluids have been involved in the formation of each deposit examined. The Mount Bonnie deposit is shown to have a genesis linked with closely associated basic intrusives. In contrast the Woodcutters deposit is shown to have formed at a lower temperature (150°C) and the sulphide, from which the metal sulphides formed, came from an organic-rich carbonate environment. The Browns deposit formed as a result of both of these processes. All carbonate examined is shown to have a marine origin.

When the isotopic evidence is compared with the geological evidence the results show close agreement.

Precambrian palaeomagnetism of Australia

J. W. G. Giddings

It is presently uncertain whether orogenic zones in the Precambrian represent an episode of ocean basin closure (plate tectonic model), or were generated *in situ* between crustal blocks that have remained contiguous (single continent model). Palaeomagnetic measurements have the potential to distinguish between the two models: in the former a number of individual polar wander paths will coalesce at the time of the suturing of the blocks, while the latter is manifested by a single apparent polar wander path.

Australia provides a suitable testing ground for the two models. Geologically, the Australian Platform comprises a welded assemblage of Precambrian crustal blocks

separated by a network of younger mobile belts. 29 palaeomagnetic poles from 9 crustal blocks are now available for analysis. They comprise:

(i) 16 poles from isotopically dated (Rb-Sr method) Precambrian formations belonging to 8 crustal blocks, 9 of the poles relating to the Yilgarn Block. The poles range in age from 2500 m.y. to the latest Precambrian.

(ii) 10 poles from certain haematite orebodies developed in the banded iron formations of the Yilgarn, Gawler and Pilbara Blocks, and the Hamersley Basin. Geological criteria enable broad age limits to be assigned to these poles.

(iii) 3 poles for which maximum ages are known.

Consideration of the data shows that the dated poles lie chronologically in sequence along a single apparent polar wander path. The orebody poles also fall on this path in positions which do not violate the geological constraints on their ages. The path can therefore be used to provide closer limits on the ages of ore formation. An average rate of apparent polar wander of 0.3°/m.y. calculated from the path is the same as that found from Precambrian and Phanerozoic paths of other continents. Palaeoclimatic implications of the common path are its prediction of:

(i) Tropical palaeolatitudes for nothern Australia during much of the Carpentarian (1800 m.y.-1400 m.y.) at a time when there was widespread accumulation there of carbonates, including stromatolitic reefs—sediment types used as palaeoclimatic indicators of tropical conditions.

(ii) Polar latitudes for Australia at two distinct periods in the Late Precambrian within the age range 1150 m.y.-620 m.y. This finding correlates with the abundant geological evidence for two distinct, widespread glaciations about this time.

Precambrian palaeomagnetic data for Australia thus favour the single continent model in which the mobile belts result from *in situ* development between essentially contiguous cratons. However, opening and closing of small intercratonic ocean basins (of the order 1500 km) cannot be ruled out in view of the experimental errors inherent in the palaeomagnetic and isotopic dating techniques. It must be stressed, though, that before an unequivocal statement can be made regarding the nature of the mobile belts much work remains to be done in Australia to refine the apparent polar wander path. It is noted, however, that the conclusion reached from the Australian palaeomagnetic data is supported by similar work in Africa and North America for which considerably greater numbers of palaeomagnetic results are available for analysis.

Correlation of Precambrian rocks

M. R. Walter

Rational mineral exploration programs require a sound geological framework, the basis for which is the correlation of rock bodies. More direct uses of correlation in exploration depend on the fact that some types of ore deposits are temporally restricted—few banded iron formations are younger than 1800 m.y. old and few major lead-zinc ore deposits are older than that. Intercontinental correlation can be used with pre-drift assemblies of continental plates to locate segments of mineralized belts disrupted during drifting.

The present status of 6 methods of correlation will be very briefly reviewed. These are the use of: 1. distinctive rock types (e.g. tillites, iron formations); 2. isotopic dating of sediments; 3. palaeomagnetic pole positions; 4. palaeomagnetic reversal patterns; 5. microfossils; 6. stromatolites. This review is based on papers and discussions at the IGCP conference in Moscow in 1975.

The correlation of distinctive rock types is a time-honoured process and in the Precambrian involves especially the use of banded iron formations and glaciogenic rocks. The thick, extensive iron formations are Early Proterozoic, apparently clustering in age at about 2.0 b.y. Iron formations are common in the Archaean, but these are associated with volcanics and greywackes, whereas the Proterozoic examples accompanying extensive dolomites and limestones. However, there are also occasional younger banded iron formations. Glaciogenic rocks fall into two groups, Early Proterozoic and latest Proterozoic. The belief that glaciogenic rock units are markedly diachronous because glaciation was restricted to polar locations does not withstand critical examination. In Australia there were two latest Proterozoic glacial episodes which are probably approximately synchronous across the continent. The Early Proterozoic glaciation has not yet been recognised here.

Rb-Sr and K-Ar dating of glauconite can provide reliable results if numerous determinations are made, but isolated datings are of little or no value since the results are frequently spurious. Rb-Sr whole-rock isochron dating of fine-grained detrital rocks is successfully used here in Australia. Again, isolated datings may be of little value since detrital micas and feldspars may be mixed with diagenetic minerals in a system that was never isotopically homogenised. In some cases at least it is possible to separate out the diagenetic micas and date only these. This method had been used successfully on North African Precambrian sediments.

It is apparent that once an apparent polar wander curve is well established, when a pole position is determined for a rock body it can be plotted on the curve and dated in relation to other units. Limitations to this method are that the establishment of such a curve depends on the use of other dating methods, and even when precise dates are available the imprecision of the magnetic record and measurements will result in dating uncertainities of ± 50 m.y. In the absence of a precise curve, pole positions can still be used for local correlation. Because of recent instrumental advances this method can now be applied to carbonate sediments as well as red beds and igneous rocks.

The use of palaeomagnetic reversal patterns for correlation in the Precambrian is much the same as matching the magnetic 'stripes' on the sea floor. Patterns of reversals can be distinctive, and can be detected in sedimentary rocks. During at least some periods in the past (e.g. the Permian) rates of reversal were much lower than during the Cainozoic. Reversals detected in rocks from these periods are potentially very useful for extremely precise correlation. This method is currently being investigated in North America and Australia.

Precambrian microfossils are not rare, contrary to what was once thought, and are commonly found in black shales and fine-grained cherts. In the USSR they have been used in biostratigraphy for some years. Within the Proterozoic this is a very promising method, although much basic research remains to be done. Significant recent discoveries include that of a fossil microbiota in the Nabberu Basin (W.A.) iron formation that is indistinguishable from that in the Gunflint and Biwabik Iron Formations of North America. It has also recently been suggested that there are biostratigraphically useful sudden size increases in several groups of microfossils at about 1.4 and 1.0 b.y. ago.

Stromatolites have been used in Precambrian biostratigraphy for only the past 17 years, so this method is still in its infancy. It is now apparent that the form and fabric of stromatolites are controlled by both biological and physical factors. While this means that it is particularly difficult to interpret these features, it also means that stromatolites are useful in both biostratigraphy and palaeoenvironmental analyses. Stromatolites are being used to group sedimentary rocks into broad units, with time spans averaging 300 m.y., and finer subdivisions also seem possible. Stromatolites are powerful tools for precise intrabasinal correlation. With careful observation in the field and a minimum of laboratory investigation a wealth of information can be gained of use in making local correlations.

No one method of interbasinal correlation in the Precambrian is wholely reliable. When attempting correlations as many methods as possible should be used in combination, to allow mutual checking and refinement.

Mineral prospects of the Arunta Block, NT

A. J. Stewart

The Arunta Block is the mass of Precambrian basement rocks situated between Alice Springs and Barrow Creek in the southern part of the Northern Territory. Since 1970, BMR has mapped about two-thirds of the Arunta Block, erected a tentative stratigraphic sequence in the metamorphic rocks, and outlined the geological history. All known data on mineral occurrences have been collected and collated. A program of isotopic dating is currently in progress, and first results have already been published.

The Arunta Block comprises Early Proterozoic (or older) sedimentary and

volcanic rocks which were complexly deformed and initially metamorphosed 1800-1700 m.y. ago. The metamorphic rocks are grouped into three divisions separated by unconformities; the first division in places comprises two subdivisions separated by another major stratigraphic break. The metamorphic facies in all three divisions range up to granulite. The first division comprises interlayered felsic and mafic metavolcanic rocks and subordinate metasediments, followed by pelitic schist, gneiss, micaceous metasandstone and subordinate metavolcanics of division 2, and then by metamorphosed quartzite, pelite, carbonate and acid volcanics in division 3. All three divisions are intruded by granite, and a diorite-tonalite-granite complex is also present. Most of the granites date at around 1700 m.y., but intermittent granitic intrusion continued to about 1000 m.y. ago. Other igneous rocks in the Arunta Block are a differentiated basic complex with kimberlitic affinities, and a carbonate; both these intrusions are close to a deep crustal fracture, the Woolanga Lineament, in the eastern part of the Block.

In addition to the stratigraphic subdivision, the Arunta Block can be divided into two geographic zones, northern and southern. The northern zone is characterised by an almost total absence of rocks of division 1: rocks of divisions 2 and 3 are generally at greenschist or low amphibolite metamorphic facies; and most granites in the Arunta Block are located in the northern zone. In contrast, the southern zone contains almost all the division 1 rocks (granulites), rocks of divisions 2 and 3 are generally at amphibolite facies, and granites are few and small.

Mineral occurrences in the Arunta Block can be grouped into five types, based on origin. The distribution of the various types follows the northern and southern zones of the Block.

1. *Stratabound*

(1) *Oonagalabi type.* These are small to medium-size copper-lead-zinc-(bismuth) occurrences lying along the stratigraphic break in division 1 of the metamorphic rocks, in the southern Arunta zone. Sulphide minerals are present in three adjacent rock-types which are present at almost every occurrence: (i) magnesium-rich rocks, containing abundant cordierite, anthophyllite, phlogopite, and enstatite, as well as sapphirine; (ii) forsterite marble; and (iii) quartz-magnetite rock. This type of deposit may be a metamorphosed soil or an early part of a metamorphosed evaporite sequence, but neither hypothesis explains all features of the deposits. (2) *Jervois type.* These are small to medium-size copper-lead-zinc occurrences in pelitic schist in division 2 of the metamorphic rocks, in the northern Arunta zone. The country rocks also include amphibolite and calc-silicate rock in some occurrences.

2. *Igneous*

(a) *Acid.* Granitic pegmatites occur in or near the granites in the northern zone of the Arunta Block. They contain copper, lead, tin, tantalum, and tungsten. The Jinka Granite is the source of tungsten, molybdenum and copper which were metasomatically introduced into nearby calcsilicate country rock.

(b) *Basic.* Small amounts of copper minerals occur along faults and joints in many orthoamphibolite bodies in the southern Arunta zone.

(c) *Ultrabasic.* Chromium occurs in two small exposures of serpentinite in the southern zone.

3. *Occurrences formed by mobilization*

Gold occurs in pyrite in quartz and quartz-carbonate veins in the southeast of the Block. The lodes formed during greenschist facies metamorphism of the Arunta basement and unconformably overlying Heavitree Quartzite during the Late Palaeozoic. Small quartzose lodes of gold and copper occur in fault and shear zones cutting schist of division 2 in the northern Arunta zone. Abundant coarse muscovite occurs in cross-cutting pegmatites in the Harts Range in the eastern part of the southern Arunta zone; the pegmatites are metamorphic segregations that were 'sweated out' of metapelitic gneisses of division 2.

4. *Occurrences formed by weathering*

Small areas of laterite on carbonate rocks of the third metamorphic division contain up to 60 percent manganese. Uranium, as carnotite and uraninite, occurs in Late Palaeozoic sandstone and Quarternary calcrete overlying the Arunta Block, and is thought to be derived from granites in the Arunta Block.

5. *Occurrences of unknown origin*

Fluorite and fluorite-barite veins cut several granite masses in the northern Arunta zone. Some of the veins that cut the Jinka Granite also cut Late Proterozoic sediments which unconformably overlie the Granite.

The copper occurrences are the most numerous in the Arunta Block, but most are small and uneconomic. There is no evidence for large stratabound deposits of the Oonagalabi type; maximum assay results at Oonagalabi itself are 1 percent Cu and 1.6 percent Zn over a width of 40 metres. The pegmatite coppers are rich, but very small; one is being worked by a small mining company, operated by aboriginals. The orthoamphibolite coppers appear to be little more than concentrations of background copper localized during metamorphism and faulting. The dioritic complex may be worth prospecting as a possibly porphyry copper; two small copper-bearing calcite veins cut orthoamphibolite which is intruded by the dioritic rocks, but copper minerals are not known in the dioritic rocks themselves.

The tungsten pegmatite occurrences are small, but one is rich enough to support a small syndicate operation. The metasomatic tungsten-molybdenum deposit is also being worked by a small syndicate. The other mineralized pegmatites are all too small to warrant exploiting for metals; some are used as sources of gemstones and mineral specimens.

The gold deposits in the southeast Arunta are (or were) rich, but small; the easily worked near-surface ore has been extracted, and the remaining unoxidized ore is not economic. Large amounts of mica still exist in the Harts Range, but cannot compete with imported material.

The fluorite-barite veins in the Jinka Granite have been prospected and evaluated, but are subeconomic at present prices. The uranium occurrences are still being evaluated, but in any case they face strong competition from the large deposits in other parts of the Northern Territory.

The location of the kimberlitic intrusion and carbonatite body, both of mantle origin, along the Woolanga Lineament suggests the possibility that diamond-bearing kimberlites and rare-earth-bearing carbonatites may be present elsewhere along the Lineament, concealed beneath superficial Cainozoic sediments.

Plates and volcanoes in Papua New Guinea

R. W. Johnson

Present-day tectonism and volcanism in Papua New Guinea are governed by the relative movements of two minor plates caught between the larger, converging, Pacific and Indo-Australian plates. It has been suggested that either two or three minor plates were involved; and it has been argued either that instantaneous poles of rotation for all the plate boundaries were a long way from Papua New Guinea, or that some poles of rotation may be within, or close to, Papua New Guinea.

Fourteen volcanoes in Papua New Guinea have erupted this century, and ten of these are found at the seismically highly active southern margin of the South Bismarck plate. This plate margin is therefore a critical one for volcanologists, and the volcanology group at BMR has, on the basis of field and petrological studies, attempted to establish a broad tectonic framework to account for the volcanism.

The south Bismarck Sea volcanoes coincide with two convergent plate boundaries: (1) a western arc off the north coast of mainland Papua New Guinea extends from the Schouten Islands to the western end of New Britain, and is associated with the Indo-Australian/South Bismarck plate boundary; (2) an eastern arc, overlying the northward-dipping New Britain Benioff zone, is associated with the boundary between the Solomon Sea and South Bismarck plates.

The compositions of rocks from the western arc change along the volcanic chain. Because the present-day pole of rotation for the Indo-Australian/South Bismarck plate boundary could be in the northwestern part of mainland Papua New Guinea, and because rate of plate convergence probably governs the thermal regime under any one part of the arc, it is postulated that primary mantle-derived magmas are produced under unique sets of conditions under different parts of the western arc, giving rise to contrasting magma compositions at different volcanoes along the arc. The compositions of volcanic rocks in the eastern arc change progressively northwards with increasing depth to the underlying Benioff zone. The unusual distribution pattern of the eastern arc

volcanoes may be due to the thermal influence of a thrust slice beneath west New Britain, and to the proximity of instantaneous poles of rotation in, or near, the Gulf of Papua.

These and related studies in other volcanic areas in Papua New Guinea lead to the following general conclusions:

(1) Most plate boundaries in Papua New Guinea are zones of deformation, and the only boundaries that can be represented by a single line are those defined by the axis of the submarine trench south of New Britain and west of Bougainville Island. In particular, the Ramu and Markham valleys on mainland Papua New Guinea are considered to represent a collision zone between a Tertiary island-arc and the northern margin of the Australian continent, and the presence of the western arc volcanoes cannot be reconciled with the models that interpret the axes of the Ramu and Markham valleys as a present-day plate boundary.

(2) Models which assume that the present-day poles of rotation are a long way from Papua New Guinea are probably less realistic than those which regard them as nearby. This applies particularly to the boundaries at the southern margin of the South Bismarck plate.

(3) Evidence for the present-day existence of a third minor plate north of the South Bismarck plate is not compelling. Plate boundaries may have existed in the zone north of Manus Island and north and east of New Ireland and Bougainville Island, but there is little seismicity and, like the Ramu and Markham valleys, the zone is probably best regarded as a possible site of former plate boundaries.

Information on former plate boundaries is critical to an understanding of early Cainozoic magmatism and metallogenesis in Papua New Guinea. Mineralization of the Cu-Au-Mo type is associated with Tertiary island-arc type igneous rocks in several parts of Papua New Guinea, and there is now a need for extending the present studies on contemporary plate boundaries and active volcanism to older igneous formations and their associated tectonic regimes.

The Median Tectonic Line in New Guinea—a continent-island arc collision suture

R. J. Ryburn

The term Median Tectonic Line was first used in Japan for the major fault separating two contrasting metamorphic terrains of late Mesozoic age—the high-pressure low-temperature Sanbagawa belt and the low-pressure high-temperature Rycke belt. Similar paired metamorphic belts have since been recognized in many of the young orogenic belts bordering the Pacific Ocean (and elsewhere), notably in California, New Zealand, and Sulawesi. In most areas the high-pressure belt lies on the oceanward side of a contemporaneous low-pressure belt, from which it is separated by a 'median tectonic line'. The high-pressure belt is characterized by sporadic occurrences of blueschist containing lawsonite, glaucophane, aragonite, and omphacite, by the abundance of dismembered ophiolites, and by the absence of intrusives coeval with the metamorphism. The low-pressure belt contains metamorphic minerals characteristic of a medium to high geothermal gradient (andalusite, sillimanite, cordierite), and abundant calc-alkaline intrusives and volcanics.

Paired metamorphic belts can be explained in terms of the plate tectonic model for convergent plate boundaries. Subduction of oceanic lithosphere results in a marked depression of the isotherms in the subducted slab—conditions suitable for blue schist-facies metamorphism. Thus the high-pressure belt is made up of sediments and fragments of oceanic crust that have been subducted and subsequently uplifted. The low-pressure high-temperature belt corresponds to eroded parts of the volcanic arc overlying the subduction zone, where magmatism has resulted in a high geothermal gradient. It is important to note that the 'median tectonic line' is usually a vertical fault produced by isostatic uplift of the subducted material after subduction has ceased, and usually lies nearer the volcanic arc than the underthrust. In some circumstances, however, the underthrust is preserved beneath relatively intact ophiolite sequences at the leading edge of the overriding plate. These sequences represent oceanic crust and upper mantle forming a basement to the volcanic arc, and are commonly tilted towards the arc by buoyant upsurge of the underlying subducted material.

Knowledge of New Guinea geology has reached a stage that allows tentative recognition of an early to mid-Tertiary median tectonic line and paired metamorphic belts. Unlike most other examples, the high-pressure low-temperature terrain lies on the continental side of the low-pressure belt. Blueschist-facies rocks, mostly metamorphosed ophiolites (gabbros and volcanics), are known from the northern fall of the central ranges in Irian Java, from southern tributaries of the Sepik River, and from south of the Papuan Ultramafic Belt. Low-grade metasediments and dismembered ophiolites are also common in the high-pressure belt. In the low-pressure belt, or North New Guinea Arc, volcanics and intrusives of Eocene to Oligocene age are widespread. Owing to the shallow depth of erosion, low-pressure high-temperature metamorphics are not widely exposed, but are present in the Sepik Valley. The age of metamorphism in both belts appears to be Oligocene, the same as in New Caledonia. Northward-dipping intact ophiolite sequences, probably basement to the North New Guinea Arc, include the Papuan Ultramafic Belt, the Marum Complex, and several smaller bodies in the south Sepik area.

The North New Guinea Arc is interpreted as an eastward extension of the Indonesian arc system that was impacted by the northern margin of the Australian continent in about the late Oligocene. Throughout the early Tertiary, oceanic crust north of the continent was consumed in a northward-dipping subduction zone beneath the North New Guinea Arc. Thus the median tectonic line in New Guinea is thought to approximate to the collision zone. The presence of late Tertiary intrusives in the central ranges of New Guinea, and two small occurrences of blueschist on the north coast of Irian Jaya, suggest that 'flipping' may have taken place during the collision, followed by southward subduction in the late Tertiary.

The model proposed here has some implications for the location of mineral deposits in New Guinea. Apart from the porphyry-copper potential of the North New Guinea Arc, and lateritic nickel associated with the ultramafic bodies near the median tectonic line, the blueschists and other meta-ophiolites are a favourable environment for cupriferous bedded pyrite lenses similar to those in the Sanbagawa belt in Japan. Jade may yet be found in the high-pressure belt, as chloromelanitite, a close relative of jade, occurs in the south Sepik blueschists.*

* Jadeite has recently been reported from the northern fall of the central ranges in Irian Jaya (C. Brooks, pers. comm.).

Beach ridges, sea-level changes and heavy minerals—some preliminary results

P. J. Cook

Many relative changes of sea level have taken place during the Quaternary, mainly in response to fluctuations in the volumes of ice in the Arctic and Antarctic. During still-stands of sea level there is extensive mechanical working and reworking of strandline deposits which in places results in heavy mineral deposits. The current state of knowledge suggests that the richest heavy mineral deposits are associated with high sea-level stands, and that the longer the still-stand, the richer those deposits are likely to be. Therefore if a precise sea level curve can be established it should be possible to forecast the periods in which heavy mineral deposits are most likely to have formed. Consequently as an aid to the exploration of these deposits, BMR is not only compiling information on known deposits but is also examining beach ridge sequences onshore and offshore in order to help define a sea-level curve with greater precision.

Work by BMR on beach ridges in the Gulf of Carpentaria (Smart), and Broad Sound (Cook, Polach) supports the idea that sea level stabilized at about 6000 years BP. Offshore work on the north NSW and south Queensland coast (Jones) has shown that there are a number of features associated with Quaternary shorelines, the most prominent of which are at depths of about 20-30 m (late Holocene), 40-50 m, 77-85 m, 105-120 m and 160-180 m. The 20-30 m feature has been sampled by drilling (Planet), but to date none of the deeper submerged features have been sampled. Uranium-series dating of coral material from the Newcastle and Evans Head areas (Marshall, Thom) has now proved that the Inlier Barrier formed during the last inter-

glacial period when sea level was somewhat higher than the present-day level.

The best developed onshore beach ridge sequence in Australia is that in southeast South Australia. A cooperative program by BMR (Cook, Colwell), the S.A. Dept. of Mines (Lindsay, Firman) and Flinders University (von der Borch, Schwebel) is currently being undertaken in this region in the hope of using it to establish a sea level curve for a continental coast. The drilling program to date has made it possible to establish fairly precisely the Quaternary coastal sequence in this region although absolute ages are not available at the present time. Because of its well-developed beach ridge sequence the area has attracted a number of exploration companies looking for heavy mineral deposits. Results obtained from our drilling program indicate that, in general, heavy minerals are not abundant. The greatest heavy mineral concentrations (up to 1.2% total heavies) are found not in the beach ridges but in a non-outcropping marine sand unit which underlies the eastern half of the region and any future exploration effort should probably be directed at this unit.

Recent palaeomagnetic work on the sequence has shown that all the ridges, with the exception of East Naracoorte Range, were formed during the Brunhes normal polarity epoch. This suggests that there have been at least 12-15 major changes in sea level within the past 700 000 years.

Habitat of Petroleum as related to maturation indices Gippsland Basin, Vic.

S. Ozimic

It is generally accepted that the source of hydrocarbons in the Gippsland Basin is the organic matter dispersed in sediments of the Late Cretaceous to Early Tertiary Latrobe Group. Comparison of the composition and the degree of maturation of the sediments of the Strzelecki, Latrobe and the Seaspray Groups reveal that only the Latrobe Group sediments satisfy the requirements necessary for the generation of the hydrocarbons encountered in the basin.

The source rocks of the Latrobe Group have been buried deeply enough and for a sufficient length of time for the diagenetic formation of hydrocarbons from exinitic (spores, pollen, cuticle, resin and algae) vitrinitic and inertinitic constitutents. Present day temperatures (up to 160°C) are assumed to approximate the maximum palaeo-temperatures.

The composition of the hydrocarbons from the Gippsland Basin (dry gas, condensate, oil and gas with a high content of CO_2) indicates a range of different sources and the nature of migration.

The source of gas with a high CO_2 content (e.g. the Marlin—Deep reservoir contains 21% CO_2) is speculative. It may be related to volcanic activity (contact metamorphism) which could have liberated CO_2 through heating calcareous and/or coaly material, or to bacterial action in the early stage of the diagenesis of the Latrobe Group sediments. Dry gas in the Golden Beach No. 1A reservoir is probably biogeneic in origin. The results of coal-rank analyses from different offshore wells (68-81% carbon) indicate an oil and wet gas province. This appears to be consistent with the observed liquid/gas ratios of the hydrocarbon accumulations. Moisture content and calorific values of coals of the Latrobe Group from the offshore wells show a direct relationship to depth of burial and the type of associated hydrocarbons.

Temperature gradients (1.5-2.5° C/100 m) observed in the individual offshore wells vary considerably.

Present-day distribution of the hydrocarbons throughout the basin is a function of the nature of folding (non-compressional), time of migration (late Eocene and Oligocene) and the sealing off of the Latrobe Group sediments, by the transgressive, calcareous and shaly sediments of the Lakes Entrance Formation.

The stratigraphy and structural evolution of the Great Australian Bight Basin

J. B. Willcox

A regional interpretation of BMR seismic profiles along the southern margin of Australia, between 120° and 141°E, indicates that 200 to 500 m of sediment underlies most of the continental shelf and the western Eyre Terrace, and that the section is continuous with the Upper Cretaceous and Tertiary of the Eucla Basin. A section up to 10 km thick in the Great Australian Bight Basin; that is, under the outer edge of the continental shelf, Ceduna Terrace and eastern Eyre Terrace, and under the continental rise south of the terraces, is subdivided by four unconformities. By analogy with the well-documented section in the Otway Basin, and by comparing the structural style with that suggested in Falvey's model for the formation of Atlantic-type continental margins, the section is considered to comprise four units: a Lower Cretaceous fluviatile—lacustrine unit (Otway Group equivalent); an Upper Cretaceous and lower Paleocene, mainly fluviatile-deltaic unit (Sherbrook Group equivalent); an upper Paleocene and Eocene shallow marine clastic unit (Wangerrip and Nirranda Group equivalents); and an Oligocene to Recent prograded carbonate shelf unit (Heytesbury Group equivalent). These rocks overlie crystalline and sedimentary basement of Precambrian age. The proposed stratigraphy is consistent with the log of Shell's Potoroo No. 1 well which is located on the northern margin of the basin (130°46′E, 33°23′S).

Beneath the extensive continental rise south of the Eyre and Ceduna Terraces, similar unconformities occur and 2-3 km of Great Australian Bight Basin sediments appear to be present. Oceanic basement, characterized by numerous diffractions and by Number 22 (upper Paleocene), appears to be in contact with faulted Cretaceous rocks at the foot of the continental rise. On some profiles, pockets of sediment accoustically similar to the proposed upper Cretaceous unit lie between knolls of oceanic basement and this may indicate that the initial intrusion of oceanic material took place along several fractures.

The basement and Lower Cretaceous rocks are sliced by extensive normal faults which trend parallel to the continental margin. In general, the fault-blocks are downthrown southward and tilted northward; beneath the Ceduna Terrace they form an elongated structural basin. The Upper Cretaceous and lower Paleocene sediments which fill this basin are faulted at the margins only, probably by rejuvenation of the Lower Cretaceous faults.

The earliest geological event deduced in the interpretation is the erosion of basement probably during the Permo-Carboniferous ice age. In the early Mesozoic, fault-bounded troughs probably formed near the edge of the present continental shelf (e.g. Polda Trough) and possibly south of the Eyre Terrace. During the Early Cretaceous, fluviatile and lacustrine sediments were deposited south of the basement which now underlies the continental shelf and western Eyre Terrace. Shallow marine sediments may have been deposited southwest of the basin during this period, as indicated by marine influence in Early Cretaceous sediments in Potoroo No. 1. Towards the end of the Early Cretaceous a thermally induced arch may have formed along the foot of the present continental rise, and the resulting tension was relieved by normal faulting and formation of an incipient rift. By the early part of the Late Cretaceous a structural rift-valley basin had formed. This was followed by a marine incursion, which probably spread from the west. Fluviatile and deltaic sediments were deposited in the subsiding rift-valley basin during most of the Late Cretaceous and early Paleocene. The readjustment of fault-blocks near the basin margins in the mid-Late Cretaceous caused a minor unconformity. In the upper Paleocene, commencement of seafloor spreading led to subsidence of the southern fault-blocks and formation of the southern margin. A marine transgression resulted in deposition of shallow marine clastic sediments in the late Paleocene and Eocene. By the Oligocene, the source of detritus had been largely eroded down, and the northward drift of Australia into a warmer latitude probably resulted in the change to carbonate sedimentation. As the margin continued to subside, a shelf of prograded carbonate sands built southwards and pelagic carbonates were deposited on the continental rise.

The main difference between this interpretation and the one presented by Bouef & Doust (*APEA J.*, 1975) is that the 'break-up unconformity' is believed to be higher in the section, resulting in the post-break-up Tertiary section being about 600 m instead of 3 km thick. The Upper Cretaceous is correspondingly thicker.

Potoroo No. 1, together with Echidna No. 1 and Platypus No. 1 which are located at the eastern end of the basin (Duntroon Embayment), cannot be regarded as an adequate test of its petroleum potential. Potoroo lies 100 km north of the depositional axes of the Cretaceous and Tertiary sediments, in an area where most of the Lower Cretaceous is faulted out and where

the Upper Cretaceous is relatively thin. Numerous faults separate this well from the major part of the basin which lies beyond the continental shelf. The favourable reservoir sands encountered in the Upper Cretaceous and Neocomian may persist into the deep water part of the basin and suitable source rocks may occur as a result of the more marine conditions expected in that area. The depth of burial of the Lower Cretaceous and lower part of the Upper Cretaceous sediments suggests that they maybe sufficiently mature for generation of hydrocarbons.

Extension of the Lovelle Depression, Galilee Basin, Qld

P. L. Harrison and J. A. Bauer

The Galilee Basin formed by periodic downwarping during Late Carboniferous, Permian and Triassic times and received mainly terrestrial sediments comprising sandstones and siltstones with thick coal sequences in the Lower and Upper Permian. The western part of the Galilee Basin consists of the Lovelle Depression, a northeast-trending trough of Permian and Triassic sediments up to 700 m thick, west of the Cork Fault. The margins of the Lovelle Depression were poorly known from scattered petroleum wells, water-bores and limited seismic traverses.

Economic interest in the Galilee Basin sediments result from the possible presence of oil, gas or coal. By analogy with the Permian sequences of the Cooper Basin and Bowen Basins, the Galilee Basin could contain commercial quantities of hydrocarbons.

Regional gravity and magnetic interpretation have not generally been useful in defining the sedimentary thickness because the gravity anomalies appear to reflect basement density variations and the magnetic anomalies to reflect basement lithological variations.

The main objective of the seismic survey carried out in 1975 was to further define the extent and thickness of Galilee Basin sediments in the Lovelle Depression.

An additional objective was to verify the presence of a possible sedimentary sequence about 5000 m thick beneath the Eromanga Basin sequence which was indicated on a single seismic line south of Ooroonoo No. 1 well.

Four strong reflections were selected for mapping. They were identified in the Lovelle Downs No. 1 well section as:

Horizon A	Near base of Toolebuc Formation (Cretaceous)
Horizon B	Near top of Hooray Sandstone (Lower Cretaceous/Upper Jurassic)
Horizon C	Near top of Permian
Horizon D	Basement

Preliminary interpretation indicates that Galilee Basin sediments in the Lovelle Depression are more extensive than previously realized. The first complete northwesterly seismic cross-section over the Lovelle Depression was obtained; this cross-section shows that the sediments thin gradually towards the western margin, and that the eastern margin probably lies east of the Holberton Structure, the previously inferred margin. The maximum thickness of the Permian sediments was about 500 m in the southeast.

Results of this survey, together with review of a company line south of Ooroonoo No. 1 well, indicate Permian sediments are about 200 m thick 70 km south of the well and that the well may have been drilled on a local basement high.

The southern margin of the Lovelle Depression is therefore not yet defined. However a direct link with the Cooper Basin is unlikely because a seismic line in the northwestern part of the Cooper Basin indicates complete thinning of the Permian and Triassic sediments of the Cooper Basin about 100 km south of the presently known extent of the Lovelle Depression. A large unexplored area however remains between the Lovelle Depression and the northwestern Cooper Basin.

Two major faults were mapped. The Holberton Structure, previously known from geological mapping, corresponds to a major fault in the sub-surface with up to 300 m of downthrow to the west. Another major fault appears to be a southerly continuation of the Cork Fault.

The survey also discovered a basement high having an amplitude of 300 m at basement level; depth to the top of the high is 1400 m. The structure has apparent axial lengths of 7 km and 3 km, and is inferred to trend approximately northwest, parallel to the regional basement trends inferred from the gravity and magnetic anomalies.

The presence of a sedimentary (or possibly metamorphic) sequence up to 7500 m thick beneath the Permian sediments near Mount Windsor was confirmed. The sequence is known only from seismic work and could be one of several older sequences which exploration wells and water-bores have intersected in the area (Proterozoic sediments to the west, metasediments to the east and Palaeozoic carbonates of the Georgina Basin to the northwest).

Further seismic work is required to better define the margins of the Lovelle Depression especially in the unexplored area between the Galilee and Cooper Basins where the thickness of the Permian sediments is unknown. Follow-up work is required to demonstrate whether the basement high found during the survey is a closed structure. More detailed seismic coverage is required where regional coverage indicates a reasonably thick Permian section to determine whether other similar basement highs may be present in the Lovelle Depression.

Reassessing the mineral potential of the Georgetown Inlier, Qld

J. H. C. Bain

Early in 1972, BMR, in collaboration with GSQ, began a re-examination of the Georgetown Inlier in North Queensland—an area of Precambrian and Palaeozoic rocks, including several small abandoned mining districts. It was soon established that during the preceding ten years exploration activity in the region had been patchy and lightweight and that the region was poorly rated. To reassess the mineral resources and potential of the region and to stimulate exploration the Bureau began remapping the region at 1:100 000 scale; in addition airborne radiometric and magnetic surveys were flown to revise and augment available regional geophysical data. Systematic regional stream-sediment geochemistry was also initiated to check for indications of possibly mineralized areas that might be overlooked during geological mapping, and to provide a sound regional base for more detailed prospecting by exploration companies.

A north-south strip 50 km by 150 km in the central part of the Inlier was selected as a test area to determine whether or not the chosen multidisciplinary approach could contribute significantly to our reappraisal of the region. This test strip and some adjacent areas have now been geologically and geophysically surveyed although the geochemical surveys are still in progress. Even though this work is incomplete, it is already apparent that the more numerous and accurate data now available can significantly improve assessment of the region.

Furthermore, recent discoveries by BMR and exploration companies clearly indicate that the Inlier has greater mineral potential than was previously evident: Central Coast Exploration's recently announced Maureen Uranium deposit is an example of this. The mineralization is contained in epiclastic sediments at the base of an Upper Palaeozoic acid volcanic sequence, and is believed to be a metasomatic replacement deposit which formed when ascending hydrothermal fluids, derived from a late-stage intrusive equivalent of the volcanic rocks, spread out on intersecting a favourable host—the basal arkose. Our mapping of the nearby Carboniferous Newcastle Range Volcanics shows that such sediments are sporadically present where previously none were known or inferred, and that mineralized fracture zones are also present in the overlying volcanics and related dykes. It can now be postulated that epiclastic sediments are present in all, or most, of the numerous Upper Palaeozoic acid volcanic sequences in the Cairns-Townsville hinterland. These volcanics also have common chemical and structural characteristics, and thus the region may now be regarded as a potential new uranium province. Concentrations of Mo, F, Sn, As, Bi and W are common throughout the province.

Additional mineral potential is indicated by the presence of at least three extensive zones of hydrothermally altered rock with copper mineralization (porphyry copper deposits), at Mount Darcy, Mount Turner and near Cardross; and three large zones of auriferous quartz-sericite alteration in granite—the Kidston breccia pipe, the Jubilee Plunger reef, and the Mount Hogan gold mines area.

The gold deposits of the Etheridge Goldfield in the central part of the Inlier, previously thought to be Precambrian and derived from granite, may have formed during the Palaeozoic by lateral secretion-type processes from stratiform concentrations in the Proterozoic metasedimentary rocks. If this as yet untested hypothesis is correct, the region may also have some potential for Homestake-type gold deposits.

R75/292(3) Cat. No. 76 3375 9

Australian Mineral Industry 1974 Review

The Australian Mineral Industry Annual Review and associated Quarterly Reviews have been issued regularly since 1948. The current Annual Review (ix + 424 pp, $13.00) covers as far as practicable developments, both domestic and international, in 1974 and in the first half of 1975; full statistical coverage is necessarily limited to the end of 1974.

Information is presented in four parts. Part 1—the General Review—includes salient statistics of the Australian mineral industry and summarises recent developments in the industry at both the national and international levels under the headings of production, mineral processing, self-sufficiency, trade, prices, mineral exploration and Government assistance and controls.

Part 2—Commodity Review—reviews individual mineral commodities (Abrasives to Zirconium) from the viewpoint of domestic mine production, smelting and refining, overseas trade, consumption, prices, exploration and new developments, and overseas review.

Part 3—Mining Census—tabulates statistics extracted from the Mining Census (which appears in condensed form in Part 1), and some mineral processing statistics from the Manufacturing Census.

Part 4—Miscellaneous—details quantum and value data of mineral output provided by Departments of Mines in the various states; and provides miscellaneous information such as principal mineral producers, ore buyers and mineral dealers, mining services, industrial and professional organisations and development associations, and publications available from the Bureau of Mineral Resources.

Forthcoming papers in the Journal

The 1:5 000 000 coloured Gravity Map of Australia is now available. To coincide with its release a number of papers on gravity in Australia will form part of Number 4 of this volume, scheduled to appear in December 1976. Titles of these papers are listed below. This number will also contain coloured Bouguer and free air gravity maps of the Australian region.

J. C. Dooley and B. C. Barlow
A short history of gravimetry in Australia

W. Anfiloff, B. C. Barlow, A. S. Murray, D. Denham and R. Sanford
Compilation and production of the 1976 Gravity Map of Australia

S. P. Mathur
Relation of Bouguer anomalies to crustal structure in central and southwestern Australia

P. Wellman
The gravity field of the Australian basement

J. C. Dooley
Variation of crustal mass over the Australian region

P. Wellman
Regional variation of gravity and isostatic equilibrium of the Australian crust

A. Fraser
Gravity provinces and their nomenclature

P. A. Symonds and J. B. Willcox
The gravity field of offshore Australia—a brief description

O. Terron, W. Anfiloff, F. J. Moss and P. Wellman
A selected bibliography of Australian gravimetry

Contents

Page

G. Jacobson, P. H. Vanden Broek, and J. R. Kellett
Environmental geology for urban development—Tuggeranong, Australian Capital Territory 175

W. Mayo
Numerical techniques applied to the geochemistry of some estuarine sediments from Broad Sound, Queensland 193

N. F. Exon and J. B. Willcox
Mesozoic outcrops on the lower continental slope off Exmouth Western Australia . 205

J. Smart
The nature and origin of beach ridges, western Cape York Peninsula, Queensland . 211

S. K. Skwarko, Robert S. Nicoll, and K. S. W. Campbell
The Late Triassic molluscs, conodonts and brachiopods of the Kuta Formation, Papua New Guinea 219

Peter J. Davies, B. M. Radke, and C. R. Robison
The evolution of One Tree Reef, Southern Great Barrier Reef, Queensland 231

Notes

G. R. Pettifer and J. Smart
Resistivity methods in the search for groundwater, Cape York Peninsula, Queensland . 241

P. J. Davies and D. B. Stewart
Scuba-operated coring device 246

E. K. Carter and K. Modrak
The Registry of Stratigraphic Names 247

Discussion

R. A. Callen
Tentative correlation of onshore and lacustrine stratigraphy, Lake Frome area, South Australia 248

Abstracts

The 5th BMR Symposium, April 1976 251